



Practical implementation of real-time fish classification from acoustic broadband echo sounder data

Author(s): B. Berges, J. van de Sande, B. Quesson, S. Sakinan, E. van Helmond,
A. van Heijningen, D. Burggraaf, S. Fassler

Wageningen University &
Research report C076/19



Europese Unie,
Europees Fonds voor maritieme zaken en visserij



WAGENINGEN
UNIVERSITY & RESEARCH

Practical implementation of real-time fish classification from acoustic broadband echo sounder data

Author(s): B. Berges, J. van de Sande, B. Quesson, S. Sakinan, E. van Helmond, A. van Heijningen, D. Burgraaf, S. Fassler

Wageningen Marine Research
IJmuiden, August 2019

CONFIDENTIAL no

Wageningen Marine Research report C076/19



Europese Unie,
Europees Fonds voor maritieme zaken en visserij



Client: RVZ
Attn.: Liesbeth Smits, Martin Pastoors
By e-mail: lsmits@pelagicfish.eu, m.pastoors@pelagicfish.eu

This report can be downloaded for free from <https://doi.org/10.18174/497323>
Wageningen Marine Research provides no printed copies of reports.



Europese Unie,
Europees Fonds voor maritieme zaken en visserij

This report has been produced with financial support of the European Fisheries Fund: Investment in sustainable fisheries.



Wageningen Marine Research is ISO 9001:2015 certified.

© Wageningen Marine Research

Wageningen Marine Research, an institute within the legal entity Stichting Wageningen Research (a foundation under Dutch private law) represented by Dr. M.C.Th. Scholten, Managing Director

KvK nr. 09098104,
WMR BTW nr. NL 8113.83.696.B16.
Code BIC/SWIFT address: RABONL2U
IBAN code: NL 73 RABO 0373599285

Wageningen Marine Research accepts no liability for consequential damage, nor for damage resulting from applications of the results of work or other data obtained from Wageningen Marine Research. Client indemnifies Wageningen Marine Research from claims of third parties in connection with this application. All rights reserved. No part of this publication may be reproduced and / or published, photocopied or used in any other way without the written permission of the publisher or author.

A_4_3_2 V29 (2019)

Contents

| | |
|--|-----------|
| Practical implementation of real-time fish classification from acoustic broadband echo sounder data | 1 |
| Executive summary | 5 |
| 1 Introduction | 8 |
| 1.1 Assignment | 8 |
| 2 Data collection and database | 11 |
| 2.1 Data collection | 12 |
| 2.2 Database | 17 |
| 3 Calibration | 20 |
| 3.1 Operational procedure | 20 |
| 3.2 Data processing | 22 |
| 3.3 Results | 26 |
| 3.3.1 Baseline analysis of Tridens II calibration data | 27 |
| 3.3.2 Analysis of inter-annual calibration data from fishing vessels | 34 |
| 4 Data processing and demonstrator software | 38 |
| 4.1 Processing chain | 38 |
| 4.1.1 Pre-processor | 39 |
| 4.1.2 Image Processor | 41 |
| 4.1.3 Data manager | 47 |
| 4.1.4 Replayer | 47 |
| 4.2 Graphical user interface | 47 |
| 4.2.1 Echogram display | 48 |
| 4.2.2 Classification display | 48 |
| 4.2.3 Control panel | 49 |
| 4.2.4 Length estimation | 52 |
| 4.2.5 Disturbance analysis | 52 |
| 5 Data analysis | 54 |
| 5.1 Frequency response analysis | 54 |
| 5.1.1 Method | 54 |
| 5.1.2 Results | 55 |
| 5.2 Noise analysis | 58 |
| 5.2.1 Background noise level | 58 |
| 5.2.2 Interference noise | 60 |
| 6 Species identification | 62 |
| 6.1 TNO classification | 63 |
| 6.1.1 Method | 63 |
| 6.1.2 Results | 64 |
| 6.2 WMR classifier | 71 |
| 6.2.1 Method | 71 |
| 6.2.2 Results | 75 |
| 6.3 Combined classifier | 81 |

| | | |
|----------|---|------------|
| 6.4 | Impact of reduction in data richness on classification accuracy | 82 |
| 6.4.1 | Feasibility | 83 |
| 6.4.2 | Expected operating range | 84 |
| 6.4.3 | Classification of data with reduced frequency bandwidth (ES80 FM) | 85 |
| 7 | Length estimation | 88 |
| 7.1 | Method | 88 |
| 7.2 | Results | 90 |
| 8 | Conclusions and recommendations | 95 |
| 8.1 | Conclusions | 95 |
| 8.2 | Recommendations | 96 |
| | Quality Assurance | 97 |
| | Acknowledgements | 98 |
| | Project management and dissemination activities | 99 |
| | References | 100 |
| | Table of figures | 103 |
| | Table of tables | 108 |
| | Justification | 109 |
| | Annex I: calibration additional information | 110 |
| | Annex II: automatic report generation | 113 |
| | Annex III: Calibration manual | 118 |
| | Annex V: project dissemination and presentations | 136 |
| IV.1 | presentation at the 2017 ASA conference (Boston, USA) | 136 |
| IV.2 | presentation at 2019 WGFAST (Galway, Ireland) | 140 |
| IV.3 | DG MARE newsletter (2019) | 144 |
| IV.4 | Presentation at PFA science day | 145 |

Executive summary



Europese Unie, Europees Fonds
voor Maritieme Zaken en Visserij

In the context of new policies restricting the discarding of fish at sea, this project aims at further improving the selectivity of the Dutch pelagic fishery. More specifically, broadband active acoustics is used to discriminate fish species and size them.

Downward active acoustic systems, so called echosounders are used routinely on board fishing vessels to monitor the water column. Here, the simrad EK80 echosounder is used. Though the EK80 is commonly operated in narrowband mode (CW), a broadband mode (FM) is also available. The use of the latter is advantageous because of: (1) the ability to determine the frequency response over wider frequency bands (2) the increased range resolution. The data richness from the EK80 in FM mode can be used for accurate species recognition, especially for species with a swim bladder that are hard to differentiate using CW mode (e.g. Horse Mackerel and Herring). The challenges of working of the EK80 FM is twofold: (1) increased noise due to higher interference with other acoustic equipment; (2) generation of a substantial amount of data.

The purpose of this document is to report the final results of the realFishEcho project. This project aims at developing and implementing real-time species identification and fish sizing algorithms. This is done using data collected by commercial vessels. Through a period of four years, data were collected by the Alida (SCH6) and the Afrika (SCH24) fishing vessels (FV) across the North Sea (Figure ES.1(a)). A total of 19 terabyte (TB) of acoustic data together with haul composition and length measurements were collected. Within this project, improved data processing was developed with accurate calculation and correction of the acoustic signal. Specific procedures for efficient handling of the data (e.g. building of a database) was also put in place.

Accurate calibration is an important step for cross-vessel application of the species classification algorithms developed in this project. The Alida (SCH6) FV calibrated the EK80 FM every year since 2015 and the Afrika (SCH24) FV in 2016. Large discrepancies were found between different calibration trials. These discrepancies (though only for FM mode) are similar to those found on research fishing vessel (RFV) Tridens II. They are problematic for cross vessel application, more specifically (1) the merging of data from different vessels and (2) the application of species recognition algorithms trained using data from different vessels. This issue needs to be investigated further through dedicated experimentation. During future calibration trials, it is important to reduce potential bias by:

- Calibrating the equipment in favourable conditions (weather, location, time of day)
- Following calibration guidelines (Annex III)

Within the realFishEcho project, two species classifiers were independently developed by WMR and TNO. Both use a machine learning approach that draw on the collected data. A species classifier combining both algorithms is also devised. With such an approach, the accuracy of the species classifier depends on the amount and diversity of the data collected. Using the large amount of data collected by the Alida (SCH6) FV, accurate and robust species classifiers are derived (Figure ES.2(b)). The results exemplify high accuracy levels of species classification (TNO: 95.6%, WMR: 94.7%). Expectedly, Mackerel is identified very accurately (>99%). Accuracies for Herring and Horse Mackerel are also very high (>91%). The data from the Afrika (SCH24) FV were also tested independently and also resulted in very high scores. However, because the data collected by this FV were limited in term of spatial and time coverage, the resulting species classifier lacks robustness and testing. Furthermore, because of the discrepancies between calibrations trials, it was not possible to fully combine the data from the Alida (SCH6) and the Afrika (SCH24).

Classification was further tested on two other species: Sardine and Sprat. Whilst the species classification accuracy for Sprat is low (~65%), Sardine exemplifies high scores (90%). However, the data available for these species is very limited and the classifiers that include those species lack robustness. Overall, the amount of data for Herring, Horse Mackerel and Mackerel is extensive (and

exemplify good spatial coverage of the North Sea) but data of other species such as Sprat and Sardine is needed for the practical implementation of a classifier including more species. The reduction in data richness (e.g. mimicking the fisheries version ES80 instead of the scientific version EK80) overall hampers the accuracy of the classifiers.

A specific software (ECHO software) implementing the improved acoustic data processing was developed. The ECHO software allows real-time visualisation and has the following features (Figure ES.2):

- Figure ES.2 panel C: Aid in data recording.
- Figure ES.2 panel A: Echogram viewing with user specified options (e.g. filtering or viewing over specific frequency bands).
- Figure ES.2 panel B: Viewing of species identification results (Herring, Horse Mackerel, Mackerel)
- Figure ES.2 panel E: Noise disturbance indicator.

In addition to species identification, the project investigated the use of the EK80 FM for sizing fish. The method employed uses the increased range resolution provided by the EK80 in FM mode to identify the boundaries of single fish detections. Preliminary results show that it is possible to differentiate different length classes (e.g. between 10 cm and 25 cm) when single fish targets are detected. However, The method needs further investigation with more data, especially with the coverage of a large range of length classes for different species.

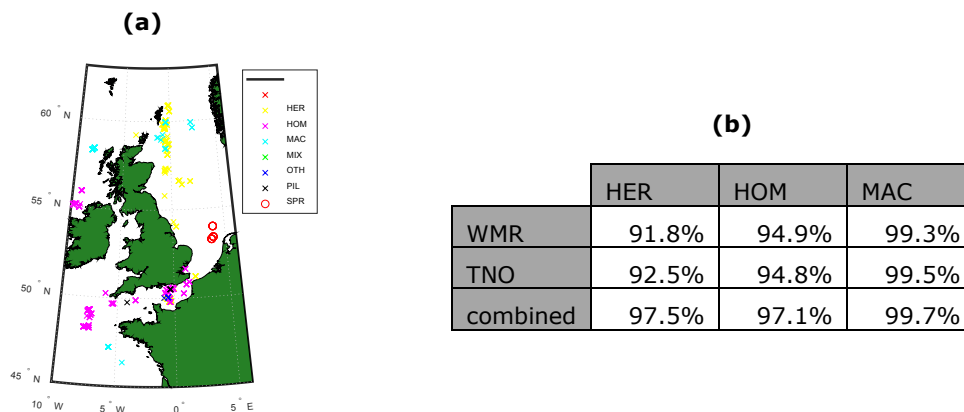


Figure ES.1: Results from the realFishEcho project. (a) Overview of the EK80 FM data collected through the course of this project. Each marker represents an imaged fish school. Data were collected by the Alida (SCH6) and the Afrika (SCH24) FVs. (b) Accuracy of the three species identification algorithms developed in this project (TNO, WMR and combined classifiers). These were developed for the three species with extensive data available: Herring, Horse Mackerel, Mackerel.

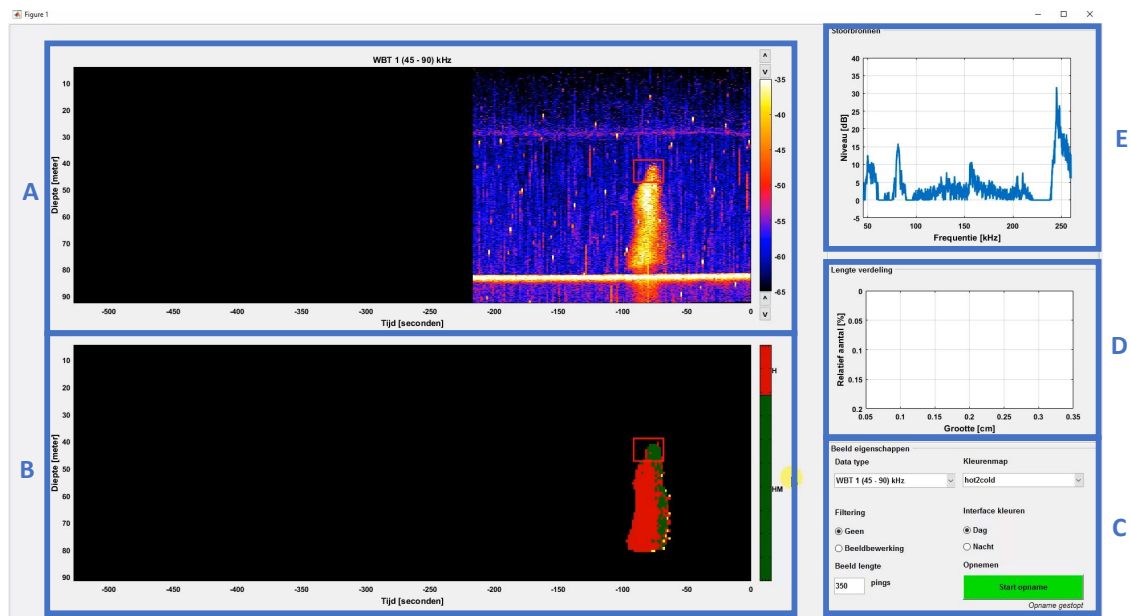


Figure ES.2: Screenshot of the Graphical User Interface (GUI) of the demonstrator, used on board by the skipper. Panel A: streaming echogram display. The display of the data can be changed using options the control panel (Panel C). Panel B: classification display, showing the detected schools and the estimated species type by the classifier. Panel C: control panel with the different visualization settings that can be selected by the user. Visualization settings are: different Wide Band Transceiver (WBT) to visualise; change in colour scheme; filtering of the echogram; number of pings to display. Panel D: visualisation of length estimation results. This feature is not implemented yet. Panel E: Disturbance analysis panel, displaying a frequency spectrum computed on the detected interferences in the echograms. This indicates the operating frequencies of narrowband interferences (other sonars).

1 Introduction

The EU has by means of new policy [1] restricted the discarding of fish at sea (e.g. not allowed to discard undersize quota species). As a result, the fishing industry now requires improved methods to identify fish species and sizes before the catch process begins. Active acoustics are the methods of choice for probing the surrounding of the vessel. More specifically, calibrated downward looking active acoustic devices, so called scientific echosounders [2] (combination of a transducer and a transceiver) are able to detect fish schools efficiently but also quantify these if the system is calibrated. Furthermore, because of their high accuracy and precision, scientific echosounders have the potential to classify imaged fish schools

For decades, echosounders have used narrowband as signal to send in the water, effectively measuring scattering levels in the water column around a specific frequency with a limited bandwidth. Using echosounders operating simultaneously at different frequencies, one is able to determine the echo strength of targets at “discrete” frequencies. This acoustic footprint can be used to discriminate different fish species [3]–[5]. However, while species discrimination algorithms have high performance for species that exemplify large biological differences (e.g. swimbladder against non-swimbladdered species), it often fails at successfully discriminating species with similar biological properties.

Scientific echosounders are now able to operate in broadband (as opposed to narrowband) robustly. The pulse consists of a chirp signal that sweeps a range of frequency through time. The resulting acoustic scattering measurements from an echosounder is then resolved over a wide frequency band as opposed to “discrete” frequencies for a narrowband system. Simultaneous measurements from different echosounders yield the backscattering frequency content over several wide frequency ranges. Another advantage of using a broadband pulse is the increased echogram resolution through pulse compression [6]. There are two main drawbacks of using broadband echosounders: 1) the higher noise level as acoustic energy is spread across wider frequency bands, and 2) the large volume of data that are generated. However, data from multi-frequency broadband echosounders is more rich than data from multi-frequency narrowband systems. This can for example be used to overcome the limitations encountered with species identification using narrowband systems. In addition, the very high range resolution has potential for fish sizing applications.

The purpose of this document is to report the final results of the realFishEcho project. This project aims at developing and implementing real-time species identification and fish sizing algorithms. This is done using data collected by commercial vessels. In the realFishEcho project, simrad EK80 Wide Band Transceivers (WBT) that had been installed on board three commercial fishing vessels (FV) are used to drive the corresponding transducers in broadband. These echosounder were calibrated and used to collect a large amount of data across the North Sea, English Channel and West of the UK for different fish species. From this large database, species identification algorithms are developed and implemented in a real-time software. This software package is installed on FVs and helps skippers to take better-informed decisions about targeted species while fishing. In addition, a length estimation methodology is developed and tested.

1.1 Assignment

The realFishEcho project runs in collaboration between Wageningen Marine Research (WMR), Redersvereniging voor de Zeevisserij (RVZ) and TNO. The development of the different tasks within this project is based on data collected by three commercial freezer trawlers:

- Afrika (SCH24)
- Alida (SCH6)

-
- Willem van der Zwan (SCH302)¹

In addition, research fishing vessel (RFV) Tridens II provided data of opportunity collected during acoustic surveys conducted by WMR.

In this study, all participating FVs except the Willem van der Zwan (SCH302) FV used an EK80 system running in Frequency Modulated mode (FM, named "EK80 FM" further in this report), i.e. broadband. This is different from the EK80 system running in Continuous Wave mode (CW, named "EK80 CW" further in this report), i.e. narrowband. The EK80 system is provided by SIMRAD. Three Wide Band Transducers (WBT) frequency channels are used here: 70 kHz, 120 kHz and 200 kHz. The depth at which the system was operated is limited to ~160 m due to the noise limitation of the 120 kHz and 200 kHz WBT channels.

This project ran over three years (June 2016 to May 2019) and is divided into 5 work packages (WP) which are then divided into tasks (T). The breakdown of these WPs and tasks is given in Table 1-1. Results for the first two years of the project were reported in two progress reports [7], [8]. A dedicated report describing the methodology for the species identification algorithms was also produced [9]. The different WPs are:

WP 1: system calibration

A set of three WBT frequency channels (70 kHz, 120 kHz, 200 kHz) were calibrated in FM mode on board each vessel involved in the project. Calibration trials on board the FVs was attempted if possible once a year to keep track of the efficiency of the transducer. Calibration was performed by the crew of each FV with the assistance of scientists. The data from each trial were scrutinized and analysed thoroughly and compared. For this project, the calibration was essential for cross vessel application of the species identification algorithms and the merging of data between different vessels.

WP 2: data collection

Acoustic data were collected by FVs and analysed afterwards. The acoustic data were collected around fishing operations and associated with biological data collected after each haul (species composition, length frequency distribution). The main species targeted by the FVs in this project were Mackerel, Horse mackerel and Herring and to a lesser extend Sprat and Sardine. The data collection also includes regular calibration trials. Visits of scientists on board the FVs were performed to test the software developed in operational conditions.

In order to handle the large amount of data generated, a data handling procedure was developed to reduce the data collected to single fish schools and organize these into a database.

WP 3: data processing and analysis

Drawing on work from a previous project [10], the pre-processing of the acoustic data needed to be improved.

The effect of various variables (depth, species, area etc.) on the acoustic frequency response was investigated using the large amount of data collected by the different FVs.

Using a machine learning approach, two independent species classification methods were developed. A combined species classifier was also be devised.

A method for estimating fish size using broadband echosounders was developed and tested on a small data set.

WP 4: software development

The developments in term of data pre-processing was implemented in a demonstrator software that allowed the skippers to benefit from enhanced echogram visualization.

The species discrimination algorithms developed in WP3 was implemented into the demonstrator software with real-time visualization.

¹ In practice, no broadband data was collected on board SCH302 during the course of the project, as the vessel was targeting narrowband data instead.

Table 1-1: breakdown of the WPs and tasks within the realFishEcho project. Corresponding report sections are also given.

| Item # | Tasks | Section |
|------------|---|-------------------|
| WP1 | System calibration | |
| T1.1 | Calibration in the field | Section 3 (p20) |
| WP2 | Data collection | |
| T2.1 | fishing trips (mackerel, horse mackerel, herring, sprat) | Section 2.1 (p12) |
| T2.2 | research trips (mackerel, herring, sprat) | |
| WP3 | Data processing & analysis | |
| T3.1 | fishing trips (mackerel, horse mackerel, herring, sprat) | Section 5 (p54) |
| T3.2 | research trip (mackerel, herring, sprat) | |
| T3.3 | database setup | Section 2.2 (p17) |
| T3.4 | species identification algorithm improvement | Section 6 (p62) |
| T3.5 | fish length estimation method development | Section 7 (p88) |
| WP4 | Demonstrator software development | |
| T4.1 | first demonstrator software version (GUI 1): pre-processing, imaging, noise reduction, school detection, species classification | Section 4 (p38) |
| T4.2 | second demonstrator software version (GUI 2): implementation of updated species classification and length estimation | |
| T4.3 | installation, test & evaluation GUI 1 | |
| T4.4 | installation, test & evaluation GUI 2 | |
| WP5 | Management, communication & reporting | |
| T5.1 | Project progress monitoring & reporting | p99 |
| T5.2 | Project management and communication | |
| T5.3 | Report and presentation of results | |

2 Data collection and database

In the realFishEcho project, data were collected from 2017 to 2019 using the EK80 FM at three WBT frequency channels: 70 kHz, 120 kHz and 200 kHz. Three FVs were involved in the data collection effort: Alida (SCH6), Afrika (SCH24), Willem van der Zwan (SCH302)². Because of the limitation in depth of the 120 kHz and 200 kHz channels, no data deeper than ~160 m was collected. This section describes the protocol for data collection and presents the wealth of data collected through the course of the project.

The EK80 system is the successor of the EK60 system. The latter has been used for decades for acoustic surveys and is known for its consistency and robustness. While the EK80 works similarly to the EK60 in Continuous wave mode (CW, narrow band), it also offers broadband capabilities when operating in Frequency Modulated mode (FM, broadband). EK80 FM offers advantages in term of target discrimination (by resolving backscattering intensity over large frequency bands) and range resolution (through matched filtering). Whilst scientific methods for the processing of narrow band echosounders is well established [11], the use of broadband echosounders is relatively new in the field of fisheries acoustics though it has been used in the past [12].

The working principle of the EK80 is exemplified in Figure 2-1 for a single WBT frequency channel. An acoustic transducer is coupled to the EK80 system (i.e. transceiver) for: (1) transmission of input signals that is further converted into acoustic waves, and (2) reception of the signals that results from the measurements of the scattered acoustic waves. The functioning of the EK80 relies on firmware updates. Then, the EK80 system interfaces with the EK80 or the ES80 software (installed on a separate computer). Both software allow:

- The visualization of data.
- The configuration of the system (e.g. pulse length, ramping, frequency range).
- The logging of raw data in the *.RAW format.

The data collected also uses calibration values in order for the echosounder to derive absolute acoustic intensity levels. Calibration is paramount in order to compare results from different vessels. Calibration is obtained after dedicated trials where measured acoustic intensity levels can be compared with those from calibration spheres (theoretically known acoustic response) [3, 4]. Further explanation on the need for calibration is explained in Section 3. The EK80 software has a specific Graphical User Interface (GUI) where the state and quality of the calibration can be monitored. The result of a calibration trial is:

- A set of values that are stored within the EK08 software but also in output files.
- An update of beam at the level of the EK80 transducer.

The EK80 software (as opposed to ES80) is a version that offers more possibilities in term of customization (pulse length, pulse ramping, frequency range). At the contrary, the settings from the ES80 software is limited which hampers the quality of data collected with this software. More specifically the following can only be achieved with the EK80 software:

- Maximized frequency range
- adjustable pulse ramping
- Setting pulse length

For these reasons, only data collected using the EK80 software are used in this project. Data collected with the EK80 software (as opposed to ES80) with a maximum frequency range is highly desirable for maximizing the success rate of the species identification. However, because the ES80 is optimized for visualization, this software is preferred by skippers on board commercial vessels. It is therefore beneficial to explore the use of data collected with the ES80 for classification purposes. This is presented in Section 6.4.3.

² However, see footnote 1 on page 12

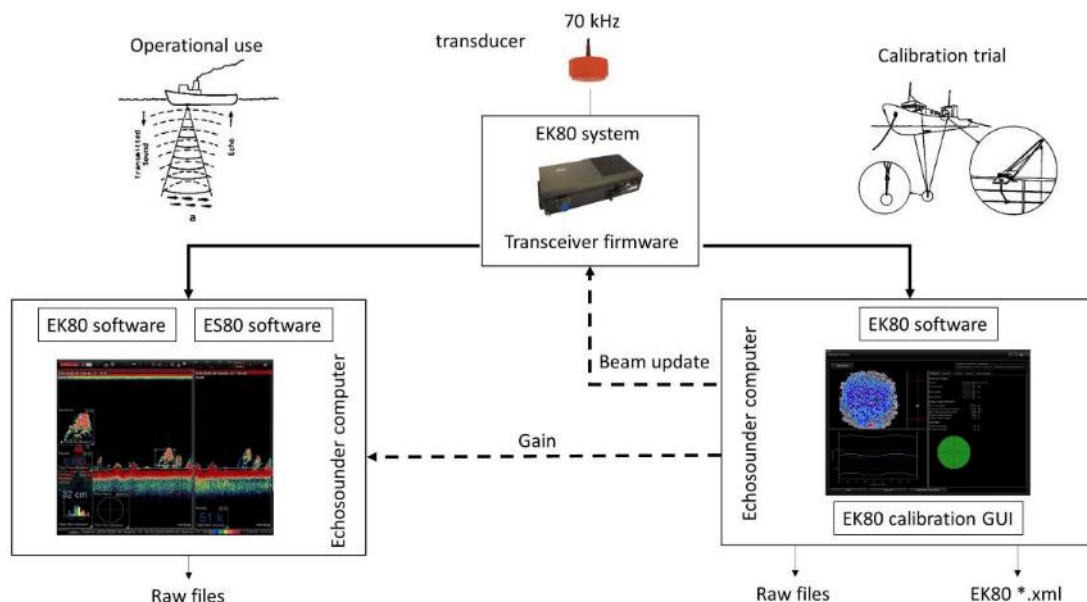


Figure 2-1: working principles of the EK80 system for an individual WBT frequency channel. Most often, several WBT channels operate simultaneously (or sequentially) on FVs. In operational use, the EK80 system (combination of transducer and transceiver) probes the water column in the acoustic beam. Subsequent echo returns can be displayed as echograms by the EK80 or ES 80 software. These software are also able to record data in the *.RAW format. Each EK80 system has a specific set of calibration values: gain and beam update. These are determined during dedicated calibration trials that are performed using the standard sphere method [13], [14] (see Section 3).

2.1 Data collection

Through the course of this project, two types of data were collected on board the FVs: calibration data and data around fishing activities. EK80 FM data from a previous project [10] are also used. Though the collection of EK80 FM data on board Dutch FVs is relatively new, collection of narrowband acoustic data (EK60 and EK80 CW) was already undertaken in previous projects [15]–[17] and the crew from the different FVs were familiar with scientific requirements at the start of the project.

The setting for the EK80 FM used here are presented in Table 2-1. In order to sweep a range of frequencies, the EK80 FM uses so called chirp signals which have a changing frequency with time. Here, a signal with linear increase of frequency is used (LFM up). A standard pulse duration of 1.024 ms is used with maximum transmit power and frequency bandwidth for each WBT channel. Another important transmit signal characteristic is the ramping, which refers to the speed at which the transmitted pulse in the water reaches its maximum amplitude level. Options available in the EK80 software are “fast” and “slow” ramping. The difference between a “fast” and “slow” ramping pulse for the EK80 FM is exemplified in Figure 2-2(a) and (b). A fast ramping maximizes the effective frequency bandwidth and range resolution of the data at the expense of higher noise (compared to slow ramping) generated by side lobes from the match filter. The difference in spectra for “fast” and “slow” ramping pulses is shown in Figure 2-2(c) and (d).

Table 2-1: EK80 settings used during data collection.

| Channel | Pulse type | Pulse duration (ms) | Power (W) | Start Frequency (Hz) | End Frequency (Hz) | Ramping |
|---------|------------|---------------------|-----------|----------------------|--------------------|---------|
| 70 kHz | LFM Up | 1.024 | 750 | 45000 | 90000 | Fast |
| 120 kHz | LFM Up | 1.024 | 250 | 90000 | 170000 | Fast |
| 200 kHz | LFM Up | 1.024 | 120 | 160000 | 260000 | Fast |

(a)

(b)

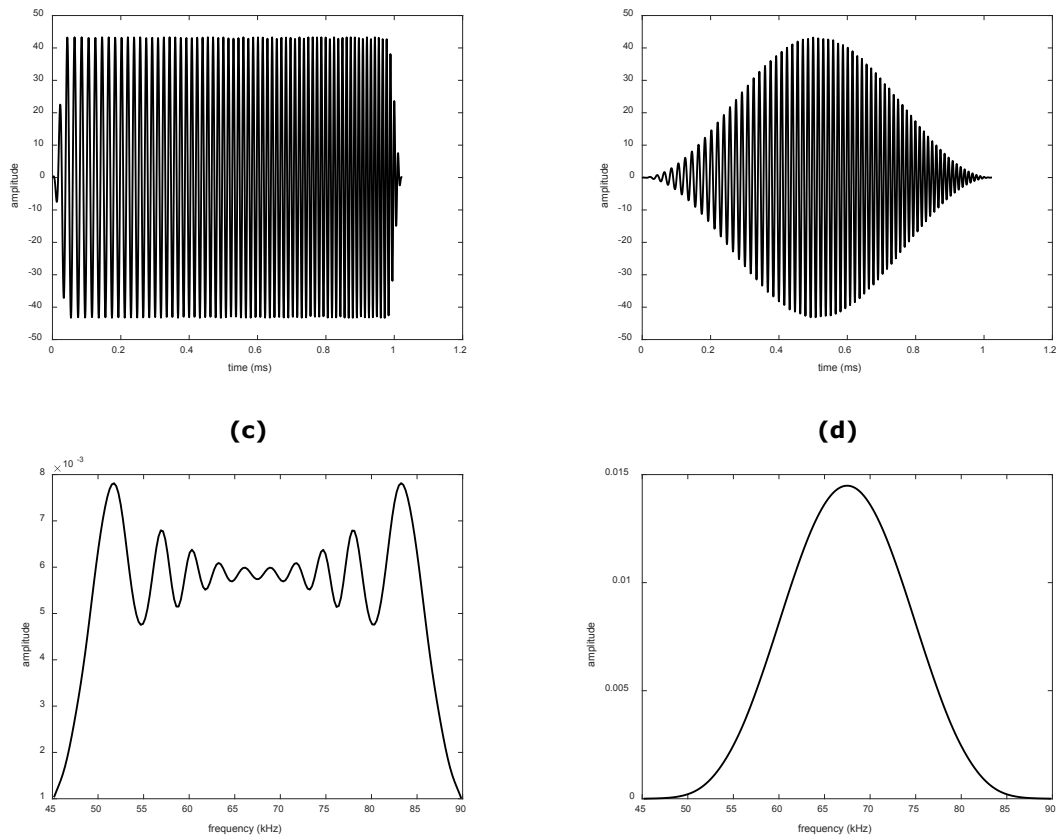


Figure 2-2: comparison of fast and slow ramping acoustic pulses used by the EK80 FM. (a) fast ramping time signal. (b) slow ramping time signal. (c) frequency content of a fast ramping pulse. (d) frequency content of a slow ramping pulse.

Calibration data consisted of single day trials were the standard calibration spheres method was used [13], [14]. Based on Fassler et al. [16, p. Annex B], a calibration manual was devised, describing the calibration procedure for both the EK80 FM and the EK80 CW. This manual is given in Annex III. The operational processing and data processing is described in Section 3.

Across the calibration data sets, four different sphere sizes (tungsten carbide, WC) were used (Table 2-2): 15 mm, 22 mm, 25 mm and 38.1 mm. Three WBT channels were calibrated: 70 kHz, 120 kHz and 200 kHz. Data collected onboard RFV Tridens II are used as a baseline for comparison with calibration on board the FVs in Section 3. No calibration data was collected onboard FV Willem van der Zwan (SCH302).

As shown in Table 2-2, the size of each calibration data set is variable. This is due to each specific setups, especially in term of weather. If conditions are optimal, the calibration of a single WBT channel against a specific sphere takes about 20 minutes. If weather conditions are inclement, it can last for 1-2 hours. The location where each calibration was undertaken is shown in Figure 2-3(a), (b) and (c). The calibration of RFV Tridens II is routinely performed in Scapa Flow (Scotland, shown in Figure 2-3(c)). Calibration of the Afrika (SCH24) FV was also calibrated in Scapa Flow (Figure 2-3(a)). The Alida (SCH6) FV calibrated in Scapa Flow and in open sea (Figure 2-3(b)). Whilst timing for calibration on board the FVs is opportunistic between fishing operations, calibration in open sea is not optimal.

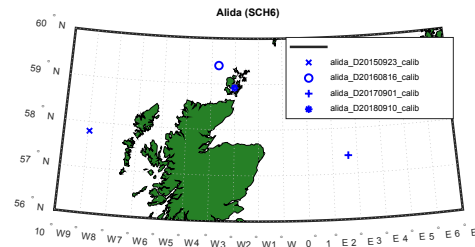
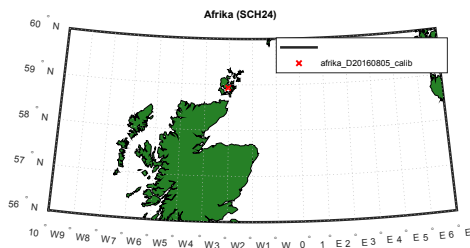
Table 2-2: overview of the calibration trials performed through the course of this project.

| date | data set size (GB) | Frequencies (kHz) | Sphere sizes (tungsten carbide, WC) | Non target channels set as passive |
|--------|--------------------|-------------------|-------------------------------------|------------------------------------|
| Alida | | | | |
| Sep/18 | 39 | 70/120/200 | 15 mm/22 mm/38.1 mm | yes |
| Sep/17 | 128 | 70/120/200 | 25 mm/38.1 mm | no |
| Aug/16 | 52.6 | 70/120/200 | 22 mm/25 mm/38.1 mm | no |

| | | | | |
|------------|------|------------|---------------------|-----|
| Sep/15 | 7.9 | 70/200/200 | 15 mm/22 mm/38.1 mm | no |
| Afrika | | | | |
| Aug/16 | 24.1 | 70/120/200 | 22 mm/25 mm/38.1 mm | no |
| Tridens II | | | | |
| Jun/19 | 60 | 70/120/200 | 22 mm/25 mm/38.1 mm | yes |
| Jun/18 | 18.4 | 70/120/200 | 15 mm/22 mm/38.1 mm | no |
| Jun/17 | 9 | 70/120/200 | 22 mm/25 mm/38.1 mm | no |
| Jun/16 | 90.1 | 70/120/200 | 22 mm/38.1 mm | no |
| Jun/15 | 20.4 | 70/120/200 | 22 mm/38.1 mm | no |

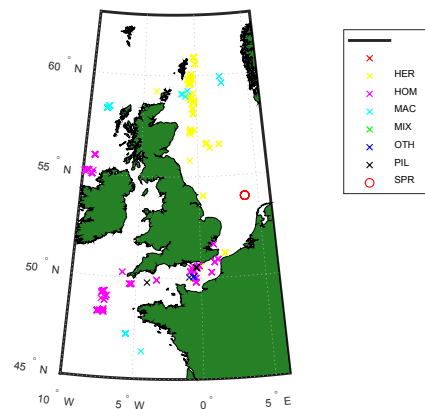
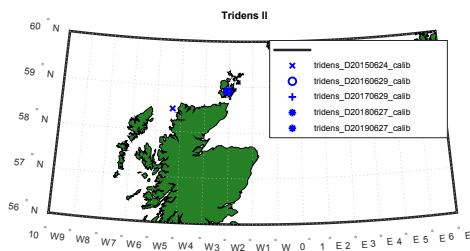
(a)

(b)



(c)

(d)



(e)

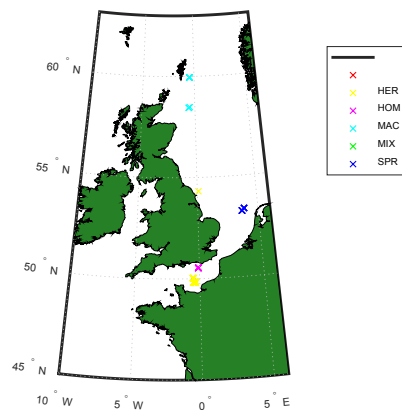


Figure 2-3: distribution of data collected in the realFishEcho project. (a) Location of calibration data sets (Table 2-2) for the Afrika (SCH24) FV. (b) Location of calibration data sets (Table 2-2) for the Alida (SCH6) FV. (c) Location of calibration data sets (Table 2-2) for RfV Tridens II. (d) and (e): Individually detected fish school for the different data sets (Table 2-3), separated by FV, Alida (SCH6) is shown in (d) and Afrika (SCH24) is shown in (e).

The routine acoustic data were collected across the North Sea, the English Channel and at the west and north of Ireland (Figure 2-3(a) for the Alida (SCH6) FV and Figure 2-3(b) for the Afrika (SCH24) FV). Collection of EK80 FM data is particularly challenging because of the amount of data generated (~1TB of data per day if recorded continuously). Though onboard automatic processing and reduction of data is possible, this functionality was not available at the time of the project. Consequently, the amount of data generated had to be managed by manual recording around fishing activities. The skippers of the respective vessels ensured that recording was only active during fishing operations. Specific user settings were prepared on each vessel. Omnidirectional SONARs (not synchronized with the EK80) were used during fishing operations and produced interference noise in specific frequency bands (see Section 5.2.2). This noise was managed at the post-processing stage (bad ping detection, see Section 4). Alongside acoustic data, species composition and fish length measurements were collected for each haul. The combination of biological data and acoustic data are used. Regular communication was kept with skippers via WhatsApp and TeamViewer for assistance.

A summary of the data collected through the course of this project together with data collected previously is shown in Table 2-3. Prior to December 2017, data collection was hampered by the running of two separate parallel data collection programs (realFishEcho and SEAT³ projects). From this date, arrangements were made so FV Alida (SCH6) focused on the collection of EK80 FM data (realFishEcho project) while FV Willem van der Zwan (SCH302) only collected EK80 CW data (SEAT project). FV Afrika (SCH24) only effectively started collecting EK80 FM data from September 2018. Prior to this date, this FV was conducting fishing in the west of Africa. The sizes of the different data sets were substantial and well correlated with biological data since December 2017. Each data set corresponds to a fishing trip for a given vessel. After each trip, the acoustic data collected are processed and filtered and each fish school is extracted. These acoustic traces are then associated with species if there is matching fishing activity with a composition of more than 95% of a single species. Using this species allocation to acoustic detections for all the data sets, one obtains the following for the most represented species:

- Herring: 218 schools correlated with biological samples. Of these, 16 schools have associated length measurements.
- Horse Mackerel: 266 schools correlated with biological samples. Of these, 138 schools have associated length measurements.
- Mackerel: 38 schools correlated with biological samples. Of these, 34 schools have associated length measurements.
- Sprat: 19 schools correlated with biological samples. Of these, 13 schools have associated length measurements.
- PIL: 7 schools correlated with biological samples. Of these, 7 schools have associated length measurements.

A summary per species for each vessel is given in Table 2-4. It is important to note that the number of detected schools for Mackerel is low but the total number of pings is high. This is because detected Mackerel schools have a much larger number of pings per schools. Contrarily, Herring, Horse Mackerel, Sprat and Sardine have a low number of pings per school. The proportion of data collected between the different species reflects the distribution of the fishing effort of the vessels involved in this project. For example, Sprat and Sardine are only targeted sparsely over a year. Consequently, data for Sprat and Sardine is limited. The impact of this low amount of data for adding either Sprat or Sardine as a species for the identification algorithms will be discussed in Section 6.

An overview of the length measurements for the different species is shown in Figure 2-4. For Herring, there is a spread across different sizes with a mode for the length distributions between 25 cm and 30 cm. For Horse Mackerel, most hauls sampled exemplify length frequency distributions with a mode at ~23 cm. There is also a lack of diversity in length classes for Mackerel (measured length frequencies with mode at 35 cm). Sprat and Sardine exemplify dominant length of 10 cm and 20 cm respectively.

³ SEAT: School Exploration and Analysis Tool. See: *Sustainovate 2017 Improved Selectivity of Small Pelagics iun the North Sea & North Atlantic Using SEAT*

Table 2-3: overview of the data collected through the course of the project.

| Acoustic data | | | Biological data | | | Matching acoustic/bio data |
|---------------------|--------------------|----------------------------|-----------------|--------------------------------------|---------------------|----------------------------|
| date | data set size (GB) | number of detected schools | length data | nb of hauls with length measurements | Species composition | |
| Alida | | | | | | |
| Feb/19 | 1500 | 104 | yes | TBD | HOM, MAC | 72 |
| Oct/18 | 1900 | 42 | yes | 43 | HOM, PIL, MAC | 33 |
| Sep/18 | 37 | 4 | yes | 4 | HER | 3 |
| Aug/18 | 1500 | 64 | yes | 81 | HER, MAC | 54 |
| Jul/18 | 1500 | 99 | yes | 26 | HER | 68 |
| Mar/18 | 1800 | 72 | yes | 34 | HOM, WBH, MAC | 12 |
| Jan/18 | 1160 | 98 | yes | 18 | HOM | 16 |
| Dec/17 | 2100 | 77 | yes | 16 | HOM, HER, SPR | 23 |
| Aug/17 | 44 | 3 | no | | HER | 0 |
| Oct/16 | 1210 | 52 | no | | HOM | 6 |
| Aug/16 | 1140 | 77 | no | | HER | 0 |
| Dec/14 | 40 | 12 | no | | MAC | 2 |
| Oct/14 | 67 | 18 | no | | HOM | 5 |
| Aug/14 | 77 | 15 | no | | HER | 3 |
| Afrika | | | | | | |
| Feb/19 | 1000 | TBD | yes | 38 | HOM, MAC | 5 |
| Dec/18 | 1000 | TBD | yes | 62 | HER, SPR | 56 |
| Oct/18 | 2800 | 196 | yes | 28 | MAC, HOM | 47 |
| Sep/18 | 205 | 15 | yes | 41 | HER | 2 |
| Dec/16 | 61 | 13 | no | | HER | 0 |
| Aug/16 | 83 | 26 | no | | HER | 0 |
| Willem van der Zwan | | | | | | |
| Sep/17 | 579 | 11 | no | | HER | 3 |

Table 2-4: summary of data collected by species.

| Alida | | | | | | |
|--------------------------------------|-------|-------|------|------|------|------|
| | HER | HOM | MAC | SPR | PIL | MIX |
| Number of schools | 174 | 200 | 23 | 6 | 7 | 11 |
| number of pixels (x10 ⁶) | 52 | 70 | 22 | 1 | 1 | 3 |
| number of pings | 24799 | 32440 | 3660 | 870 | 705 | 2204 |
| mean height | 20 | 13.2 | 34.6 | 15.3 | 17.6 | 12.3 |
| Afrika | | | | | | |
| | HER | HOM | MAC | SPR | PIL | MIX |
| Number of schools | 44 | 19 | 15 | 13 | 0 | 0 |
| number of pixels | 26 | 28 | 9 | 9 | | |
| number of pings | 10613 | 8636 | 2085 | 4043 | | |
| mean height | 17 | 18 | 35.6 | 11 | | |

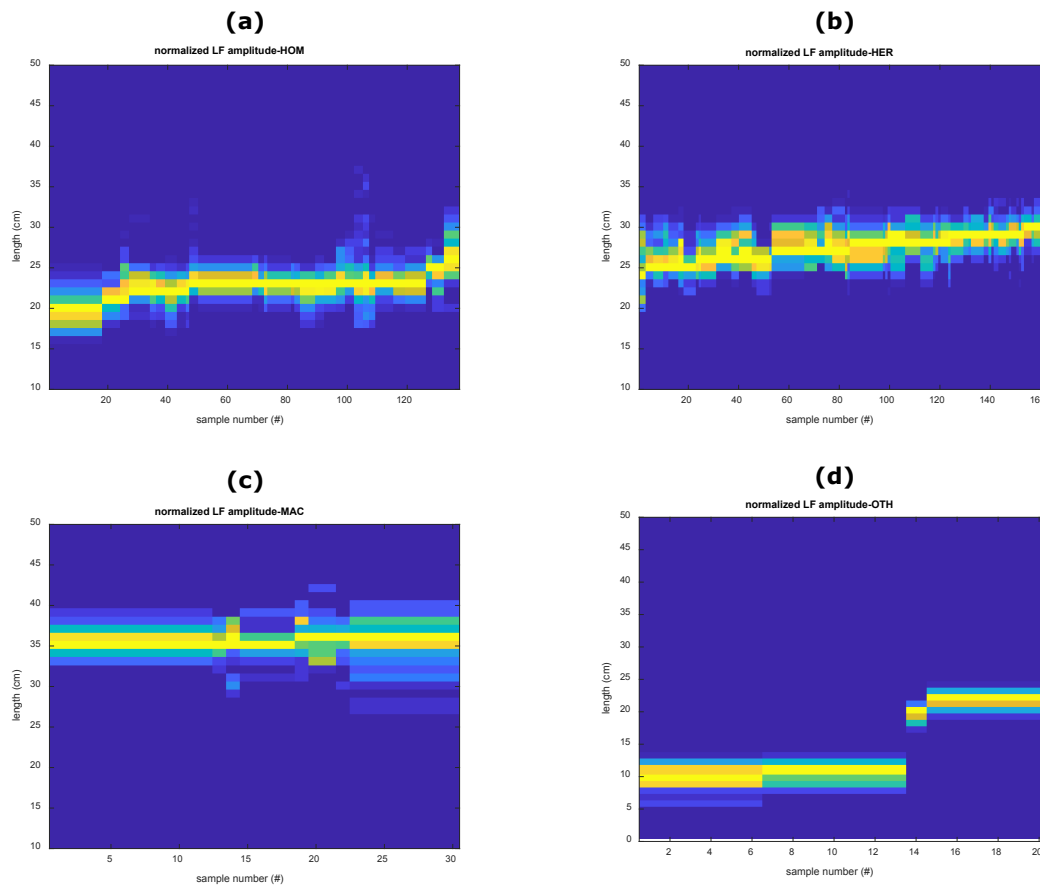


Figure 2-4: length measurements collected through the course of this project for the different species. The different length frequencies are normalized plotted together for comparison. The samples are sorted in ascending order. (a) Herring. (b) Horse Mackerel. (c) Mackerel. (d) Sprat and Sardine.

Until September 2018, acoustic data were recorded directly using the EK80 software. From September 2018 on board the FV Afrika (SCH24) and October 2018 on board the FV Alida (SCH6), the demonstrator software (ECHO software) was used as the main interface. The first version consisted of limited functionalities. Only echogram visualization and data recording features were enabled (the species identification was disabled). A full version of the ECHO software was then installed with real-time species identification features. For data recording, the ECHO software needs the EK80 software to continuously record data so stored files can be managed. A thorough description of the ECHO software is given in Section 4.2. Prior to the installation of the ECHO software, the collection of data using the EK80 software was challenging for the skippers because the EK80 echograms appear noisy and are not useable without data cleaning. They usually prefer the ES80 software. While data are optimized for display with the ES80 software, this is not the case for the EK80 software. However, though data collected using the EK80 software appears as more noisy, it contains more information because of the larger available bandwidth. This issue was solved with the ECHO software which allowed one to collect data with the EK80 software and display filtered data, alleviating the drawbacks of using the EK80.

2.2 Database

The total amount of data collected through the course of this project totalled 19 TB (Table 2-3). This is mostly due to the data richness from the EK80 FM. In comparison, data in CW mode generates ~20 times less space. Therefore, it is paramount to have a robust and consistent data management. Here, the data are managed as follows after each trip (Table 2-3):

1. Copying of the data on a separate HDD onboard the FV initiated few days prior to return to port.
2. Collecting HDD from the FV in port.
3. Processing of data using automatic routines and data pre-processing of ECHO software (see Section 4). This consists in data reduction and detection of bad pings and individual schools (Figure 2-5).

4. Manual scrutiny of detected schools, e.g. deleting false detections.
5. Format biological data (species composition, length frequency per haul per species).
6. Update database ground truth table (individual fish schools information and association with species composition and length frequency).

Following this process, each data set is saved in a specific hierarchical folder tree. An example is showed in Figure 2-6. Out of the acoustic processing, MATLAB workspaces with the data in a specific format (Figure 2-6, "Workspace" folder) together with echograms at each frequency (Figure 2-6, "Echograms" folder) are generated for each school. Calibration associated to the data set is stored in a specific location (Figure 2-6, "Calibration" folder). When computing the frequency response, schools are divided into cells. This is computed in a separate process and also stored in the corresponding database folder (Figure 2-6, "Results" folder). The biological data are stored after formatting and acoustic data processing in the "ground truth folder" (Figure 2-6). The biological data used here were collected through the PFA self-sampling program. Amongst Dutch freezer trawlers, this defines clear protocols for length measurements and data formatting [18], [19].

The biological data are used to associate species to each school matching the following criteria:

1. The fish school is within the timing of a fishing operation (shooting and hauling of the fishing net).
2. The haul contains more than 95% of a single species.

The species contained in the fish schools imaged through acoustics are not necessarily represented by the observed species composition in associated haul. This is because the fishing operation does not necessarily capture the entirety of the imaged fish schools (e.g. fishing occurs at selective depths). While matching with depth can be applied, the approach used here matches timing between the acoustic records and the fishing operations and uses a filtering to hauls with a monochromatic species composition (>95%). The latter ensures a strong relationship between the acoustic data and the species composition.

In order to have a selective access to the data, a summary table of the entire data base is updated after the inclusion of a new data set. This table contains high level information on each school for both acoustics (time, position, Sv at different frequencies, school length etc...) and biology (associated species, associated length frequency).

This data set format was also used to generate report for each trip. Though still under development, this feature is to be used in the future to provide a prompt and succinct feedback to the FVs. An example report for the data set collected by the Alida (SCH6) in December 2017 is given in Annex II.

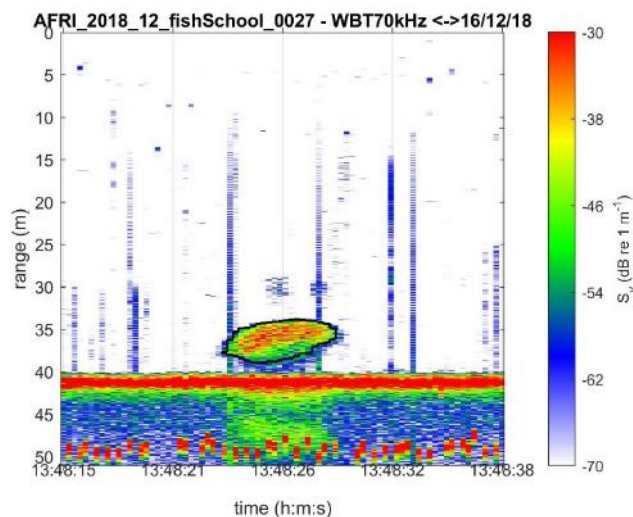


Figure 2-5: echogram example of reduced data. The data of the fish school is selected with 30 pings before and after the school and converted into a specific data format. The thick solid black represents the boundary of the school.

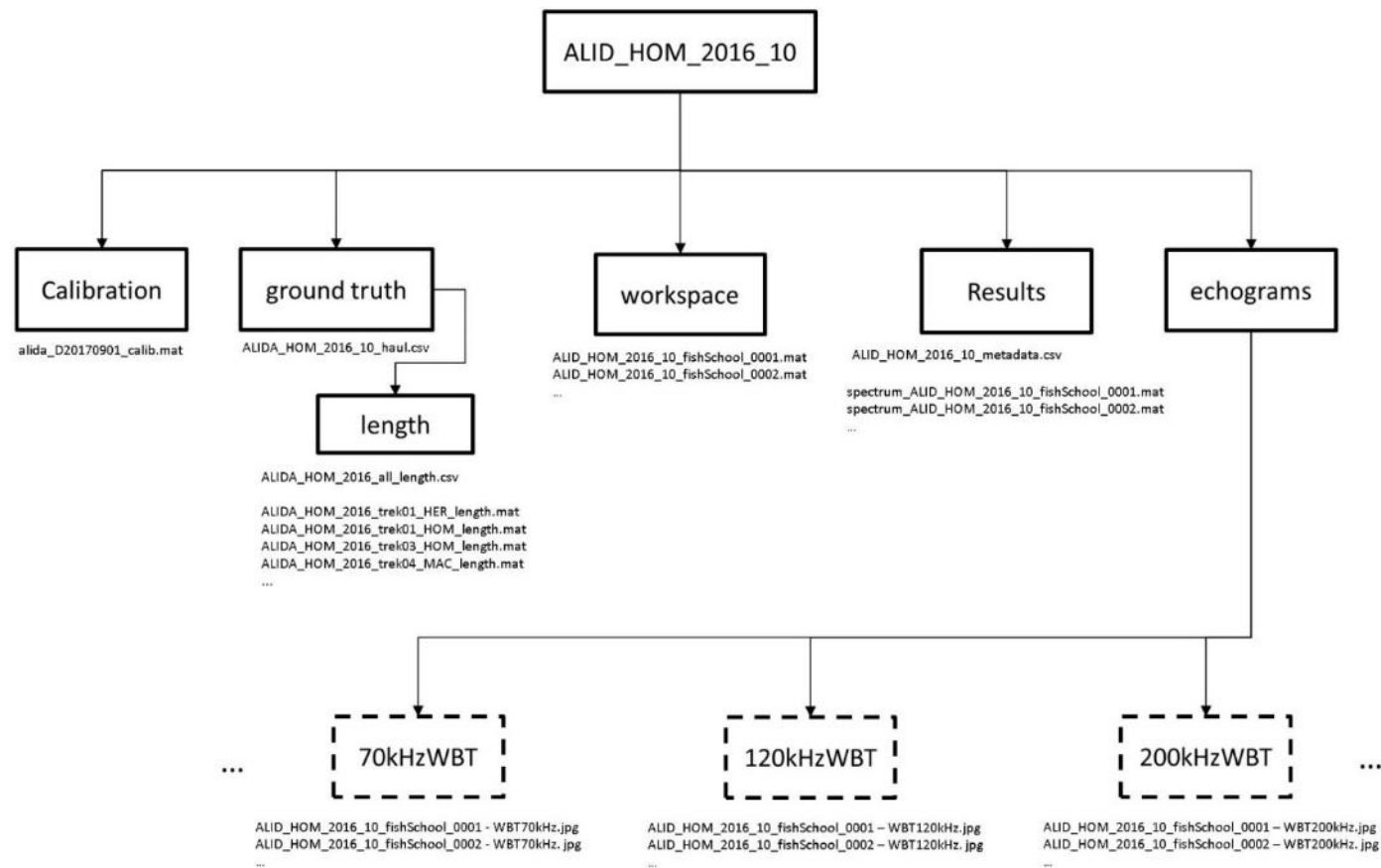


Figure 2-6: example organisational tree of a single data set. This data organisation is the basis for the analysis carried out in this project. A single data set is associated to each trip from each fishing vessel. Here, the data set ALID_HOM_2016_10 is exemplified and corresponds to the data collected by the Alida (SCH6) in October 2016 which mostly consisted in Horse Mackerel (HOM). After a semi-automatic processing and reduction of the raw data, only the data containing fish schools are retained. The data for the trip are then organised following the folder tree presented here which consists of: (1) the associated calibration set (2) the associated ground truth (catch composition and length frequency), (3) the acoustic data for each detected school, (4) the cell based spectra for each school and fish school metadata, (5) echogram for each school for each WBT channel (70 kHz, 120 kHz, 200 kHz).

3 Calibration

In this section, the work undertaken for the calibration of the echosounders on board the different vessels is presented. Calibration is an important step of the acoustic data collection process. It enables the echosounder to provide absolute acoustic measurements. This is paramount for the consistency of the data collected but also the consistency between different platforms (differences between echosounders and background conditions). Echosounder calibration has been very topical for the last 30 years and remains an important topic in the scientific community [14] in an effort to provide standardized procedures [13], [20]. The most commonly used procedure involves the use of standard spheres (known size and material properties). With such a target, the acoustic response at various frequencies can be calculated theoretically [21] and provide the base for the correction needed for each individual echosounder. The calibration procedure is generally performed in advance of the data collection, at least once per year.

Reliability of the species classification and size estimation algorithms depends on the accuracy of the calibration. While standard instruction procedures are provided by the echosounder manufacturers, experience and knowledge are needed when assessing the quality of the results. Furthermore, while procedures for narrowband systems have been refined for the last 30 years [13], [14], calibration procedures for broadband systems (e.g. EK80 FM) are still under development and require further and more elaborate efforts. In addition, calibration on board commercial vessels is more time consuming and can be particularly challenging for the crew who are not as familiar as scientists with these operations. However, the involvement of the crew is highly desired. On this point, some progress had been achieved by WMR in the last years with projects involving Dutch pelagic trawlers [10], [15], [17]. However, further progress is needed to make the fishing vessels fully autonomous in terms of data collection with adequate data quality, especially for the EK80 FM.

The calibration of the EK 80 FM is more complex than for narrow band echosounders (e.g. EK60, EK80 CW). The EK 80 FM provides active acoustic measurements across continuous large frequency bands. During the calibration, the challenge is to maintain accuracy and sensitivity over the entire frequency band rather than focusing on discrete frequencies. Calibration has been a straightforward task for the earlier generation echo sounders (narrowband, e.g. EK60, EK80 CW) because corrections for transducer gain and beam-pattern characteristics were needed only at one frequency per channel. However for a broadband system, one needs to cover the entire frequency range instead of discrete frequency points. In addition, the use of calibration spheres for the coverage of the full frequency range has one main drawback. The acoustic response from a given calibration sphere has regions of the spectrum that are not usable because the acoustic intensity is predicted to be infinitesimally small due to the phase cancellation. In practice, one is unable to infer calibration gains in these regions. Therefore, a combination of different calibration spheres is needed in order to cover the entire frequency range for a broadband system. Tungsten Carbide calibration spheres are used here.

3.1 Operational procedure

The calibration procedure employed here is the standard sphere method [13], [14]. This method is most commonly used during acoustic surveys where a high precision calibration is needed. It consists on placing a sphere of known size and material in front of the echosounder to be calibrated. The system can then be calibrated against the theoretical response of the sphere. The EK80 software has a specific interface for calibration using the standard spheres method.

The operational procedure is thoroughly described in a dedicated calibration manual (Annex III). It was devised so the crew from the FVs could be autonomous with performing a calibration. This is advantageous as time windows on board the FVs for calibration is limited due to tight fishing activities planning. The procedure consists of several main operations: (1) attaching one or several spheres to

different points on the vessel's deck using fishing lines, (2) placing the spheres under the vessel, (3) moving the spheres under the vessel using the fishing lines (either manually or using automated systems). While several spheres are usually placed in the water at the same time, the calibration of each frequency channel is done against a specific sphere.

Once the targeted sphere is centred below a given transducer, the calibration operation starts for each WBT channel. The calibration for a specific WBT channel covers the whole frequency band of this WBT channel. A typical echogram is shown in Figure 3-1(a) where the echo trace from two calibration spheres can be observed. Once the calibration procedure starts, one uses the interface shown in Figure 3-1(b). From this display, the state and quality of the calibration can be monitored. The calibration is complete once the calibration sphere has been detected several times in all the different beam sectors, providing a good enough spatial coverage. Each sphere detection is compared against the theoretical response. While the combination of all these detections provides calibration values, the measurement uncertainty is given by the corresponding standard deviation. Depending on weather conditions, this operation can last from 20 minutes to several hour. This procedure is repeated for each WBT channel. The resulting calibration for each WBT channel consist on a frequency dependent gain offsets and frequency dependent beam patterns. The quality of the calibration can be assessed with the EK80 software (coverage, error estimation). When these are applied, the calibrated system is able to provide absolute measurements. In practice, if the calibration is of good quality it allows comparison between different EK80 systems installed on different vessels.

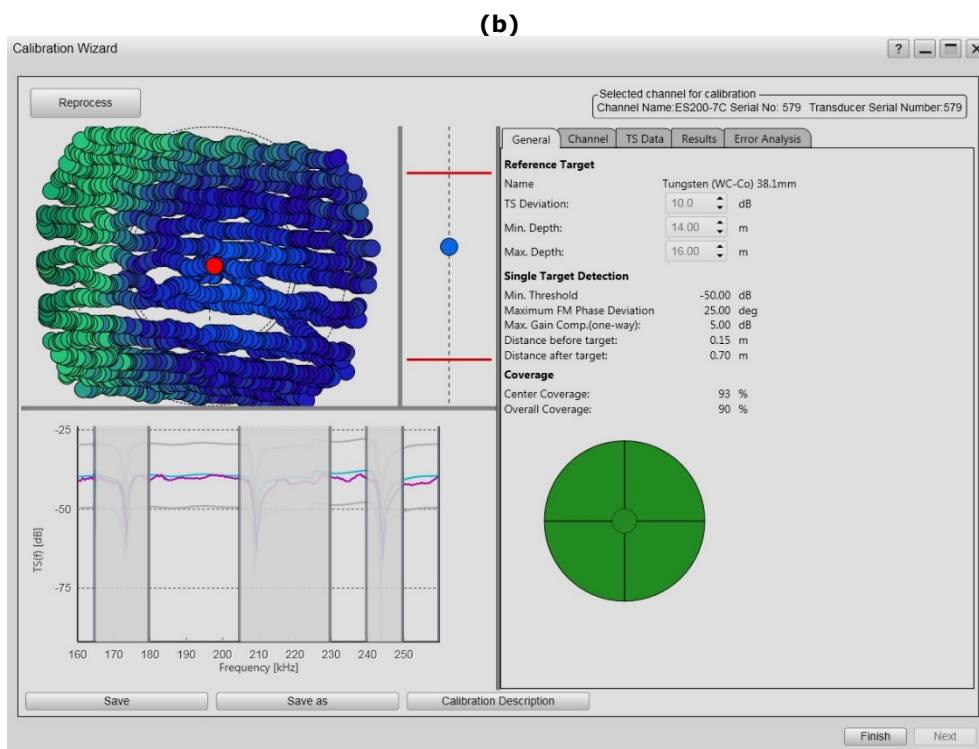
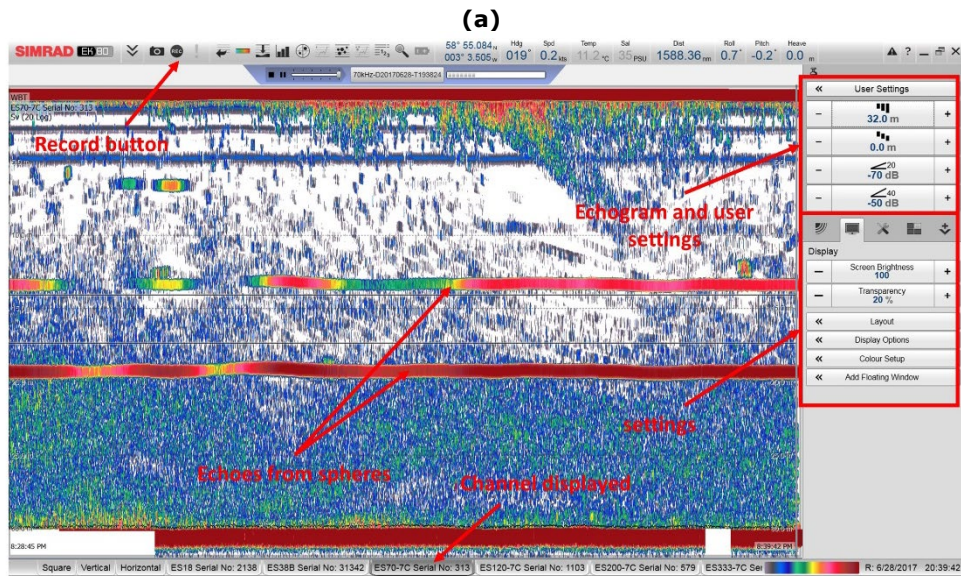


Figure 3-1: (a) echogram display after deployment of the calibration spheres. (b) EK80 interface used for calibration.

3.2 Data processing

The data collected through the calibration procedure consist of two types of files: raw acoustic records and an output calibration file (*.xml, direct output from the EK80 software). While the EK80 software provides calibration outputs, MATLAB code was developed in order to revisit the raw calibration files. This software was developed because:

- While the EK80 software produces calibration outputs, one cannot control the processing and the calculation of calibration gains. Because the calibration operation is paramount for cross vessel application of the identification algorithms, it is important to be able to optimize and investigate in depth the processing of the data.
- The EK80 calibration output (*.xml files) only contains limited information on the calibration trial and therefore limits the analysis.
- The current EK80 software is unable to read past data (2015 calibration data collected by the Alida (SCH6)).

- It is likely that the EK80 calibration software will be updated in the future which may make it impossible to apply classifiers to data sets calibrated in different ways.

In practice, several calibration spheres are suspended in the water but the EK80 calibration software tracks the location and data acquisition of a single sphere in the water column. This is done through the processing of sphere detection in a specified depth interval. While other spheres in the water are not being focused on during this procedure, the raw data can be revisited in order to derive additional calibration gains. The final results of a calibration trial then consists of gains at frequencies computed for each sphere for each EK80 FM channel (i.e. frequency). Because the gains are computed over a large frequency band, some regions of the spectrum are not useable because of dips in the spectrum. These dips are specific to each sphere size. This is exemplified in Figure 3-2 where calibration gains can be inferred in the green while red regions are not useable. The number of dips increases with frequency. The larger the size the more dip regions are present from a lower frequency. For frequencies within the dip regions, gain can be calculated through interpolation or tentatively by combining different spheres (combine different workable frequency regions).

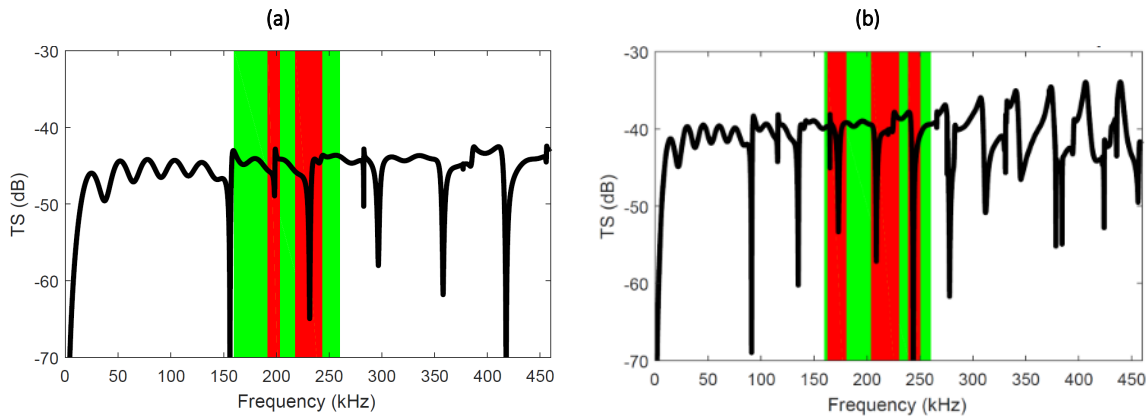


Figure 3-2: theoretical target strength (TS) vs frequency. This analytically inferred TS is used to compare measurements of the EK80 FM against and in turn determine calibration gains at different frequencies. The solid black line is the theoretical target strength. The shaded area represents the working range of the EK80 FM 120 kHz channel. The subsequent green and red areas are the useable and non-useable frequency ranges for calibration respectively. (a) 22 mm WC calibration sphere. (b) 38.1 mm WC calibration sphere.

An initial depth interval around the sphere is setup. The uncompensated target strength equation used here is similar to those from narrowband systems [22]–[24]:

$$TS_{\text{uncomp}}(f) = 10 \times \log_{10}(p_{rx}(f)) + 40 \times \log_{10}(r_{\text{target}}) + 2 \times \alpha(f) \times r_{\text{target}} - 10 \times \log_{10}\left(\frac{t_x \times \lambda^2}{16\pi^2}\right) - 2G_f, \quad \text{Equation 3-1}$$

with r_{target} the range of the target, $\alpha(f)$ the frequency dependent absorption loss calculated using [25], [26], t_x the transmit power, λ the wavelength ($\lambda = 2 \times \pi \times f$) and G_f the calibration gain. The quantity $p_{rx}(f)$ is the received power expressed as:

$$p_{rx}(f) = \left(\frac{|y_r(f)/y_t(f)|}{4}\right)^2 \times \left(\frac{|R_{tx} + Z_{trd}|}{R_{rx}}\right)^2 \times \frac{1}{|Z_{trd}'|}, \quad \text{Equation 3-2}$$

with R_{tx} and R_{rx} the internal resistance of the transceiver in transmission and reception respectively, Z_{trd} the complex transducer impedance, y_r the fft of the matched filtered beamformed signal and $y_t(f)$ the fft of the matched filtered input signal replica. Both time signals are filtered using a hanning window prior to the fft. The received signal that undergoes the fft is selected as follows:

- The maximum within the selected window for sphere detection is defined as the sphere detection
- A window is applied to select the signal that is further processed with the fft. The window is defined by its length in m but also the proportion of the signal prior and after the sphere detection.

This processing is exemplified in Figure 3-3. The uncompensated target strength calculated is therefore representative of a short window around the sphere detection.

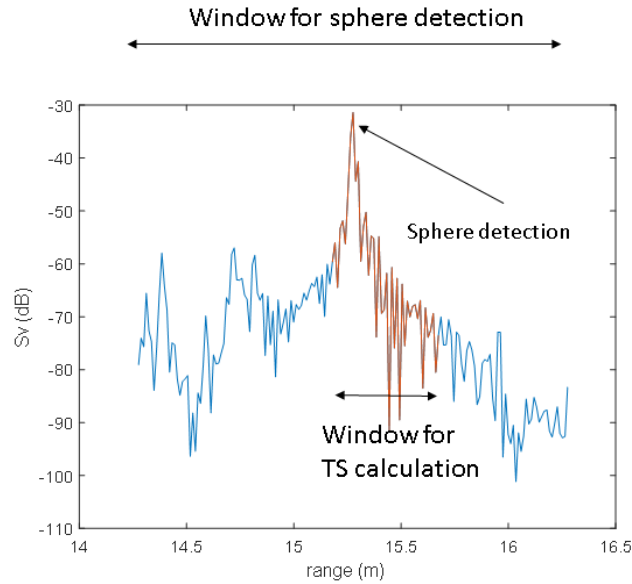


Figure 3-3: S_v time series example around a calibration sphere, exemplifying the different time windows used for sphere detection and TS calculation.

After the calculation of the uncompensated target strength $TS_{\text{uncomp}}(f)$, the target strength is compensated for the target position in the beam:

$$TS_{\text{comp}} = TS_{\text{uncomp}} + C(f, a, b). \quad \text{Equation 3-3}$$

The quantity $C(f, a, b)$ is the beam compensation function as a function of frequency and alongside and athwart side angles. This function is based on the LOBE algorithm employed by Simrad. The gain is then calculated as:

$$G_{f_{\text{new}}} = \frac{(TS_{\text{comp}} - TS_{\text{th}})}{2} + G_f, \quad \text{Equation 3-4}$$

with TS_{th} the theoretical target strength of the targeted sphere. The gain calculation is only performed and stored if the following detection criteria are met:

- The prominence of the peak of the sphere detection within the window for TS calculation is higher than a set threshold
- The signal to noise ratio (SNR) is higher than a set threshold. The signal to noise ratio is computed as the ratio of acoustic power between the window for sphere detection and the window for TS calculation (Figure 3-4(a))
- The mean compensation factor $C(f, a, b)$ is below a set threshold
- The compensated TS is within upper and lower bounds offsets from the theoretical TS (Figure 3-4(b))

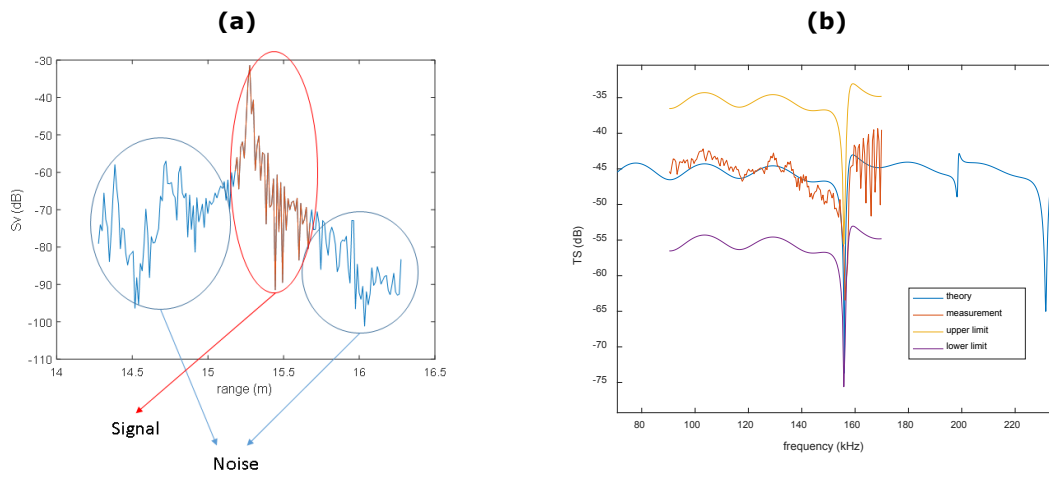


Figure 3-4: working examples of criteria used for calibration sphere detection. (a) SNR is calculated as the ratio of acoustic power between the window for sphere detection and the window for TS calculation. (b) Only the detection with compensated TS is within upper and lower bounds offsets from the theoretical TS is considered a successful detection.

If the detection criteria are met, the location of the sphere is updated. If not, the sphere location remains the same. This way the sphere is tracked across the pings. This process is automatized so the calibration processing can be performed in batch. An overview of the processing workflow is shown in Figure 3-5.

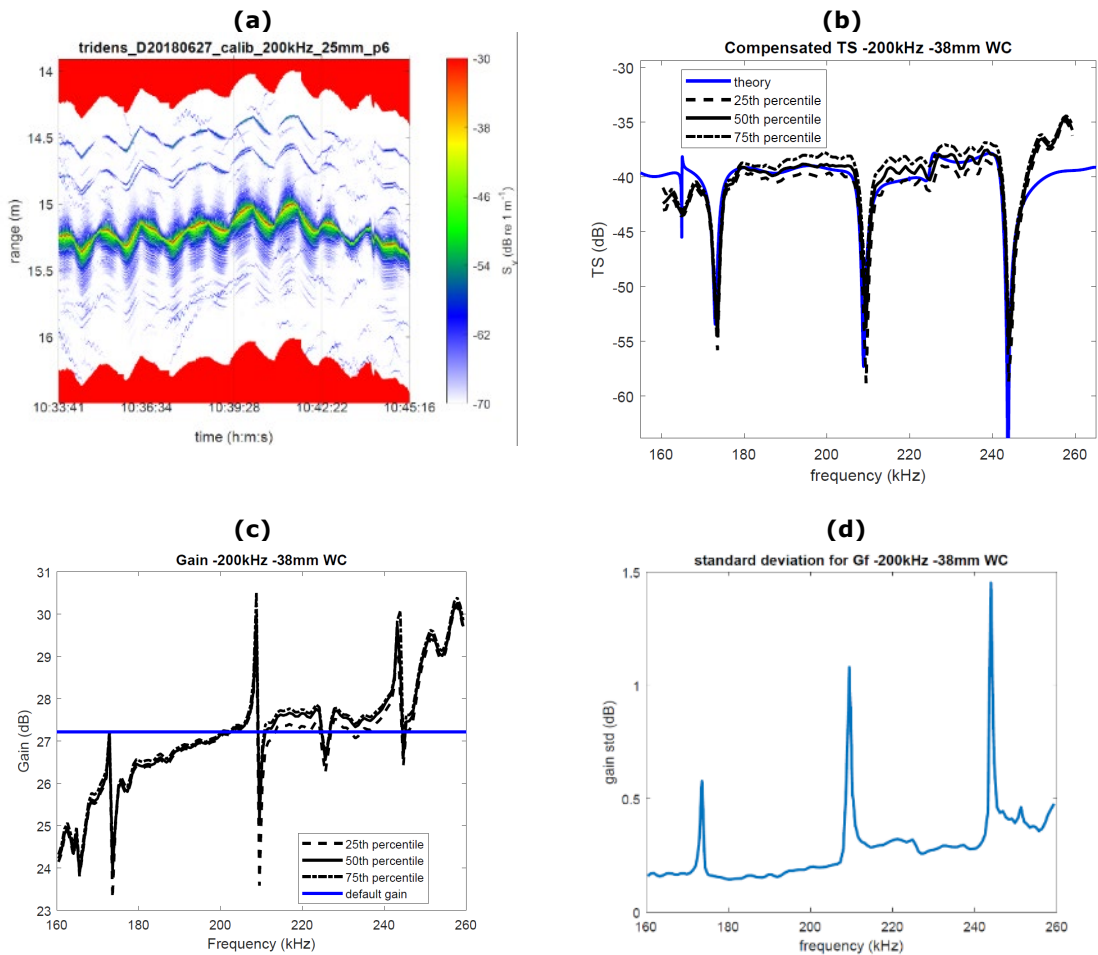


Figure 3-5: calibration processing workflow. Reading each raw files, the targeted calibration sphere is tracked through the pings (a). For each detection, target strength can be calculated and compared to the theoretical target strength (b). The difference in level is effectively the gain (c). It is important to note that outside dip regions the gain values are erroneous and are therefore not used. These are shown here as an examples In the null regions, the gain is interpolated. The different detections allow one to assess the accuracy of the calibration exercise. The accuracy is commonly expressed as the standard deviation in gain, estimated from gains estimated from every single detections (d).

3.3 Results

Calibration outputs consist of the gain and measurement error (standard deviation in gain). The gain corresponds to the offset that needs to be applied to the data so the echosounder provides absolute measurements. This quantity is specific to each EK80 system installation (combination of transducer and transceiver). The standard deviation gain is calculated using the gain obtained from each single sphere detection and it provides an estimate of the accuracy of the results. Data exemplifying a large spread between the results from the different detections is associated with large standard deviation values. It is desirable to reduce the standard deviation as much as possible. In CW mode, the gain and standard deviation consist of a single values while in FM mode, these are frequency dependent.

For narrow band systems (and therefore EK80 in CW mode), the at sea calibration is well established with decades of research and acoustic surveys on the different generation of simrad echosounder (EK500, EK60, EK80). Several studies showed that these systems produce similar measurements [27]–[31]. At sea practice of calibration exemplifying limited deviation gain. For example, historical calibration from Tridens II from EK60 and EK80 CW systems is shown in Figure 3-6. It can be observed that the gain remains stable. The drop of ~ 2 dB for the EK80 CW in March and June 2018 corresponds to a malfunction of the transceiver that was replaced in June 2019. Standard deviation typically does not exceed 0.3 dB and calibration with an rms error value exceeding 0.5 B is usually repeated.

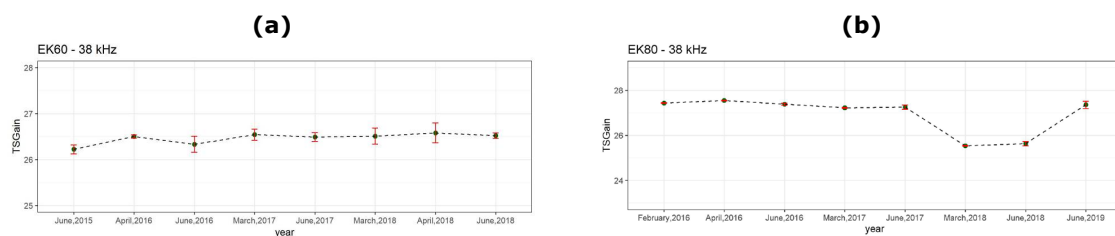


Figure 3-6: historical calibration gain for the narrow band echosounders EK60 and EK80 CW onboard Tridens II. The drop of ~ 2 dB for the EK80 CW in March and June 2018 corresponds to a malfunction of the transceiver that was replaced in June 2019.

In contrast, while calibration of broadband active acoustic systems is common both at sea and in water tanks [32]–[34], experience with routine at sea calibration of systems such as the EK80 FM is lacking. This is mainly due to the difficulty in using these systems for acoustic survey purposes (large data size, processing handling). For this study, it is therefore important to have a baseline for comparison prior to the analysis of the calibration data collected onboard FVs. To that purpose, calibration data from RFV Tridens II are analysed. These are high quality data and provide robust assessment for the subsequent analysis of FVs calibration data.

It is important to note that discrepancies in calibration gains were often observed when using the EK80 software, especially at the 120 kHz and 200 kHz WBT channels (Figure 3-7). This type of discrepancy motivated the development of MATLAB routine in order to investigate in depth the sources of error.

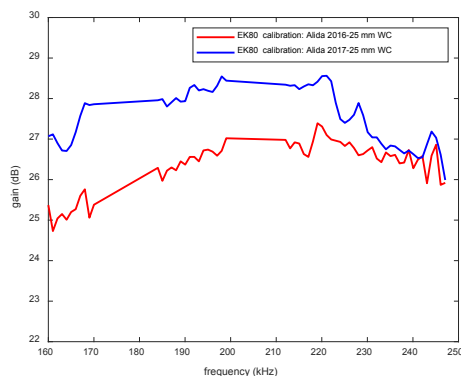


Figure 3-7: example of discrepancies in calibration gains after the processing of the data using the EK80 calibration software. The blue line is the calibration on the 25 mm WC sphere in 2016. The red line is the calibration on the 25 mm WC sphere in 2017.

3.3.1 Baseline analysis of Tridens II calibration data

The RFV Tridens II is used yearly for different type of scientific surveys, among which acoustic surveys. Prior to each acoustic surveys, the EK80 onboard the vessel is calibrated in CW mode. Also, during the herring acoustic survey (HERAS, [35]), the EK80 is usually further calibrated in FM mode in Scapa flow (Scotland ~30 m depth). The Scapa flow site is advantageous for calibration because it is a sheltered area, providing low background noise level conditions. Table 2-2 gives an overview of the EK80 FM calibration data collected during this survey since 2015. Because Tridens II is used for scientific purposes, the quality of the data collected is higher and provide a strong basis for the assessment of at sea sphere calibration. Here, these data are used as a baseline to assess:

- The best calibration settings to be used for the analysis of fishing vessel calibration
- The variation of the calibration outputs against different parameters: sphere type, frequency, background noise
- The variation of the calibration outputs between the different years.

The analysis presented here is divided into two sections. First, the data on 26th and 27th June 2019 are analysed. The data collected since 2015 are then compared.

3.3.1.1 At sea calibration variability

In June 2019 the calibration outputs from different spheres in different setups were investigated (four setups,

Table 3-1). The different setups were chosen in order to investigate:

- The influence of different calibration spheres: 38. 1 mm WC; 25 mm WC; 25 mm WC 3 attachment points; 22 mm WC; 22 mm WC 3 attachment points. It is important to note that for the two 22 mm WC spheres investigated, only data at 200 kHz were collected.
- The influence of different sphere setups, particularly whether having several spheres in the water is influential.

Photographs of the different spheres used are shown in Figure 3-8. For the 25 mm WC and 22 mm WC, two attachment setups were used:

- the one commonly used with a single monofilament glued at the top of the calibration sphere. This filament is attached to a single line further attached to four lines connected to winches.
- a three monofilament attachment. One filament is attached to a weight downward while each of the two other filaments is connected to two lines connected to the winches on port and starboard.

Setup 2 was specifically used to investigate the effect of having a filament attached to the sphere in the centre line. With a three monofilament attachment setup, the centre line of the sphere is free of disturbance.

Table 3-1: summary of the various setup investigated using calibration data collected onboard Tridens II RFV in June 2019.

| channel | target sphere | setup in water |
|------------|-------------------|--|
| 70/120/200 | 38.1 mm WC | Setup 1: 38.1 mm WC/63 mm Co |
| 70/120/200 | 25 mm WC 3 points | Setup 2: 25 mm WC 3 points/25 mm WC |
| 70/120/200 | 25 mm WC | Setup 2: 25 mm WC 3 points/25 mm WC |
| 70/120/200 | 25 mm WC | Setup 3: 25 mm WC |
| 200 | 22 mm WC 3 points | Setup 4: 22 mm WC 3 points/22 mm WC |
| 200 | 22 mm WC | Setup 4: 22 mm WC 3 points/22 mm WC |

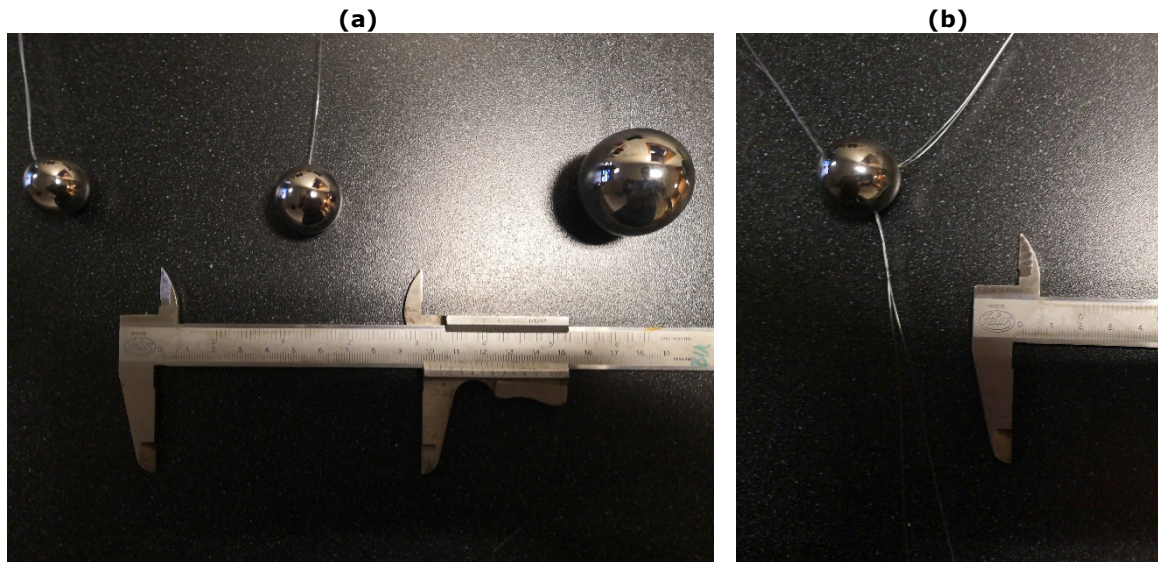


Figure 3-8: calibration spheres used during the calibration trial. (a) single attachment point calibration spheres used in the experiment (22 mm WC, 25 mm WC, 38.1 mm WC). (b) example of a three attachment points calibration spheres (25 mm WC displayed here though a 22 mm WC sphere with three attachment points was also used).

The collection of the data was done using the EK80 calibration software, as described in Section 3.1. The data were further analysed following the procedure given in Section 3.2. The settings are as follows:

- Proportion of signal prior and after sphere detection: 50%/50%
- Window for TS calculation: 0.5 m
- peak prominence: 10
- SNR threshold: 10 dB
- Mean compensation threshold: 2 dB
- TS deviation: 10 dB

The results for the different setups (Table 3-1) are shown in Figure 3-9 (calibration gain and standard deviation of the different frequency channels). Associated SNR levels (Figure 3-4(a)) are presented in Figure 3-10 as boxplot. These are indicative of noise levels around the sphere. High noise level is detrimental for the accurate calculation of TS. Variation in noise is mainly due to changing conditions in the water column (particles in the water) or slight differences in setup (e.g. nodes connecting the different lines).

For the 70 kHz channel (45 kHz to 90 kHz), despite varying level in standard deviation (Figure 3-9(b)), the calibration gain between the different spheres and setups is consistent. The gain between the 25 mm WC spheres (red, black and blue solid lines) is within 0.1 dB and a larger offset can be observed between the 25 mm WC spheres and the 38.1 mm WC sphere (up to 0.5 dB at 90 kHz). The associated measurements have varying noise levels (Figure 3-10(a)) with the data for the 38.1 mm sphere exemplifying the highest SNR and lowest standard deviation (Figure 3-9(b)).

Compared to the 70 kHz calibration, the discrepancies are larger for the 120 kHz channel. The two 25 mm WC spheres deployed during setup 2 present similar calibration gain (within 0.15 dB), standard deviation and SNR (Figure 3-9 and Figure 3-10(b)). In contrast, the 25 mm WC sphere from setup 3 (single calibration sphere in the water) deviates in gain by up to 0.9 dB compared to its deployment for

setup 2. This could be explained by the somewhat lower SNR associated with higher standard deviation. In time domain, the response of a calibration sphere consists of a strong first return (acoustic wave from front interface) and returns from subsequent modes (circumferential waves) [6], [36]. Though the front interface is high and unlikely to be influenced unless SNR is very low, circumferential waves have a much smaller amplitude and a decrease in SNR can be influential. Though the decrease in SNR between the two 25 mm WC spheres observed in Figure 3-10(b) ("25 mm WC" and "25 mm WC single") is limited (2 dB), it could have an influence on low amplitude circumferential waves and then affect the overall gain and standard deviation. Despite having the highest SNR, the calibration based on the 38.1 mm WC sphere exemplifies the highest standard deviation and large deviation in gain compared to other spheres (1 dB at 150 kHz). This suggest that high standard deviation is not necessarily associated with low SNR.

For the 200 kHz, the differences between the setups and spheres are very important (Figure 3-9 and Figure 3-10(c)). Excluding the 38.1 mm WC sphere, the lowest standard deviation levels are associated with highest SNRs (blue, pink and black solid lines in Figure 3-9(b)). Using the same 25 mm WC sphere in two different setups leads to very different results in term of gain and standard deviation (black and red solid lines in Figure 3-9). The difference in gain is particularly important (2.4 dB at 230 kHz). The main reason for this discrepancy seems to be the lower SNR for the 25 mm WC in setup 3. Also, similar deviation in gain is observed between the two 22 mm WC spheres in setup 4 (pink and yellow solid lines in Figure 3-9). A drop in SNR could also be a strong factor for this discrepancy. Similarly to the results from the 120 kHz channel, though the drop in SNR is limited, it could be influential for circumferential waves, then affecting the overall frequency response and standard deviation between measurements. Contrarily, despite having the highest SNR, the 38.1 mm WC sphere exemplifies a very high standard deviation and deviates substantially compared to the lowest standard deviation measurements from other spheres (25 mm WC spheres of setup 2, 3 points 22 mm WC sphere from setup 4). Though miss match in sphere properties for the different calculations can explain variation between spheres, the comparison of the same 25 mm WC sphere in different setups (red and black solid lines Figure 3-9) shows that it cannot be the only explanatory variable.

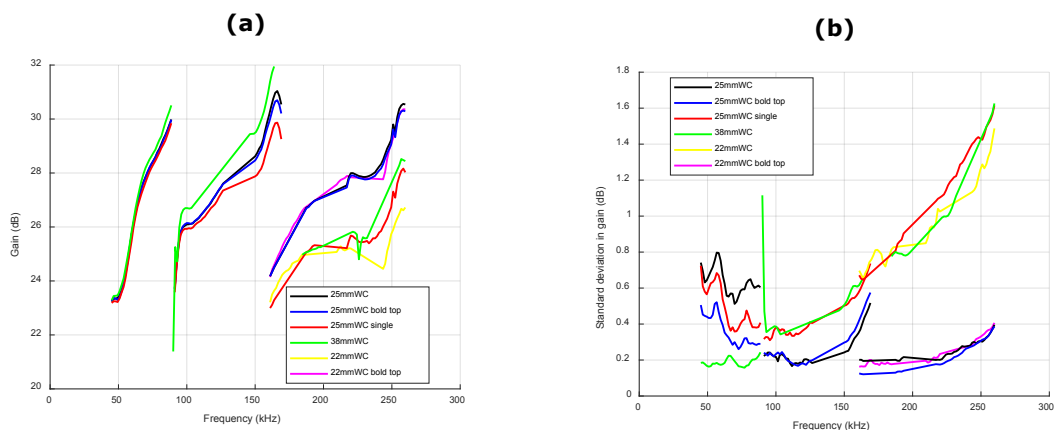


Figure 3-9: gain and standard deviation for the different setups used (Table 3-1). Spheres labelled as "bold top" are those with a 3 monofilament attachment, allowing the top of the sphere to be free when setup in the water. The sphere labelled as "25 mm WC single" corresponds to the case of the 25 mm WC sphere without other sphere in the water.

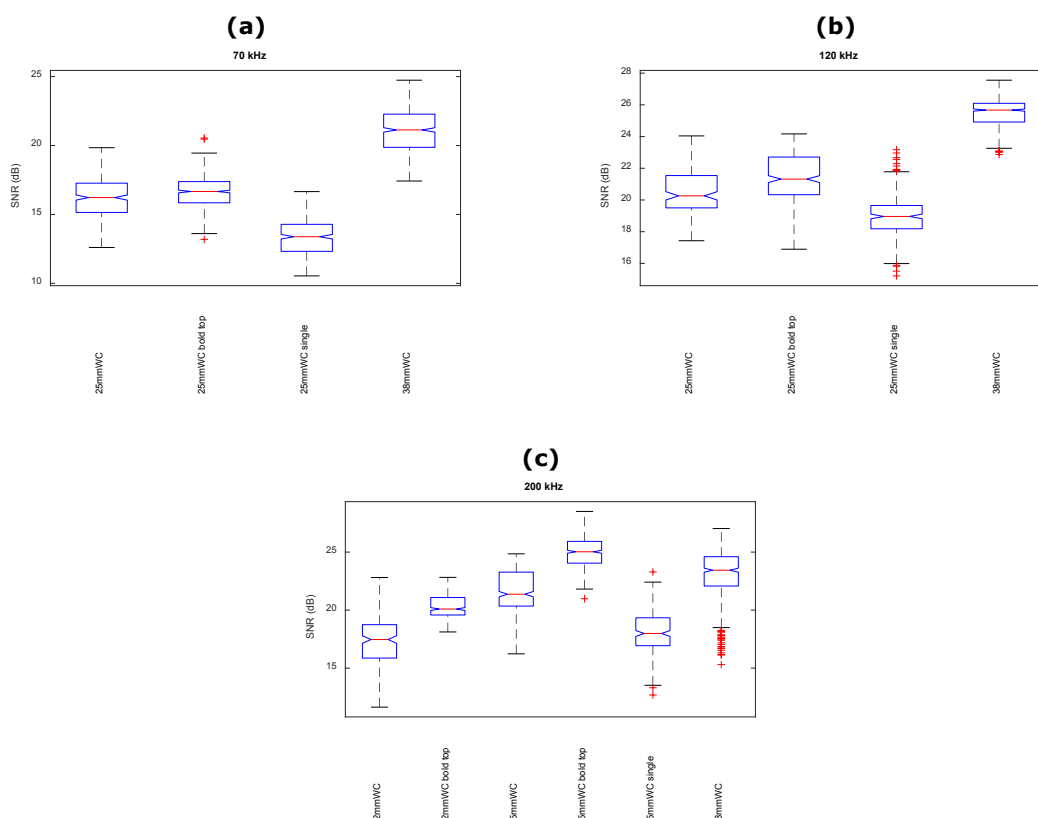


Figure 3-10: boxplot of the signal to noise ratio of selected pings for the different data sets investigated here. (a) 70 kHz WBT channel. (b) 120 kHz WBT channel. (c) 200 kHz WBT channel.

The results from this experiment suggests that:

- Calibration is overall consistent between the data sets for the 70 kHz channel.
- Calibration gain is very sensitive to SNR for the 120 kHz and 200 kHz channels. This is exemplified by changing calibration gains obtained using the same sphere but under different SNR conditions.
- The 38.1 mm WC calibration sphere has very low performance for the 120 kHz and 200 kHz channels. At these frequencies, the standard deviation in gain is high under high SNR.

The trends observed here would need to be investigated further through a combination of measurements in a water tank and at sea.

3.3.1.2 Inter-annual variability of at sea calibration

As shown in Table 2-2, RFV Tridens II was calibrated every year since 2015. While Section 3.3.1.1 investigated the variability within a given data set, the inter-annual variability is the focus of this section.

It is important to note that the settings between each set of measurements differs in pulse length and ramping. The different settings for each set of data is provided in Table I.1 in Annex I. Though a set of different settings induces a different calibration gain, the change is expected to be limited. Data that have similar settings to those used for the data collection (Table 2-1) are the 2017 and 2019 data sets.

The resulting calibration gain for the different data sets are shown in Figure 3-11(a), (c) and (e) for the different frequency channels. Similarly to what was observed in Section 3.3.1.1, the calibration gain is most sensitive at the highest frequency channels (120 kHz and 200 kHz, Figure 3-11(c) and (e)) and most consistent at 70 kHz (Figure 3-11(a)). The 120 kHz channel exemplifies outliers gain with: the calibration against the 38.1 mm WC from 2016 and 2019 (Figure 3-11(c)). The other seven calibration gains are relatively similar in trend and level. For the 200 kHz channel, a large discrepancy was observed between the 25 mm WC sphere and both the 22 mm WC and 38.1 mm WC spheres in the previous section (Figure 3-9(a)). This is confirmed with the comparison with data sets from previous years (Figure 3-11 (e)). Compared to other data sets, the data from 2019 for the 22 mm WC and 38.1 mm WC spheres have a suspiciously low calibration gain (~2.5 dB difference with other data sets). However, if these data are omitted, the differences in calibration gain between the data sets remain substantial (in the order of 0.5-1 dB).

In order to investigate the effect of SNR further, the average deviation of measured compensated TS from the theoretical TS. It is plotted for each frequency channel in Figure 3-11(b), (d) and (f). It is important to note that the TS deviation from the theory is dependent on spheres type and vessel. However, an average deviation higher than ± 2 dB is somewhat high. For 70 kHz (Figure 3-11(b)), the consistency between inferred calibration gains is confirmed with relatively low dispersion in TS deviation between the different measurements. For 120 kHz and 200 kHz (Figure 3-11(e) and (f)), outliers in term of TS deviation can be observed: (1) 38.1 mm WC from 2016 for 120 kHz, (2) 38.1 mm WC and 22 mm WC from 2019 for 200 kHz. These correspond to the erroneous calibration gains observed in Figure 3-11(c) and (e). Though SNR levels for these measurements are relatively low, they are not the lowest in the series of measurements. This suggest that SNR is affecting the quality of the calibration but is not the only explanatory factor.

In conclusion, the comparison of the different calibration data sets from the RFV Tridens II shows high variability for the high WBT frequency channels (120 kHz and 200 kHz). This is similar to what is presented in Section 3.3.1.1, i.e. variability between different calibration sets.

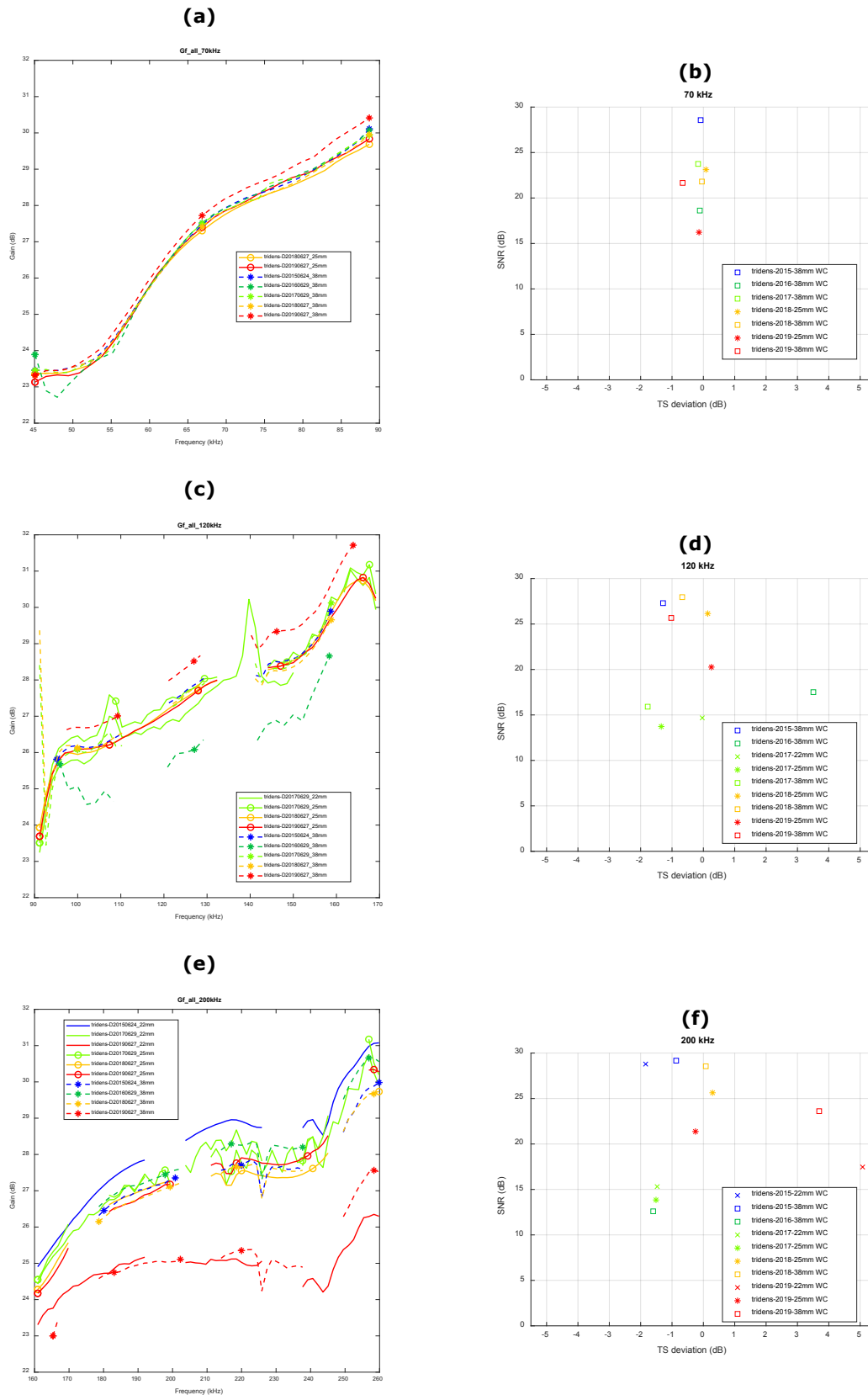


Figure 3-11: comparison of calibration outputs computed from calibration data collected by Tridens II between 2015 and 2019. (a) calibration gains at 70 kHz channel. (c) calibration gains at 120 kHz channel. (e) calibration gains at 200 kHz channel. For each plot, the difference in marker and line type is associated with different sphere types while the differences in colour is associated with different years (i.e. different data sets). The different data sets presented here are: 2015 (blue colour), 2016 (dark green colour), 2017 (bright green colour), 2018 (yellow colour), 2019 (red colour). The different spheres are: 22 mm WC (solid lines), 25 mm WC (solid lines with circle markers), 38.1 mm WC (dashed lines with star markers). Data sets with settings as those listed in Table 2-1 are 2017 and 2019. (b) (d) (f): deviation from theoretical TS (TS error) against Signal to Noise Ratio (SNR) for the different combinations of year, frequencies and sphere type.

3.3.2 Analysis of inter-annual calibration data from fishing vessels

The Willem van der Zwan (SCH302) FV only collected a limited amount of data (Table 2-3) and did not perform any calibration of the EK80 FM. The Alida (SCH6) FV performed four calibrations since 2015 and the Afrika (SCH24) FV only performed a calibration in 2016 (Table 2-2). The differences between the different calibration sets is investigated here. The subsequent settings for each trial is given in Annex I (Table I.1). It is important to note that there are differences between settings (e.g. 1.024 and 2.048 pulse lengths depending on the data set). This can generate discrepancies between the results of different data sets though these changes should remain limited. Only the data collected on board the Alida (SCH6) FV in September 2017 and September 2018 comply to the settings used for data collection (Table 2-1). The reason for differences in EK80 FM settings is miscommunication with skippers and lack of directions. To remedy this point, a calibration manual with instructions was created (Annex III).

First, data with correct EK80 FM settings (Table 2-1) are investigated (2017 and 2018 calibration data collected by the Alida (SCH6) FV). The sphere targeted for these calibrations was the 38.1 mm WC. The comparison of the frequency dependent calibration gains is shown in Figure 3-12(a). Discrepancies can be observed, especially for the 200 kHz channel. For this channel, the differences in Signal to Noise Ratio (SNR) is substantial (Figure 3-12(b)) with a decrease in mean level of 15 dB for the 2017 data set. As an example, Figure 3-12(c) shows the compensated TS frequency response for two individual target detections positioned similarly in the beam (i.e. similar beam position compensation). The data with the lowest SNR (2017 series in Figure 3-12) is more variable. The resulting TS with uncertainty bounds (25th and 75th percentiles) is shown in Figure 3-12(d) and differences between the two data sets can further be observed with a higher TS for the noisier data. As for the 2019 calibration for RFV Tridens II presented in Section 3.3.1.1, this suggests that increased noise levels impacts the calibration results substantially at high frequencies.

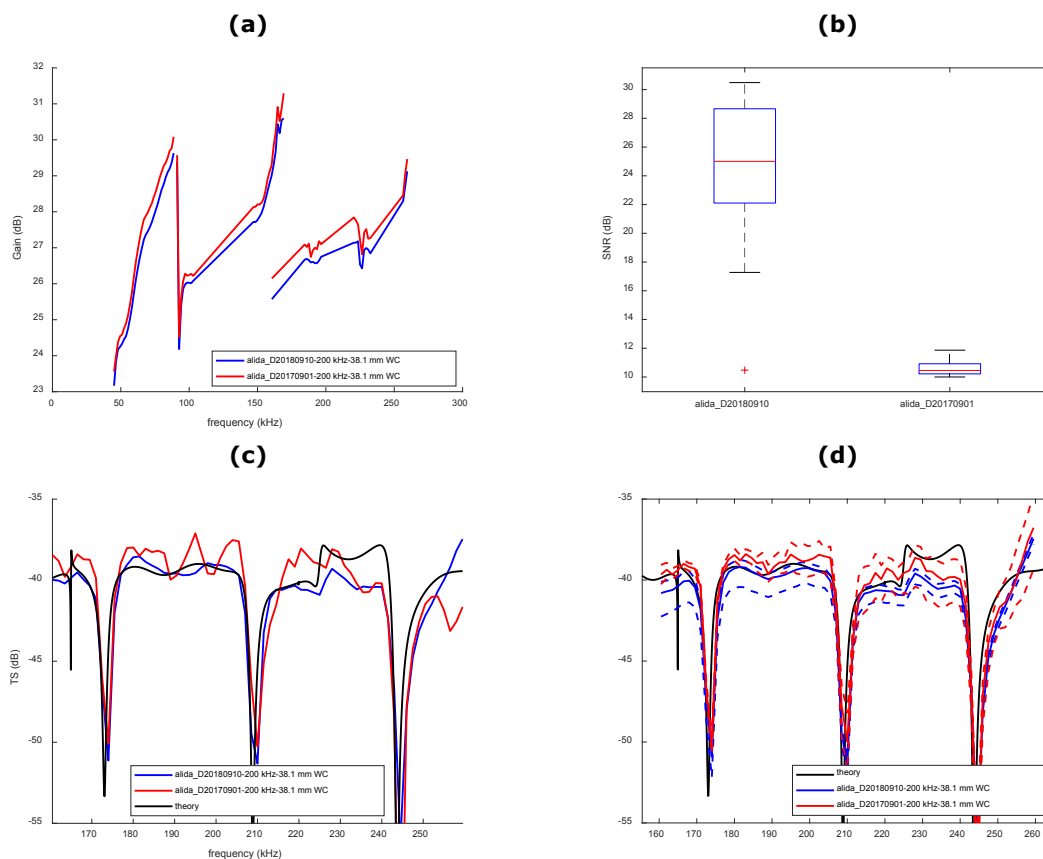


Figure 3-12: comparison of calibration data collected from a 38.1 mm WC sphere by the Alida (SCH6) in 2017 and in 2018. (a) calibration gain from 2018 and 2017 data sets. (b) boxplot of SNR for each detected hit. The 2018 data set showed here exemplifies high SNR. (c) frequency compensated TS for a single hit in the same location in the beam (i.e. equivalent compensation). (d) summary plot for compensated TS across all the sphere detections with 50th, 25th and 75th percentiles for both data sets. The solid black line in the theoretical frequency response.

The comparison between all the calibration data sets from the FVs is presented in Figure 3-13 for the three frequency channels of interest. Calibration gains are shown in Figure 3-13(a), (c) and (e) and SNR against TS deviation from theory in Figure 3-13(b), (d) and (f). Similarly to previous results, results are most consistent for the 70 kHz channel while more sensitive for the 200 kHz channel. However, the differences in calibration gain between data sets is greater than those presented in Section 3.3.1.2. For example, the calibration gain for the 70 kHz channel (Figure 3-13(a)) exemplifies differences of ~1 dB in the middle of the frequency band, even between data sets with similar SNR levels. This could be explained by differences in calibration settings (sphere netting, line setup, EK80 FM settings). Differences for the 120 kHz and 200 kHz channels are greater (Figure 3-13(c) and (e)) and no clear correlation between SNR and TS deviation is observed (Figure 3-13(d) and (f)). Similar observations were made for the analysis of the calibration data collected onboard the RFV Tridens II (Section 3.3.1), suggesting that the source of the discrepancies between the data sets lies within the calibration method at sea and the increased sensitivity induced by the use of broadband acoustics.

In practice, newest calibration gain values are used to correct the raw data. For example, for acoustic surveys using narrowband systems (EK60, EK80 CW), calibration is performed prior to the survey operations and these calibration results are used directly for the analysis. Calibration of narrowband systems is known to be stable [14], [37]. However, discrepancies between data sets exemplified here for the EK80 FM (onboard RFV and FVs) are high whilst alteration of the calibration gain of an echosounder through time is expected to be minor. The differences between calibration gains computed here are then not genuine. The introduction of such differences between data sets would result in substantial biases that would in turn be detrimental to the performance of the species identification algorithms (Section 6). As a result, a single calibration set is used for each vessel: 2016 calibration with 38.1mm WC sphere for the Afrika; 2017 calibration with 38.1mm WC sphere for the Alida. As shown in Section 6, this is severely hampering the cross vessel application of the species identification algorithms (i.e. the ability to harmonize data between vessels).

Though the study here investigated several data sets inconclusively, it would need to be investigated further to better pinpoint the sources of error. Also, novel processing methods could be tested. For example, a peak calibration instead of a full response calibration (current processing method) could improve the stability of the results and therefore the accuracy. It has been proposed in the literature to use the response from the front interface (first return) but only for short pulse signals [6], [36]. Alternatively, the EK80 FM between different vessels could be calibrated against each other using fish school marks if the FVs are conducting fishing operations at the time and location.

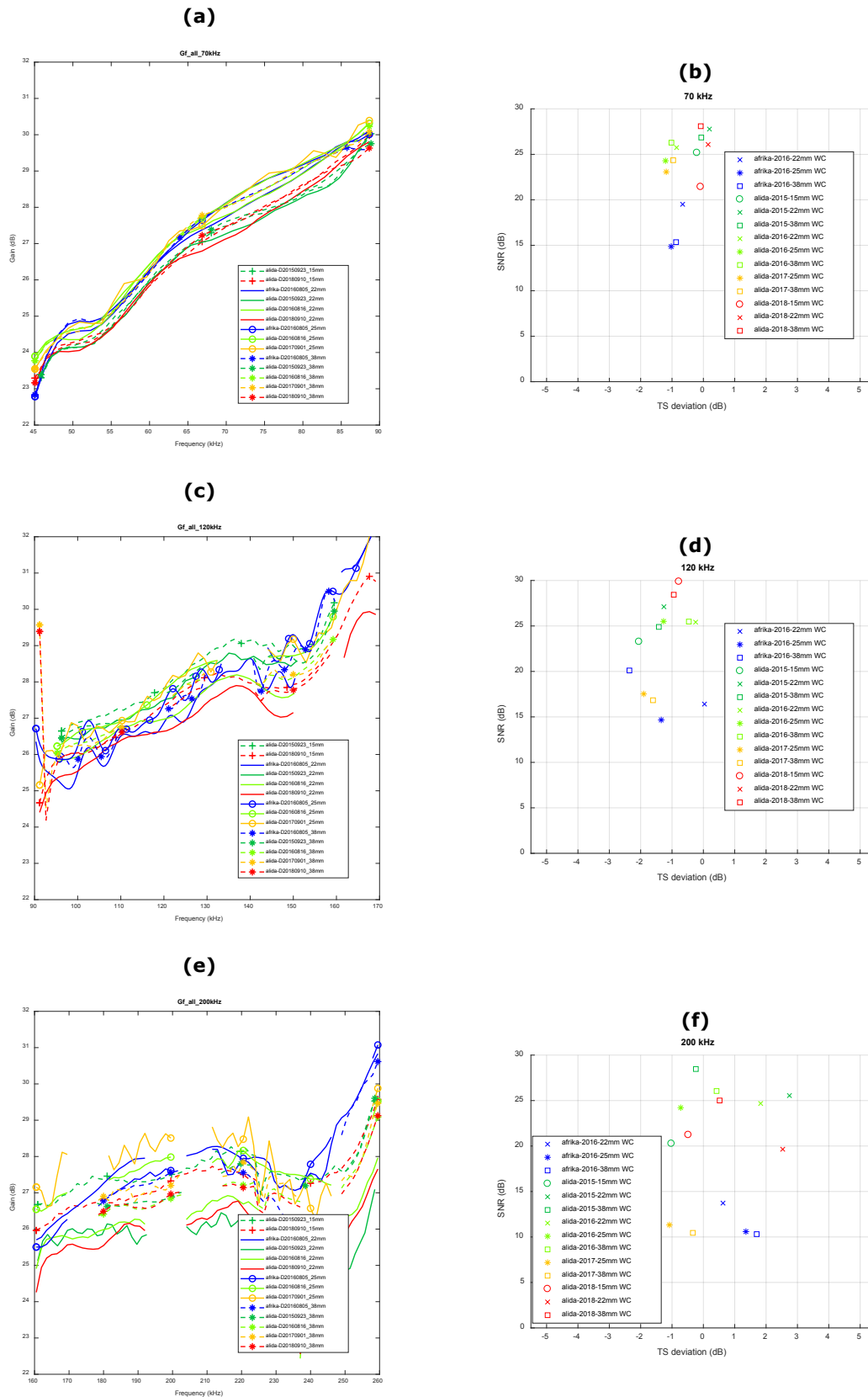


Figure 3-13: comparison of calibration outputs computed from calibration data collected by FVs between 2015 and 2018: (a) 70 kHz channel (c) 120 kHz channel (e) 200 kHz channel. For each plot, the difference in marker and line type is associated with different sphere types while the differences in colour is associated with different years and vessel (i.e. different data sets). The different data sets presented here are: Afrika (SCH24) 2016 (blue colour), Alida (SCH6) 2015 (dark green colour), Alida (SCH6) 2016 (bright green colour), Alida (SCH6) 2017 (yellow colour), Alida (SCH6) 2018 (red colour). The different spheres are: 15 mm WC, (dashed line with cross markers) 22 mm WC (solid lines), 25 mm WC (solid lines with circle markers), 38.1 mm WC (dashed lines with star markers). Data sets with settings as those listed in Table 2-1 are 2017 and 2018. (b) (d) (f): deviation from theoretical TS (TS error) against SNR for the different combinations of year, frequencies and sphere type.

Overall, large variability between the different calibration sets from the FVs was found, especially for the 120 kHz and 200 kHz WBT frequency channels. Such variability was also observed in the baseline analysis of RV Tridens II (Section 3.3.1) though this is slightly higher for the FVs. This suggests that the calibration trials performed on FVs yield results with similar accuracy and precision as the RFV Tridens II.

It is clear that high frequency channels (120 and 200 kHz) are sensitive to noise (Figure 3-9, Figure 3-12) but the comparison of different data sets did not reveal a clear trends between SNR and deviation from the theoretical response (Figure 3-11, Figure 3-13). There are several sources of error that in combination with each other could cause subsequent deviation in gain:

- Different SNR levels
- Cross talk between channels if other channels than the one being calibrated are not set as passive
- Different settings (pulse length, ramping)
- Difference in sphere parameters (e.g. aging, inaccuracy in material properties)

While calibration of the EK80 CW (narrowband) is well established and documented due to the worldwide use of the preceding SIMRAD echosounders (EK500, EK60), the wealth of experience with at sea calibration of the EK80 FM system is currently lacking. More research is needed to identify the different sources of error and caveats. For example, a study comparing different size spheres calibrated in a water tank and at sea could reveal the disturbances introduced by at sea operations. In light of the variability of results observed between years and vessels, it is important to minimize controllable sources of error as much as possible by:

- Calibrating the equipment in favourable conditions (weather, location, time of day)
- Ensuring settings are in line with expectations. For this project, these are those listed in Table 2-1
- Following guidelines. Of particular importance is ensuring that other channels than the one being calibrated are set as passive to avoid cross talks

Specific calibration guidelines for the EK80 FM and EK80 CW are described in a dedicated calibration manual (Annex III).

4 Data processing and demonstrator software

This section describes the data processing chain that was developed within this project. This is used by the ECHO software which was developed (WP4, Table 1-1) to aid skippers from commercial vessels with species identification and length estimation based on the acoustic records.

The ECHO software currently classifies the following fish species: Herring, Horse Mackerel, Mackerel and possibly Sardine or Sprat. Classification algorithms are in place within the ECHO software and both are using a machine learning approach (see Section 6). The training of the algorithms relies on data collected by the commercial vessels, including calibration

4.1 Processing chain

For both the offline reprocessing as well as for the online demonstrator, data from the EK80 sonar is read from recorded files. The recorded files contain individual pings of raw sensor data that must be converted to an image of a fish school (when present) with an accompanying classification output. To ensure consistency in results between the offline processing and the demonstrator, the software is developed such that it can be used in both offline (playback) and online operating mode. This means that all modules described below use internal round-robin buffering for real-time data streaming, such that each module delivers the exact same output, independent of operating mode. A schematic overview of the processing chain is depicted in Figure 4-1. The orange disks correspond to static or temporary data storage. The blue boxes represent individual processing threads. Since with broadband acoustics the amount of data entering the system is significant (roughly 10 MB/s as opposed to < 0.5 MB/s for CW), the processing chain must be very fast to process all data in real-time. Hence, multiple threads are launched that each perform part of the processing. This section briefly describes the individual threads in the processing chain.

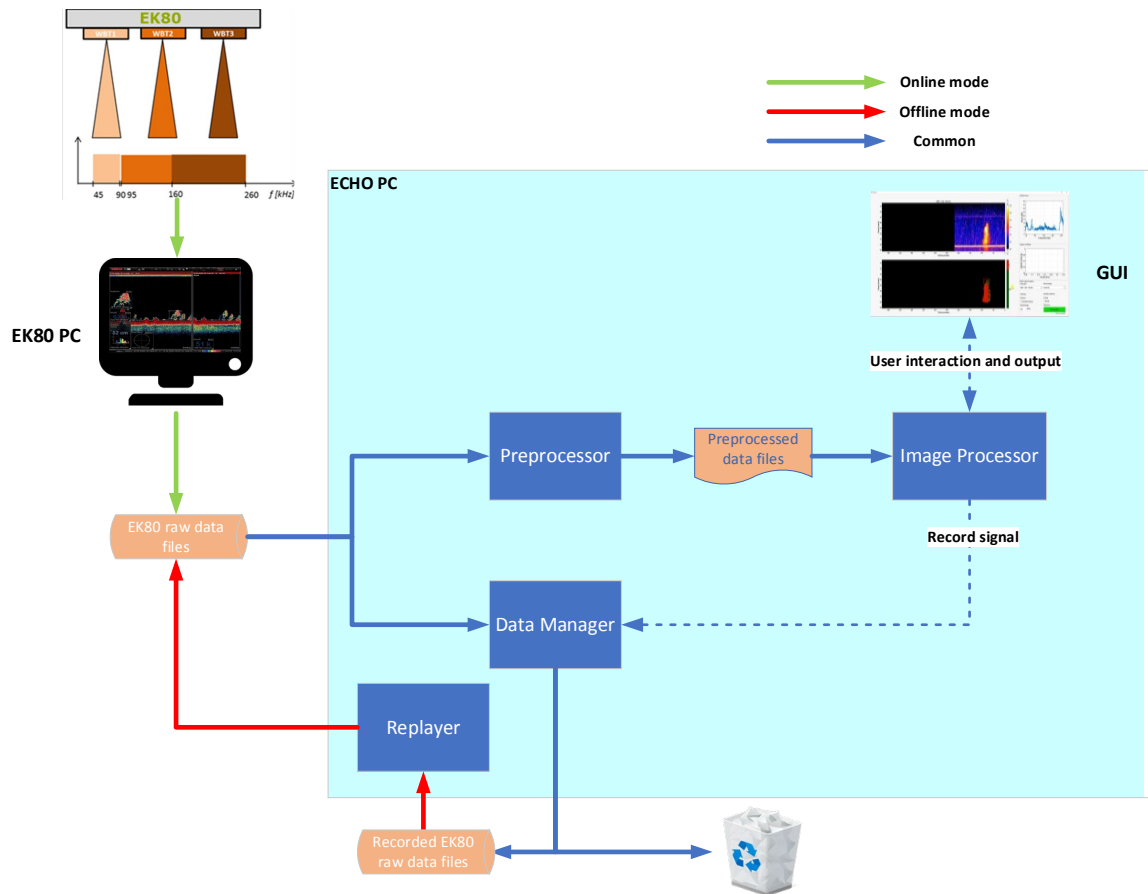


Figure 4-1: Schematic overview of the processing chain of the demonstrator, suited for both online and offline processing.

4.1.1 Pre-processor

The pre-processing module continuously reads new, raw data files coming in that are stored on disk either by the EK80 or by the replaying module. The pre-processor performs the important sonar processing steps required to convert raw sound pressure levels to Target Strength (TS) levels, used to construct an echogram and perform classification with. Sonar processing consists of a number of steps, depicted in Figure 4-2, which are briefly explained here.

TX-signal reconstruction: Based on the sonar settings stored in the data, the pulse that was originally transmitted by the sonar is reconstructed. Sonar settings include pulse length, pulse slope, start/stop frequency, transmission power, transducer impedance and data reduction filter settings.

RX-signal reconstruction: Similar to reconstruction of the TX-signal, the acoustic data received by the sonar is converted to normal acoustic units.

Matched filtering: A convolution is performed between the TX-signal and the RX-signal. This is a common technique to improve the Signal-to-Noise Ratio (SNR) and signal resolution.

Beamforming: Each Wide-Band Transceiver (WBT) consists of four quadrants that each transmit the same acoustic signal. The signals they receive are combined by averaging to create a directional beam perpendicular to the face of the transceiver and therewith suppressing noise and interferers from other directions. This increases the SNR.

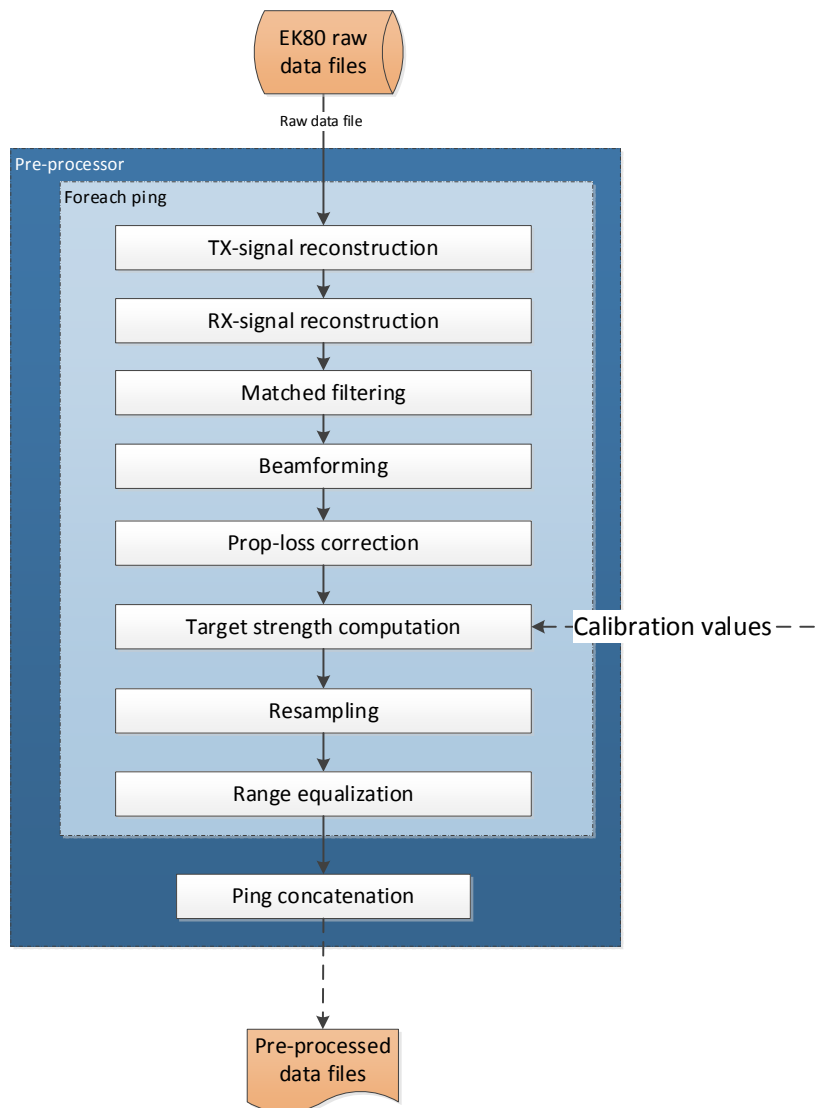


Figure 4-2: Block diagram indicating the processing steps of the pre-processor.

Prop-loss correction: On the resulting acoustic signal, propagation loss correction is applied. Propagation loss is a result of geometrical spreading of the sound while it propagates through the water. This is compensated for. The same accounts for absorption of the sound by the sea water, depending on temperature, depth, salinity, acidity and frequency of the sound.

Target strength computation: Each acoustic sample is converted to a target strength level, based on the transmission power and gain and centre frequency of the transceiver. Corrections are applied for the calibration levels of the transceiver. The resulting target strength is the final level that is used as indication for the target's acoustic properties.

Resampling: To facilitate rapid processing, the data of all three transceivers are resampled to the same sampling frequency. This is convenient when image processing results of the transceivers need to be combined.

Range equalization: The pings of the different transceivers are cropped to have the exact same dimensions, again to facilitate the image processing steps later in the processing chain.

Ping concatenation: Pings are collected in small chunks that are finally written to the collection of pre-processed data files, from where they will be read again by the Image Processor.

4.1.2 Image Processor

The image processing thread is responsible for converting the pings containing target strengths to processed images with detected schools and corresponding classification results. The results are visualized in the Graphical User Interface (GUI) that also allows user interaction to start/stop a recording session and switch between different types of echogram views (see Section 4.2). The Image Processor comprises quite a number of independent modules that are chained together (Figure 4-3). The example outputs of the modules described below, will be given for an entire echogram, in order to get a good impression of the functionality of each module. Note that in the real-time demonstrator, all processing is done in small chunks of roughly 8 pings, that together construct a running stream of outputs. The chunks are buffered internally in each module to make sure that all operations give the same result as when the entire echogram of e.g. 150 pings would be put in.

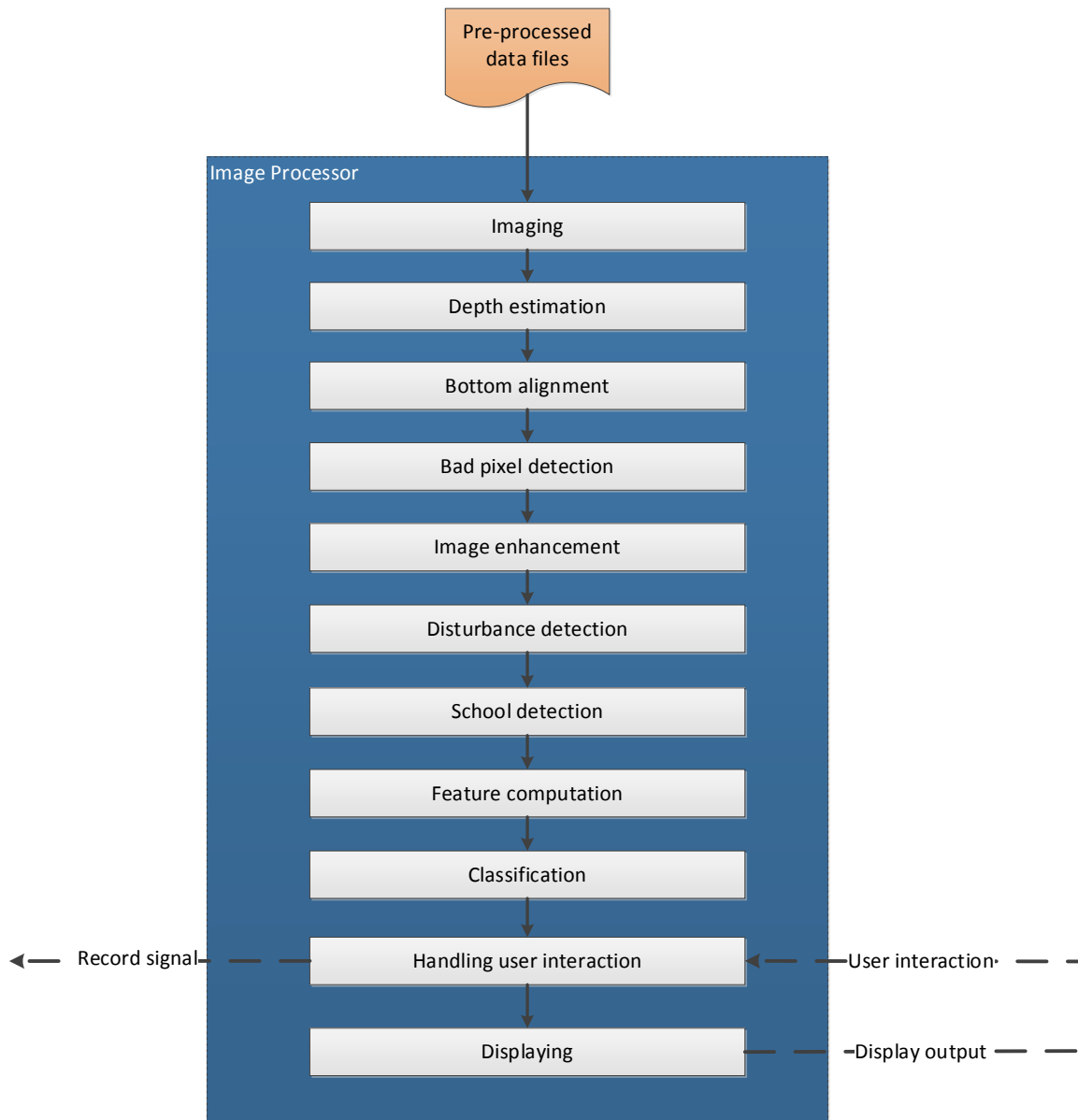


Figure 4-3: Block diagram indicating the processing modules of the image processor.

4.1.2.1 Imaging

Internal storage is continuously scanned for new, pre-processed data files. Data files are loaded and buffered/concatenated, together constructing a streaming echogram (Figure 4-4).

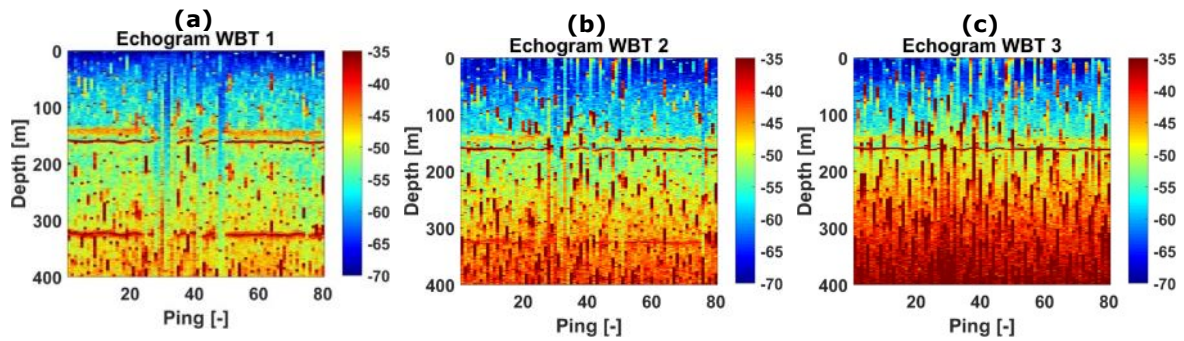


Figure 4-4: Example echograms of the three Wide-Band Transceivers: 70 kHz (a); 120 kHz (b); 200 kHz (c).

4.1.2.2 Depth estimation

Based on the data in the echograms, the depth is estimated per ping. Depth estimation is required to ensure that 'no fish' detections are done below the bottom. Also it reduces the amount of data to process, since data below the bottom return can be cut off. Depth estimation is performed for only a single transceiver and applied to all three transceivers. Since transceivers are pinging simultaneously, this ensures the different echograms do not misalign in case a different depth would be estimated for one of the transceivers. In Figure 4-5 some plots can be observed of the depth estimation process. First, an average depth estimate is made to avoid detecting interference as bottom. To this end, the echogram is slightly filtered to stretch out the bottom return (b). This is done to reduce the effect of ship heave caused by surface waves. The median intensity levels as function of depth are then computed (c). As observable, the intensity level increases as function of depth. This is caused by transceiver noise that is amplified after propagation loss correction. To remove this increase, the local intensity trend is removed with a moving median filter, resulting in a straight line with a short bump caused by the bottom return (c). This is defined as the estimate of average depth. Finally, the actual depth per ping is determined by looking for the maximum level, within a range bracket around the average depth (d).

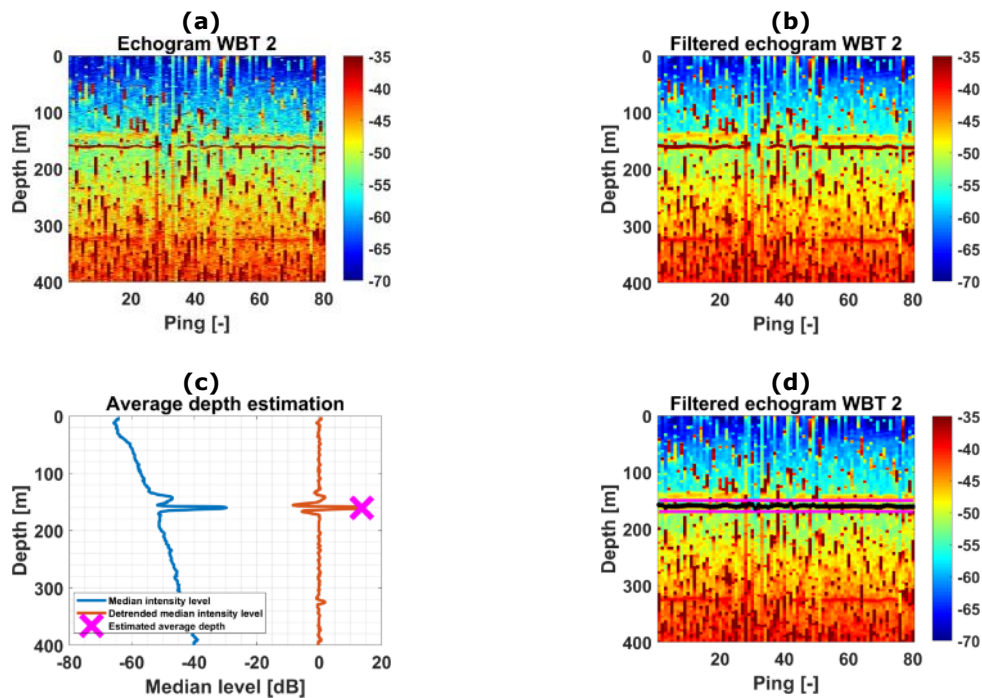


Figure 4-5: Steps in the depth estimation process. The input echogram of WBT2 (a). A slightly filtered version of the echogram in which the bottom is spread out (b). The median intensity levels of the pings and the estimated average depth (c). The depth estimation bracket indicated in magenta and the depth estimated per ping indicated by black crosses (d).

4.1.2.3 Bottom alignment

The depth estimates per ping are used to align the image. All pings are shifted either forward or backward in time such that all pings in the output image have a depth that equals the average depth. In this case the shape of the school remains preserved. All data more than 10 meters below the bottom

is cut off, such that only the relevant information in the image remains. In Figure 4-6 the result of this operation is displayed.

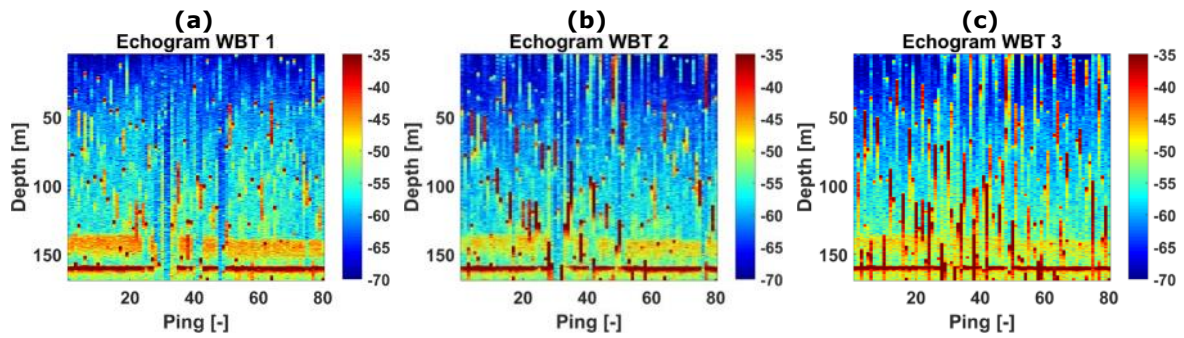


Figure 4-6: Bottom-aligned, truncated echograms of the three Wide-Band Transceivers: 70 kHz (a); 120 kHz (b); 200 kHz (c).

4.1.2.4 Bad pixel detection

Bad pixel groups are a collection of pixels in the image that contain interference (red stripes) or lack of energy. Interference stripes are mainly caused by other sonars pinging in the same frequency band. A lack of energy is the result of sound not properly penetrating the water. This can be caused by air bubbles around the face of the transceiver as a result of surface waves, possibly in combination with a relatively low weight of the ship in the beginning of a trip. These parts of the image severely distort the perceived acoustic signal of the school at those locations and malform the frequency spectrum. As a result, species classification cannot be done for those parts. To avoid that these parts are being classified, they need to be detected. Figure 4-7 briefly summarizes some steps in this process. The image is first slightly filtered in the range direction to avoid detecting individual pixels as noise, that genuinely have a somewhat higher value, for example in fish schools. Noise stripes normally lead to a number of close-by pixels that are bad, and not individual, isolated pixels. Subsequently a template is created that defines the average expected pixel levels. The two echograms are subtracted and a difference image remains. Any pixels with a difference larger than a certain threshold level are assigned as bad.

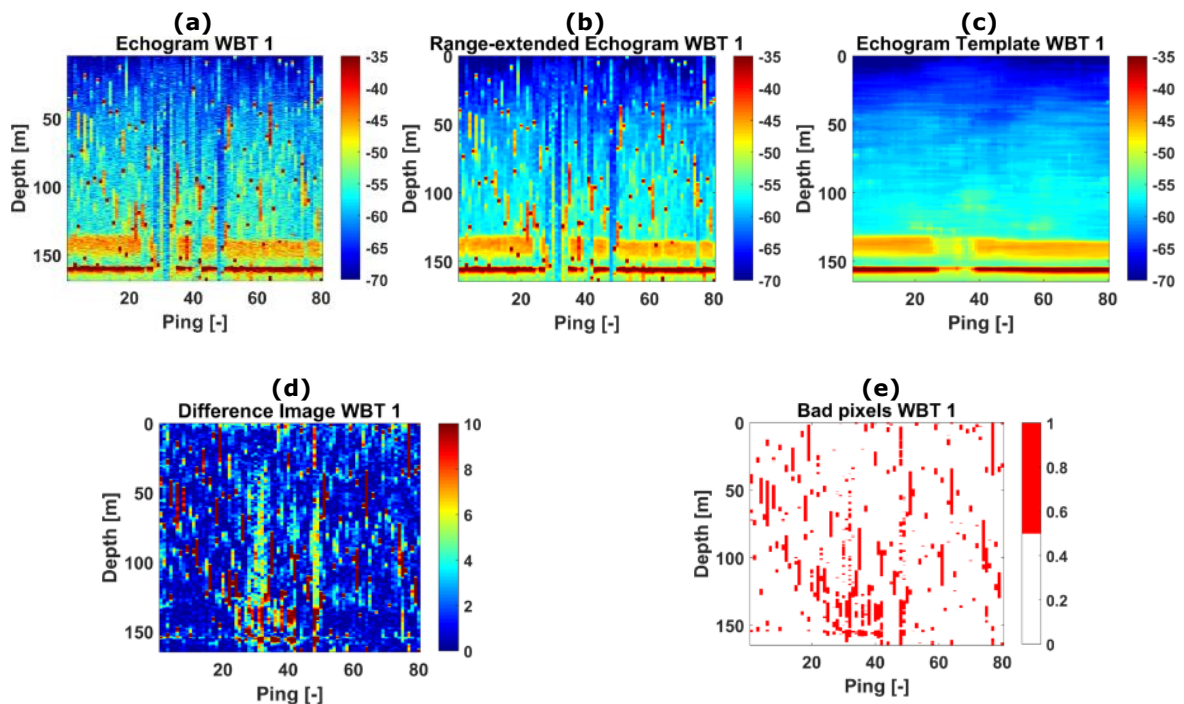


Figure 4-7: Processing steps in bad pixel detection. Example input echogram (a) of WBT 70 kHz. Range-filtered echogram to avoid assigning isolated pixels as 'bad' (b). Background template indicating expected signal levels (c). Deviation of echogram from template (d). Pixel groups assigned as 'bad' (e).

4.1.2.5 Image enhancement

The image enhancement module replaces the bad pixels in the echograms with new pixels based on an interpolation of their neighbouring pixels. This is done purely for visual purposes. This image will be presented as echogram to the skipper interface. It has filtered away interferences while preserving high detail. Additionally, a smoothed version of the echogram will be created by this module to serve as stable input in school detection. Figure 4-8 shows both results for the three echograms.

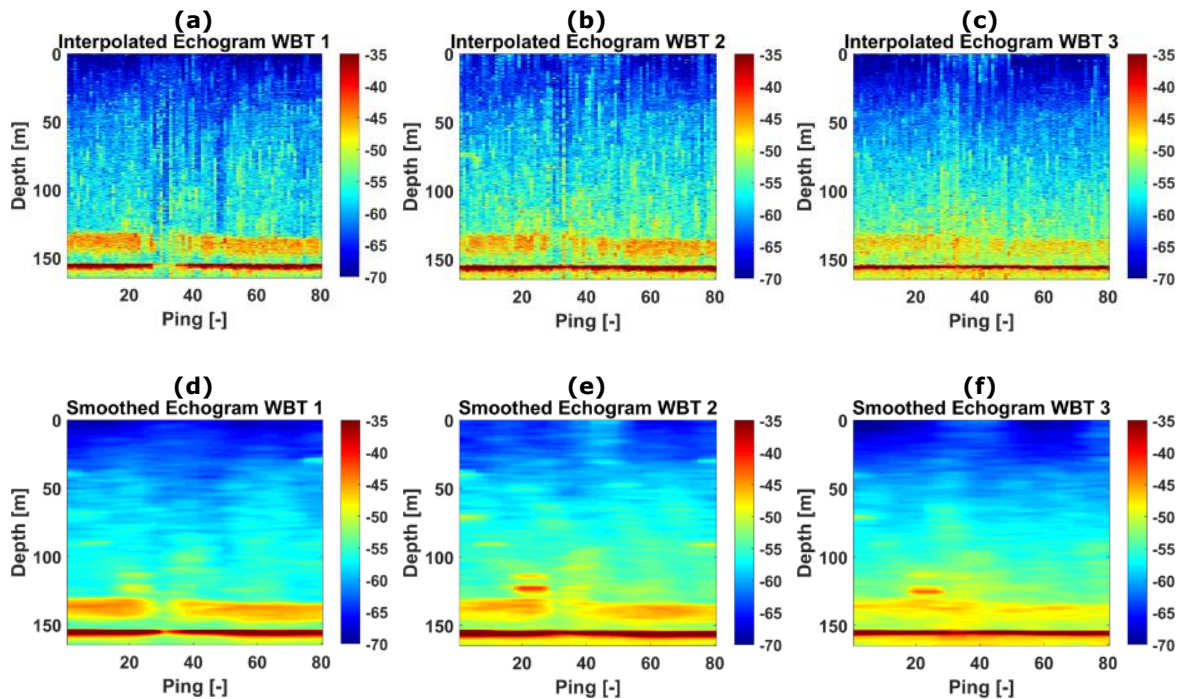


Figure 4-8: example of the image enhancement processing.

(a), (b), (c): Interpolated echograms in which noise has been filtered out while image detail remains. (a) 70 kHz WBT. (c) 120 kHz WBT. (c) 200 kHz WBT

(d), (e), (f): Smoothed echograms that are used as input to the school detection module. They are a strongly filtered version of the original echograms to avoid noise being mistakenly detected as fish. (d) 70 kHz WBT. (e) 120 kHz WBT. (f) 200 kHz WBT.

4.1.2.6 Disturbance detection

The mask indicating bad pixels is used to detect and analyse narrowband disturbances within the frequency bands covered by the three transceivers. This is done to give the skipper an impression on the cause of current disturbances, such that it could take action to reduce the interference in its sonar images. Disturbances in general are interferences caused by other sonars. They express themselves as vertical stripes in the echogram. These vertical stripes are detected and a frequency analysis is performed on the extracted audio. Figure 4-9 shows a number of images describing the steps of this process. The bad pixel mask is filtered to maintain only prominent, narrowband disturbances. The resulting spectral analysis shows two dominant spikes at interfering frequencies of 14 dB above the background level.

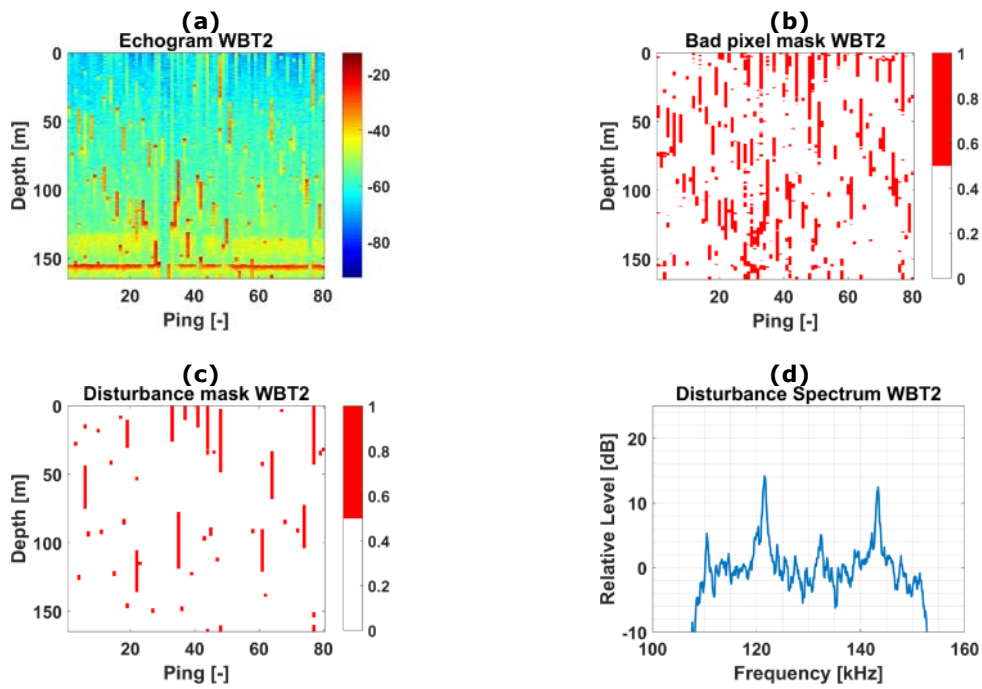


Figure 4-9: Steps describing the disturbance detection and analysis process. Input echogram (a). Initial bad pixel mask detected in the bad pixel detection module (b). Filtered bad pixel mask, indicating the locations of the dominant interferences (c). Spectrum of the analysed interferences showing two dominant, narrowband peaks of interfering sonars (d).

4.1.2.7 School detection

Using the smoothed echograms from the image enhancement module, fish are automatically detected. All three echograms are thresholded to deliver a mask that indicates the presence of fish. Bad pixels, detected in the bad pixel detection module, are removed from the mask, such that they will not be classified. By applying some image erosion and dilation, any remaining noise is filtered out. The detection masks of the individual transceivers are combined to form a single detection mask. Per pixel at least two out of three transceivers should have a detection for it to be assigned to the final mask. This additional step filters out some more transceiver-dependent noise. The detection mask for the example school considered in this section is given in Figure 4-10.

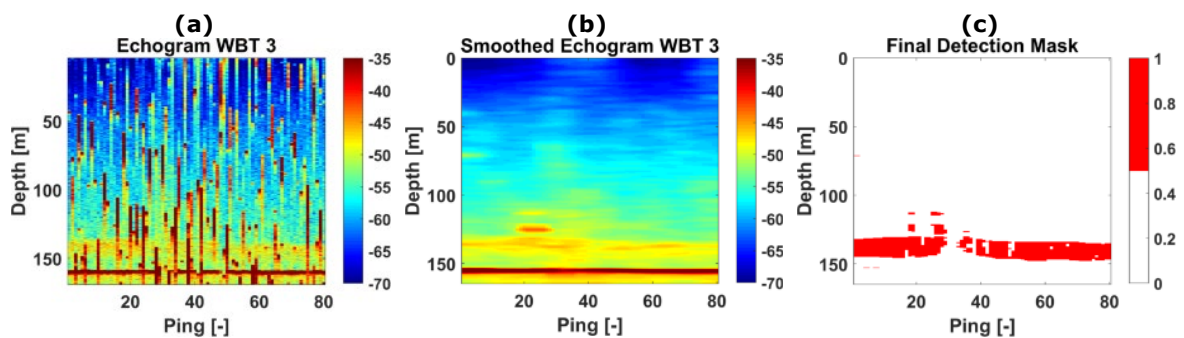


Figure 4-10: Steps describing the school detection process. One of the input echograms (a). The filtered version of the echogram (b). The final school detection mask after combining the detection masks of the three transceivers (c).

In the detection process, a threshold must be exceeded for pixels to be detected as fish. A difficulty with the EK80 is its limited operating range. The presence of ship noise (either electrical, thermal etc.) causes the SNR to decrease with increasing depth. Since the acoustic signal is amplified to compensate for propagation loss, stationary background noise is also being amplified. When depth increases, the amplified background noise levels also increase as a result of this, up to a point where it crosses the detection threshold. At this point noise is detected as fish. This is a normal physical limitation which in practice indicates the sonar has reached its limits at that depth. However, there is a transition window where classification may still be possible when increasing the threshold level. When doing this, the effective operating depth for the classifier could be increased with 25 to 50 meters. This has led to a

dynamic detection threshold that increases as function of range (i.e. depth). Figure 4-11 shows this adjustment for a single ping. It must be noted that the received acoustic signal at these larger depths will start to become more dominated by background noise, making it more difficult to classify the fish school. Based on the recorded data sets, the current operating range up to which classification seems feasible is estimated to be at least roughly 200m. The actual range depends on ship type and varying noise conditions. More on this topic is described in Section 5.2 (noise analysis) and Section 6.4 (effect of SNR reduction).

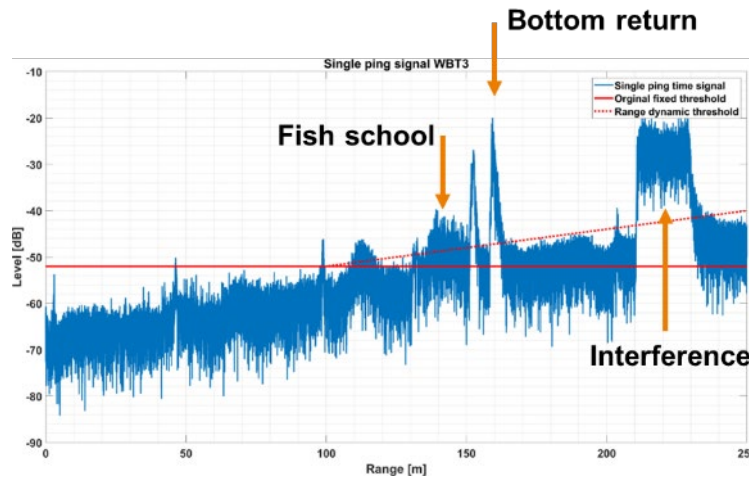


Figure 4-11: Example time signal of a single ping of WBT3, after correction for propagation loss. After a certain range the noise exceeds the detection threshold. By applying a range-dynamic detection threshold, the operating range of the demonstrator can be slightly increased.

4.1.2.8 Feature computation

In this module features are computed that serve as input to the Classification module. The echograms are split into small cells. A cell is a time window of 1.6 m in length within a single ping. A ping has multiple consecutive cells. Only the cells that are within the detection mask are used in feature computation and classification. The same features are computed for each cell. Each cell will later be classified individually. In Figure 4-12 the division in cells is given for the example echogram. The division of the school into smaller parts allows the classification of mixed schools as opposed to only homogenous schools. This is a desire of fishermen since schools that contain a mix of Horse Mackerel and Mackerel are being caught regularly, which is undesirable.

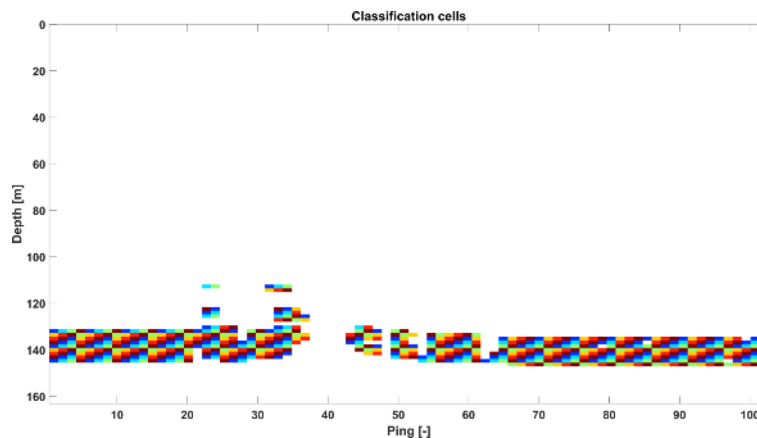


Figure 4-12: Division in cells of the example school. On each cell, time signal and spectral features are computed after which they are classified. A single cell is roughly 1.6m in length.

4.1.2.9 Classification

Each cell is classified individually using the features computed for that cell. The classification output is one of the species types with which the classifier was trained. Figure 4-13 gives the classification result for the given example school. Classification is described in more detail in Section 6.

4.1.2.10 Handling user interaction

This module handles input from the user to modify display settings and to enable/disable recording. Any change in recording status is forwarded to the data management module. User interaction has no effect on the classification result. Effort has been put in being able to automatically derive all underlying processing settings, since the processing settings can be complex to understand for an operator. Settings in this regard relate to e.g. filter lengths in image enhancement, thresholds for school and noise detection etc. These settings are automatically derived based on, among others, image quality metrics and estimated environmental conditions. A more detailed description of display settings and the user interface is given below (Section 4.2).

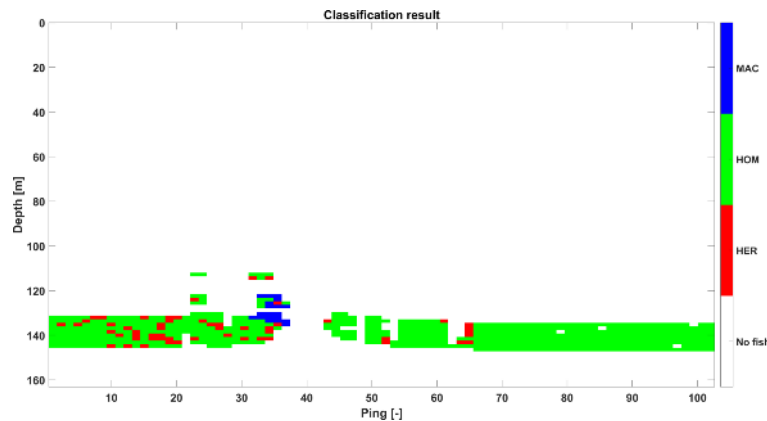


Figure 4-13: Classification result for the given example school, where the colour of each cell indicates the estimated species type as which it is classified.

4.1.2.11 Displaying

The (enhanced) echograms and classification results are finally displayed to the user in the Graphical User Interface (GUI). A more detailed description of the user interface is given below (Section 4.2).

4.1.3 Data manager

The data manager handles the removal and relocation of raw data files based on user input. Since the amount of data generated by the broadband echosounders is very large (roughly 10 MB/s), it is not possible to keep all data that is recorded during the entire trip on an external storage device. And because the data recorded by the EK80 software must first be stored in order to be able to process it with the demonstrator software, this data must be removed after it has been processed in case it is not relevant to the skipper (i.e. when no fish present). The skipper uses the recording button on the GUI to indicate whether data should be removed or remain stored. This signal is passed to the data manager, which on its turn removes processed data files or moves them to a permanent storage folder.

4.1.4 Replayer

With the replayer it is possible to replay recorded data files in offline mode. The replayer acts as the EK80 and feeds recorded data files in real time (or faster) to the demonstrator in a streaming fashion. In case files are large (minutes), which is the case when they are recorded in an earlier stage of the project, the data files are split into smaller chunks with which new, small files are generated. In this way the EK80 operation is simulated which is useful for development purposes. With this functionality, the real-time capabilities of the online demonstrator can be tested. Also the exact operation of the demonstrator can be reviewed offline. This can be useful to reproduce any issues noted by the skipper during online use.

4.2 Graphical user interface

The Graphical User Interface (GUI) is used to enable user interaction with the demonstrator software and to display echograms and classification results. Additionally it provides a number of options to adjust

the representation of (intermediate) results. Figure 4-14 depicts the GUI that is used in the demonstrator. The different panels are indicated with letters and will be described here.

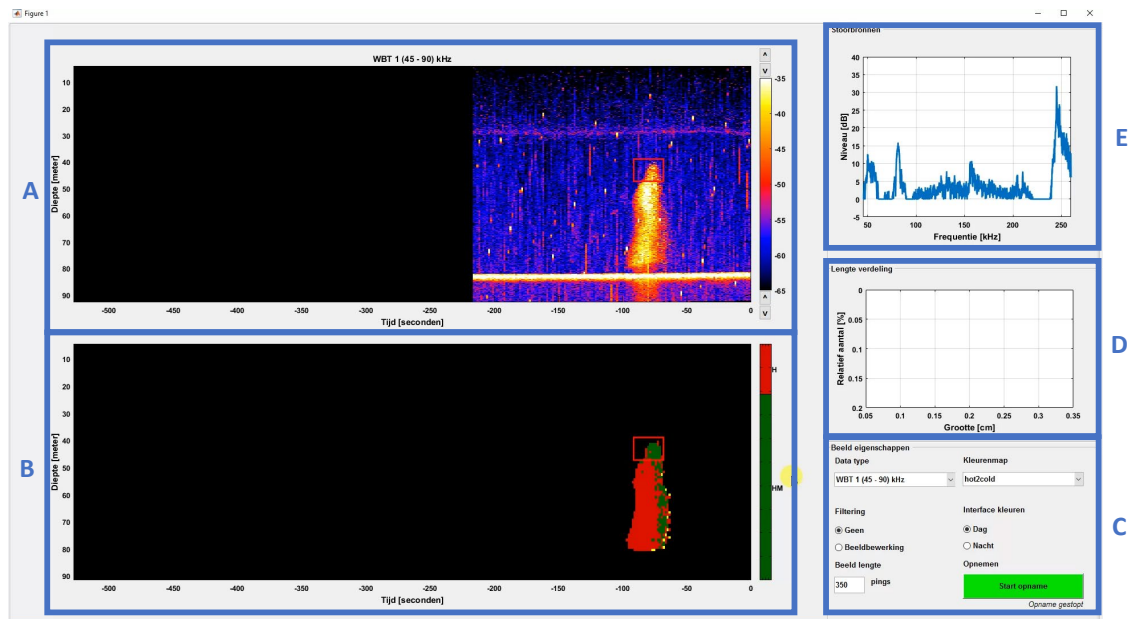


Figure 4-14: Screenshot of the Graphical User Interface (GUI) of the demonstrator, used on board by the skipper.

4.2.1 Echogram display

The panel A in Figure 4-14 displays the echogram of one of the transceivers or a sub band of that transceiver (further expanded in Figure 4-15). The small bar on the side indicates the used colour scale. Using the up and down buttons on both sides of the bar, the upper and lower limit of the colour scale can be adjusted. In Panel E in Figure 4-14, other visualization settings can be modified.

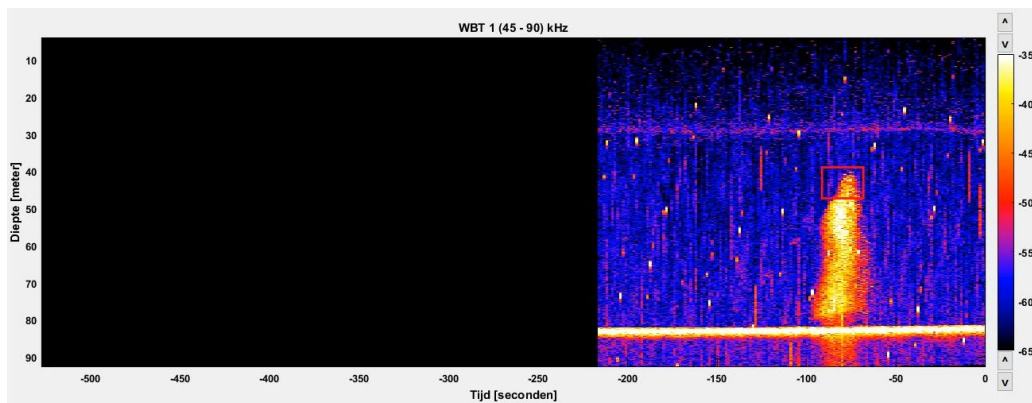


Figure 4-15: Screenshot of the streaming echogram display.

4.2.2 Classification display

The panel B in Figure 4-14 displays the classification result of the automatically detected school (further expanded in Figure 4-16). Each cell of the school has a classification result, indicating the expected output species. Each species has a predefined colour. This results in a coloured image of the school indicating at which location which species is expected. The colour bar on the right is dynamic and provides the relative amount of a certain species in the image by means of the height of each sub bar. At the same time it serves as a legend that couples the colour to the type of species. In case the red selection box is drawn, as shown in the image, the statistics in the colour bar are given for that specific area. Note that this box can be drawn in both the echogram display as well as this classification display.

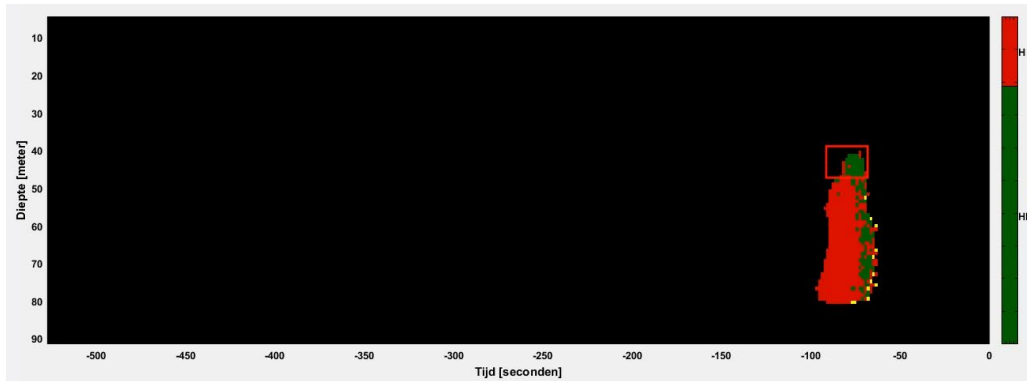


Figure 4-16: Screenshot of the classification display, showing the detected schools and the estimated species type by the classifier.

4.2.3 Control panel

Panel C in Figure 4-14 is the control panel (further expanded in Figure 4-17). With the control panel, the display settings of the echogram can be modified and recording can be enabled/disabled.



Figure 4-17: Control panel with the different visualization settings that can be selected by the user.

The following parameters (in Dutch) in the control panel can be adjusted:

a. Data type (Figure 4-18):

Can be used to select a particular transceiver of which to display the echogram. It is also possible to select a small sub band. This is known to be useful for the skippers since:

- Interference of other sonars with a frequency range outside the sub band will be filtered out
- Resolution of the image is decreased, which makes it easier to see very sparse, scattered fish

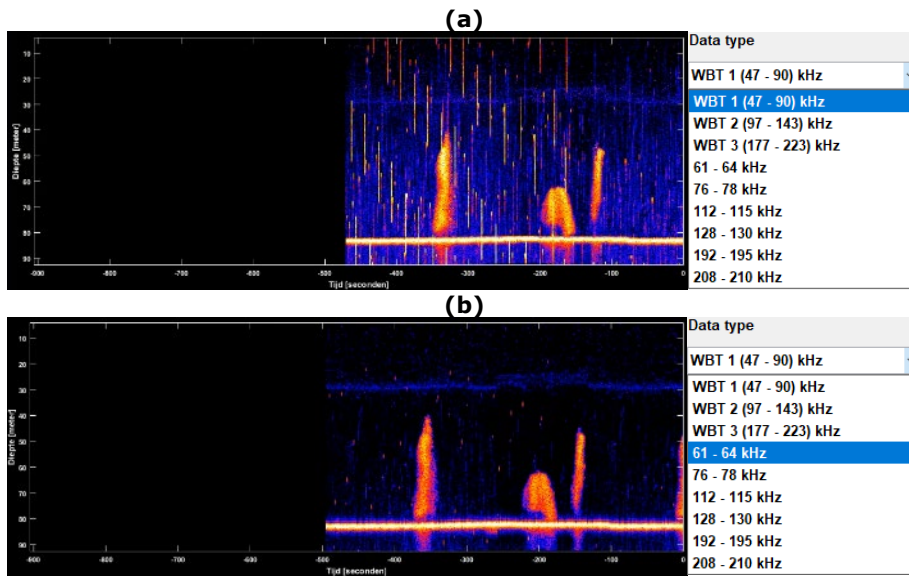


Figure 4-18: Screenshots of the echogram of the same transceiver, displayed in different frequency bands: (a) full 70 kHz WBT channel band, 47-90 kHz; (b) partial frequency band from 70 kHz WBT channel, 61-64 kHz. The frequency band is selectable in the data type menu.

b. Filtering (Figure 4-19):

Can be used to switch between the regular echogram and a filtered version of the echogram. In the filtered version, the noise is filtered out using image processing techniques. This provides a more clear, denoised echogram to the user.

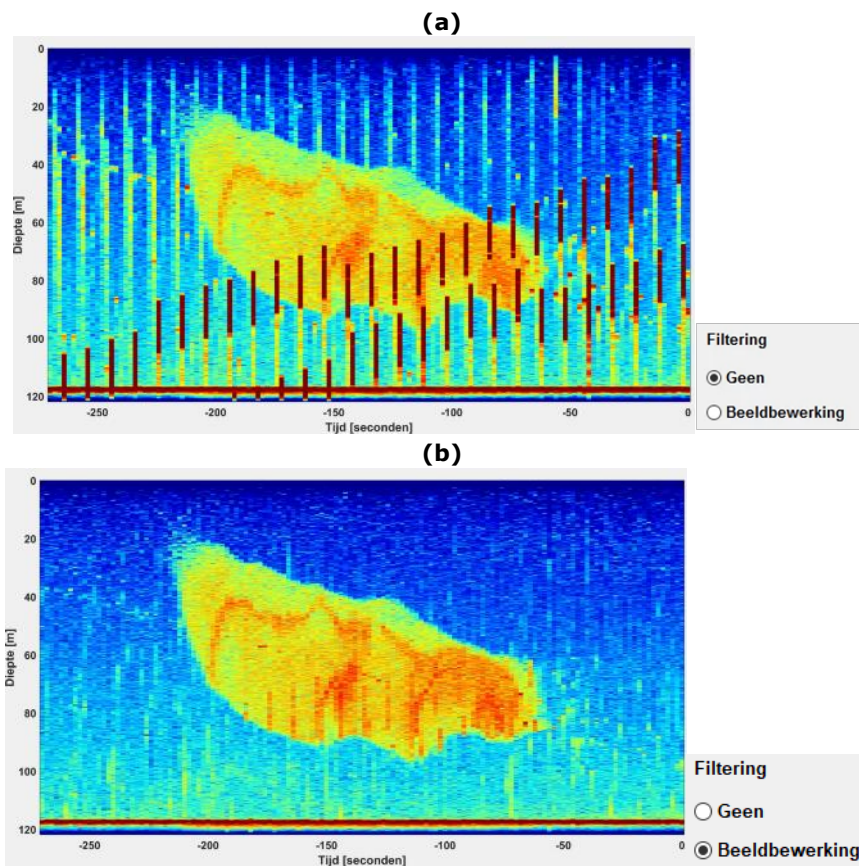


Figure 4-19: Screenshots of the same echogram, displayed without (a) and with (b) image enhancement, selectable using the filtering buttons.

c. Beeld lengte (Figure 4-20):

Allows to extend the history length of the echogram up to half an hour in length.

Beeld lengte
350 pings

Figure 4-20: Image length box to modify the history length of the echogram.

d. Kleurenmap (Figure 4-21):

Allows to use different types of colormaps to display the echogram with.

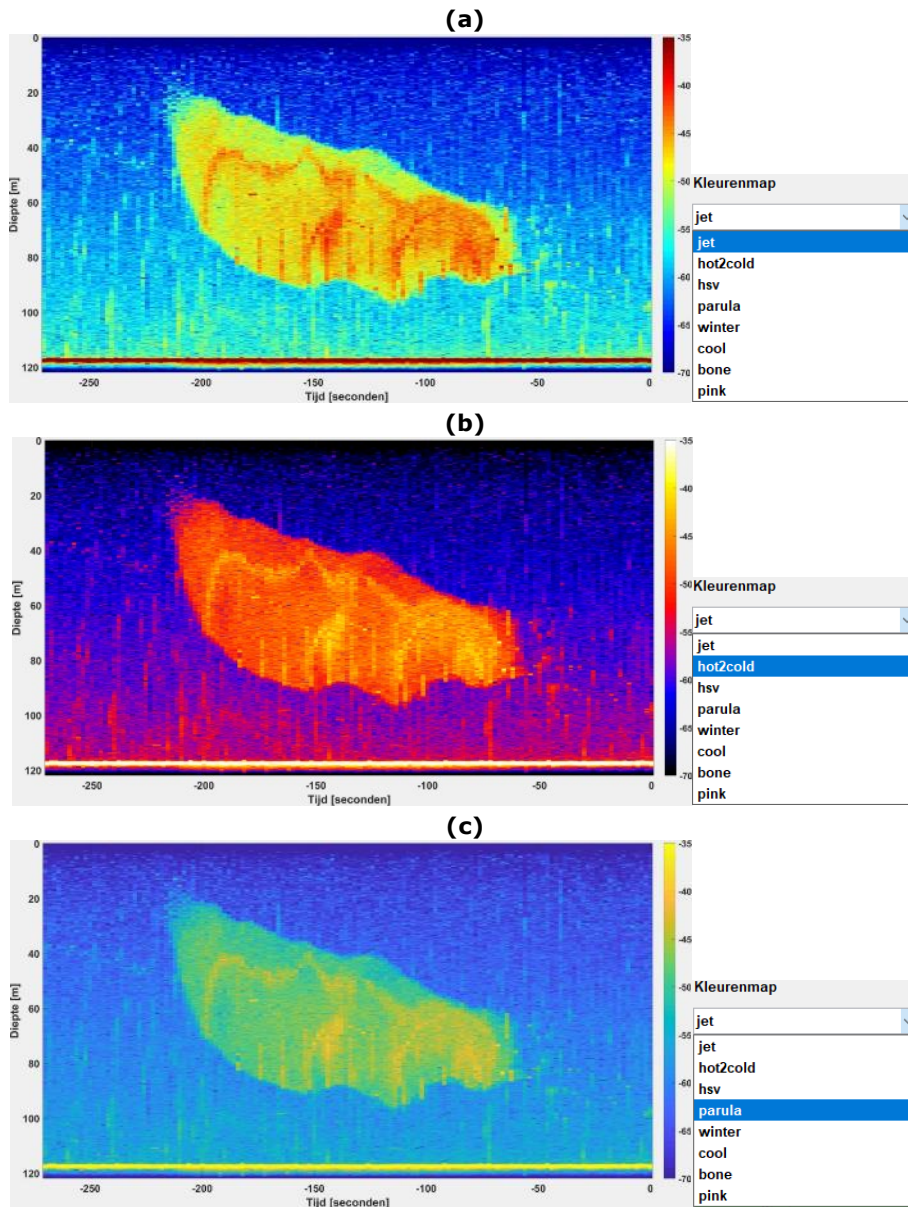


Figure 4-21: Screenshots of the same echogram displayed with different colour scaling maps: (a) jet;(b) hot2cold; (c) parula. The colour scheme is selectable in the colour map menu.

e. Interface kleuren (Figure 4-22):

Allows the user to switch between day and night mode. In night mode the background colours of the interface are turned to black to avoid overexposure of the eyes.

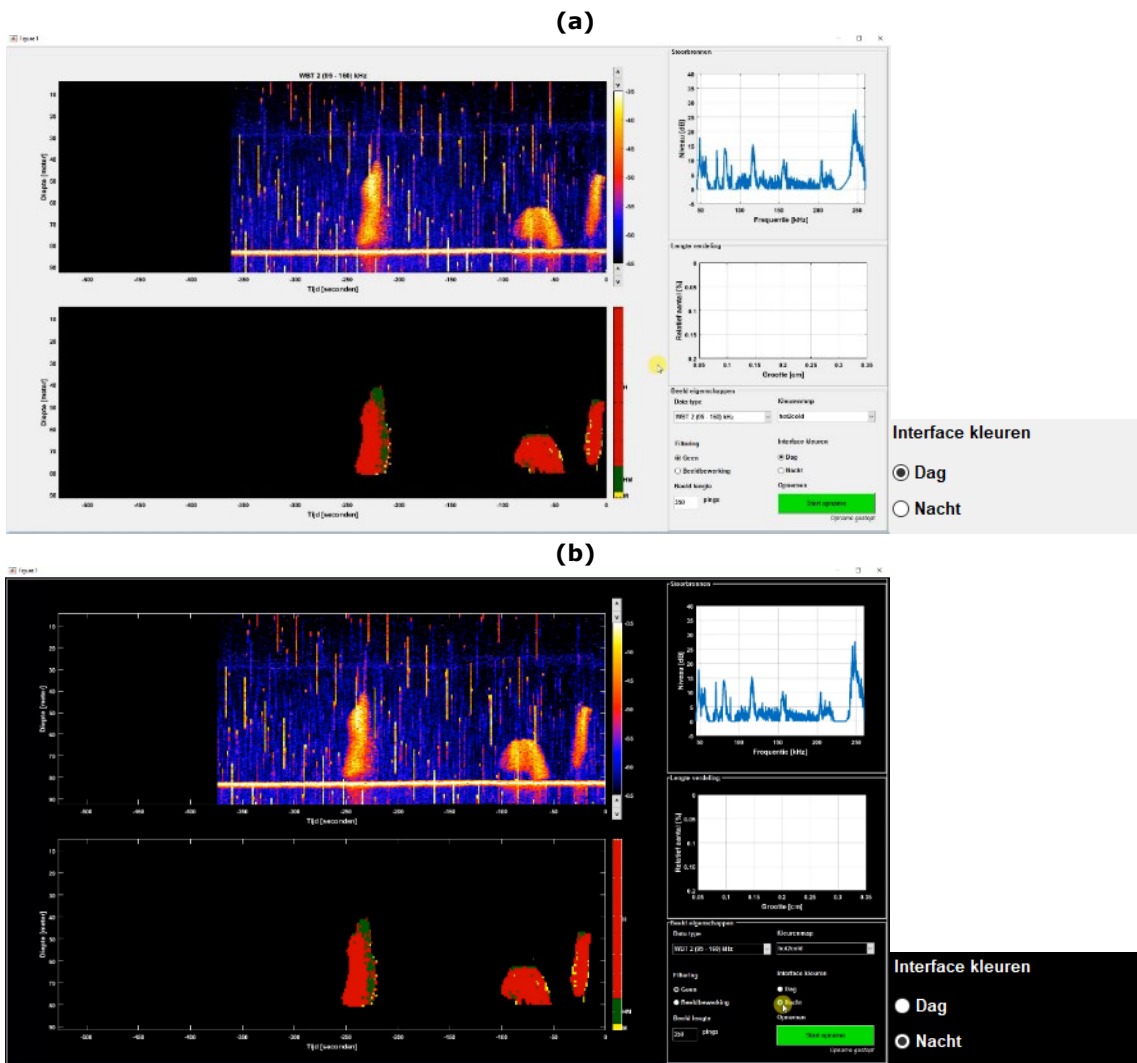


Figure 4-22: GUI screens in day (a) and night (b) mode, selectable in the interface colours menu.

f. Opnemen (Figure 4-23):

Button to enable or disable recording. The signal is passed to the data manager that deletes or permanently stores processed files.

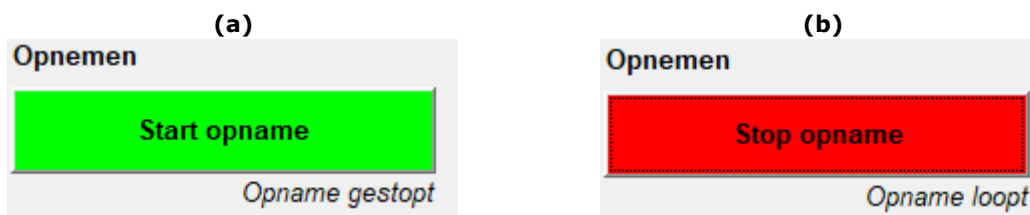


Figure 4-23: Data recording button in different modes: not recording (a) and recording (b).

4.2.4 Length estimation

This is displayed in panel D shown in Figure 4-14. This feature is currently disabled. The development of the size estimation method is described in Section 7.

4.2.5 Disturbance analysis

This is displayed in panel E in Figure 4-14. An expanded view is shown in Figure 4-24. It provides a graph with a spectral analysis of any present interfering sources. As described in the section on the processing chain, interferences (mainly caused by other sonars) are automatically detected in the echogram. A spectral analysis of these interferences is done and presented to the user. In this way it

can get an impression on which sonars are disturbing the image and possibly disable these interferers. In case an interferer is disabled, the noise peak will disappear from the disturbance graph within a few seconds.

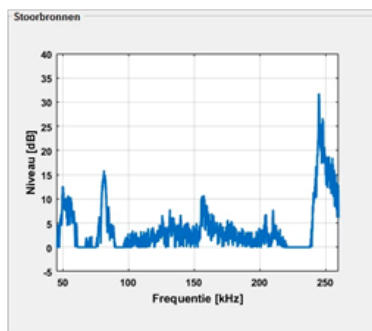


Figure 4-24: Disturbance analysis panel, displaying a frequency spectrum computed on the detected interferences in the echograms. This indicates the operating frequencies of narrowband interferences (other sonars).

5 Data analysis

In this section, the analysis of the data collected in the project (Table 2-3) is presented. First, the differences in frequency response between schools is investigated. This is important as the frequency content is one of the most important feature for classification (Section 6). Then, an analysis of the noise encountered in the acoustic data for the Alida (SCH6) and Afrika (SCH24) FVs is presented. Though mitigated through specific processing (see Section 4.1.2.6), high noise and disturbance levels limits the classification ability by reducing the amount of data that can be used for classification.

5.1 Frequency response analysis

5.1.1 Method

As explained in Section 2.2, individual fish schools in the database are “ground thruthed” with the species composition from each haul. When correlated in time with a haul containing mostly a single species, the school is given a species type. The species associated with the data in the database are: Herring (HER), Horse Mackerel (HOM), Mackerel (MAC), Sprat (SPR) and Sardine (PIL).

Prior to the analysis of individual spectrum, these need to undergo three specific processing steps:

- Down sampling as one is only interested in trends over large frequency bandwidths and fine frequency resolution is not needed.
- Smoothing because the spectrum in individual cells can be very variable in frequency. Smoothing is therefore applied.
- Normalization in order to be able to compare spectra with different absolute amplitude.

The processing is as follows. First, the raw spectrum (Figure 5-1(a), black line) is down sampled and smoothed. The down sampling is using an interpolation in 2 kHz steps in the following frequency bands (Figure 5-1(a), red line): 60-80 kHz; 110-150 kHz; 170-240 kHz. The frequency bands correspond to those from each WBT channel with the first and last 20 kHz cropped. This is because the spectrum is less stable on the edge of each frequency band. The down sampling operation reduces the spectrum to 68 frequency samples. This down sampled spectrum is smoothed using a rolling average over 8 samples (Figure 5-1(a), blue line). The smoothed spectra is then z-normalized (Figure 5-1(b)):

$$S_{znorm} = \frac{S_{smooth} - \overline{S_{smooth}}}{std(S)} \quad \text{Equation 5-1}$$

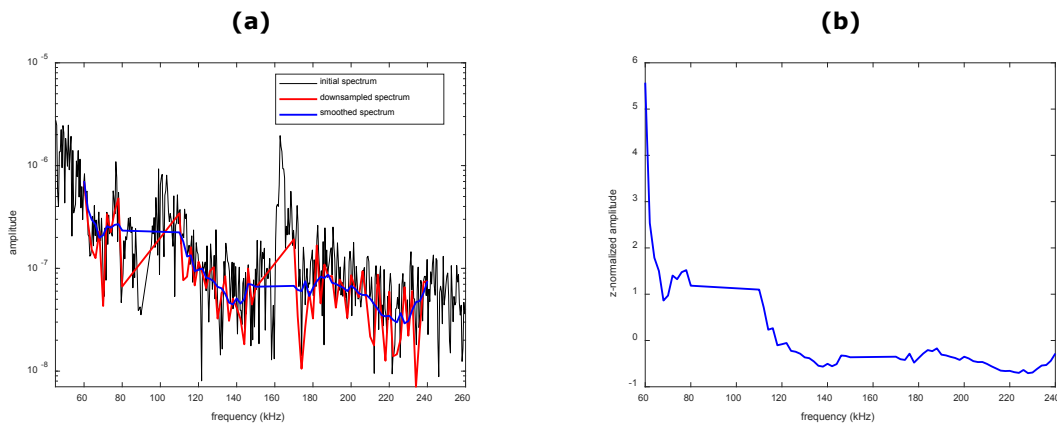


Figure 5-1: example of spectral down sampling used when deriving spectral features. (a) down sampling (red line) and smoothing (blue line) operation applied to the raw spectrum (thin black line), (b) resulting spectrum after down sampling, smoothing and normalisation.

Each z-normalized spectrum is used to compare different schools. The workflow for this analysis is shown in Figure 5-2. Each school in the data base undergoes the processing above (Figure 5-2(a)). For each school, the distance between each pair of spectra is computed, yielding a distance matrix for the school. The distance matrix in each school is used to exclude outlier cells through clustering (Figure 5-2(b) and (c)). The remaining spectra are then averaged and the corresponding spectrum is associated to the school. A new distance matrix is computed between the average spectrum from every school. Using this distance matrix, a multidimensional scaling (MDS) is used to investigate the similarities between schools and the impact of different parameters (school species, length classes, region).

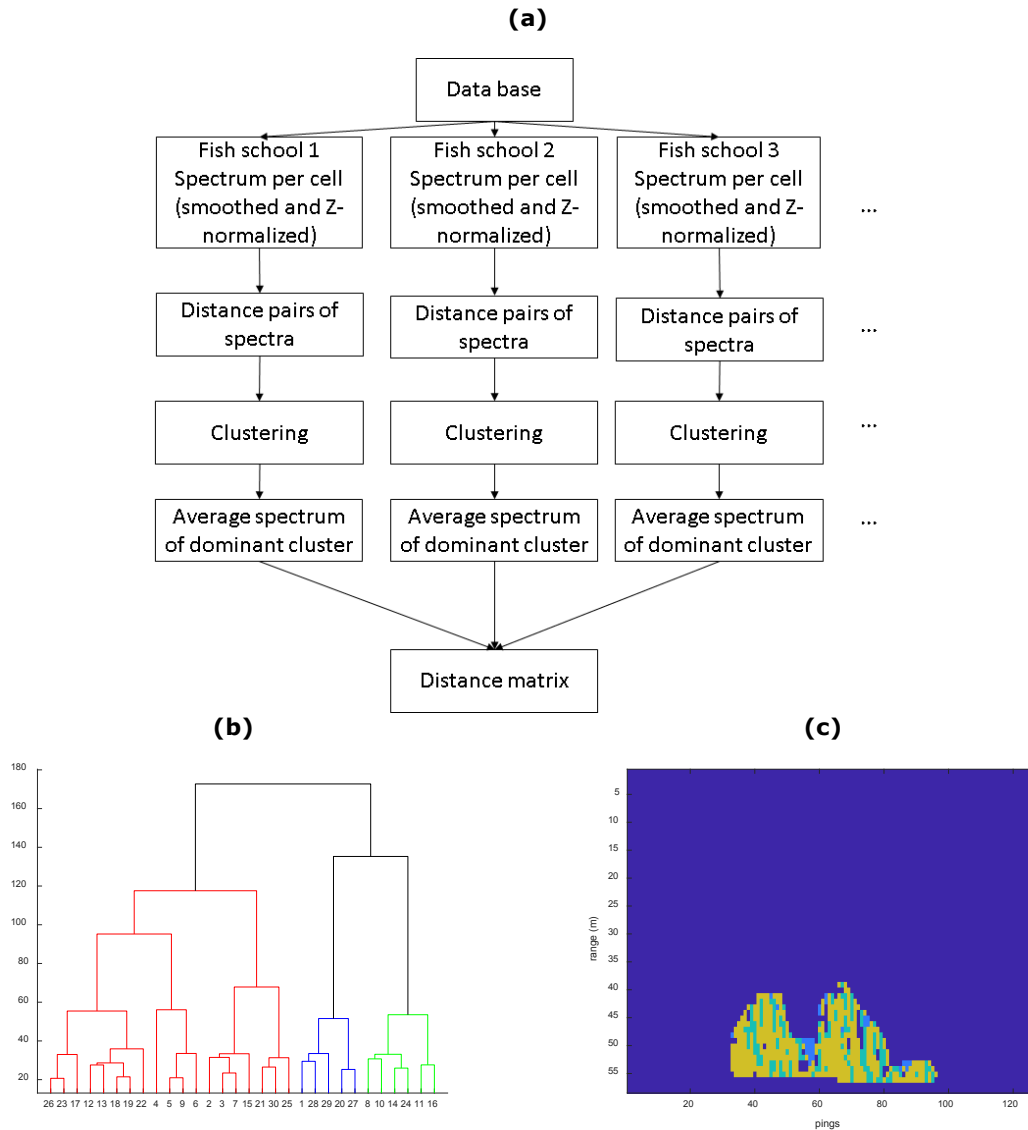


Figure 5-2: frequency response analysis. (a) *processing workflow for the frequency response analysis, i.e. comparison between different spectra.* (b) *example Dendrogram plot used to discard outlier clusters.* (c) *location of the different clusters in the school. The clusters that have less than 5% cells of the total number of cells in the school are discarded.*

5.1.2 Results

In this analysis, only the data from the Alida (SCH6) FV are included. This is because the differences with data from the Afrika (SCH24) are potentially biased due to calibration errors (see Section 3). Using the method described in Section, 5.1.1, the spectra from the different “ground truthed” schools are compared using a distance matrix. There are five different species available in the data set (Table 2-4). The differences between the schools is shown as a multidimensional plot. This type of plot allows one to visualize similarities between different instances in a reduced number of dimensions. Here, this is visualized in a two dimensional space.

First, the different species are compared in Figure 5-3. It can be observed that Mackerel schools are very distinct. They also exemplify a large spread. This suggests that the average spectrum between Mackerel schools is variable though separated from the spectra of the other species. The other four species investigated here are swimbladdered species (Herring, Horse Mackerel, Sprat, Sardine) and demonstrate a strong overlap. For Sprat and Sardine, only few schools are available in the database (Table 2-4), making this investigation limited for these species. In contrast, Herring and Horse Mackerel are represented by numerous schools in the database (Table 2-4). It can be observed that though there is overlap, some schools are distinctively separated. The use of other features than the frequency response can improve the discrimination power (see Section 6).

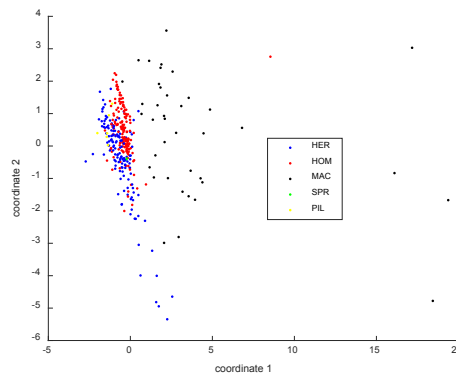


Figure 5-3: MDS plot representing the distance between each ground thruthed school in the database (for the Alida (SCH6) FV data). Each dot represents a school. The different species are differentiated with different colours: Herring (HER, blue), Horse Mackerel (HOM, red); Mackerel (MAC, black); Sprat (SPR, green); Sardine (PIL, yellow). It is important to note that only few schools for Sprat and Sardine are available and these overlap with Herring and Horse Mackerel.

Figure 5-3 shows the comparison by species. However, there are other potentially strong explanatory factors: fish length, geographical location. Using a MDS plot, the effect of these factors is shown in Figure 5-4. First, the data collected by the Alida (SCH6) FV is divided into five regions. These regions were defined manually to separate the data into the different areas of the North Sea, English Channel, and West of the UK. The five regions are shown in Figure 5-4(a) as follows:

- Region constrained as: $45^{\circ} \text{N} < \text{latitude} < 53^{\circ} \text{N}$ and $10^{\circ} \text{W} < \text{longitude} < 5^{\circ} \text{W}$. This region corresponds to the West of the English Channel (blue colour in Figure 5-4(a) and (b));
- Region constrained as: $49^{\circ} \text{N} < \text{latitude} < 52^{\circ} \text{N}$ and $5^{\circ} \text{W} < \text{longitude} < 2.5^{\circ} \text{E}$. This region corresponds to the English Channel (red colour in Figure 5-4(a) and (b)).
- Region constrained as: $52^{\circ} \text{N} < \text{latitude} < 57^{\circ} \text{N}$ and $4^{\circ} \text{W} < \text{longitude} < 8^{\circ} \text{E}$. This region corresponds to the central region of the North Sea (black colour in Figure 5-4(a) and (b)).
- Region constrained as: $57^{\circ} \text{N} < \text{latitude} < 65^{\circ} \text{N}$ and $4^{\circ} \text{W} < \text{longitude} < 8^{\circ} \text{W}$. This corresponds to the Orkney-Shetland region (green colour in Figure 5-4(a) and (b)).
- Region constrained as: $53^{\circ} \text{N} < \text{latitude} < 65^{\circ} \text{N}$ and $15^{\circ} \text{W} < \text{longitude} < 5^{\circ} \text{W}$. This region corresponds to the North/North West of Ireland (yellow colour in Figure 5-4(a) and (b)).

The similarities between the individual schools in the different regions is shown in Figure 5-4(b). One can observe that the acoustic finger prints are the highest variability in the channel and Orkney-Shetland region. Horse Mackerel schools at the West of the Channel and at the North of Ireland exemplify less variability. The finger print for Horse Mackerel in the West of Ireland is particularly distinct. This was observed in a previous study using narrow band data (EK60 and EK80 CW) [29].

The plot exemplifying the differences between length classes is presented in Figure 5-4(c) for Herring and in Figure 5-4(d) for Horse Mackerel. A length class associated with a school is determined as the mode of the length frequency distribution of the associated biological measurements. For Herring (Figure 5-4(c)), there is no clear differentiation between length classes though each length class is represented by several schools. Regarding Horse Mackerel (Figure 5-4(d)), the schools in the database are mostly associated with length frequency distributions with a mode at 23 cm. Though 26 cm length classes seem to be distinct (yellow open circles), more measurements are needed to draw conclusive relationships.

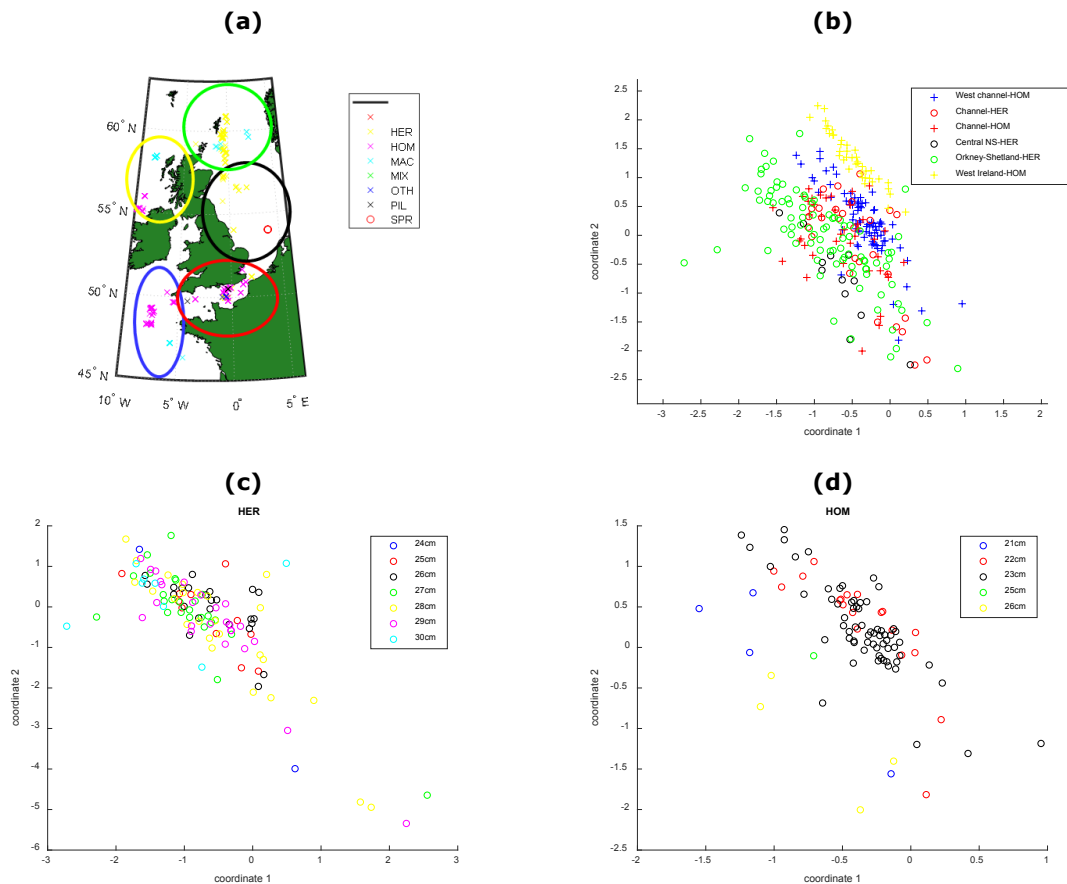


Figure 5-4: fish school comparison with respect to different areas and length classes.
 (a): Spatial division of the data. The approximate extend of the different areas is shown by circles of different colours: the yellow circle is the West of Ireland region; the green circle is the Orkney-Shetland region; the red circle is the channel region; the blue circle is the west of channel region.
 (b): corresponding MDS plot with colour scheme in line with (a) for the comparison between different geographical areas. The different species are represented by different marker types: plus signs represent Horse Mackerel schools; open circles are the Herring schools.
 (c) and (d): MDS plot comparing different length classes for the two main swimbladdered species observed in this project: Herring (c) and Horse Mackerel (d).

In previous plots, the frequency response analysis is presented in the form of MDS plots. Whilst it shows the similarity between different schools, one is unable to assess the frequency ranges that are most important to discriminate different school. In that aim, the averaged relative frequency response for the different species in the different data sets are compared. The frequency used as reference for the relative frequency response is 60 kHz (i.e. the relative level is of 0 dB at this frequency). The results are shown in Figure 5-5. Similarly to Figure 5-3, a large overlap can be observed for swimbladdered species (Herring and Horse Mackerel) and the acoustic finger print for Mackerel is more distinct. Horse Mackerel in the West of Ireland is distinctive, as observed in Figure 5-4(d) and in [29]. In term of differences in the frequency content, Herring and Horse Mackerel are most distinctive from 170 kHz to 250 kHz. This corresponds to the frequencies measured by the 200 kHz WBT channel. This distinct feature exemplifies the advantage of using broadband instead of narrowband. Whilst narrowband systems can be operated at multiple frequencies it is not able to cover frequencies as a finer resolution. The EK80 operated in CW mode is only able to provide backscattering level at discrete frequencies 70 kHz 120 kHz 200 kHz with input signals spanning only few kHz. The EK80 in CW mode would therefore not be able to capture the changes in relative level between 170 kHz and 250 kHz. It is important to note that the EK80 CW is able to also span 18 kHz and 38 kHz which are potentially informative for discriminating different species. However, a mixture of WBT channels operating in CW (18 kHz, 38 kHz) and FM (70 kHz, 120 kHz, 200 kHz) can be used to optimize the ability to discriminate species.

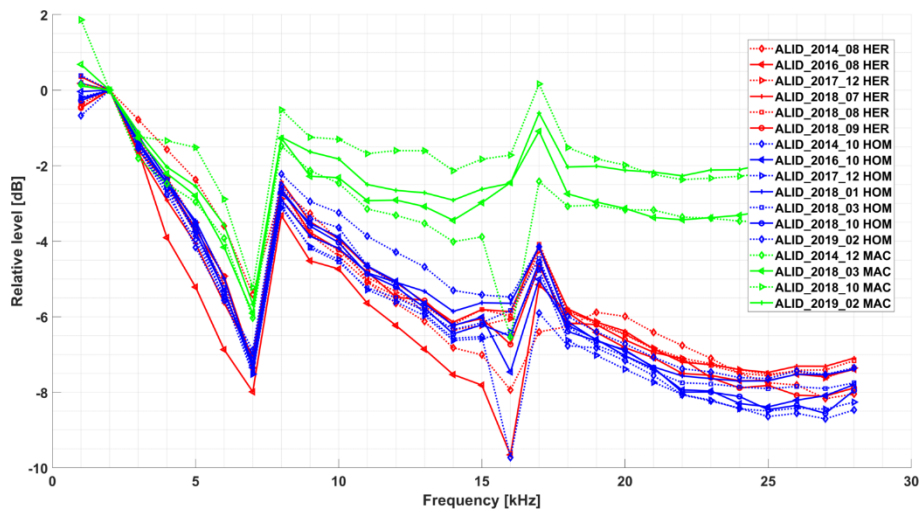


Figure 5-5: average relative frequency response (at 60 kHz) for the different data sets and species (Table 2-4)

5.2 Noise analysis

5.2.1 Background noise level

First, the background noise level is investigated for the FVs involved in the data collection (Alida (SCH6) and Afrika (SCH24)). Background noise is persistent and homogeneous through time. It is caused by the intrinsic environment of the transducer (e.g. vessel noise, electrical noise). Often, it is hard to reduce background noise level as vessel and echosounder configurations are usually fixed. Reduction in background noise level is done at the vessel design phase and/or the echosounder installation. Because this type of noise is persistent, it hampers the ability of the echosounder to use data below a certain Signal to Noise Ratio (SNR). This SNR is specific to each echosounder and decreases with frequency and range. Therefore, the larger the depth the higher the impact of noise. Whilst the sonar equation [38] can be used to calculate range independent intensity, it is only useable when the received signal is higher than the background noise. If this is not the case, the effective returned signal is masked. In short, the background noise level determines the maximum range at which each WBT can operate. In Figure 5-6 echograms are given for all three transceivers for both the FVs, together with plots of the average ping levels in the echogram. The echograms are recorded with all other interfering sonars disabled. For the purpose of background noise comparison, the data has deliberately not been compensated for propagation loss. To get an impression on background noise, one must look at the levels at which the signal is stationary, a few tens of meters beyond the first bottom hit. For this particular recording, it is clear that the background noise of the Alida (SCH6) is roughly 4 to 5 dB higher than that of the Afrika (SCH24) for all three transceivers.

It must be kept in mind though that the amount of background noise is observed to vary significantly between data sets; predominantly the Alida (SCH6) has recorded data sets with noise levels that are substantially higher. As a final illustration, echograms from the two FVs (70 WBT frequency channel) of two recording sets are shown in Figure 5-7(a) and (b). The difference in background colour can clearly be observed. This is again further exemplified in Figure 5-7(c) with an offset of 10 dB in favour of the Afrika. The difference in background noise needs to be accounted for in the data pre-processing through adjusted thresholds (e.g. to avoid miss detections).

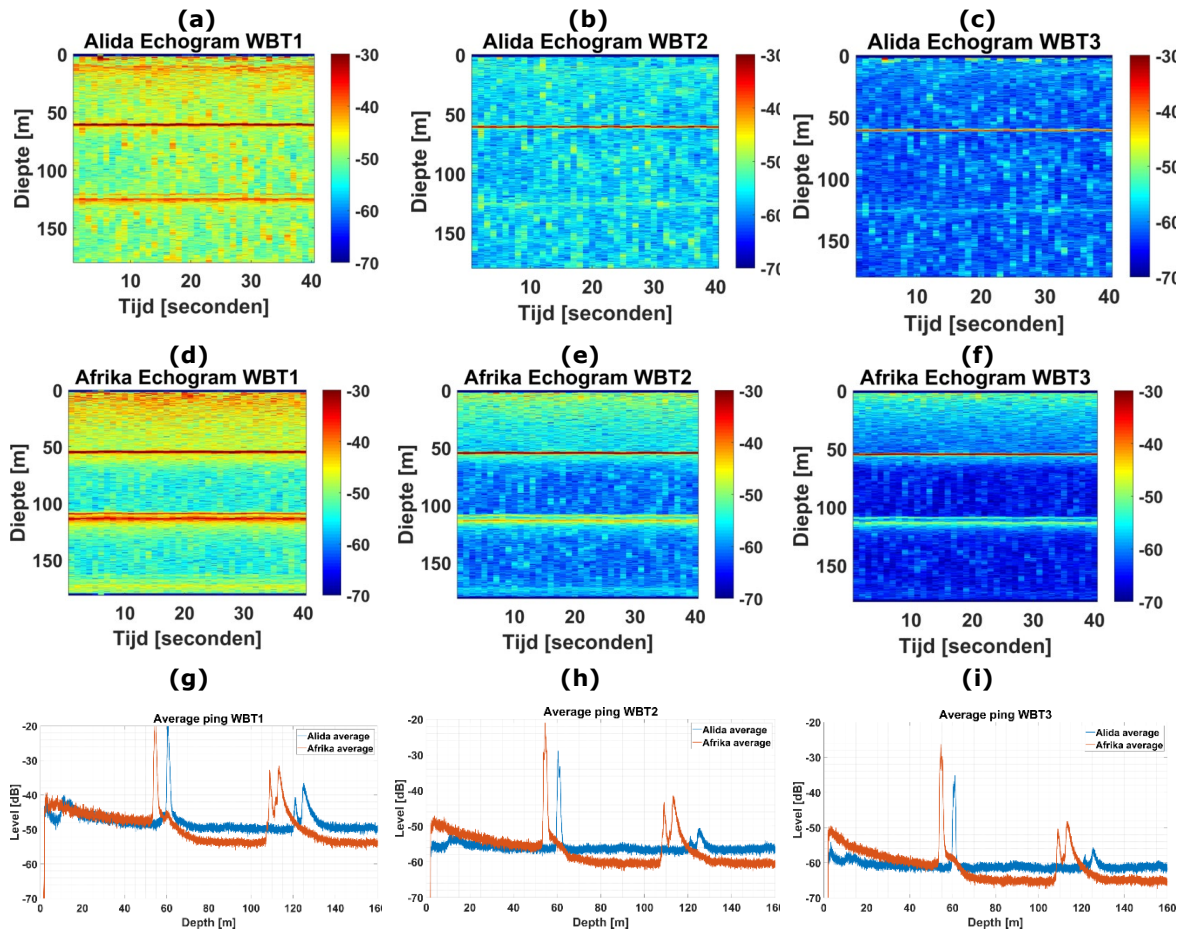


Figure 5-6: Echograms of the Alida (SCH6) (a,b,c) and Afrika (SCH24) (d,e,f) with all interfering sonars disabled. The data is not compensated for propagation loss in order to get an estimate of stationary background noise levels that are observable below the bottom return. In (g,h,i) plots of the median ping levels are given for the two vessels.

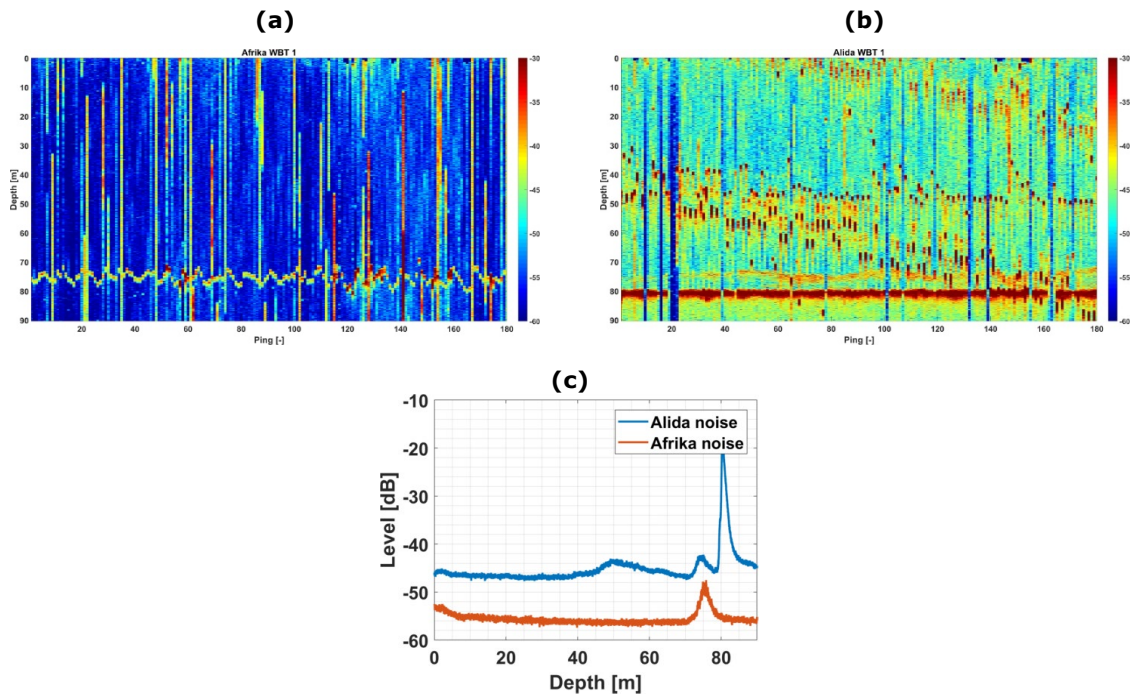


Figure 5-7: background noise level for the Alida (SCH6) and Afrika (SCH24) FVs. (a) 70 kHz WBT echogram from the Afrika (SCH24) FV. (b) 70 kHz WBT echogram from the Afrika (SCH6) FV. (c) corresponding Average (median) ping of corresponding echograms ((a) and (b)), not corrected for prop-loss.

5.2.2 Interference noise

Alongside background noise, another type of noise is common when using echosounders: interference noise. Interference noise is generated by acoustic equipment running alongside the echosounder. This is particularly the case if the frequency ranges at which the acoustic equipment operate are shared. Moreover, the transmission of an acoustic wave at a specific frequency is associated with subsequent components at higher frequencies (so called harmonics). Though the higher harmonics have a lower intensity than the fundamental component, these can spread to higher frequency bands and impact other acoustic sensors. In the case of the EK80, the harmonics from lower frequency WBT channels can impact the higher frequency ones. In practice, the use of different type of pulse (LFM up, LFM down) and sequential pinging can be used to minimize this potential noise. However, the level of cross-talk between WBT channels has not been shown particularly substantial to date.

Furthermore, on board fishing vessels, several acoustic equipment are used for probing the surrounding of the vessel. A non-exhaustive list includes [2]: echosounders, omnidirectional sonars, multi-beam. Whilst the different acoustic equipment can be synchronized, pinging in a sequence, it is at the cost of lower ping rate and expensive synchronisation unit. On board the FVs engaged in this project, no ping synchronisation was employed. As a result, interference noise was present. This is exemplified for the Afrika (SCH24) FV in echograms in Figure 5-8(a) (70 kHz WBT channel), Figure 5-8(d) (120 kHz WBT channel) and Figure 5-8(g) (200 kHz WBT channel). For the 70 kHz WBT channel, there two types of interference around 54 kHz (Figure 5-8(b)) and 80 kHz (Figure 5-8(c)), most likely induced by the use of the low frequency omnidirectional SONAR (SIMRAD SU90). Higher harmonics are present for the 120 kHz WBT channel with subsequent disturbances in the spectra of smaller amplitude (Figure 5-8(e) and (f)). For the 200 kHz WBT channel, a combination of two interferences affects the data at: 164 kHz (Figure 5-8(h), JRC doppler profiler) and 240 kHz (Figure 5-8(i), Kayo high frequency SONAR).

Though high interference noise is detrimental, it is somewhat less impactful than a high background noise. In practice, interference noise can be managed through processing with for example bad pings detection (see Section 4.1.2.6). The different level of interference noise between the vessel need to be accounted for individually through the fine tuning of the processing settings (e.g. threshold, erosion/dilation filters for the fish detection steps). This is done automatically in the demonstrator software (see Section 4.1.2.7).

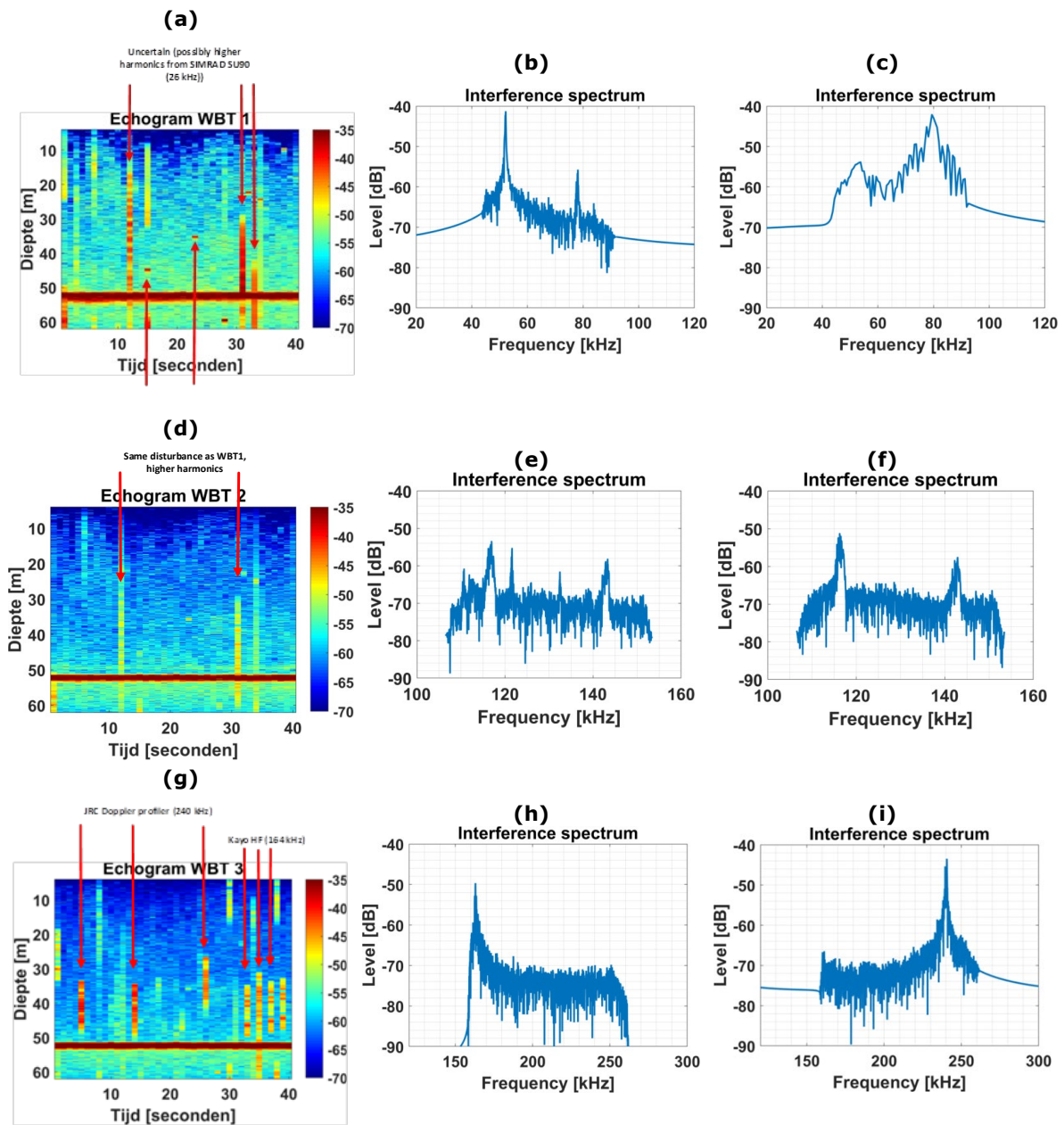


Figure 5-8: interference noise on board the Afrika (SCH24) FV. The noise is exemplified for each WBT frequency channel in echograms: 70 kHz WBT channel (a), 120 kHz WBT channel (d), 200 kHz WBT channel (g). The interference spectra for the difference interference noise are shown in separate plots: interference at 54 kHz (b), interference at 80 kHz (c), interference spectra for two pings with disturbances for the 120 kHz WBT channel (e and f), interference at 164 kHz (h), interference at 240 kHz (i)

6 Species identification

Two species identification algorithms developed separately by WMR and TNO are presented in this section. Results of the combination of these two classifiers is also shown. These methods draw on the experience gained from previous projects [10], [39] and are further developed. There is general improvements benefiting the species classification algorithm: (1) enhanced (i.e. more accurate) data pre-processing (2) access to more data (3) improved data organisation (4) development of a specific data format for algorithm training. The development of improved data organisation and specific data format allows one to reduce each data sets to fish schools and therefore to update the algorithm with new data more easily. In term of data, three data sets were available from only one vessel in the last project [10]. Within this project, the number of data sets has been expanded to twenty (Table 2-3). The species considered are Horse Mackerel, Herring, Mackerel and tentatively Sprat.

The machine learning approach used here requires the association between fish school in the database and species (Section 2.2). This is done by matching biological data with the acoustically detected fish school. As explained in Section 2.2, this is done by associating species to fish school within the timing of fishing operations that caught monochromatic species composition (<95% of a single species).

Both algorithms described here are based on the acoustic pre-processing described in Section 4. The region detected as schools (Figure 6-1(a)) are further divided into cells (Figure 6-1(b)) while noisy sections (e.g. interference with other acoustic equipment such as omnidirectional SONARs) of the echogram are not considered. In a ping, a cell is a window of 1.6 m in range (i.e. height). Specific processing details are given in Section 4.1.2. For each cell, a specific set of features are calculated. Features are divided into time signal features and spectral features. The features effectively are a reduction of data to make sure a classifier can derive boundaries to distinguish species. Hence, the features are derived such that data is reduced, while maintaining important signature information specific to a certain species. A machine learning approach is then used to derive an algorithm able to differentiate different species based on these features. The set of features used is specific to each algorithm (WMR and TNO classifiers). Results from the combination of the classifiers is also provided in this section.

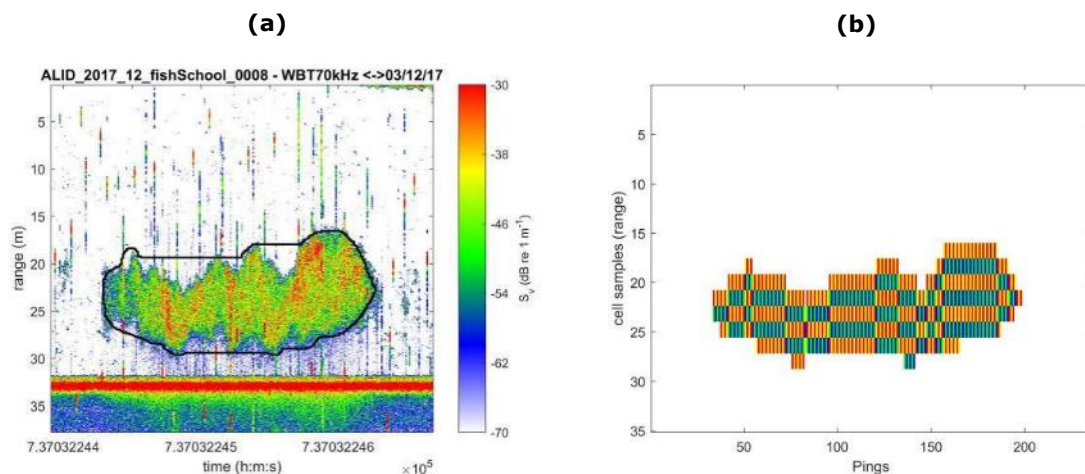


Figure 6-1: example of a fish school being divided into different cells. Each cell is associated with its time signal and corresponding spectrum. This constitutes the basis for the analysis and classifier training. Classification is computed for each cell. (a) Echogram of a fish school. (b) corresponding cell division.

6.1 TNO classification

6.1.1 Method

Deriving suitable features is key for classification to work well. Figure 6-2 provides an example plot of two extracted features for the different species. Each point represents the feature values of a single cell. It is clear that, as expected, the feature values of Herring and Horse Mackerel are closer to each other than those of Mackerel. The lines indicate classification boundaries derived by different types of classifiers. The side of the boundary at which a feature pair resides, determines to which species type it would be assigned. The type of classifier determines two major aspects of the classifier:

- Its performance/score
- Its robustness for variation within species

A more complex classifier can give better performance on a given data set, but it can potentially derive boundaries that are not natural and/or can be driven by noisy data points. Boundaries also can become too strict, leaving no space for any variation within a species. Hence, it should always be kept in mind that the available data set is only a subset of the species. It does not per definition represent the signature of the entire species or contain all possible variation within a species. It is good practice to find a balance between performance and robustness, where a more simple classifier can get preference because of its robustness on the cost of slightly reduced score. Classifiers used in the examples below (Figure 6-2) are:

- linear classifiers: Normal densities based linear classifier (LDC/Bayes Normal 1), Nearest Mean linear Classifier (NMC)
- quadratic classifiers: Normal densities based quadratic classifier (QDC/Bayes Normal 2), Uncorrelated normal densities based quadratic classifier (UDC/Bayes Normal U)
- other: Support Vector Classifier (SVC), Parzen Classifier (ParzenC), Nearest Neighbour Classifier (KNNC)

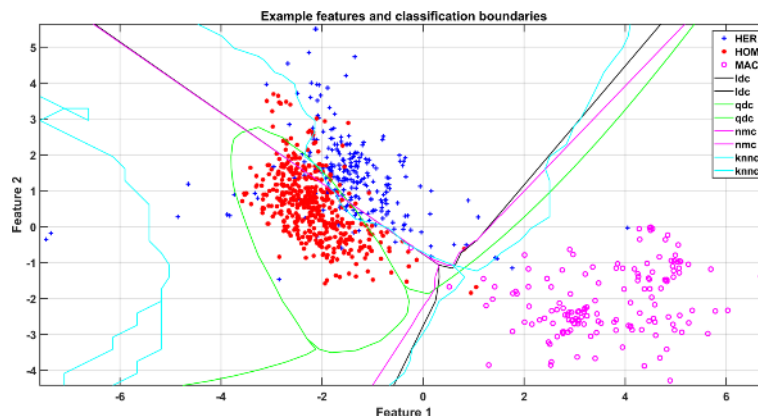


Figure 6-2: Plot of two example features computed for the entire dataset. Each marker indicates the feature values of a different species. The coloured lines indicate the species boundaries derived by a number of different types of classifiers.

A large number of features has been derived manually, which are not all used in classification. Reduction of the number of features is required to avoid the risk of overtraining, which means a classifier has high performance for the data set on which it is trained, but lacks robustness for new datasets. Again, a balance must be found between the number of features used and the classification performance, where a smaller number of features is preferred.

Features are ranked based on how well they can discriminate between species. This is done using forward feature selection [40] based on the sum of the Mahalanobis distances [41]. The ranked features are used in the evaluation of different types of classifiers. In classifier evaluation, different classifiers are trained and tested using an increasing amount of features. This gives insight in the optimal number of features to use. Figure 6-3 gives a plot of classifier evaluation for an increasing number of ranked features. Depending on the type of classifier, a number between 5 and 10 features is a good choice, leading to an average score of roughly 85 to 95 %. The use of a larger number of features will lead to overtraining for some classifiers (curse of dimensionality [42]).

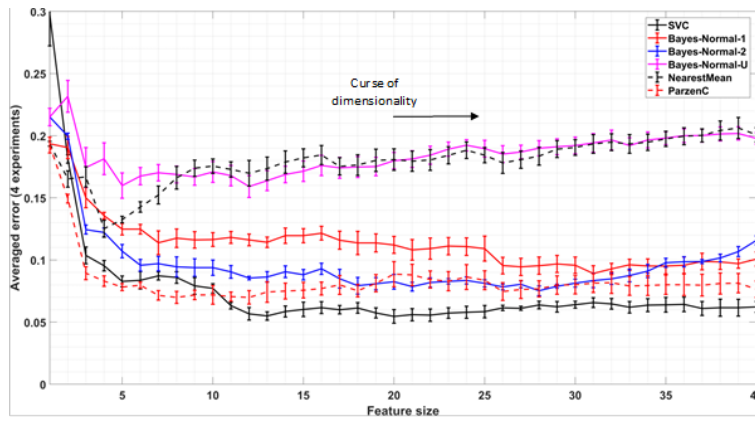


Figure 6-3: Plot of the expected classification performance as a function of the number of features used. Each line represents the result of a different type of classifier.

6.1.2 Results

The selected features and classifier are evaluated using the recorded data sets. Classification scores are estimated by multiple test iterations of a classifier. Each iteration, the total set of data is split in an independent training set and test set. The classifier is trained with the training set. The trained classifier is evaluated with the test set. Finally, the scores of the iterations are averaged to get a performance indication.

To avoid performance biases, some additional constraints are set to the training and test sets:

- Each fish school is bound to contribute only a certain maximum number of cells to the training and test data sets. This is done to avoid very large schools to dominate the process. It is not desired if the overall classification score would be 95% because a single, large school scores 100% and 10 small schools score 0%.
- Also each fishing trip is bound to contribute only a certain maximum number of cells to the training and test data sets. Since there is more variation within a species *between* fishing trips than there is *within* a fishing trip, the same bias is avoided that a trip with a large number of schools scores perfect, while some trips with a few schools score very poor.

Two types of results will be described below. In the first section the data of all trips will be used, while still meeting the above constraints. In the second section, the performance for each trip is analysed individually to recognize any remaining biases or overtraining.

6.1.2.1 Main TNO classifier

In the first test, the data sets of all fishing trips are collected to form one big data set with the three main species (HER, HOM, MAC). The cell selection criterion described above is applied, such that each trip and each school roughly delivers an equal amount of input data. Figure 6-4 plots the resulting confusion matrix averaged over 20 iterations on the total collected data set. The numbers on the diagonal are the classification scores per species.

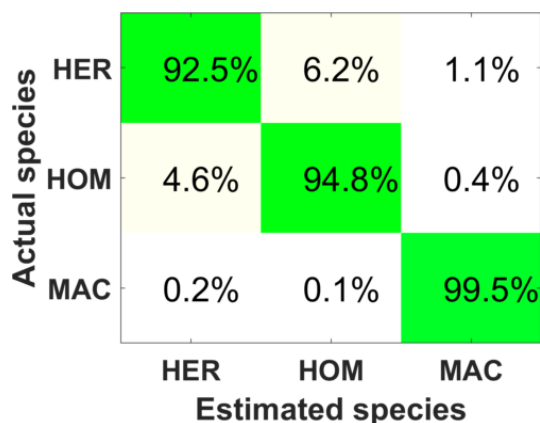


Figure 6-4: Confusion matrix for the used classifier when using all data sets. The percentages on the diagonal are the scores per species type.

The classification performance is computed for each individual fishing trip to recognize any remaining trip biases. In addition, leave-one-out tests are performed for each trip. This means that all data of the concerning trip is removed from the *training* set. A classifier is then trained with all data from the other trips, of which the classification performance then is evaluated on the concerning trip. This test gives a reasonably good impression on the robustness of the classifier and in particular the performance that can be expected in practice. Figure 6-5 displays the results of both types of tests. Data set-*inclusive* test results are indicated by a cross; data set-*exclusive* results are indicated by the filled dot. Conclusion is that the inclusive and exclusive results on average are relative close to each other. This indicates the classifier is robust against variations within a species. Again, it should be noted that the classifier is designed as such: not the highest score possible, but with significant robustness against variation. There are two data sets that show a larger difference:

- ALID/2017/12: This data set, recorded in the Channel, seems very important in defining the boundaries between Herring and Horse Mackerel. The difference between these species in this data set is the smallest of all data sets. The average relative spectral difference is in the order of 0.4 dB, which is very low, not yet taking into account variations within the species. Hence, it should preferably be included in training.
- ALID/2019/02: This set of Horse Mackerel data is the only one recorded on the North-West of Ireland. Earlier research [29] has shown that this species has a different frequency spectrum than at other locations, possibly caused by significant differences in fish size. This difference is confirmed by the data recordings. The classifier is able to recognize this new pattern successfully (95% score), however the score is lower (64%) when it has not learned the new pattern yet.

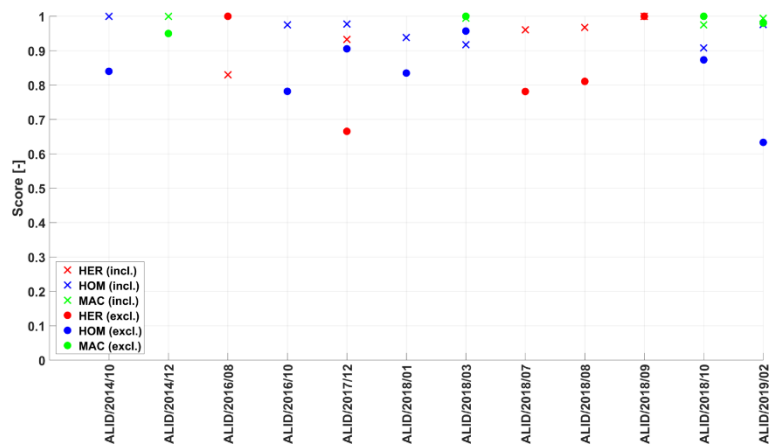


Figure 6-5: Classification score per fishing trip. Each trip can contain multiple species types. Crosses indicate the results for data set-inclusive training, filled dots indicate the results for data set-exclusive training.

All results described above apply to homogenous schools of fish. In practice this means that at least 90% of the part of the school that was actually caught, was reported to consist of a single species type. The current approach with cell-based classification allows classification of mixed schools as well. Though the results are difficult to verify, skippers report successful classification of mixed schools of Horse Mackerel and Mackerel or Herring and Mackerel. As an illustration, Figure 6-6 shows an example result of a mixed school consisting of Herring and Mackerel.

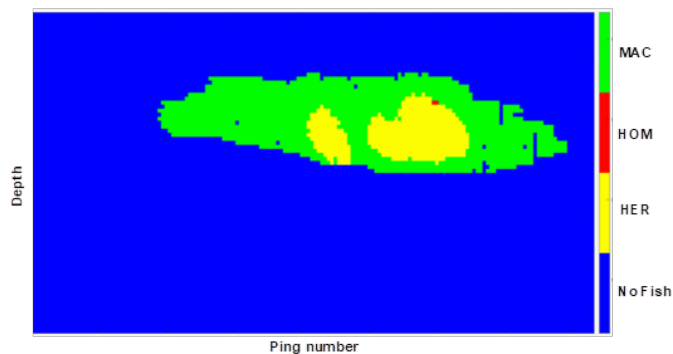


Figure 6-6: Example of the classification result of a school that likely contains different species types.

6.1.2.2 Classification of Afrika data

All results described in this section are generated with data recorded by the Alida, since the Alida has recorded significantly enough data to say something statistically meaningful about classification performance. Another issue still remaining is accurate calibration which would allow merging of data sets between vessels, but also apply a classifier trained with data on one vessel to data on another vessel. Despite these issues, still a classification result will be given for the data recorded by the Afrika. Figure 6-7(a) provides the classification results of the relatively small amount of data recorded by the Afrika, when training the classifier with the Afrika data. The scores are in line with the scores for the Alida, which is expected. Figure 6-7(b) finally shows the results when applying the classifier trained with Alida data to the Afrika data set. Both data sets are effectively processed without any calibration set, since the current calibration results are not accurate enough yet. Hence, the transceiver responses of the two vessels in this case are taken to be equal. Though the scores of the Alida classifier on the Afrika data are not very bad, proper calibration can definitely improve the classification results by 10 to 15 %.

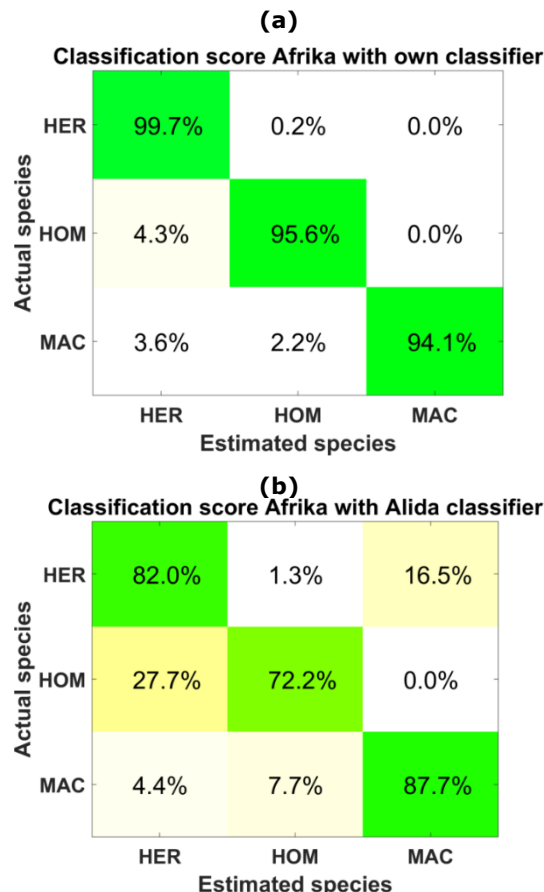


Figure 6-7: Confusion matrix when classifying Afrika data with a classifier also trained with Afrika data.. The percentages on the diagonal are the scores per species type.

6.1.2.3 4th species inclusion

The described results provide the classification performance for three species. One of the goals of the project was to add a 4th species to the classifier. However, hardly any data of a 4th species has been collected by the Alida (only 7 Sprat schools, Table 2-4). Though it is statistically all but significant, some brief tests have been performed to classify Sprat as a 4th species, using the few schools collected. Figure 6-8 shows the confusion matrix. The average score of Sprat is around 67%, while the score of Herring slightly decreases to 80%. There is overall a decrease in accuracy compared to the baseline classifier (Figure 6-4, three species: HER, HOM and MAC). This decrease is induced by the inclusion of the fourth species and is due to: (1) the closeness of SPR with HER and HOM; (2) the low amount of data available for SPR. The low amount of data available for SPR is particularly detrimental in the training phase of the algorithm. In practice, the amount of data used for training must be of equal proportions between the different species and be representative enough (different depths, geographical areas, time of year etc.). As a result, the inclusion of SPR lowers the amount of data used for training. The training is in turn less

representative of the variability in the data for HER, HOM and MAC. The relative conservative score of 67% can be declared by the fact that Sprat is acoustically very similar to Horse Mackerel. In practice there is an advantage however, since Sprat and Horse Mackerel do not reside in the same area. Hence, in these areas Horse Mackerel can be replaced by Sprat in the classifier, which means classification could also be done successfully for Sprat, based on this small set of results.

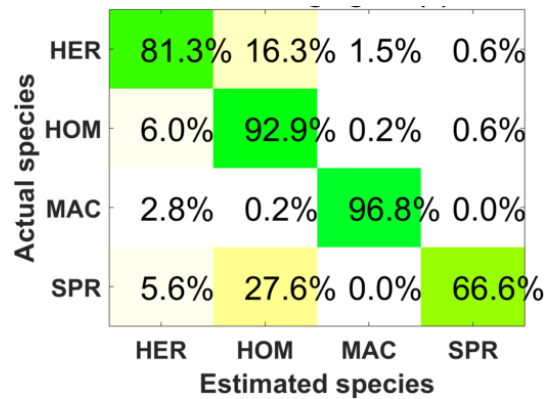


Figure 6-8: Confusion matrix when adding Sprat as a fourth species. Sprat is partly classified as Horse Mackerel, but since these two species do not reside in the same area, Horse Mackerel could be replaced by Sprat in the relevant areas.

6.1.2.4 Classification resolution

As described earlier, to be able to support classification of schools containing a mix of different species, schools are divided into smaller chunks, which are classified individually. The smallest possible chunk is called a cell and is chosen to be defined as a window of 1.4 m in length within a single ping. A cell can be classified individually. Delivering a classification result per cell will result in a highly detailed image that defines the distribution of species within a school. The downside of classifying on a per-cell basis is that the data within a cell can be very noisy as result of reflections of sound within the school. This leads to frequency dependent constructive and destructive interference, which may cause the perceived spectrum to deviate from the actual spectrum of the corresponding species type.

In order to increase stability of the perceived spectrum, neighbouring cells can be combined by statistical averaging or median filtering at the cost of reduced classification resolution; i.e. a resulting classification image with less detail. However, because of the small size of a cell, it should be kept in mind that single cell resolution will practically not be required, given the fact that also in mixed schools, species of the same type are typically clustered together spanning a few square meters in size. To this end different settings for cell averaging have been analysed. Figure 6-9 schematically depicts this median filtering process. For each cell, neighbouring cells are selected up to a maximum distance, defined by the number of averaging cells. These cells are combined by taking their median to construct a new value for the considered cell, in practice called a moving median filter. This process is done for the spectra and for all feature values.

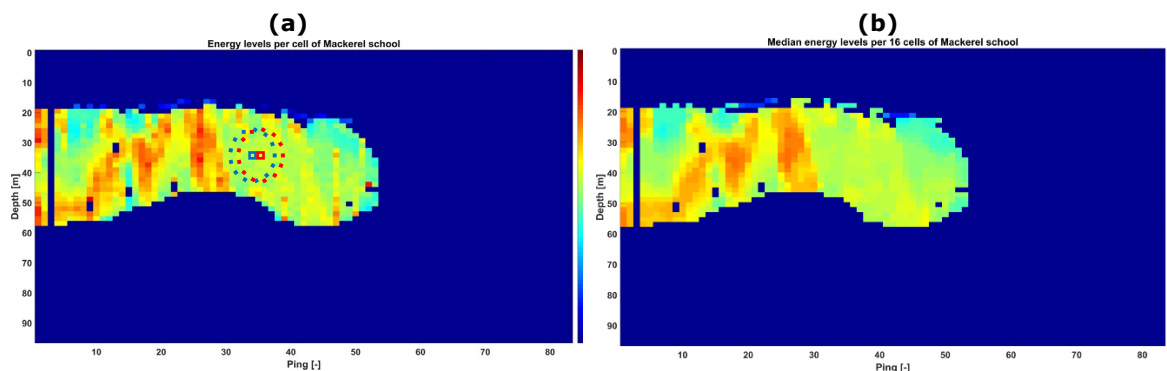


Figure 6-9: Illustration of the cell averaging process. The original cell values (a), in this case simply representing energy, are filtered with a sliding median window to deliver the averaged values (b). The resulting cells are still put into the classifier individually.

Figure 6-10 shows the spectra of a school of Herring and a school of Horse Mackerel for different numbers of averaging cells. The use of more averaging cells corresponds to the average spectrum of a larger area within the school. The two darker lines indicate the average spectrum of the entire school. The light-coloured lines represent the averages of the sub-averages of the schools. It is clear that, as expected, a decrease in number of averaging cells increases the variability in the spectrum. As an indication: 32 cells correspond to an area in the school of roughly 8 x 8 m.

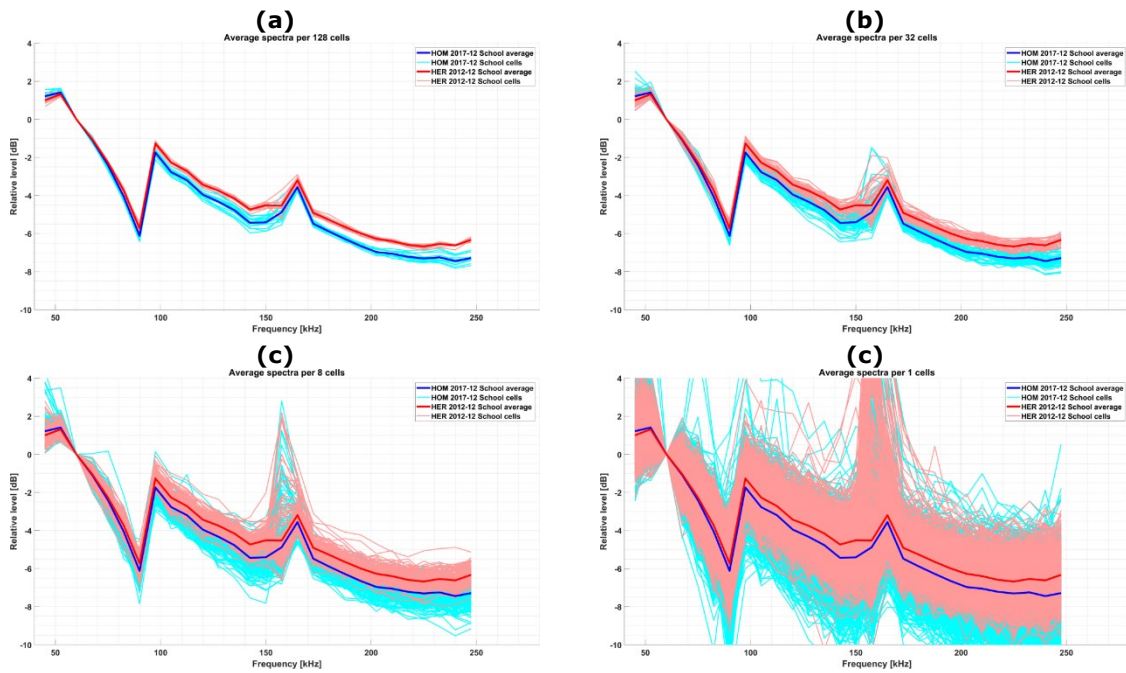


Figure 6-10: Spectra for different numbers of cells used in averaging for Horse Mackerel and Herring. The use of more cells leads to more stable spectra. Since the two species types are very similar, it is beneficial to have stable spectra. (a) averaging over 128 cells. (b) averaging over 32 cells. (c) averaging over 8 cells. (d) no averaging.

Figure 6-11 shows the classification results for a number of fishing trips when applying different numbers of averaging cells. It is clear the scores increase when using more averaging. It should be mentioned that the utilized features and type of classifier are chosen to work with averaged cells. It is well possible that a more complex classifier performs better with a smaller amount of averaging cells. However, the current classifier and features have been chosen for their robustness, in combination with the fact that single cell classification in practice is not a requirement. When schools would be expected to be homogenous classification scores would head to 100%. The current number of averaging cells in the demonstrator software is set to 64.

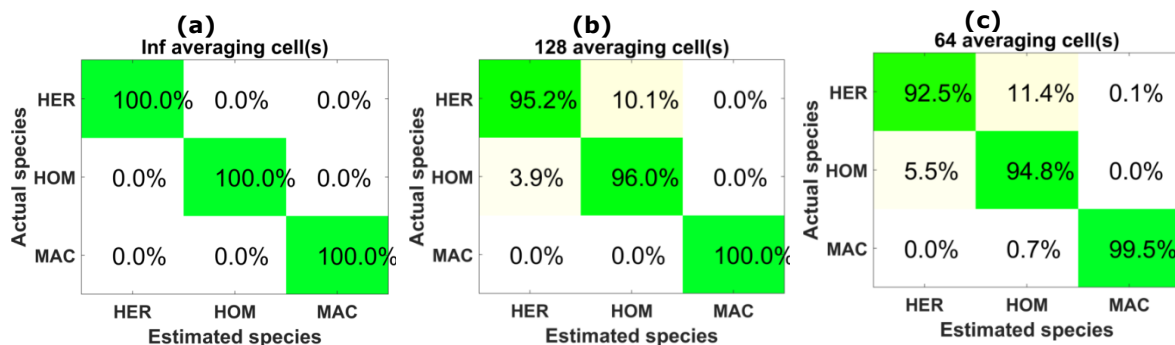


Figure 6-11: Confusion matrices indicating classification scores per species for different numbers of averaging cells. The use of fewer averaging cells will decrease the classification performance. (a) averaging over all available cells for each school. (b) averaging over 128 cells. (c) averaging over 64 cells.

6.1.2.5 Sensitivity to calibration error

In the sets of available species, Herring and Horse Mackerel have a very similar acoustic response. When looking at the average spectra of these two species, the relative differences between the spectra are in the order of 0.5 to 1 dB. This accounts for the average species spectrum. Moreover, between schools of the same species, there is also some variation, as well as within parts of the school. Spectral variations within a species can be the result of differences in fish size or composition.

As a result of the small differences, very high accuracy of all processing steps is crucial. One of the important steps in cross-vessel applicability is calibration of the acoustic transceivers. In order for a classifier that is trained with data recorded on one vessel, to give a similar result with the hardware on another vessel, calibration has to be performed with high accuracy. This section will evaluate the effect of calibration errors on the classification result to get an impression on required calibration accuracy.

Several types of calibration errors are assessed with varying magnitude:

- Adding a linear trend as function of frequency to one or more transceivers.
- Adding an offset to one of the transceivers. Note that addition of the same offset to all transceivers has no effect since the relative spectra are used.
- Adding a resonance curve to one or more transceivers.

In this test, a classifier is trained with the original fish school data. Subsequently the school data is being altered using the modified calibration values. The trained classifier is evaluated/tested with the new, modified data. The difference in classification scores between the original and the modified set gives an indication of the effect of the error on classification. For the test only Horse Mackerel and Herring are used since these are the ones predominantly affected by small errors.

Figure 6-12 shows classification scores for the different types of errors, with Figure 6-12(a) and (b) showing the reference situation with no modification of the calibration values. Though the results represent only a subset of potential errors, it gives a first impression on the effect of calibration errors on the classification scores. Based on the given results, offset errors to a particular WBT seem to result in the largest error, especially for the 200 WBT channel. As also expected from the spectral plots, an error of 1 dB severely deteriorates the classification accuracy. Taking into account some additional variation within a species to come in yet unknown data sets, calibration accuracy should definitely be better than 0.5dB, and preferably below 0.3 dB.

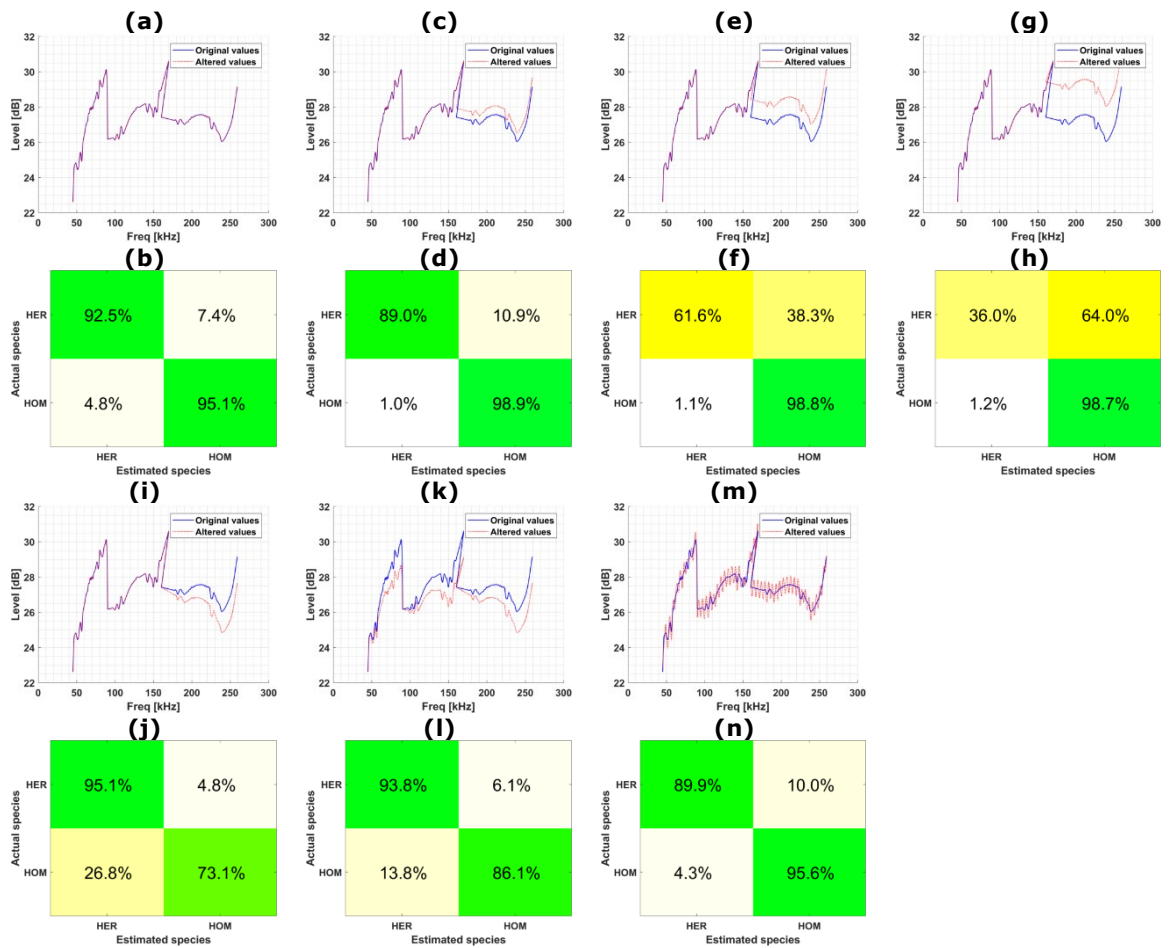


Figure 6-12: results of classifier testing against erroneous calibration. Each scenario has a figure pair showing the change in calibration gain and resulting classification accuracy.

(a) and (b): reference classification score with unaltered calibration values

(c) and (d): Classification score with 0.5 dB offset added to the 200 kHz WBT channel.

(e) and (f): Classification score with 1 dB offset added to the 200 kHz WBT channel.

(g) and (h): Classification score with 2 dB offset added to the 200 kHz WBT channel.

(i) and (j): Classification score with 1 dB linearly increasing trend added to the 200 kHz WBT channel.

(k) and (l): Classification score with 1 dB linearly increasing trend added to all WBT channels.

(m) and (n): Classification score with 0.5 dB sinusoid added to all WBT channels.

6.2 WMR classifier

In a previous project [10], the frequency response classification was performed using a dynamic factor analysis [43]. This allowed to determined different frequency response trends between fish species. In the realFishEcho project, a machine learning approach is used based on signal features, more specifically a Neural Network (NN). Neural Network was proven to be effective solely based on frequency response using a small data set [39]. The benefits of using a NN are: (1) its known ability for pattern recognition [44]; (2) the easiness to improve training as the number of data sets available grows; (3) the potential ability to provide information at a cell level; (4) the probabilistic results.

6.2.1 Method

6.2.1.1 Background

The WMR classification uses a machine learning approach, more specifically a Neural Network method (NN) [12], [44]. This consists of interconnected processing elements that after appropriate training are able to solve a specific problem. Here, the problem consists on determining the fish species given a set of features derived for each cell (Figure 6-1).

A NN is typically constituted of several layers of neurons: input layers, hidden layers where undergoes the classification process (through application of weights, biases and operators) and output layers, yielding the final scores for the classification.

Here, the input to the NN is a set of spectral and time features (Section 6.2.1.2) calculated for each cell for the three WBT channels (70 kHz, 120 kHz, 200 kHz). Prior to entering the NN, these are normalized, a process that consists of bounding the maximum and minimum of each spectrum between -1 and 1 based on two threshold boundaries. The features are expected to vary between fish species, length classes and to a lessened extent with depth and area [2], [10], [45]. This is further fed into the various layers of the NN. For the purpose of pattern recognition, only one hidden layer is used here. The subsequent equation of the NN is:

$$a = f_2(w_2 \times f_1(w_1 \times p + b_1) + b_2), \quad \text{Equation 6-1}$$

with a the vector of outputs (fish species classes), p the vector of inputs (features for a single cell). The quantities w_1 , b_1 and f_1 are respectively the weight matrix, bias vector and operator function for the hidden layer and w_2 , b_2 and f_2 the same quantities for the output layer. The adjustment of the weights (w_1 , w_2) and biases (b_1 , b_2) is performed prior to the use of the NN in a real situation, during a process a training, validating and testing the NN. A schematic of the NN architecture used here is shown in Figure 6-13, it consists of:

- 31 inputs (31 features for each cell)
- 3 outputs (4 for the inclusion of Sprat as an additional species)
- 62 nodes in the hidden layer.
- A sigmoid function as operator for the hidden layer
- A softmax function as operator for the output layer

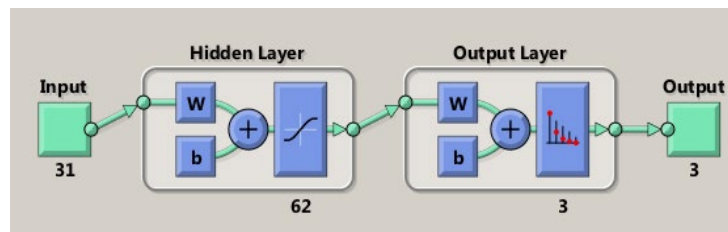


Figure 6-13: schematic of neural network architecture.

6.2.1.2 Features calculation

A combination of time and spectral (i.e. frequency) features are used for the WMR classifier. More specifically, a total of 31 features derived for each single cell. These are summarized in Table 6-1. It is important to note that the time features are derived for each WBT channel (70 kHz, 120 kHz, 200 kHz). Therefore, each time feature consists of three values.

Table 6-1: listing of features used for the WMR species identification. The time features are derived for each WBT channel and are then a set of 3 value each.

| Feature name | Feature type | Number of features | Description |
|--|--------------|--------------------|--|
| S_v | Time | 3 | backscattering volume coefficient [40] down sampled at the cell level. |
| SNR | Time | 3 | difference in dB between S_v in the cell and S_v in the same ping but outside the masked pixels (fish school detection, Section 4.1.2). |
| mean | Time | 3 | Mean of distribution estimated by fitting a normal distribution to the distribution of S_v in the cell. |
| standard deviation | Time | 3 | Standard deviation of distribution estimated by fitting a normal distribution to the distribution of S_v in the cell. |
| kurtosis | Time | 3 | Kurtosis of distribution of S_v in the cell. |
| skewness | Time | 3 | skewness of distribution of S_v in the cell. |
| number of peaks | Time | 3 | estimated using a peak detected on the amplitude signal (beam formed and matched filtered), using a threshold for the peak prominence of 0.25. |
| 10 principal components spectral decomposition | Spectral | 10 | Decomposition of relative spectra into 10 principal components based on prior SVD decomposition. |

Prior to the calculation of the spectral features, the spectrum of cell undergoes a specific processing. The spectrum in each cell is down sampled, smoothed and z-normalized using the approach described in Section 5.1.1. A semi-random selection of cells is then selected for further Single Value Decomposition (SVD) of the matrix of selected S_{znorm} , S_{znorm} . This matrix is of size $n_s \times n_{sel}$ with n_s the number of sample of a single spectrum (down sampling to 68 samples is used here) and n_{sel} the number of selected cells (user defined). The specific selection process is further explained in Section 6.2.1.3. The SVD of S_{znorm} yields [44], [46]:

$$S_{znorm} = U \times S \times V^T. \quad \text{Equation 6-2}$$

The matrix U is square of size $n_s \times n_s$ and a truncated U_{trunc} version (of size $n_s \times n_{trunc}$) can be used to truncate S_{znorm} vectors into n_{trunc} components:

$$S_{trunc} = S_{znorm} \times U^T. \quad \text{Equation 6-3}$$

A truncation number $n_{trunc} = 10$ is used here, i.e. each spectrum S_{znorm} of n_s samples is truncated into 10 components. This constitutes the 10 spectral features for each cell. Whilst time features can be directly derived from each cell, the processing employed for spectral features implies that an external matrix (U_{trunc}) is needed for the truncation of the spectrum Figure 6-14.

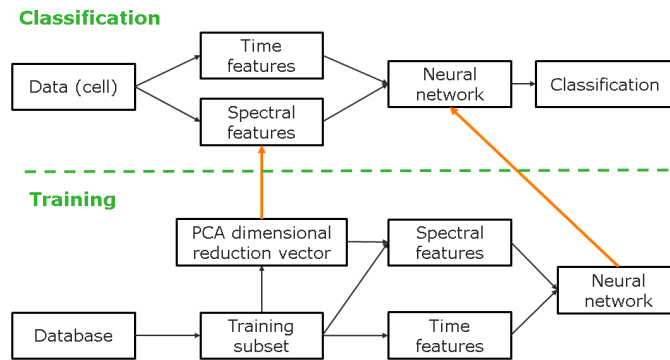


Figure 6-14: workflow diagram for training and operational use of the WMR classifier. For the training of the NN, time features are derived from each cell but spectral features use the spectrum from each cell and a matrix U_{trunc} that was calculated from the training set. In operational use, the algorithm uses two inputs: the training neural network and the matrix U_{trunc} . The latter is used for the calculation of spectral features.

The feature calculation is applied to all cells from all the recorded schools across the data sets. Averaging of each features across cells can also be applied (similarly to Section 6.1). Only a subsample is used for training, the other cells are used to assess the performance of the algorithm (Section 6.2.1.3).

6.2.1.3 Neural network training and assessment

In order to train the NN and build the U_{trunc} matrix (for the calculation of spectral features), a specific strategy is employed in order not bias the training set toward: (1) large schools in data sets; (2) large data sets compared to smaller ones. The selection process for the data selected for training is done for each selected species as follows:

1. Define number of cells per species $n_{species}$.
2. For each single species, the $n_{species}$ cells are spread equally across the relevant data sets (i.e. those containing the currently selected species). Each data set have an allocated $n_{alloc} = n_{species}/N_{data\ sets}$ with $N_{data\ sets}$ the number of data sets with the current species. This works under the following constraint:
 - If $n_{alloc} > n_{cells\ set}/2$ (with $n_{cells\ set}$ the number of cells in the selected data set), $n_{alloc} = n_{cells\ set}/2$.
3. For a species within a data set, the n_{alloc} cells are spread equally between the schools in this data set. Each school of the selected species have $n_{school} = n_{alloc}/N_{schools}$ with $N_{schools}$ the number of schools of the selected species for the selected data set. This works under the following constraint:
 - $n_{school} > n_{cells\ school}/2$ (with $n_{cells\ school}$ the number of cells of the selected school), $n_{school} = n_{cells\ school}/2$.
4. Cells non allocated in the process are reallocated to eligible data sets and schools.

For each school, the defined n_{school} are selected randomly. The total number of cells used for training is then $n_{species} \times N_{species}$ and only constitute a small subset of all the data available.

For the training of the NN, the training subset is divided into three components:

- Training (70% of subset): these data are used to compute weights and biases through various iterations.
- Validation (15% of subset): these data are used to validate the NN and make sure it does not become too specialised with respect to the training data.
- Testing (15% of subset): these data are used to assess the performance of the NN after the training it completed.

The training process is exemplified in Figure 6-15(a). The training component is made of several input samples (time and spectral features from cells) together with associated outputs (fish species classes). The weight and biases are adjusted for each sample using a backpropagation algorithm[44]. This is repeated several times over the training data set component and each iteration is called an "epoch" (x-axis in Figure 6-15(a)). At the end of each epoch, an error index is calculated (y-axis in Figure 6-15(a), cross-entropy [44] in this instance) for the training data set and the validation data set. The validation component is used to ensure that the NN does not loose generality (i.e. is not too specialised to the training component). Therefore, the optimal training is where the performance of the validation component is maximized (i.e. minimized error). After the end of each epoch, the NN is applied to the

testing data set component. The training performance can be summarized in a matrix of scores (so called confusion matrix, Figure 6-15(b)).

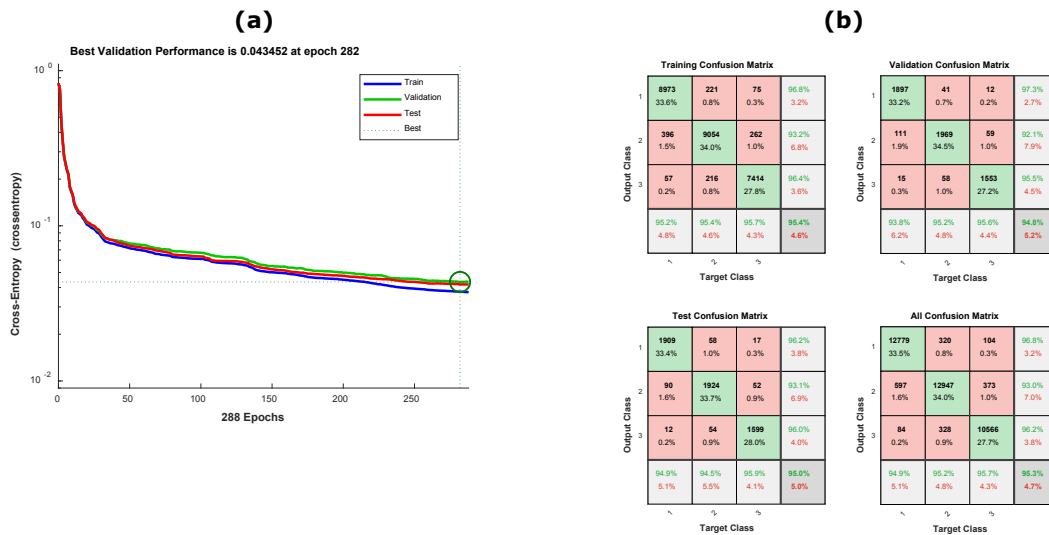


Figure 6-15: results from a NN training process. (a) Cross-entropy error index across epochs. (b) confusion matrix summarizing scores for training, validation and test data sets.

The training of the NN only applies to a small number of samples, selected using the routine described in Section 6.2.1.3. Typically, one uses $n_{\text{species}} = 5000$ to 10000 samples per species. For example, the total number of samples available for Horse mackerel using all the data sets from the Alida (SCH6) FV is 140000. The testing of the NN is done through two separate analysis:

- An analysis using all the samples not used for training
- A one data set out analysis: within a pool of data sets, a NN configuration is tested blindly by training the NN on all data sets except one sequentially for all data sets available. For example, in the case of the classifier based on the Alida (SCH6) FV data, there is 13 data sets available. The main WMR classifier is derived using a subsample of the data and tested against the cells not selected for training. In addition, training over 12 data sets and testing against the data set not included is performed. This mimics the situation encountered in the field where the data collected will not be included for training of the NN.

Classification is performed per cell (allowing the classification of mixed schools) and tested against the different data sets. Two classification examples (Herring and Mackerel schools) are shown in Figure 6-16 together with the associated echogram. The classification output from each cell takes the form of a probability for each species. The determined species is taken as the one associated with the maximum probability score amongst the classified species. It is important to note that the classifier allocates species to each cells based on the species input during training. Therefore, the classification of species outside the one used for training will result in misclassification.

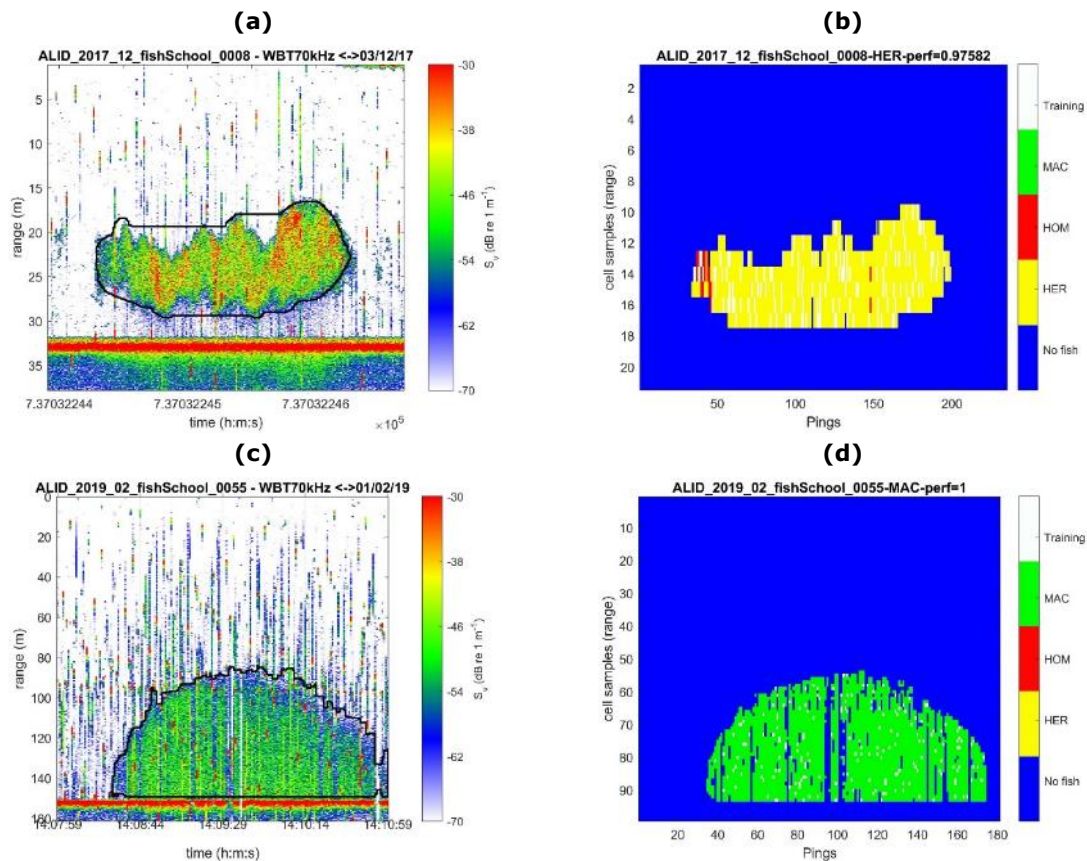


Figure 6-16: classification examples for two fish schools (HER and MAC). (a) and (b) echogram and subsequent classification of a Herring fish school. (c) and (d) echogram and subsequent classification of a Mackerel fish school.

6.2.2 Results

6.2.2.1 Main WMR classifier

The main WMR classifier is based on the method presented in Section 6.2.1. This consists on: (1) the calculation of signal features for every cells available in a data set; (2) the training of a NN on a subsample of the data. Here, the classifier is based on all the data collected by the Alida (SCH6) FV (Table 2-3). From 2014 to 2019, data are divided into 13 data sets with various species. The species included in the classifier are those that are the most substantially represented (Table 2-4):

- Herring (HER, 52x10⁶ pixels)
- Horse Mackerel (HOM, 70x10⁶ pixels)
- Mackerel (MAC, 22x10⁶ pixels)

Whilst the inclusion of additional species is possible, species must be represented with an equal amount of samples for the training process. If the number of samples available for a species is limited, one can: (1) use duplicates of the samples for this species; (2) decrease the number of samples used for the species with more numerous samples. The acoustic backscatter varies with species but also with variables such as area, time of year or depth. In addition, it was shown in Section 5.1 that the frequency response exemplifies a large variance. Prior to the inclusion of a new species, it is then paramount that its acoustic backscatter variability is represented in the data used for training. The inclusion of a species with limited data available will result in higher misclassification, especially on cases not represented in the data set (depth ranges, areas etc...).

The results of testing on all the cells not used for training is shown in Figure 6-17. This is for different cell averaging: no averaging (Figure 6-17(a)); averaging over 10 cells (Figure 6-17(b)); averaging over 30 cells (Figure 6-17(c)); averaging over 60 cells (Figure 6-17(d)); averaging over 500 cells (Figure 6-17(e)). The classification score increases with the number of cell used for averaging. This is because of the large variability between cells within each school. The averaging reduces the variability and in turn allows a more accurate classification. However, whilst classification is done for each individual cell, an increased cell averaging decreases the effective resolution. For example, the configuration of

averaging over 500 cells is in effect a classification where all the cells are averaged, i.e. using a single cell per school. The choice of the amount of averaging is then a balance between improvement in classification score and cell resolution. If no averaging is used, the accuracy of the classification is 80.4% with 94.7% for Mackerel, 78.9% for Horse Mackerel and 75.8% for Herring. The high score for Mackerel compared to the other two species is expected because it is a non swimbladdered species as opposed to Herring and Horse Mackerel. The lowest score of 75.8% for Herring is due to the high variability between cells. A good compromise between accuracy and resolution is an averaging over 30 cells. This exemplifies an accuracy of 93.5% with a lowest score for Herring of 90.3% (Figure 6-17(c)).

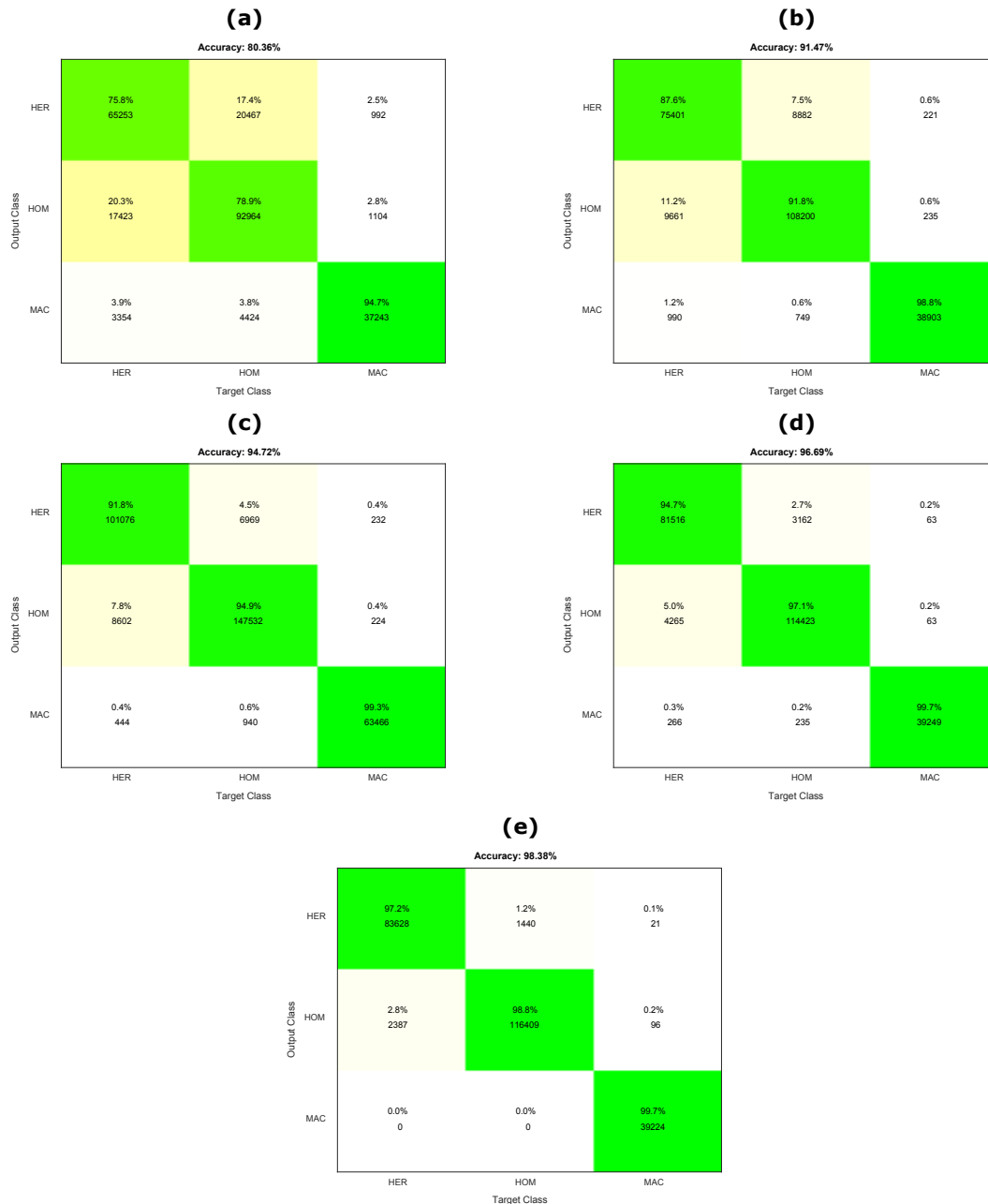


Figure 6-17: classification results of the WMR classifier for different cell averaging configurations. The results are presented as confusion matrix for the WMR classifier trained and tested on data from the Alida (SCH6). (a) no cell averaging. (b) 10 cells averaging. (c) 30 cells averaging. (d) 60 cells averaging. (e) 500 cells averaging.

In Figure 6-17, the WMR classifier was tested against all non-selected cells for training. However, a sub-sample of all the available Alida (SCH6) FV data was used for training. Therefore, each data set is represented in the training. Whilst this constitutes the classifier with optimal training, the classification method can be tested with a leave one out analysis. This test consists in leaving one data set for training at a time and test the classifier on this sole data set. It mimics a more realistic situation for the classifier where the data it is be used against are not included for training (i.e. a blind test). The results for all

the cell averaging configurations is shown in Figure 6-18. Across all the configurations, there are data sets that exemplify significant drops when tested blindly (cross markers compared to open circle markers for the different colours), most notably the data collected by the Alida (SCH6) FV in December 2017 (ALID_2017_12 on the x-axis). For this data set, the baseline accuracy of ~78% drops to ~40% if it is classified without prior information. This shows that this data set provides a new set of information to the classifier. As in Figure 6-17, the scores increase with increased amount of averaging. It is also noticeable that with no averaging (Figure 6-18(a)), some blind scores are higher than the baseline score. This is because each case is independently trained (different cells selected for each training) and there is variability in the accuracy score. The accuracy variability decreases with increased averaging because of decreased variability between cells. The classifier selected for implementation is the one using a 30 cell averaging (Figure 6-18(c)).

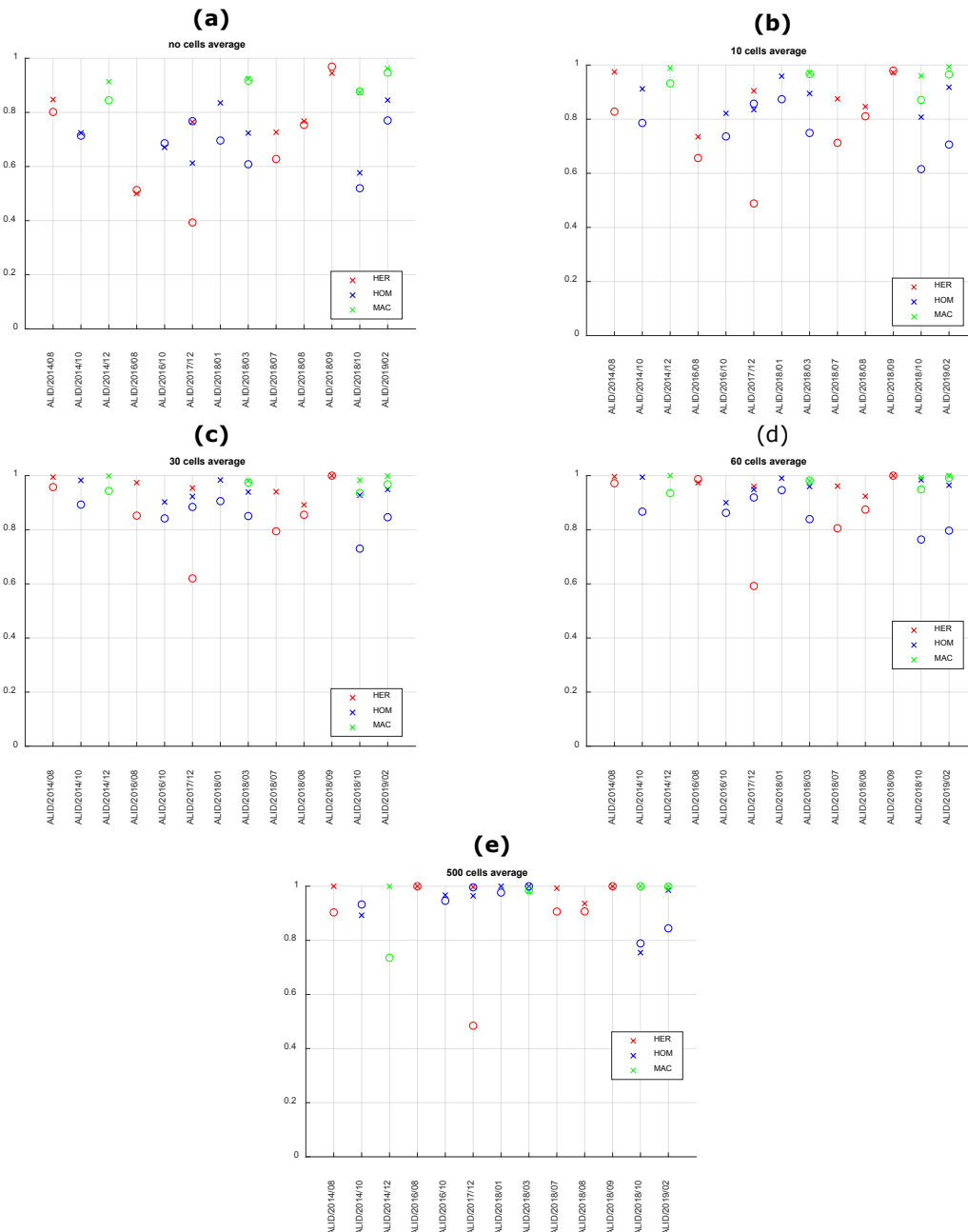


Figure 6-18: testing of the WMR classifier with one data set dropped at a time. The data sets are those collected by the Alida (SCH6) FV (Table 2-3). Cross markers are the baseline scores for each data set and each species (combined results presented in Figure 6-17) while open circle markers are the score from the leave one out test. (a) no cell averaging of features. (b) feature averaging over 10 cells. (c) feature averaging over 30 cells. (d) feature averaging over 60 cells. (e) feature averaging over 500 cells.

6.2.2.2 Sensitivity to calibration error

An important application for extended use of the results of this project is the ability to transpose the WMR classifier trained using data from a specific vessel to another vessel. In theory this should be

enabled with calibration of the echosounder. However, in the case of the Alida (SCH6) and Afrika (SCH24) Fvs, several discrepancies were found for the calibration (Section 3.3.2). Though slight differences in calibration gain between years and between FVs are expected, the differences between calibration gains found here are too high to be genuine, especially for the 120 kHz and 200 kHz WBT channels. It is therefore important to test the sensitivity of the WMR classifier against various offsets levels in calibration gains for the different WBT channels. Positive offsets from 0.5 dB to 3 dB for all WBT channels are tested. Results are presented in Figure 6-19. The sensitivity between the WBT channels can be observed. The 70 kHz WBT channel is robust against calibration offsets with a small decrease in classification score (Figure 6-19(a)). Contrarily, the 120 kHz and 200 kHz WBT channels are much more sensitive (Figure 6-19(b) and (c)). The decrease in accuracy occurs for specific species (Horse mackerel for the 120 kHz WBT channel and Herring for the 200 kHz WBT channel). Offset in calibration gain lead to severe misclassification with for example a score of 20% for Herring in the case of 3 dB offset in gain for the 200 kHz WBT channel (Figure 6-19(c)).

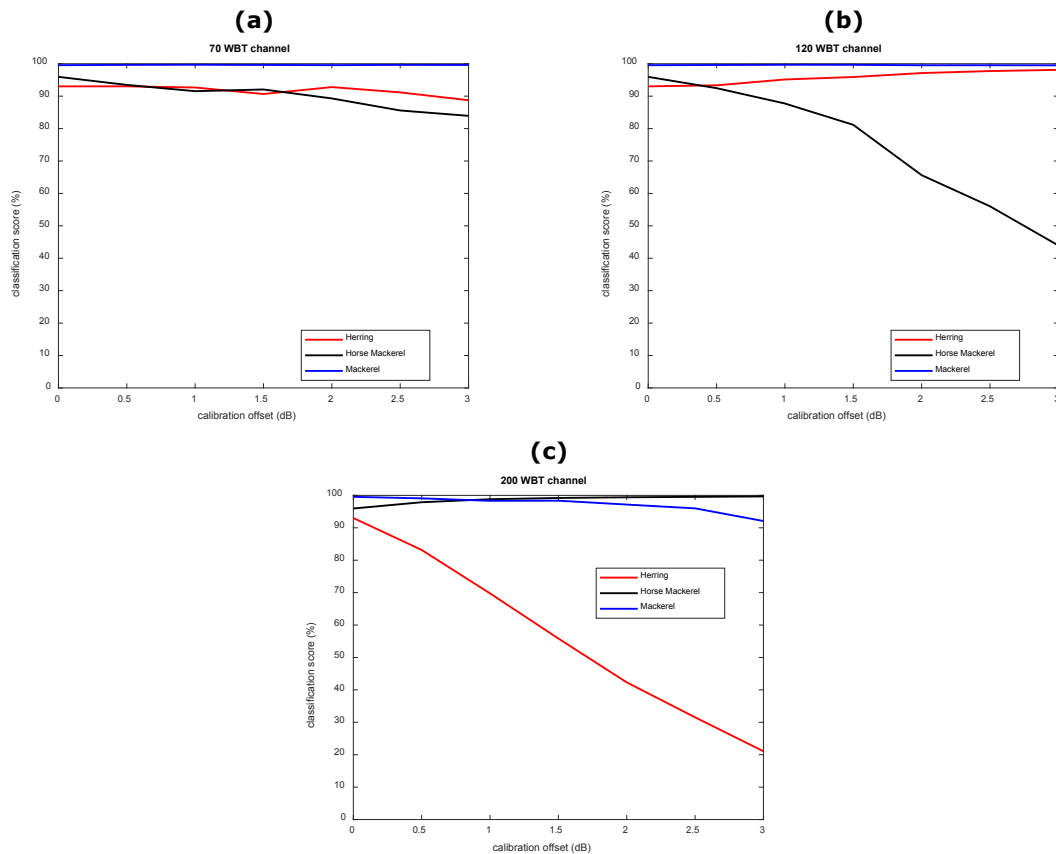


Figure 6-19: sensitivity tests. Each sensitivity test uses a offsets at a specific WBT channel: 0.5 dB, 1 dB, 1.5 dB, 2 dB, 2.5 dB and 3 dB. The 0 dB case is the baseline (Figure 6-17(c), averaging over 30 cells). Results are shown as classification score for the different species against calibration offset. (a) sensitivity test for the 70 kHz WBT channel. (b) sensitivity test for the 120 kHz channel. (c) sensitivity test for the 200 kHz channel.

The classification of the data from the Afrika (SCH24) using the classifier presented in Figure 6-17(c) is shown in Figure 6-20. For the Afrika (SCH24) data, the calibration from 2016 using the 38.1 mm sphere is used for all WBT channels. For the Alida (SCH6), the calibration from 2017 using the 38.1 mm sphere is used for all WBT channels. The comparison of the calibration gains for these two data sets is shown in Figure 6-20(a). Significant offsets can be observed (2.5 dB at 200 kHz). The classification of the Afrika data sets yields 70.2% for Herring, 97.6% for Horse Mackerel and 71.9% for Mackerel. These scores are low and most likely reflect some discrepancy in calibration gain. Whilst the differences between calibration gains is explained by the use of different echosounders in different conditions, these might not be fully genuine. This is illustrated in Section 3 that presented discrepancies between comparable data sets.

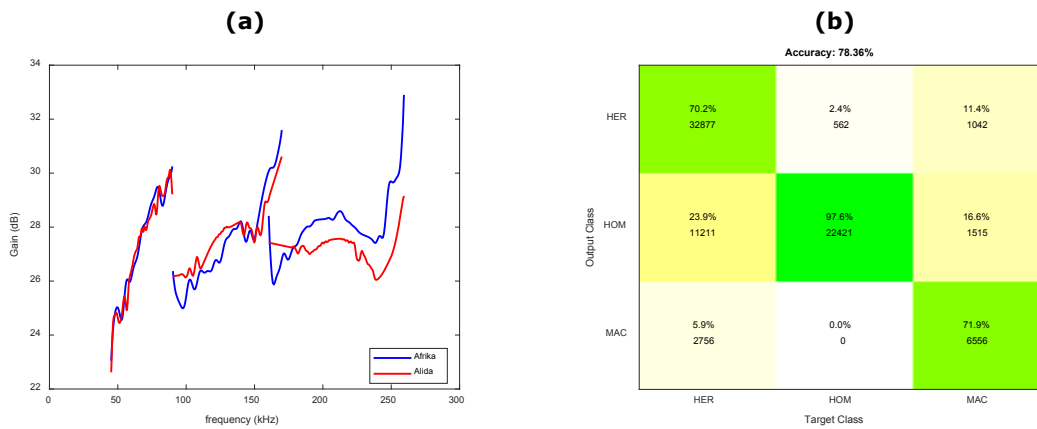


Figure 6-20: classification of the data from the Afrika (SCH24) FV using the WMR classifier trained using the data from the Alida (SCH6) FV with an averaging over 30 cells. (a) Calibration gains used for the data from the Alida (SCH6) FV and the Afrika (SCH24) FV. (b) WMR classifier results.

6.2.2.3 Classification based on Afrika (SCH24) FV data

The classification results shown in Section 6.2.2.1 are calculated using the WMR classifier trained using all the data available from the Alida (SCH6) FV. In this section the data from the Afrika (SCH24) are solely used for deriving a NN classifier. Though, the amount of data available from this vessel are limited (Table 2-3) and are for example only representative of a small regional subspace of the North Sea (Figure 2-3(c)). In comparison, the data available for the Alida (SCH6) FV is much larger (Table 2-4). The results of the classification are presented in Figure 6-21 for two configuration: no cell averaging (Figure 6-21(a)); averaging over 30 cells (Figure 6-21(b)). It can be observed that the accuracy score are high compared to those presented in Figure 6-17. This is because the classifier devised in the previous section deals with a much more diverse data set and is therefore more robust against the variation in features across the North Sea. It is important to note that it is not possible to perform a leave one out analysis (as in Figure 6-18) in the case of the classifier using only data from the Afrika (SCH24) FV. This is because the data from the Afrika (SCH24) FV only has a limited number of data sets available (Table 2-3 and Table 2-4) and HER and HOM species are only present in single data sets. If one would leave the data set where HER is present, it would not be possible to train the NN for this species. As the data set for the Afrika (SCH24) will grow the robustness of the classifier specific for this vessel will improve.

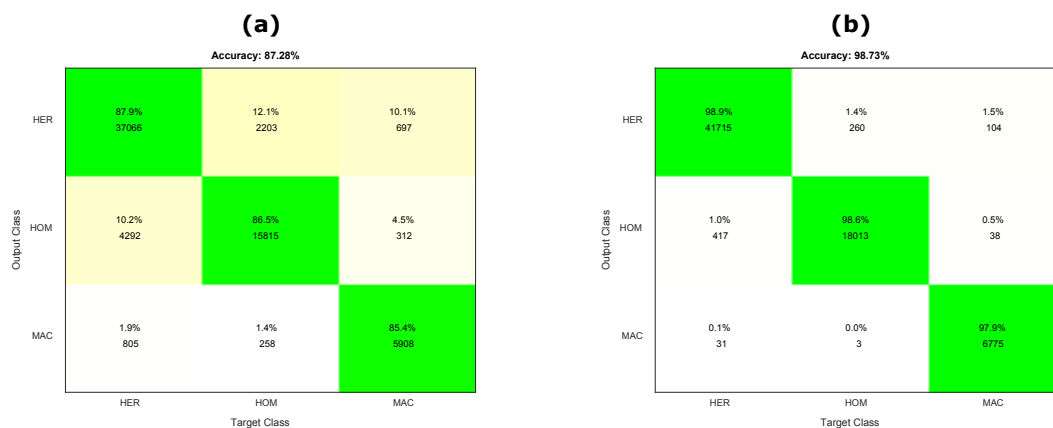


Figure 6-21: classification for different cell averaging using data from the Afrika (SCH24) FV. Results are presented as confusion matrices. (a) classification results without feature averaging. (b) classification results with an average of features over 30 cells.

6.2.2.4 4th species inclusion

In the previous sections, the devised WMR classifier was only applied to three species: Herring, Horse Mackerel and Mackerel. This is because these species represent the bulk of the data collected by the Alida (SCH6) and Afrika (SCH24) FVs (Table 2-4). Though in smaller proportions than the three main

species, the data sets contains data associated with Sprat for both the Alida (SCH6) and Afrika (SCH24) and Sardine for the Alida (SCH6) only.

First, the inclusion of Sprat as a fourth species for the classifier is tested separately with data from the Alida (SCH6) and the Afrika (SCH24). Both classifiers use a configuration with an averaging over 30 cells. The result are shown in Figure 6-22. The classifier using data from the Afrika (SCH24) exemplifies high scores (Figure 6-22(a)) as there is enough data for each species to devised a balanced training subset (Table 2-4). Contrarily, the classifier training on Alida (SCH6) data presents lower score (Figure 6-22(b)). This is particularly the case for the Sprat accuracy score (only 66%). This reduction in accuracy is mostly due to the low number of data available for Sprat in the data sets from the Alida (SCH6) FV (Table 2-4).

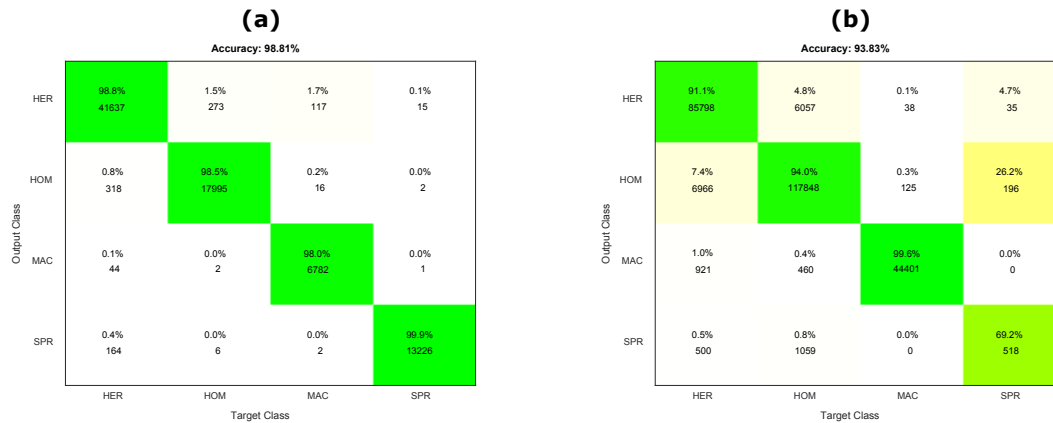


Figure 6-22: WMR classifier results of four species identification (Sprat as fourth species) using training based respectively on: (a) the data from the Afrika (SCH24) FV; (b) the data from the Alida (SCH6). The classifier uses a configuration with an averaging over 30 cells.

Furthermore, data from Sardine was collected by the Alida (SCH6) FV (Table 2-4). Similarly to Sprat data, these can be tested as a an additional classified species. The results from the classification are shown in Figure 6-23. Overall, it can be observed that the accuracy is high, similar to the levels of the baseline classifier (Section 6.2.2.1). In contrast, the classification of Sprat is much lower (Figure 6-22(b), 69.2%) (whilst Sardine has more distinct characteristics (frequency response, density etc...) leading to more contrasting features. However, as for Sprat, the amount of data available for Sardine is very limited and is only representative of a specific region (Figure 2-3). In order to add this species, it is therefore important to collect more data in order to assess the robustness of the algorithm (e.g. using a one out study as shown in Section 6.2.2.1).

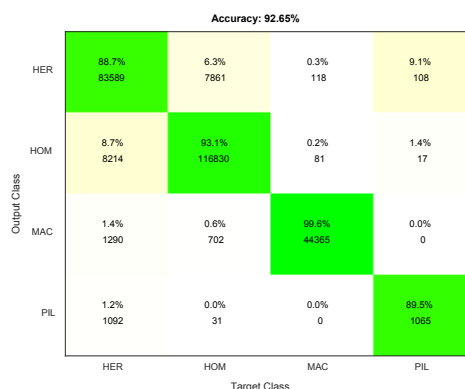


Figure 6-23: WMR classifier results of four species identification (Sardine (PIL) as fourth species) using training based on data from the Alida (SCH6) FV. The classifier uses a configuration with an averaging over 30 cells.

6.3 Combined classifier

The classifiers of TNO and WMR are developed independently. Though they both build on a mutual pre-processing chain that delivers their raw inputs, which is one of the critical factors, the independent classification approaches can and will lead to different results. The main reason for independent approaches was to increase the chances of success. Though both classifiers perform well, it is possible to improve the final classification results even further by combining the outputs of the classifiers. The idea behind this is that they may augment each other in cases where one classifier is uncertain about the result, while the other is not.

Classifier combination is performed on a single cell basis. Classifiers are combined by automatically computing and assessing the confidence levels of each classifier. For each cell the output of the classifier with the highest confidence is selected. Or in other words: the classifier that is most certain about its outcome, determines the combined classification output for that cell.

The supporting ground for this approach is given in Figure 6-24(a) and (b), where confidence masks are given for a Herring and a Horse Mackerel school, respectively. Per school, the confidence mask is given for each of the two classifiers. The low confidence levels indicate about which part of the school the classifiers are uncertain. Since both classifiers are uncertain about a different part of the school, they can 'help' each other in estimating the correct species. Figure 6-24(c) also plots the confidence levels of an example school, but in a different representation. The desired confidence augmentation in the given examples appears to be representative for the majority of the schools.

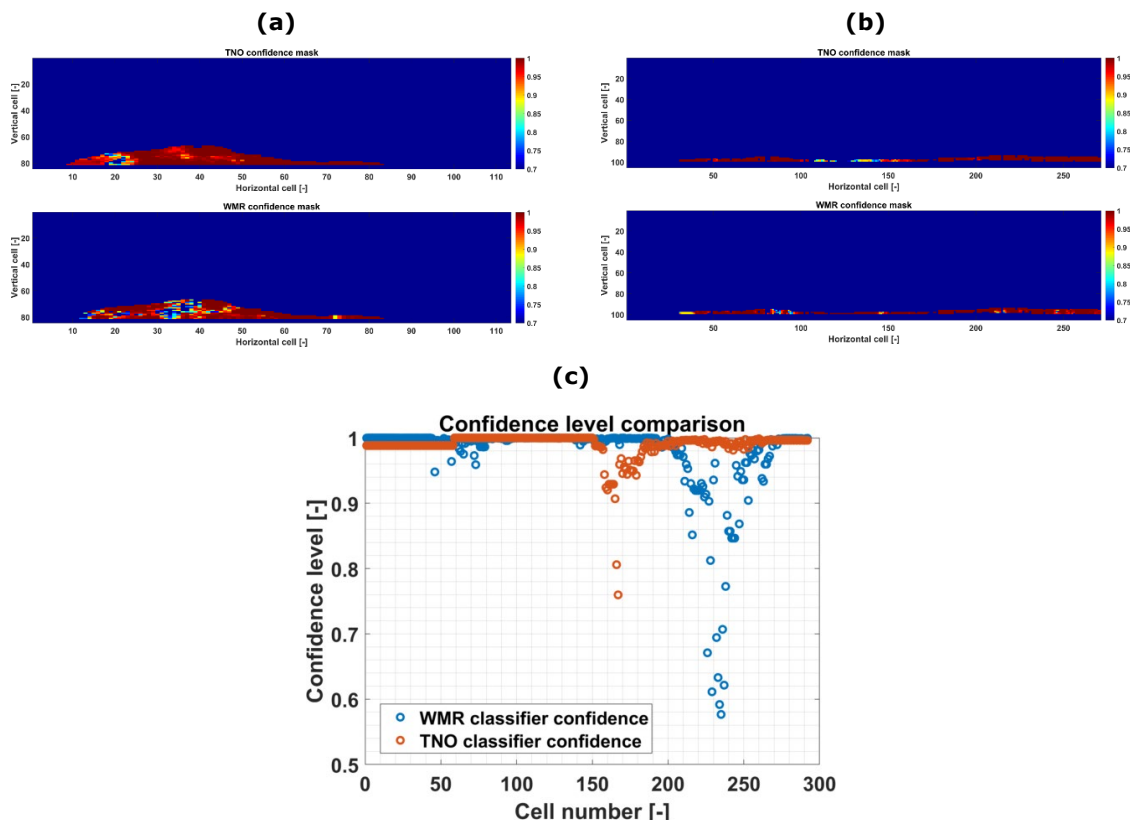


Figure 6-24: Confidence masks of both the TNO classifier and the WMR classifier for two example fish schools (a,b). Low confidence levels indicate the classifier is uncertain about the classification result for that cell. In (c) the confidence levels are plotted per cell for one of the example schools.

The described fusion approach has been applied to all existing data sets. Figure 6-25 provides the results per data set per classifier, including the combined classifier. Since the scores were already rather high, the improvement is somewhat difficult to observe. Figure 6-26 plots the average score per species of the different classifiers in a single plot, together with the confusion matrix of the combined classifier. Here, it is well observable that the combination of classifiers increases the scores even further by roughly 2 to 3 percent.

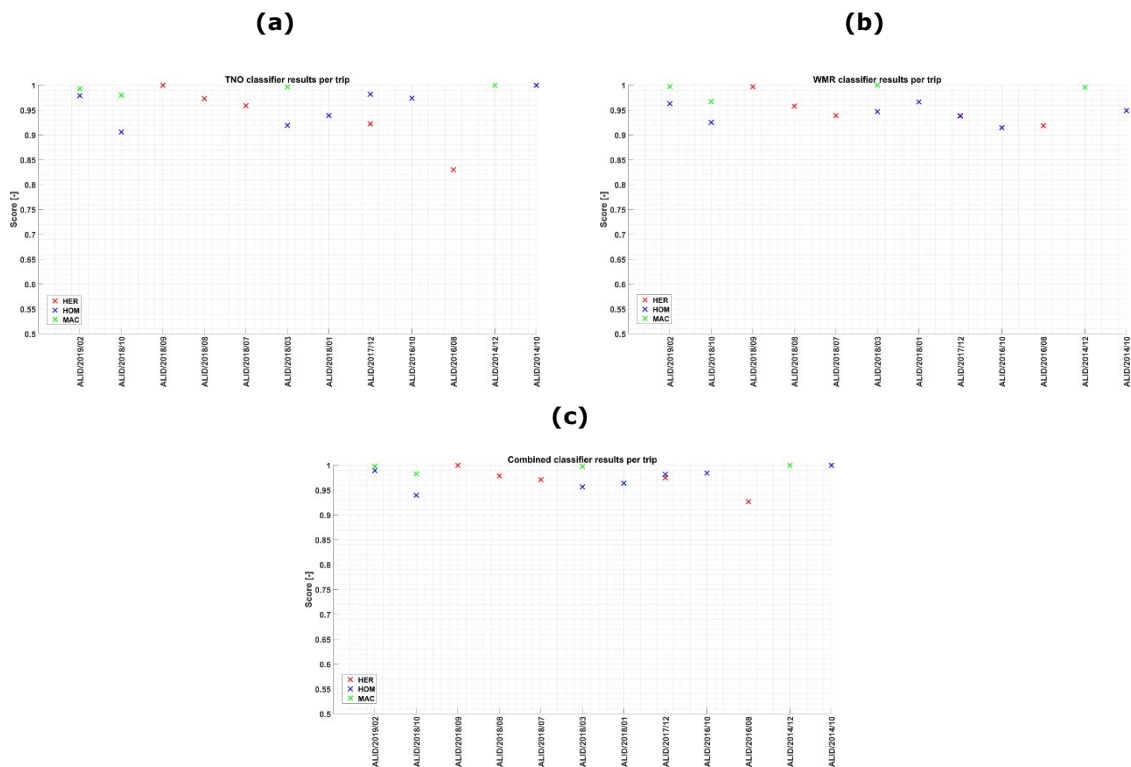


Figure 6-25: Classification scores per data set for the TNO classifier (a), WMR classifier (b) and the combined classifier (c). The combined classifier slightly outperforms both classifiers.

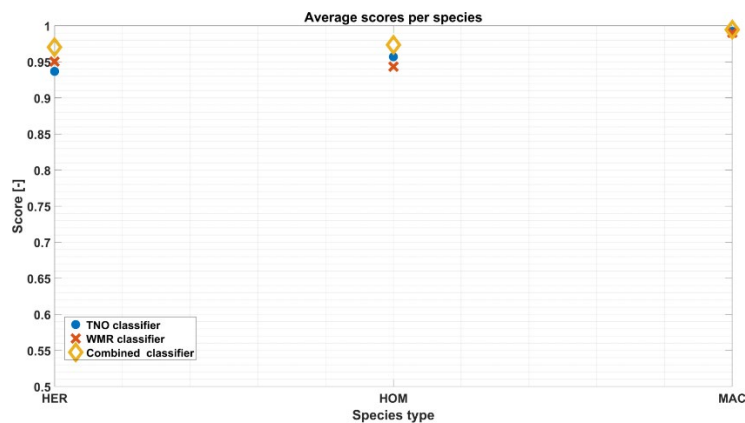


Figure 6-26: Average classification score per species type for the TNO classifier (circle markers), WMR classifier (cross markers) and the combined classifier (diamond markers). The combined classifier slightly outperforms both classifiers.

6.4 Impact of reduction in data richness on classification accuracy

A disadvantage of the EK80 sonar is its limited operating range. With the EK80 operating at maximum power, the average achievable operating depth for classification using the three WBTs is roughly 200 meters. At this range the SNR of the transceiver with the highest frequency (160-260 kHz) becomes too low. This means that the signal representation at this depth is predominantly defined by background noise and not by backscatter of fish. Since higher frequencies experience more absorption by sea water, the operating range of the transceiver with the highest frequency limits the total operating range. The maximum range depends on the amount of background noise, caused by ship noise and environmental noise. Since the amount of background noise varies in time, but also between ships, the maximum operating range also varies.

For discrimination between Herring and Horse Mackerel, which are acoustically very similar, all three transceivers currently are used to obtain high classification scores. This implies that 200 meters at this moment seems the maximum achievable operating range. However, skippers indicate it would still be very useful if classification could also be applied at larger depths to discriminate only between Horse Mackerel and Mackerel, or more general: between a fish with and without a swim bladder. This is grounded further by the fact that at depths larger than 200-250 meters, Herring and Horse Mackerel are not found in the same area at the same time, making discrimination between these two species unnecessary at these depths.

6.4.1 Feasibility

As a result, it has been assessed to what extent it is possible to discriminate between Mackerel and Horse Mackerel as well as between Mackerel and Herring with fewer than three transceivers. To this end the existing data sets are used. These sets only go up to depths of 200 meters, however this is sufficient to test the feasibility of classification with fewer transceivers. In Figure 6-27 classification scores are provided for the classification of the species pairs with three, two or only one transceiver(s), respectively. It is clear that for these pairs classification can be done well with two transceivers, but also with only a single transceiver, at the cost of a slightly reduced score. The main reason for this is that effectively the classification problem has been reduced to classification between fish with and without swim bladder. Since the difference in acoustic response for this is large enough, fewer transceivers can be used.

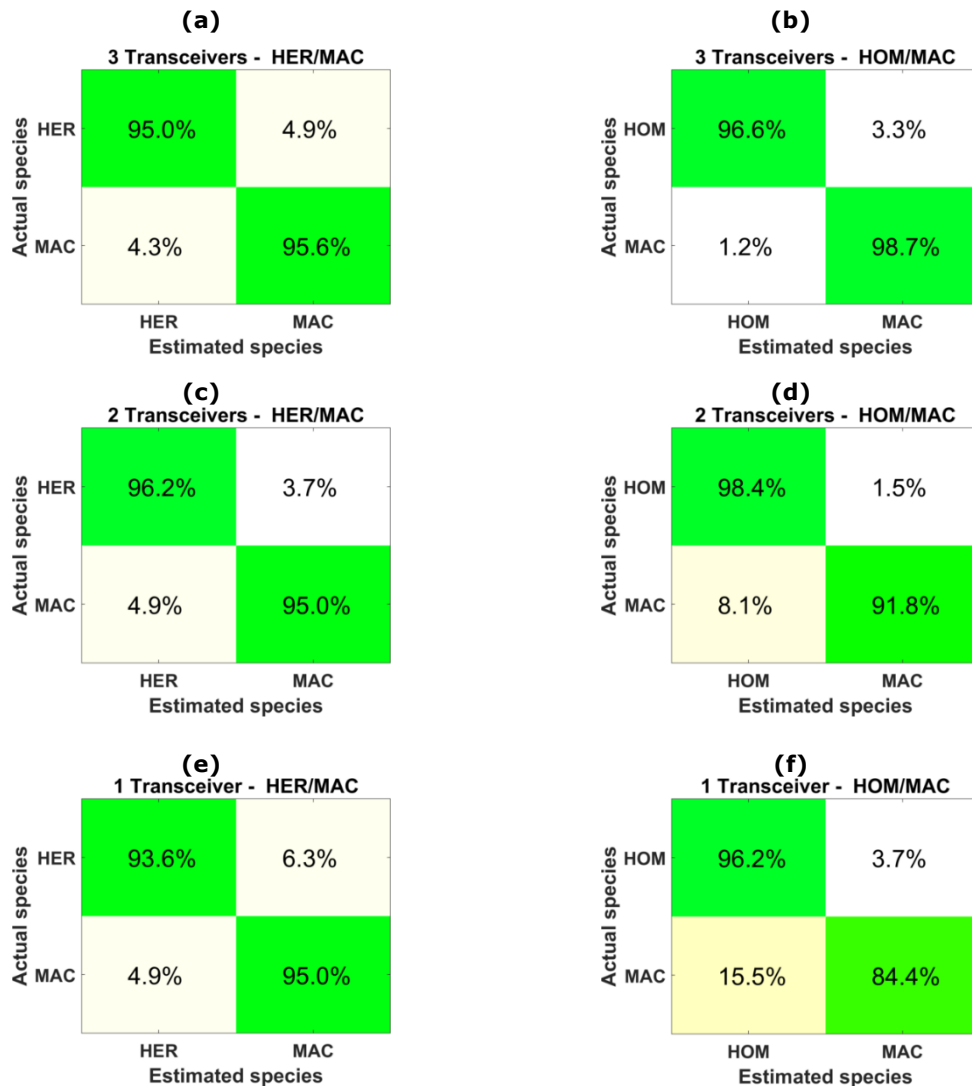


Figure 6-27: Confusion matrices for classification between Mackerel and Herring/Horse Mackerel when using a decreasing number of transceivers. The possibility of using fewer transceivers allows increasing the maximum operating depth of the classifier.

6.4.2 Expected operating range

Since classification with fewer transceivers seems to have potential for this subset of species, it is good to have an estimate of achievable operating depth. In a potential next version of the demonstrator, it is possible to design a classifier for different depth brackets and automatically switch between classifiers based on school depth. In this case a best effort is made to optimize operability. Since frequency dependent absorption loss is the dominant factor that determines the differences in maximum operating depth between the transceivers, Figure 6-28(a) depicts a plot of the absorption loss as function of depth and frequency. Based on all collected data, the average operating range with three transceivers was estimated to be roughly 200 m, with WBT3 being the limiting factor. Using this as a reference and looking at the absorption ISO line in the image, the achievable operating depths with a varying number of transceivers are estimated to be:

- 3 transceivers (WBT1, WBT2 and WBT3): ~200m
- 2 transceivers (WBT1 and WBT2): ~280m
- 1 transceiver (WBT1): ~450m

This would assume equal background noise levels in the different bands. When analysing the median sound levels of the actual echograms used in the examples in this report, the range per transceiver is slightly more conservative. When setting a maximum allowed noise level - the example threshold in Figure 6-28(b)- and intersecting it with the average background level of each transceiver, the expected ranges are as follows:

- 3 transceivers (WBT 70 kHz, WBT 120 kHz and WBT 200 kHz): ~200m
- 2 transceivers (WBT 70 kHz and WBT 120 kHz): ~260m
- 1 transceiver (WBT 70 kHz): ~370m

The difference for WBT1 can be assigned to the fact that background noise in the lower frequencies (45-90 kHz) may be a few dBs higher than in the higher frequencies (160-260 kHz). However, this gives a rough impression on achievable range with a reduced number of transceivers. Also note that when looking at Figure 6-28(b), a noise reduction of 3 dB can increase the operating range with 50 m for WBT3 and 100 m for WBT1. The given numbers are expectations for the concerning vessel (Alida). In case the dominant noise source is the ship and not the environment, which is the expectation, the maximum ranges will differ. With the lower noise levels on the Afrika for example, the expected ranges will probably be higher.

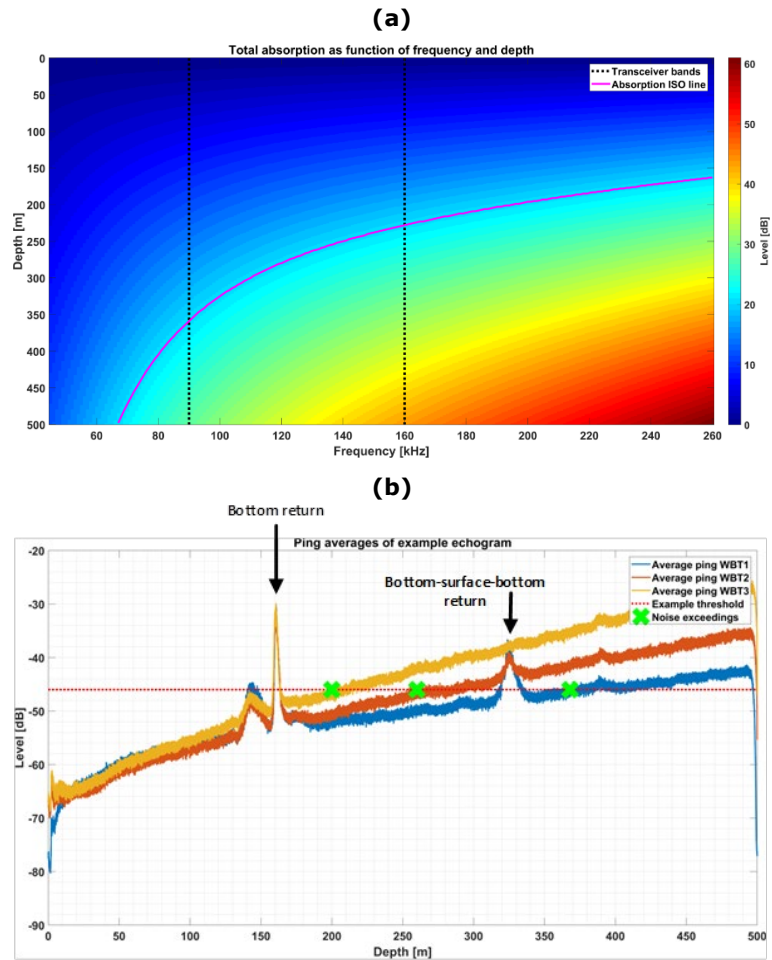


Figure 6-28: limitation in operating range with the EK80 for the different WBT of interest.
 (a) Total absorption loss as function of frequency and depth. This gives an indication of the relative, expected maximum operating depth between the transceivers.
 (b) Average time signals of an example echogram for the three transceivers after propagation loss compensation, together with an example fish school detection threshold. The three intersections show the relative achievable ranges of the transceivers.

6.4.3 Classification of data with reduced frequency bandwidth (ES80 FM)

The EK80 Simrad Wide-band transceiver discriminates itself from its ES80 sister in the width of the frequency band it is operating in. The EK80, which is used for this research, operates in bands of:

- WBT 70 kHz: 45-90 kHz
- WBT 120 kHz: 90-160 kHz
- WBT 200 kHz: 160-260 kHz

The ES80 operates in reduced bands:

- WBT 70 kHz: 56-84 kHz
- WBT 120 kHz: 96-138 kHz
- WBT 200 kHz: 180-220 kHz

As a result, the resolution of the time signal per EK80 transceiver is a factor 2 to 3 higher (more detail) than that of the ES80 transceivers. Further, the EK80 simply contains more spectral information. All together more acoustic species information is available for classification. A practical disadvantage of the EK80 version, however, is the user interface for the skipper. It contains less functionality than that of the ES80. Also the high resolution appears to be judged as a disadvantage, since very sparse schools are harder to observe visually. Hence, because the advantages of a wide band and a high resolution are in practice not well noticeable by a skipper, they prefer to use the ES80 over the EK80 during their fishing operations.

A side path of this research is to make an estimate of the expected classification performance when the ES80 sonar would be used. Since no substantial ES80 data is available, the alternative is to strongly filter the EK80 data recordings in order to mimic ES80 sonar data. To this end the EK80 data is filtered using the transmitted pulses of the ES80. This results in degraded data that has the exact same

frequency composition and time resolution as the ES80 data would have. It must be noted that this conversion still will not reconstruct an exact ES80 recording, but it gives a good first impression on what would be achievable. In Figure 6-29(a) and (b), the spectrum of a ping of the EK80 is given, together with its representation after the conversion process that mimics ES80 data. For the same ping, also part of the time signal is given in Figure 6-29(c) for a single transceiver, comparing the (unmodified) EK80 signal with the mimicked ES80 signal.

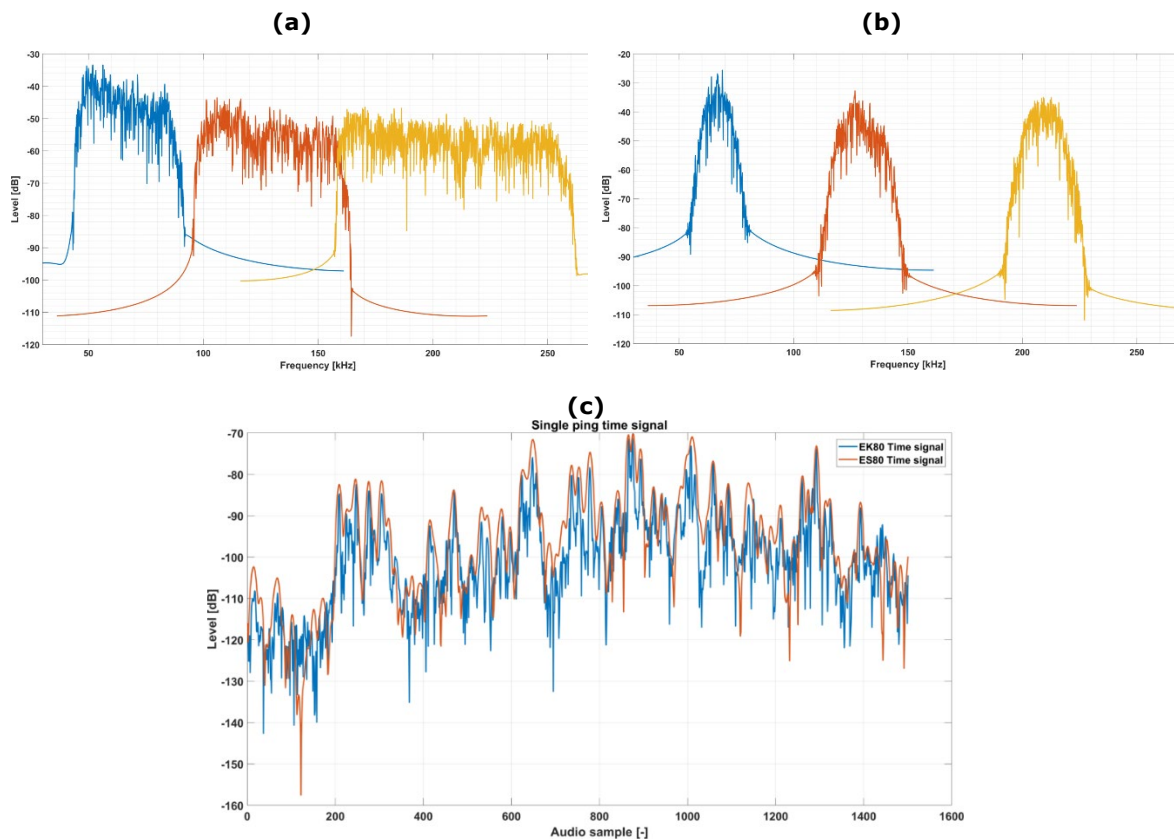


Figure 6-29: comparison of EK80 FM data with data with reduced frequency bandwidth (mimicking ES80 FM data). (a) and (b): Single ping spectrum of the three transceivers for the EK80 (a) and the mimicked ES80 data (b). (c): Time signal of part of a single ping for one of the three transceivers for the EK80 and the mimicked ES80 data.

Using the reduced data representations, a classifier is trained and evaluated in a similar way as was done for the EK80 data. Figure 6-30(a) and (b) show the same type of results. It is clear the scores are reduced when using the reduced data representation. One of the main reasons is likely related to the fact that as a result of variation within a species some key frequencies are missing. It must be noted however, that there are still some processing improvements to make, which will increase the scores of both EK80 and pseudo-ES80 classification. These processing improvements relate to further corrections for environment and school insonification, which have an effect on the spectrum.

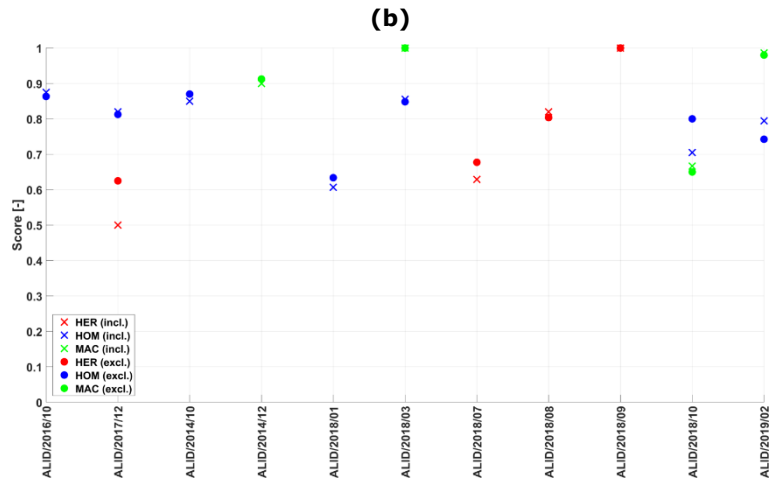
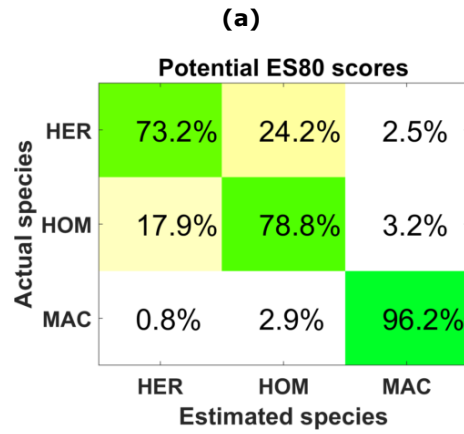


Figure 6-30: classification results using data from the Alida (SCH6) FV mimicking the ES80 FM.

(a): Confusion matrix of classification performed with mimicked ES80 data. The scores indicate potentially achievable results with ES80 data.

(b): Classification score per fishing trip using mimicked ES80 data. Each trip can contain multiple species types. Crosses indicate the results for data set-inclusive training, filled dots indicate the results for data set-exclusive training.

7 Length estimation

There are several means to sizing targets using active acoustics systems. If a relationship between TS and length can be established, it can be used for size estimation [45], [47]–[51]. However, there are several caveats to this methodology: the TS-length relationship changes with the incidence angle [52], [53]; the TS-length relationship can be specific to the species; the sizing is limited by the detection of single targets (i.e. not applicable to dense fish schools). In specific cases, it is possible to infer size distribution using an inversion on the volume backscattering strength (S_v). Inversions have been attempted successfully to infer zooplankton size distributions [2], [54]–[56] and for gas bubbles [57]–[59]. Whilst sizing of swimbladder fish is possible through inversion [60], [61], it is limited to low frequencies as this method utilizes the resonance of the swimbladder at low ka (wavenumber times the target size) regimes, i.e. at either low frequencies or small organism sizes. For higher ka regimes, the inversion is impractical as the change in TS is much less pronounced and well established than around the resonance. In a previous project [10], differences in frequency response were observed between different length classes but the data available were limited. With access to a larger data set, it was shown in Section 5.1 that there is not a clear pattern in the frequency response for the different size classes. Therefore, an alternative methodology is needed. With the increased range resolution provided by the EK80 in FM mode, a new method is emerging [62], [63]. This method utilises the high range resolution to discriminate the different boundaries from single targets. It has the potential to be more accurate than the application of the TS-length relationship. Results from controlled experiment have shown that the different target boundaries can clearly be resolved for artificial targets [62] but also for non-swimbladdered fish ([63]) and fish with swimbladder (personal contact). Here, a practical implementation of this approach is developed and tested on at sea data from the Alida (SCH6) and Afrika (SCH24) FVs.

7.1 Method

The method employed for size estimation aims at identifying the boundaries of the different body parts of the fish using the very fine range resolution provided by the EK80 in FM mode. In this mode, the range resolution is particularly high because of the use of match filtering (only possible when using broadband signals).

The size estimation algorithm applied here consists of two parts: (1) a single target detection and tracking across pings; (2) a target boundary detection around each single target detection. The detection of single targets is done for each ping by:

- Thresholding between -55 dB and -34 dB.
- Peak detection with
 - A minimum spacing between peaks of 0.6 m
 - A prominence level of the peak of 10
- Filtering of peak detections, retaining those that exemplify:
 - a standard deviation in along and across angles of less than 1°
 - an along angle within 4°
 - An across angle within 4°

Tracking of targets is done by linking the different single target detections in consecutive pings (Figure 7-1(a)). The criteria used to group two target detections is:

- Difference in depth between the two target detections of less than 0.6 m
- Difference in combined angle of less than 1.5°

Around each target detection, a new peak detection is used to find potential boundaries (Figure 7-1(b)). This is performed in a window of 0.6 m around the target detection, retaining the detections with a minimum distance between peaks of 0.03 m and a minimum prominence of 10. The angular position of boundary candidates are then compared to the angular position of the target detection. Only the closest boundary candidate is kept.

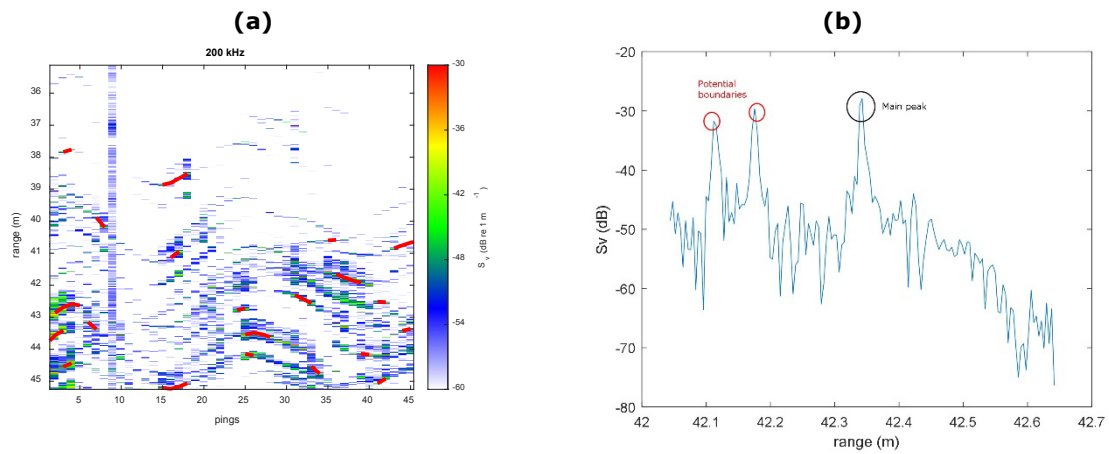


Figure 7-1: example of processing for fish size estimation. (a) EK80 FM echogram at 200 kHz with single target detection and tracking (red lines). (b) S_v time series around a single target detection. The main detection is shown as a black circle. Potential boundaries

The size estimation algorithm is applied to each WBT channel independently. The results consist of individual target detections with associated nearest boundary. The distance between the target detection and the nearest boundary d can be associated with fish size. However, it is important to note that for the same target, d will change depending on the grazing angle. The distance between the boundaries at 90° grazing angle is smallest. With increasing or decreasing angle from the 90° grazing angle, the distance d will increase (Figure 7-2). In practice, the distribution of measured distances between fish boundaries d is a combination of different grazing angles as fish in the water column exemplify varying behaviour. It is important to note that d measured dorsally (90° grazing angle) between different length classes is small. With a changing grazing angle, the measured length will reflect more the differences in length.

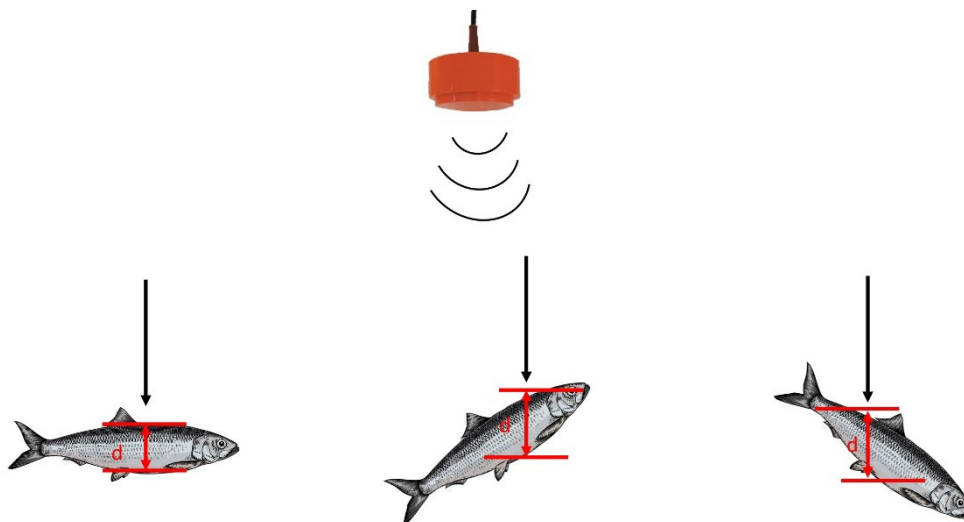


Figure 7-2: schematic exemplifying the increased distance between detected boundaries as the angle deviated from the 90° grazing angle.

The algorithm described above is applied to various acoustic records exemplifying single fish marks and intensity fish schools. Example echograms for both type of data is shown in Figure 7-3(a) and (b). The method presented here applies to single target detections only and is expected to work best on acoustic data presenting clear single fish marks (Figure 7-3(a)). However, the method is also tested against fish school type marks (Figure 7-3(a) and (b)) to test whether single targets are detectable and sizeable around the schools. The species allocation for the training and testing of the species is done for each school and in the time window of the fishing operations (see Section 2). In contrast, the acoustic records of interest here are outside the time windows where fishing was performed. This is because the echograms only exemplify low fish density which is not desirable for large scale fishing (as performed on FV involved in this project). These correspond to periods where the FV is actively searching for high

density spots. Though not ideal, the associated species and length distribution for each record is based on the day of the record, i.e. is not directly related to the catch species and length composition. The type of species encountered is Herring, Horse Mackerel, Mackerel and Sprat. The different cases span various water depths.

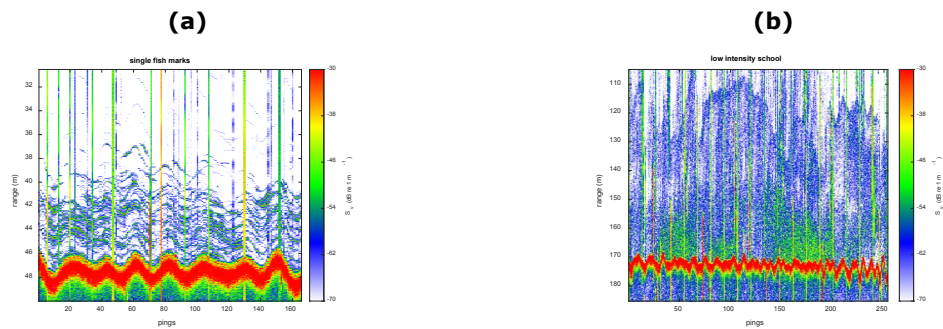


Figure 7-3: example echograms of the different data type used in this analysis. (a) single fish mark (data collected by the Afrika (SCH24) FV on 2018/12/18). (b) fish school marks (data collected by the Afrika (SCH24) FV on 2018/12/04).

Applying the algorithm described above yields single target detections and their associated boundary detection for each WBT channel. The quantity of interest is the distance between the boundary and the target detection (Figure 7-1(b)). This can be calculated and plotted as a distribution of distances. The probability density function for the distribution is then estimated using a kernel density estimation. This is done with 64 mesh points between 0 cm and 0.3 cm using a Gaussian kernel [64]. An example of kernel density estimation (200 kHz WBT channel) is shown in Figure 7-4.

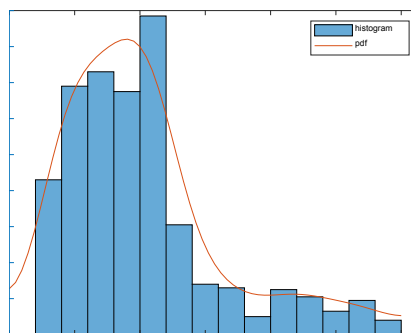


Figure 7-4: example of kernel density estimation at the 200 kHz WBT channel. The probability density function (orange line) of the distribution (blue bars) is estimated using a kernel density estimation with a Gaussian Kernel.

7.2 Results

The methodology described in Section 7.1 is tested against fourteen sets of data. These were selected manually and span different:

- Length classes (10-35 cm)
- Species (Herring, Horse Mackerel, Mackerel, Sprat)
- Depths (20-160 m)
- Acoustic mark type (single fish, low intensity schools)
- Vessel (Alida (SCH6) and Afrika (SCH24) FV)

A summary table for each data set is given in Table 7-1. The analysis results in numerous single target detection for each WBT channel used here: 70 kHz, 120 kHz, 200 kHz. The number of detection for each WBT channel is also given in Table 7-1. This quantity can vary between data sets.

Figure 7-5 shows the results for the acoustic records exemplifying single fish marks (Figure 7-3(a)). It can be observed that the size estimations is often different between the WBT channels. These differences could be due to the difference in range resolution, especially for the 70 kHz WBT channel (lowest range

resolution). The 200 kHz and 120 kHz WBT channels are overall consistent. The 200 kHz WBT channel is expected to yield the best results as it has the higher range resolution to differentiate different boundaries.

The data set from the Afrika (SCH24) FV collected on 2018/12/05 (Figure 7-5(a), black bars) exemplifies a length frequency distributions centered around 10 cm. For this case, the acoustic estimation from the 200 kHz WBT has a peak at 4.2 cm (Figure 7-5(a), blue solid line). There are two peaks for the acoustic estimation for the 120 kHz WBT, at 3.3 cm and 10 cm (Figure 7-5(a), blue dashed line). The other four data sets exemplify length frequency centered around 25 cm (Figure 7-5(c)-(e), black bars). Their acoustic estimates have peaks located between 8 cm and 10.1 cm (Figure 7-5(c)-(e), solid blue line). This shows sensitivity between different length classes (~ 10 cm Sprat and ~ 25 cm Herring/Horse Mackerel).

The results of the size estimation method applied to fish schools is shown in Figure 7-6. As for single fish marks, only one data set exemplifies small fish lengths (Sprat ~ 10 cm, Figure 7-6(a), black bars). The associated acoustic estimate using the 200 kHz WBT channel is also low (Figure 7-6(a), blue line, peak at 5 cm). In contrast, cases with swimbladder species of about 25 cm length (Figure 7-6(d)-(f)) have higher fish size estimates (~ 10 cm).

Of particular importance, the case of smaller fish size (Sprat 10 cm, data collected by the Afrika on 2018/12/05) exemplifies acoustic size estimates that are smaller than the other cases for the 200 kHz WBT channel (solid blue line in Figure 7-5). This shows the method is sensitive to different cases. Unfortunately, only a small number of samples associated with small size fish was collected through the course of this project. This exercise would need to be replicated and the method refined with additional data.

Though the analysis showed here could be indicative that the acoustic sizing based on fish boundaries is sensitive to the different length classes, there is two main caveats:

- The biological data used for comparison with acoustic estimates did not match exactly the acoustic records. It is therefore not possible to exclude a substantial contribution of other size classes than those observed in the catch.
- The data available here is limited in term of diversity. For example, only two sampled catches exemplified length classes smaller than 20 cm.

The method of sizing fish using boundary detection has been shown successful in controlled experiment setup [62], [63] and the results showed here for the 200 kHz WBT are sensitive against different length classes (~ 10 cm, ~ 25 cm, ~ 35 cm). Though further investigation is needed regarding: the sensitivity to more numerous different length classes and species; the effect of other parameters such as other parameters such as water depth, background noise, noise interference, fish behavior. To this purpose, dedicated experiments and at sea data collection will be needed.

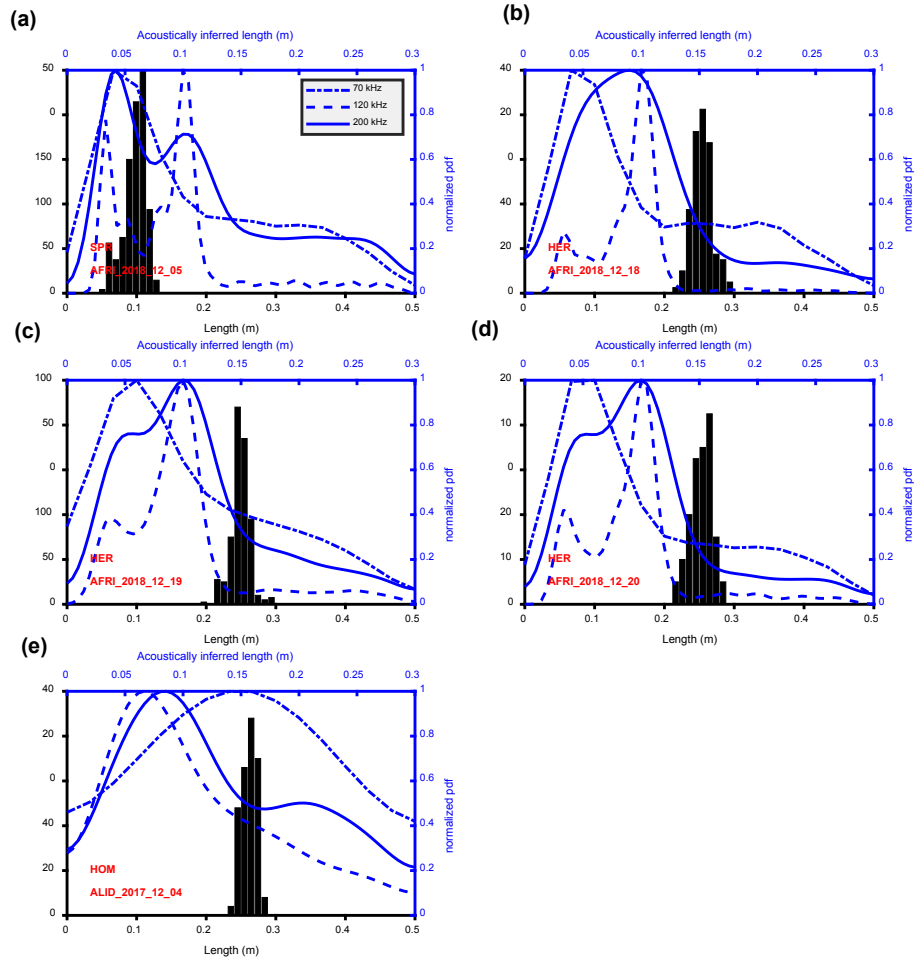


Figure 7-5: fish size estimation for single fish marks. comparison of acoustically inferred fish sizes (right axis, blue lines) against length frequency distribution for different data sets (left axis, black bars).

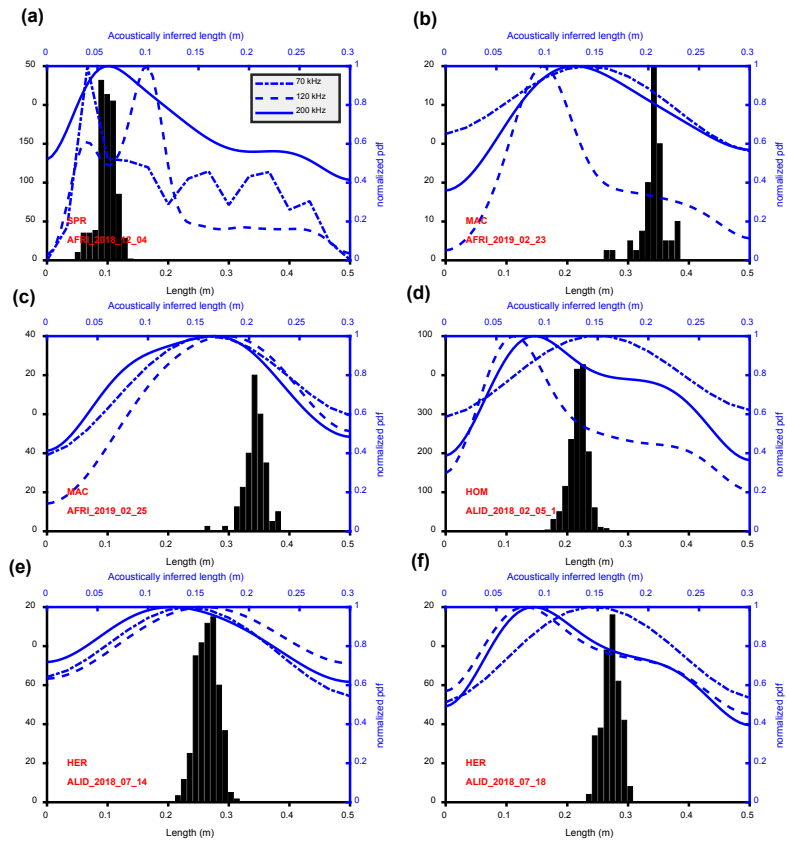


Figure 7-6: fish size estimation for single fish school marks. comparison of acoustically inferred fish sizes (right axis, blue lines) against length frequency distribution for different data sets (left axis, black bars).

Table 7-1: summary of results of the fish length estimation. Information on the data used for the study is given (date, vessel, duration, water depth, species, data type, length frequency mode) together with the number of detection at each WBT (70 kHz, 120 kHz, 200 kHz) for each record. The length frequency for the data collected by the Alida (SCH6) FV on 2017/12/04 was not available (only weight measurements) and is calculated using a weight frequency relationship (see footnote) [65].

| vessel | date | duration (minutes) | water depth | number of detections 70 kHz WBT | number of detections 120 kHz WBT | number of detections 200 kHz WBT | species | Dominant size (cm) | data type |
|--------|------------|--------------------|-------------|---------------------------------|----------------------------------|----------------------------------|---------|--------------------|---------------------|
| Afrika | 2018-12-04 | 182 | 20 | 2843 | 2448 | 2214 | SPR | 9 | fish school |
| Afrika | 2018-12-05 | 50 | 20 | 7951 | 8264 | 7129 | SPR | 11 | single target marks |
| Afrika | 2018-12-18 | 60 | 45 | 608 | 812 | 893 | HER | 26 | single target marks |
| Afrika | 2018-12-19 | 50 | 35 | 1542 | 1770 | 2136 | HER | 25 | single target marks |
| Afrika | 2018-12-20 | 80 | 35 | 1458 | 1724 | 2334 | HER | 27 | single target marks |
| Afrika | 2019-02-23 | 69 | 160 | 994 | 831 | 340 | MAC | 35 | fish school |
| Afrika | 2019-02-25 | 32 | 130 | 242 | 249 | 167 | MAC | 35 | fish school |
| Alida | 2017-12-04 | 41 | 60 | 458 | 417 | 320 | HOM | 28 ⁴ | single target marks |
| Alida | 2017-12-11 | 46 | 50 | 1457 | 2348 | 2816 | HER | 25 | fish school |
| Alida | 2018-02-05 | 100 | 120 | 3790 | 3367 | 3520 | HOM | 23 | fish school |
| Alida | 2018-07-14 | 66 | 100 | 642 | 906 | 624 | HER | 28 | fish school |
| Alida | 2018-07-17 | 53 | 120 | 919 | 1489 | 1092 | HER | 28 | fish school |
| Alida | 2018-07-18 | 158 | 120 | 6826 | 7610 | 8135 | HER | 28 | fish school |

⁴ value based on the length frequency calculated from fish weight measurements. This is done using the length-weight relationship from [65]: $L = (w/a)^{1/b}$ with $a = 0.0080$ and $b = 2.9739$.

8 Conclusions and recommendations

8.1 Conclusions

The realFishEcho project aims at developing and implementing real-time species identification and fish sizing algorithms. This is done using data collected by commercial vessels. The practical implementation of a demonstrator software for real-time viewing of acoustic data and species recognition has been implemented effectively. The software is utilizing data from the simrad EK80 echosounder operated in broadband mode (FM). The use of this operation mode for fish species identification is novel and offers two main advantages: measurement of the frequency response across large bandwidths; improved range resolution.

Through the course of the project, a large amount of data was collected (19 TB). These data (acoustics and fish sampling) were collected during fishing operations by two commercial fishing vessels: the Alida (SCH6) and the Afrika (SCH24). The coverage included the North Sea, the English Channel and the West of the UK. A range of species was sampled: Herring, Horse Mackerel, Mackerel exemplify large data size whilst Sprat, Sardine were only sparsely sampled. A protocol for handling the large amount of data has been developed: the data are first reduced to individually detected school and then saved in a database. Relevant schools are allocated species based on catch information. This database is used for efficient analysis and algorithm development.

Alongside data collection, echosounder calibration was performed on board both the Alida (SCH6) FV and Afrika (SCH24) FV. The analysis of the calibration data revealed discrepancies between different calibration trials. Similar discrepancies were found when analysing calibration data from RFV Tridens II. It is important to note that this is only for the calibration results in FM mode on these vessels. The large extend of these deviations are possibly related to various noise conditions but are unlikely to be related to genuine changes from the echosounder. The lack of precision of the calibration results is an issue for cross vessel application: merging of data from different vessel; application of species recognition algorithms trained using data from different vessels.

In line with previous studies [3], [5], the frequency response analysis of the entire data set confirmed strong overlap between swimbladdered species (Herring, Horse Mackerel, Sprat, Sardine) and good discrimination with non-swimbladdered species (Mackerel). The spectrum of Horse Mackerel in the North of Ireland were very distinct from horse mackerel in the western channel and South of Ireland. No clear relationship between was found between frequency response and fish size. The analysis of spectral trends showed that differences between swimbladdered fish species occur in the frequency bandwidth covered by the 200 kHz WBT channel.

Drawing on the large amount of data collected by fishing vessels, a machine learning approach has been used to derive two independent classifiers (TNO and WMR classifiers). These classifiers were also combined. The bulk of the data available stems from the Alida (SCH6) FV and include data for Herring, Horse Mackerel and Mackerel. The classification for these species exemplify very high accuracies (TNO: 95.6%, WMR: 93.5%, combined: 98.1%). When applied on data from the Afrika (SCH24) FV, the algorithms showed lower scores (TNO: 80.6%, WMR: 78.4%), mostly because of calibration discrepancies. The inclusion of data of Sprat and Sardine was also tested. Sprat score was low whilst Sardine was well recognized. Though, only a limited amount of data was available for these species. Further data collection is needed prior to the inclusion of these species for a robust classification. Similarly to the frequency response analysis, sensitivity tests showed that classification (both classifiers) is most impacted with bias of the 200 kHz WBT channel. This channel is also the one most variable in the calibration process. Finally, the effect of reducing the data richness was tested via: reduction in available transducers (deep water application); reduction in frequency bandwidth (mimicking the ES80 system). Both cases exemplified a decrease in score though these remain relatively high (>75 %). Using

only 1 or 2 WBTs was only able to detect difference between swimbladdered fish and non-swimbladdered fish. This could be used on board FVs under controlled conditions (e.g. in specific geographical areas).

Last, a novel method for estimating fish sizes was developed and tested. It uses the increased range resolution of the EK80 in FM mode to differentiate the boundaries of single target fish. The distance between boundaries is related to the size of the fish insonified. Here, the methodology is applied to different acoustic records exemplifying single fish marks and fish schools. The 200 WBT channel was found the most useful channel for the fish sizing estimation. For single fish type acoustic marks, one was able to see differences in acoustically inferred size distributions between fish of 10 cm size (Sprat) and 25 cm size. However, high variability was also observed which can be related to the poor ground truthing. Overall, more quality data and variety in observed fish sizes is needed to further the development of the method.

8.2 Recommendations

- For the development of a fish species recognition algorithm, it is important to have access to a large amount of data with diversity (geographical location, depth, time of year, time of day etc...).
- Inclusion of additional species to the identification algorithm is dependent on the data available for this species (amount of data and diversity).
- Automatic recording and discarding of data is desirable for seamless recording and data management on board fishing vessels
- High interference noise was experienced due to high frequency omnidirectional SONARs. It is recommended that these units are synchronised with the EK80.
- At sea calibration of the EK80 FM exemplifies unexplained variability in resulting calibration gain, both for the fishing vessels and the survey vessel. Dedicated experimentation is needed to understand and address the sources of error.
- Addition and improvement of particular echosounder pre-processing steps can further improve classification scores and robustness. These steps relate to the use of more up-to-date online environmental databases and corrections for school geometry and positioning.
- In order to reduce bias and improve classification success, it is particularly important to calibrating the echosounders in favourable conditions and follow best practices (Annex III).
- Fish sizing estimation method should be further investigated with the collection of dedicated data sets (acoustic records exemplifying single fish marks). Diversity in the data is particularly needed (i.e. large span of length classes).
- Application of the classifier at large depths is hampered by the high noise level at high frequencies (200 kHz WBT channel).
- The inclusion of additional frequencies for large depth applications (e.g. 18 kHz, 38 kHz) could improve the classification success in these scenarios, but also could allow addition of more species to discriminate between.
- The use of auxiliary features (e.g. depth, time of day, time of year) could be used to improve classification accuracy though should be used with caution. These features can potentially discriminate cases solely because there is not enough diversity in the available data.

Quality Assurance

Wageningen Marine Research utilises an ISO 9001:2015 certified quality management system. This certificate is valid until 15 December 2021. The organisation has been certified since 27 February 2001. The certification was issued by DNV GL.

Acknowledgements

Crew and skippers of the Alida (SCH6) FV, the Afrika (SCH24) FV and the Willem van der Zwan (SCH302) FV are acknowledged for their efforts in data collection. Special thanks go to Bas (skipper of the Alida (SCH6)) and his crew who were pivotal for the large scale data collection performed in this project.

The Pattern Recognition Research Group of the TU Delft, The Netherlands, is acknowledged for the use of PRTools, a pattern recognition MatLab toolbox with a variety of built-in classifiers and evaluation methods.

Gavin MaccAulay and Rokas Kubilius are acknowledged for fruitful discussions on the length estimation method.

Project management and dissemination activities

Through the course of the project, results were communicated regularly to project partners, stakeholders and scientific fora. The type of audience ranged from stakeholder from the fishery sector to scientists from different background (acoustics, fisheries). In addition, regular progress meetings were held between WMR and TNO and regular contact was kept with the skippers from the Alida (SCH6) FV and the Afrika (SCH24) FV. Numerous meetings were held with Sustainovate⁵ which ran a project (SEAT⁶) collecting data on the same fishing vessels as the realFishEcho project. The notable dissemination activities undertaken in this project are listed in the below table.

Table: dissemination activities undertaken within this project.

| Activity type | Location | Date | Audience |
|---|--------------------------------|--------|--|
| Project progress meeting | Scheveningen (The Netherlands) | Feb/17 | Science and industry project partners |
| Presentation at the acoustical Society of America conference conference: "Classification of pelagic fish using wideband echosounders" | Boston (USA) | Jun/17 | International scientists specialised in acoustics |
| Coordination between Broadband project and SEAT project | Scheveningen (The Netherlands) | Jun/17 | Science partners from realFishEcho and SEAT projects |
| Presentation at the bioacoustic day conference: "Fish species identification using wideband echosounders" | Den Helder (The Netherlands) | Oct/17 | International scientists specialised in acoustics and biology |
| Presentation at a day dedicated to the sharing of results from various species identification projects (organized by RVZ): "RealFishEcho - broadband (EK80) species recognition " | Zoetermeer (The Netherlands) | Nov/17 | Science and industry stakeholders |
| Coordination between Broadband project and SEAT project | Amsterdam (The Netherlands) | Jan/18 | Science partners from realFishEcho and SEAT projects |
| Update on project results | IJmuiden (The Netherlands) | Jun/18 | Science project partners |
| Project update and planning for at sea trials | Scheveningen (The Netherlands) | Aug/18 | Science and industry project partners |
| Remote presentation at the ICES working group WGIPS: "Fish species recognition using broadband acoustics" | Tenerife (Spain) | Jan/19 | International scientists specialised in fisheries |
| Update on project results | Zoetermeer (The Netherlands) | Feb/19 | Science and industry project partners |
| Story of the month in DG MARE newsletter | | Apr/19 | International scientists |
| Presentation at the ICES working group WGFASST: | Galway (Ireland) | Apr/19 | International scientists specialised in fisheries |
| Presentation of final results | Ijmuiden (The Netherlands) | May/19 | Science and industry stakeholders |
| Presentation of final results to participating vessels | Scheveningen (The Netherlands) | Jun/19 | Science and industry stakeholders and skippers involved in the project |
| Presentation of results to stakeholders (scientists, fleet managers, skippers) | Zoetermeer (The Netherlands) | Jun/19 | Science and industry stakeholders and skippers |

⁵ <https://sustainovate.com/>

⁶ SEAT: School Exploration and Analysis Tool. See: *Sustainovate 2017 Improved Selectivity of Small Pelagics iun the North Sea & North Atlantic Using SEAT*

References

- [1] EU, "Regulation No 1380/2013 of the European Parliament and of the Council of 11 December 2013 on the Common Fisheries Policy," *Off. J. Eur. Communities*, vol. 354, no. 22, 2013.
- [2] E. J. Simmonds and D. N. MacLennan, *Fisheries acoustics: theory and practice*, 2nd ed., no. 10. Oxford ; Ames, Iowa: Blackwell Science, 2005.
- [3] R. J. Korneliussen, Y. Heggelund, I. K. Eliassen, and G. O. Johansen, "Acoustic species identification of schooling fish," *ICES J. Mar. Sci.*, vol. 66, no. 6, pp. 1111–1118, Jul. 2009.
- [4] R. J. Korneliussen, Y. Heggelund, G. J. Macaulay, D. Patel, E. Johnsen, and I. K. Eliassen, "Acoustic identification of marine species using a feature library," *Methods Oceanogr.*, vol. 17, pp. 187–205, Dec. 2016.
- [5] R. J. Korneliussen, "The acoustic identification of Atlantic mackerel," *ICES J. Mar. Sci.*, vol. 67, no. 8, pp. 1749–1758, Nov. 2010.
- [6] T. K. Stanton and D. Chu, "Calibration of broadband active acoustic systems using a single standard spherical target.," *J. Acoust. Soc. Am.*, vol. 124, no. 1, pp. 128–36, Jul. 2008.
- [7] B. J. P. Berges, S. Sakinan, and E. van Helmond, "Practical implementation of real-time fish classification from acoustic broadband echo sounder data- RealFishEcho progress report: Year 1- June 2017," *IJmuiden Wageningen Mar. Res. (Wageningen Mar. Res. Rep. C082/17)*, p. 29, 2017.
- [8] B. J. P. Berges, S. Sakinan, and E. van Helmond, "Practical implementation of real-time fish classification from acoustic broadband echo sounder data - RealFishEcho progress report Year 2 - June 2018," *IJmuiden Wageningen Mar. Res. (Wageningen Mar. Res. Rapp. C062/18) - 42*, p. 42, 2018.
- [9] B. J. P. Bergès and E. van Helmond, "Practical implementation of real-time fish classification from acoustic broadband echo sounder data - RealFishEcho: classification algorithm improvements," *(Wageningen Mar. Res. Rapp. C010/18)*, p. 15, 2017.
- [10] S. M. M. Fassler *et al.*, "VIP report 'Use of new broadband echosounder': Techniques for improved ocean imaging and selectivity in pelagic fisheries," *IMARES Rep.*, vol. C171/15, p. 100, 2015.
- [11] D. G. Reid and E. J. Simmonds, "Image Analysis Techniques for the Study of Fish School Structure from Acoustic Survey Data," *Can. J. Fish. Aquat. Sci.*, vol. 50, no. 5, pp. 886–893, May 1993.
- [12] J. Simmonds, F. Armstrong, and P. J. Copland, "Species identification using wideband backscatter with neural network and discriminant analysis," *ICES J. Mar. Sci.*, vol. 53, no. 2, pp. 189–195, Apr. 1996.
- [13] K. G. Foote, H. P. Knudsen, G. Vestnes, D. N. MacLennan, and E. J. Simmonds, *Calibration of acoustic instruments for fish density estimation: a practical guide*. Copenhagen Denmark: International Council for the Exploration of the Sea, 1987.
- [14] D. A. Demer *et al.*, "Calibration of acoustic instruments," *ICES Coop. Res. Rep.*, vol. 326, p. 133, 2015.
- [15] T. Brunel, S. Gastauer, S. Fassler, and D. Burggraaf, "Using acoustic data from pelagic fishing vessels to monitor fish stocks," *IMARES (Report / IMARES Wageningen UR C021/13)*, p. 121, 2013.
- [16] S. M. M. Fassler, T. Brunel, A. S. Couperus, S. Gastauer, and D. Burggraaf, "VIP report acoustic data collection: implementation of the structural use of acoustic data from pelagic trawlers in scientific stock estimates (PelAcousticII)," *IJmuiden IMARES Wageningen UR (IMARES Rep. C178/15)*, p. 121, 2015.
- [17] S. M. M. Fässler, T. Brunel, S. Gastauer, and D. Burggraaf, "Acoustic data collected on pelagic fishing vessels throughout an annual cycle: Operational framework, interpretation of observations, and future perspectives," *Fish. Res.*, vol. 178, pp. 39–46, Jun. 2016.
- [18] M. Pastoors, "PFA self-sampling report 2015-2018," *PFA*, vol. 03, 2019.
- [19] M. Pastoors, "Self-sampling Manual v 2.12," *PFA2*, vol. 05, 2019.
- [20] K. G. Foote *et al.*, "Protocols for calibrating multibeam sonar," *J. Acoust. Soc. Am.*, vol. 117, no. 4, p. 2013, Apr. 2005.
- [21] D. MacLennan, "The Theory of Solid Spheres as Sonar Calibration Targets," *Scottish Fish. Res. Rep.*, no. 22, 1981.
- [22] P. Lunde and R. Korneliussen, "Power-Budget Equations and Calibration Factors for Fish Abundance Estimation Using Scientific Echo Sounder and Sonar Systems," *J. Mar. Sci. Eng.*, vol. 4, no. 3, p. 43, Jul. 2016.
- [23] P. Lunde, O. A. Pedersen, R. J. Korneliussen, F. E. Tichy, and H. Nes, *Power-budget and echo-integrator equations for fish abundance estimation*. Institute of Marine Research, Bergen, Norway,

- 2013.
- [24] P. Lunde and R. J. Korneliussen, *A unifying theory explaining different power budget formulations used in modern scientific echosounders for fish abundance estimation*. Institute of Marine Research, Bergen, Norway, 2014.
- [25] R. E. Francois and G. R. Garrison, "Sound absorption based on ocean measurements: Part I: Pure water and magnesium sulfate contributions," *J. Acoust. Soc. Am.*, vol. 72, no. 3, p. 896, 1982.
- [26] R. E. Francois and G. R. Garrison, "Sound absorption based on ocean measurements. Part II: Boric acid contribution and equation for total absorption," *J. Acoust. Soc. Am.*, vol. 72, no. 6, p. 1879, 1982.
- [27] D. A. Demer *et al.*, "2016 USA–Norway EK80 Workshop Report: Evaluation of a wideband echosounder for fisheries and marine ecosystem science," in *ICES Cooperative Research Report*, 2017, vol. 336, p. 69.
- [28] G. J. Macaulay, B. Scouling, E. Ona, and S. M. M. Fässler, "Comparisons of echo-integration performance from two multiplexed echosounders," *ICES J. Mar. Sci.*, vol. 75, no. 6, pp. 2276–2285, Dec. 2018.
- [29] S. Sakinan, D. de Haan, D. Burggraaf, and S. Fassler, "Investigation of echosounder finger prints of Dutch pelagic freezer trawlers (SEAT II) evaluation of the SEAT II joint-industry project: evaluation of the SEAT II joint-industry project," 2018.
- [30] NOAA, "EK500-EK60 comparison workshop," 2004.
- [31] J. M. Jech, K. G. Foote, D. Chu, and L. C. Hufnagle Jr., "Comparing two 38-kHz scientific echosounders," *ICES J. Mar. Sci.*, vol. 62, no. 6, pp. 1168–1179, Sep. 2005.
- [32] H. Hobæk and T. L. Nesse, "Scattering from spheres and cylinders - revisited," in *29th Symposium on Physical Acoustics*, 2006.
- [33] D. Chu and G. C. Eastland, "Calibration of a broadband acoustic transducer with a standard spherical target in the near field," *J. Acoust. Soc. Am.*, vol. 137, no. 4, pp. 2148–2157, Apr. 2015.
- [34] C. Bassett, A. De Robertis, and C. D. Wilson, "Broadband echosounder measurements of the frequency response of fishes and euphausiids in the Gulf of Alaska," *ICES J. Mar. Sci.*, vol. 75, no. 3, pp. 1131–1142, May 2018.
- [35] ICES, "Report of the Working Group on International Pelagic Surveys (WGIPS)," 2018.
- [36] L. R. Dragonette, S. K. Numrich, and L. J. Frank, "Calibration Technique for Acoustic Scattering Measurements," *J. Acoust. Soc. Am.*, vol. 69, no. 4, pp. 1186–1189, 1981.
- [37] S. Sakinan and B. J. P. Berges, "Investigation of the use of the EK80 CW during acoustic surveys on board Tridens II," *IJmuiden Wageningen Mar. Res. (Wageningen Mar. Res. Rapp.*, p. 41, 2019.
- [38] R. J. Urick, *Principles of Underwater Sound 3rd Edition*. Peninsula Pub, 1996.
- [39] A. Antona, "Remote Fish Species and Size Identification Using Broadband Echosounders," Wageningen UR, 2016.
- [40] J. Tang, S. Aleyani, and H. Liu, "Feature Selection for Classification: A Review," in *C. Aggarwal (ed.), Data Classification: Algorithms and Applications*, CRC Press, 2014, p. 29.
- [41] P. Galeano, E. Joseph, and R. E. Lillo, "The Mahalanobis Distance for Functional Data With Applications to Classification," *Technometrics*, vol. 57, no. 2, pp. 281–291, Apr. 2015.
- [42] F. Korn, B.-U. Pagel, and C. Faloutsos, "On the 'dimensionality curse' and the 'self-similarity blessing,'" *IEEE Trans. Knowl. Data Eng.*, vol. 13, no. 1, pp. 96–111, 2001.
- [43] A. F. Zuur, R. J. Fryer, I. T. Jolliffe, R. Dekker, and J. J. Beukema, "Estimating common trends in multivariate time series using dynamic factor analysis," *Environmetrics*, vol. 14, no. 7, pp. 665–685, Nov. 2003.
- [44] M. T. Hagan, H. B. Demuth, M. H. Beale, and O. De Jesús, *Neural network design*. [publisher not identified], 2014.
- [45] S. M. M. Fässler, R. Santos, N. García-Núñez, and P. G. Fernandes, "Multifrequency backscattering properties of Atlantic herring (*Clupea harengus*) and Norway pout (*Trisopterus esmarkii*)," *Can. J. Fish. Aquat. Sci.*, vol. 64, no. 2, pp. 362–374, Feb. 2007.
- [46] P. C. Hansen, *Discrete Inverse Problems: Insight and Algorithms (Fundamentals of Algorithms)*. SIAM-Society for Industrial and Applied Mathematics, 2010.
- [47] H. Peltonen and H. Balk, "The acoustic target strength of herring (*L.*) in the northern Baltic Sea," *ICES J. Mar. Sci.*, vol. 62, no. 4, pp. 803–808, Jun. 2005.
- [48] S. McClatchie and R. F. Coombs, "Low target strength fish in mixed species assemblages: the case of orange roughy," *Fish. Res.*, vol. 72, no. 2–3, pp. 185–192, May 2005.
- [49] S. M. M. Fassler and N. Gorska, "On the target strength of Baltic clupeids," *ICES J. Mar. Sci.*, vol. 66, no. 6, pp. 1184–1190, Jul. 2009.
- [50] G. Pedersen, O. R. Godo, E. Ona, and G. J. Macaulay, "A revised target strength-length estimate for blue whiting (*Micromesistius poutassou*): implications for biomass estimates," *ICES J. Mar. Sci.*, vol. 68, no. 10, pp. 2222–2228, Nov. 2011.
- [51] E. Ona, "An expanded target-strength relationship for herring," *ICES J. Mar. Sci.*, vol. 60, no. 3, pp.

-
- 493–499, Jun. 2003.
- [52] T. Okumura, T. Masaya, T. Yoshimi, and S. Kouichi, "Acoustic scattering by an arbitrarily shaped body: an application of the boundary-element method," *ICES J. Mar. Sci.*, vol. 60, no. 3, pp. 563–570, Jun. 2003.
- [53] G. Pedersen, N. O. Handegard, and E. Ona, "Lateral-aspect, target-strength measurements of in situ herring (*Clupea harengus*)," *ICES J. Mar. Sci.*, vol. 66, no. 6, pp. 1191–1196, Jul. 2009.
- [54] A. Lebourges-Dhaussy, "Caractérisation des populations planctoniques par acoustique multifréquence," *Océanis*, vol. 22, no. 1, pp. 71–92, 1996.
- [55] D. Holliday and R. Pieper, "Bioacoustical oceanography at high frequencies," *ICES J. Mar. Sci.*, vol. 52, no. 3–4, pp. 279–296, Aug. 1995.
- [56] C. Greenlaw, "Acoustical estimation of zooplankton populations," *Limnol. Ocean.*, vol. 24, no. 2, pp. 226–242, 1979.
- [57] S. Vagle and D. M. Farmer, "The Measurement of Bubble-Size Distributions by Acoustical Backscatter," *J. Atmos. Ocean. Technol.*, vol. 9, no. 5, pp. 630–644, 1992.
- [58] H. Medwin, "Counting bubbles acoustically: a review," *Ultrasonics*, vol. 15, no. 1, pp. 7–13, Jan. 1977.
- [59] H. Medwin, "Acoustical determinations of bubble-size spectra," *J. Acoust. Soc. Am.*, vol. 62, no. 4, p. 1041, Oct. 1977.
- [60] T. K. Stanton, D. Chu, J. M. Jech, and J. D. Irish, "New broadband methods for resonance classification and high-resolution imagery of fish with swimbladders using a modified commercial broadband echosounder," *ICES J. Mar. Sci.*, vol. 67, no. 2, pp. 365–378, Jan. 2010.
- [61] T. K. Stanton, C. J. Sellers, and J. M. Jech, "Resonance classification of mixed assemblages of fish with swimbladders using a modified commercial broadband acoustic echosounder at 1–6 kHz," *Can. J. Fish. Aquat. Sci.*, vol. 69, no. 5, pp. 854–868, May 2012.
- [62] R. Kubiilius, E. Ona, G. J. Macaulay, and A. Totland, "Broadband backscattering from artificial fish-like targets," *ICES Work. Gr. Fish. Acoust. Sci. Technol. 2018*, 2018.
- [63] R. Kubiilius, G. J. Macaulay, E. Ona, A. Totland, and T. Forland, "Broadband backscattering from tethered Atlantic mackerel," *ICES Work. Gr. Fish. Acoust. Sci. Technol. 2019*, 2019.
- [64] Z. I. Botev, J. F. Grotowski, and D. P. Kroese, "Kernel density estimation via diffusion," *Ann. Stat.*, vol. 38, no. 5, pp. 2916–2957, Oct. 2010.

Table of figures

Figure 2-1: working principles of the EK80 system for an individual WBT frequency channel. Most often, several WBT channels operate simultaneously (or sequentially) on FVs. In operational use, the EK80 system (combination of transducer and transceiver) probes the water column in the acoustic beam. Subsequent echo returns can be displayed as echograms by the EK80 or ES 80 software. These software are also able to record data in the *.RAW format. Each EK80 system has a specific set of calibration values: gain and beam update. These are determined during dedicated calibration trials that are performed using the standard sphere method [13], [14] (see Section 3). 12

Figure 2-2: comparison of fast and slow ramping acoustic pulses used by the EK80 FM. (a) fast ramping time signal. (b) slow ramping time signal. (c) frequency content of a fast ramping pulse. (d) frequency content of a slow ramping pulse. 13

Figure 2-3: distribution of data collected in the realFishEcho project. (a) Location of calibration data sets (Table 2-2) for the Afrika (SCH24) FV. (b) Location of calibration data sets (Table 2-2) for the Alida (SCH6) FV. (c) Location of calibration data sets (Table 2-2) for RFV Tridens II. (d) and (e): Individually detected fish school for the different data sets (Table 2-3), separated by FV, Alida (SCH6) is shown in (d) and Afrika (SCH24) is shown in (e). 14

Figure 2-4: length measurements collected through the course of this project for the different species. The different length frequencies are normalized plotted together for comparison. The samples are sorted in ascending order. (a) Herring. (b) Horse Mackerel. (c) Mackerel. (d) Sprat and Sardine. 17

Figure 2-5: echogram example of reduced data. The data of the fish school is selected with 30 pings before and after the school and converted into a specific data format. The thick solid black represents the boundary of the school. 18

Figure 2-6: example organisational tree of a single data set. This data organisation is the basis for the analysis carried out in this project. A single data set is associated to each trip from each fishing vessel. Here, the data set ALID_HOM_2016_10 is exemplified and corresponds to the data collected by the Alida (SCH6) in October 2016 which mostly consisted in Horse Mackerel (HOM). After a semi-automatic processing and reduction of the raw data, only the data containing fish schools are retained. The data for the trip are then organised following the folder tree presented here which consists of: (1) the associated calibration set (2) the associated ground truth (catch composition and length frequency), (3) the acoustic data for each detected school, (4) the cell based spectra for each school and fish school metadata, (5) echogram for each school for each WBT channel (70 kHz, 120 kHz, 200 kHz). 19

Figure 3-1: (a) echogram display after deployment of the calibration spheres. (b) EK80 interface used for calibration. 22

Figure 3-2: theoretical target strength (TS) vs frequency. This analytically inferred TS is used to compare measurements of the EK80 FM against and in turn determine calibration gains at different frequencies. The solid black line is the theoretical target strength. The shaded area represents the working range of the EK80 FM 120 kHz channel. The subsequent green and red areas are the useable and non-useable frequency ranges for calibration respectively. (a) 22 mm WC calibration sphere. (b) 38.1 mm WC calibration sphere. 23

Figure 3-3: S_v time series example around a calibration sphere, exemplifying the different time windows used for sphere detection and TS calculation. 24

Figure 3-4: working examples of criteria used for calibration sphere detection. (a) SNR is calculated as the ratio of acoustic power between the window for sphere detection and the window for TS calculation. (b) Only the detection with compensated TS is within upper and lower bounds offsets from the theoretical TS is considered a successful detection. 25

Figure 3-5: calibration processing workflow. Reading each raw files, the targeted calibration sphere is tracked through the pings (a). For each detection, target strength can be calculated and compared to the theoretical target strength (b). The difference in level is effectively the gain (c). It is important to note that outside dip regions the gain values are erroneous and are therefore not used. These are shown here as an examples. In the null regions, the gain is interpolated. The different detections allow

| | |
|---|----|
| one to assess the accuracy of the calibration exercise. The accuracy is commonly expressed as the standard deviation in gain, estimated from gains estimated from every single detections (d)..... | 25 |
| Figure 3-6: historical calibration gain for the narrow band echosounders EK60 and EK80 CW onboard Tridens II. The drop of ~2 dB for the EK80 CW in March and June 2018 corresponds to a malfunction of the transceiver that was replaced in June 2019..... | 26 |
| Figure 3-7: example of discrepancies in calibration gains after the processing of the data using the EK80 calibration software. The blue line is the calibration on the 25 mm WC sphere in 2016. The red line is the calibration on the 25 mm WC sphere in 2017..... | 27 |
| Figure 3-8: calibration spheres used during the calibration trial. (a) single attachment point calibration spheres used in the experiment (22 mm WC, 25 mm WC, 38.1 mm WC). (b) example of a three attachment points calibration spheres (25 mm WC displayed here though a 22 mm WC sphere with three attachment points was also used)..... | 29 |
| Figure 3-9: gain and standard deviation for the different setups used (.....) | 31 |
| Figure 3-10: boxplot of the signal to noise ratio of selected pings for the different data sets investigated here. (a) 70 kHz WBT channel. (b) 120 kHz WBT channel. (c) 200 kHz WBT channel. ... | 31 |
| Figure 3-11: comparison of calibration outputs computed from calibration data collected by Tridens II between 2015 and 2019. (a) calibration gains at 70 kHz channel. (c) calibration gains at 120 kHz channel. (e) calibration gains at 200 kHz channel. For each plot, the difference in marker and line type is associated with different sphere types while the differences in colour is associated with different years (i.e. different data sets). The different data sets presented here are: 2015 (blue colour), 2016 (dark green colour), 2017 (bright green colour), 2018 (yellow colour), 2019 (red colour). The different spheres are: 22 mm WC (solid lines), 25 mm WC (solid lines with circle markers), 38.1 mm WC (dashed lines with star markers). Data sets with settings as those listed in Table 2-1 are 2017 and 2019. (b) (d) (f): deviation from theoretical TS (TS error) against Signal to Noise Ratio (SNR) for the different combinations of year, frequencies and sphere type..... | 33 |
| Figure 3-12: comparison of calibration data collected from a 38.1 mm WC sphere by the Alida (SCH6) in 2017 and in 2018. (a) calibration gain from 2018 and 2017 data sets. (b) boxplot of SNR for each detected hit. The 2018 data set showed here exemplifies high SNR. (c) frequency compensated TS for a single hit in the same location in the beam (i.e. equivalent compensation). (d) summary plot for compensated TS across all the sphere detections with 50 th , 25 th and 75 th percentiles for both data sets. The solid black line in the theoretical frequency response..... | 34 |
| Figure 3-13: comparison of calibration outputs computed from calibration data collected by FVs between 2015 and 2018: (a) 70 kHz channel (c) 120 kHz channel (e) 200 kHz channel. For each plot, the difference in marker and line type is associated with different sphere types while the differences in colour is associated with different years and vessel (i.e. different data sets). The different data sets presented here are: Afrika (SCH24) 2016 (blue colour), Alida (SCH6) 2015 (dark green colour), Alida (SCH6) 2016 (bright green colour), Alida (SCH6) 2017 (yellow colour), Alida (SCH6) 2018 (red colour). The different spheres are: 15 mm WC, (dashed line with cross markers) 22 mm WC (solid lines), 25 mm WC (solid lines with circle markers), 38.1 mm WC (dashed lines with star markers). Data sets with settings as those listed in Table 2-1 are 2017 and 2018. (b) (d) (f): deviation from theoretical TS (TS error) against SNR for the different combinations of year, frequencies and sphere type..... | 36 |
| Figure 4-1: Schematic overview of the processing chain of the demonstrator, suited for both online and offline processing..... | 39 |
| Figure 4-2: Block diagram indicating the processing steps of the pre-processor..... | 40 |
| Figure 4-3: Block diagram indicating the processing modules of the image processor..... | 41 |
| Figure 4-4: Example echograms of the three Wide-Band Transceivers: 70 kHz (a); 120 kHz (b); 200 kHz (c)..... | 42 |
| Figure 4-5: Steps in the depth estimation process. The input echogram of WBT2 (a). A slightly filtered version of the echogram in which the bottom is spread out (b). The median intensity levels of the pings and the estimated average depth (c). The depth estimation bracket indicated in magenta and the depth estimated per ping indicated by black crosses (d)..... | 42 |
| Figure 4-6: Bottom-aligned, truncated echograms of the three Wide-Band Transceivers: 70 kHz (a); 120 kHz (b); 200 kHz (c)..... | 43 |
| Figure 4-7: Processing steps in bad pixel detection. Example input echogram (a) of WBT 70 kHz. Range-filtered echogram to avoid assigning isolated pixels as 'bad' (b). Background template | |

| | |
|---|----|
| <i>indicating expected signal levels (c). Deviation of echogram from template (d). Pixel groups assigned as 'bad' (e).</i> | 43 |
| Figure 4-8: <i>example of the image enhancement processing.</i> | 44 |
| Figure 4-9: <i>Steps describing the disturbance detection and analysis process. Input echogram (a). Initial bad pixel mask detected in the bad pixel detection module (b). Filtered bad pixel mask, indicating the locations of the dominant interferences (c). Spectrum of the analysed interferences showing two dominant, narrowband peaks of interfering sonars (d).</i> | 45 |
| Figure 4-10: <i>Steps describing the school detection process. One of the input echograms (a). The filtered version of the echogram (b). The final school detection mask after combining the detection masks of the three transceivers (c).</i> | 45 |
| Figure 4-11: <i>Example time signal of a single ping of WBT3, after correction for propagation loss. After a certain range the noise exceeds the detection threshold. By applying a range-dynamic detection threshold, the operating range of the demonstrator can be slightly increased.</i> | 46 |
| Figure 4-12: <i>Division in cells of the example school. On each cell, time signal and spectral features are computed after which they are classified. A single cell is roughly 1.6m in length.</i> | 46 |
| Figure 4-13: <i>Classification result for the given example school, where the colour of each cell indicates the estimated species type as which it is classified.</i> | 47 |
| Figure 4-14: <i>Screenshot of the Graphical User Interface (GUI) of the demonstrator, used on board by the skipper.</i> | 48 |
| Figure 4-15: <i>Screenshot of the streaming echogram display.</i> | 48 |
| Figure 4-16: <i>Screenshot of the classification display, showing the detected schools and the estimated species type by the classifier.</i> | 49 |
| Figure 4-17: <i>Control panel with the different visualization settings that can be selected by the user.</i> | 49 |
| Figure 4-18: <i>Screenshots of the echogram of the same transceiver, displayed in different frequency bands: (a) full 70 kHz WBT channel band, 47-90 kHz; (b) partial frequency band from 70 kHz WBT channel, 61-64 kHz. The frequency band is selectable in the data type menu.</i> | 50 |
| Figure 4-19: <i>Screenshots of the same echogram, displayed without (a) and with (b) image enhancement, selectable using the filtering buttons.</i> | 50 |
| Figure 4-20: <i>Image length box to modify the history length of the echogram.</i> | 51 |
| Figure 4-21: <i>Screenshots of the same echogram displayed with different colour scaling maps: (a) jet; (b) hot2cold; (c) parula. The colour scheme is selectable in the colour map menu.</i> | 51 |
| Figure 4-22: <i>GUI screens in day (a) and night (b) mode, selectable in the interface colours menu.</i> .. | 52 |
| Figure 4-23: <i>Data recording button in different modes: not recording (a) and recording (b).</i> | 52 |
| Figure 4-24: <i>Disturbance analysis panel, displaying a frequency spectrum computed on the detected interferences in the echograms. This indicates the operating frequencies of narrowband interferences (other sonars).</i> | 53 |
| Figure 5-1: <i>example of spectral down sampling used when deriving spectral features. (a) down sampling (red line) and smoothing (blue line) operation applied to the raw spectrum (thin black line), (b) resulting spectrum after down sampling, smoothing and normalisation.</i> | 54 |
| Figure 5-2: <i>frequency response analysis. (a) processing workflow for the frequency response analysis, i.e. comparison between different spectra. (b) example Dendrogram plot used to discard outlier clusters. (c) location of the different clusters in the school. The clusters that have less than 5% cells of the total number of cells in the school are discarded.</i> | 55 |
| Figure 5-3: <i>MDS plot representing the distance between each ground thruthed school in the database (for the Alida (SCH6) FV data). Each dot represents a school. The different species are differentiated with different colours: Herring (HER, blue), Horse Mackerel (HOM, red); Mackerel (MAC, black); Sprat (SPR, green); Sardine (PIL, yellow). It is important to note that only few schools for Sprat and Sardine are available and these overlap with Herring and Horse Mackerel.</i> | 56 |
| Figure 5-4: <i>fish school comparison with respect to different areas and length classes.</i> | 57 |
| Figure 5-5: <i>average relative frequency response (at 60 kHz) for the different data sets and species (Table 2-4)</i> | 58 |
| Figure 5-6: <i>Echograms of the Alida (SCH6) (a,b,c) and Afrika (SCH24) (d,e,f) with all interfering sonars disabled. The data is not compensated for propagation loss in order to get an estimate of stationary background noise levels that are observable below the bottom return. In (g,h,i) plots of the median ping levels are given for the two vessels.</i> | 59 |
| Figure 5-7: <i>background noise level for the Alida (SCH6) and Afrika (SCH24) FVs. (a) 70 kHz WBT echogram from the Afrika (SCH24) FV. (b) 70 kHz WBT echogram from the Afrika (SCH6) FV. (c)</i> | |

| | |
|--|----|
| corresponding Average (median) ping of corresponding echograms ((a) and (b)), not corrected for prop-loss. | 59 |
| Figure 5-8: interference noise on board the Afrika (SCH24) FV. The noise is exemplified for each WBT frequency channel in echograms: 70 kHz WBT channel (a), 120 kHz WBT channel (d), 200 kHz WBT channel (g). The interference spectra for the difference interference noise are shown in separate plots: interference at 54 kHz (b), interference at 80 kHz (c), interference spectra for two pings with disturbances for the 120 kHz WBT channel (e and f), interference at 164 kHz (h), interference at 240 kHz (i)..... | 61 |
| Figure 6-1: example of a fish school being divided into different cells. Each cell is associated with its time signal and corresponding spectrum. This constitutes the basis for the analysis and classifier training. Classification is computed for each cell. (a) Echogram of a fish school. (b) corresponding cell division..... | 62 |
| Figure 6-2: Plot of two example features computed for the entire dataset. Each marker indicates the feature values of a different species. The coloured lines indicate the species boundaries derived by a number of different types of classifiers. | 63 |
| Figure 6-3: Plot of the expected classification performance as a function of the number of features used. Each line represents the result of a different type of classifier. | 64 |
| Figure 6-4: Confusion matrix for the used classifier when using all data sets. The percentages on the diagonal are the scores per species type. | 64 |
| Figure 6-5: Classification score per fishing trip. Each trip can contain multiple species types. Crosses indicate the results for data set-inclusive training, filled dots indicate the results for data set-exclusive training. | 65 |
| Figure 6-6: Example of the classification result of a school that likely contains different species types. | 65 |
| Figure 6-7: Confusion matrix when classifying Afrika data with a classifier also trained with Afrika data.. The percentages on the diagonal are the scores per species type. | 66 |
| Figure 6-8: Confusion matrix when adding Sprat as a fourth species. Sprat is partly classified as Horse Mackerel, but since these two species do not reside in the same area, Horse Mackerel could be replaced by Sprat in the relevant areas. | 67 |
| Figure 6-9: Illustration of the cell averaging process. The original cell values (a), in this case simply representing energy, are filtered with a sliding median window to deliver the averaged values (b). The resulting cells are still put into the classifier individually. | 67 |
| Figure 6-10: Spectra for different numbers of cells used in averaging for Horse Mackerel and Herring. The use of more cells leads to more stable spectra. Since the two species types are very similar, it is beneficial to have stable spectra. (a) averaging over 128 cells. (b) averaging over 32 cells. (c) averaging over 8 cells. (d) no averaging. | 68 |
| Figure 6-11: Confusion matrices indicating classification scores per species for different numbers of averaging cells. The use of fewer averaging cells will decrease the classification performance. (a) averaging over all available cells for each school. (b) averaging over 128 cells. (c) averaging over 64 cells. | 68 |
| Figure 6-12: results of classifier testing against erroneous calibration. Each scenario has a figure pair showing the change in calibration gain and resulting classification accuracy. | 70 |
| Figure 6-13: schematic of neural network architecture..... | 71 |
| Figure 6-14: workflow diagram for training and operational use of the WMR classifier. For the training of the NN, time features are derived from each cell but spectral features use the spectrum from each cell and a matrix <i>Utrunc</i> that was calculated from the training set. In operational use, the algorithm uses two inputs: the training neural network and the matrix <i>Utrunc</i> . The latter is used for the calculation of spectral features. | 73 |
| Figure 6-15: results from a NN training process. (a) Cross-entropy error index across epochs. (b) confusion matrix summarizing scores for training, validation and test data sets. | 74 |
| Figure 6-16: classification examples for two fish schools (HER and MAC). (a) and (b) echogram and subsequent classification of a Herring fish school. (c) and (d) echogram and subsequent classification of a Mackerel fish school. | 75 |
| Figure 6-17: classification results of the WMR classifier for different cell averaging configurations. The results are presented as confusion matrix for the WMR classifier trained and tested on data from the Alida (SCH6). (a) no cell averaging. (b) 10 cells averaging. (c) 30 cells averaging. (d) 60 cells averaging. (e) 500 cells averaging. | 76 |

| | |
|---|----|
| Figure 6-18: testing of the WMR classifier with one data set dropped at a time. The data sets are those collected by the Alida (SCH6) FV (Table 2-3). Cross markers are the baseline scores for each data set and each species (combined results presented in Figure 6-17) while open circle markers are the score from the leave one out test. (a) no cell averaging of features. (b) feature averaging over 10 cells. (c) feature averaging over 30 cells. (d) feature averaging over 60 cells. (e) feature averaging over 500 cells. | 77 |
| Figure 6-19: sensitivity tests. Each sensitivity test uses a offsets at a specific WBT channel: 0.5 dB, 1 dB, 1.5 dB, 2 dB, 2.5 dB and 3 dB. The 0 dB case is the baseline (Figure 6-17(c), averaging over 30 cells). Results are shown as classification score for the different species against calibration offset. (a) sensitivity test for the 70 kHz WBT channel. (b) sensitivity test for the 120 kHz channel. (c) sensitivity test for the 200 kHz channel. | 78 |
| Figure 6-20: classification of the data from the Afrika (SCH24) FV using the WMR classifier trained using the data from the Alida (SCH6) FV with an averaging over 30 cells. (a) Calibration gains used for the data from the Alida (SCH6) FV and the Afrika (SCH24) FV. (b) WMR classifier results. | 79 |
| Figure 6-21: classification for different cell averaging using data from the Afrika (SCH24) FV. Results are presented as confusion matrices. (a) classification results without feature averaging. (b) classification results with an average of features over 30 cells. | 79 |
| Figure 6-22: WMR classifier results of four species identification (Sprat as fourth species) using training based respectively on: (a) the data from the Afrika (SCH24) FV; (b) the data from the Alida (SCH6). The classifier uses a configuration with an averaging over 30 cells. | 80 |
| Figure 6-23: WMR classifier results of four species identification (Sardine (PIL) as fourth species) using training based on data from the Alida (SCH6) FV. The classifier uses a configuration with an averaging over 30 cells. | 80 |
| Figure 6-24: Confidence masks of both the TNO classifier and the WMR classifier for two example fish schools (a,b). Low confidence levels indicate the classifier is uncertain about the classification result for that cell. In (c) the confidence levels are plotted per cell for one of the example schools. | 81 |
| Figure 6-25: Classification scores per data set for the TNO classifier (a), WMR classifier (b) and the combined classifier (c). The combined classifier slightly outperforms both classifiers. | 82 |
| Figure 6-26: Average classification score per species type for the TNO classifier (circle markers), WMR classifier (cross markers) and the combined classifier (diamond markers). The combined classifier slightly outperforms both classifiers. | 82 |
| Figure 6-27: Confusion matrices for classification between Mackerel and Herring/Horse Mackerel when using a decreasing number of transceivers. The possibility of using fewer transceivers allows increasing the maximum operating depth of the classifier. | 83 |
| Figure 6-28: limitation in operating range with the EK80 for the different WBT of interest. | 85 |
| Figure 6-29: comparison of EK80 FM data with data with reduced frequency bandwidth (mimicking ES80 FM data). | 86 |
| Figure 6-30: classification results using data from the Alida (SCH6) FV mimicking the ES80 FM. | 87 |
| Figure 7-1: example of processing for fish size estimation. (a) EK80 FM echogram at 200 kHz with single target detection and tracking (red lines). (b) S_v time series around a single target detection. The main detection is shown as a black circle. Potential boundaries | 89 |
| Figure 7-2: schematic exemplifying the increased distance between detected boundaries as the angle deviated from the 90° grazing angle. | 89 |
| Figure 7-3: example echograms of the different data type used in this analysis. (a) single fish mark (data collected by the Afrika (SCH24) FV on 2018/12/18). (b) fish school marks (data collected by the Afrika (SCH24) FV on 2018/12/04). | 90 |
| Figure 7-4: example of kernel density estimation at the 200 kHz WBT channel. The probability density function (orange line) of the distribution (blue bars) is estimated using a kernel density estimation with a Gaussian Kernel. | 90 |
| Figure 7-5: fish size estimation for single fish marks. comparison of acoustically inferred fish sizes (right axis, blue lines) against length frequency distribution for different data sets (left axis, black bars). | 92 |
| Figure 7-6: fish size estimation for single fish school marks. comparison of acoustically inferred fish sizes (right axis, blue lines) against length frequency distribution for different data sets (left axis, black bars). | 93 |

Table of tables

| | |
|---|----|
| Table 1-1: <i>breakdown of the WPs and tasks within the realFishEcho project. Corresponding report sections are also given.</i> | 10 |
| Table 2-1: <i>EK80 settings used during data collection.</i> | 12 |
| Table 2-2: <i>overview of the calibration trials performed through the course of this project.</i> | 13 |
| Table 2-3: <i>overview of the data collected through the course of the project.</i> | 16 |
| Table 2-4: <i>summary of data collected by species.</i> | 16 |
| Table 3-1: <i>summary of the various setup investigated using calibration data collected onboard Tridens II RFV in June 2019.</i> | 29 |
| Table 6-1: <i>listing of features used for the WMR species identification. The time features are derived for each WBT channel and are then a set of 3 value each.</i> | 72 |
| Table 7-1: <i>summary of results of the fish length estimation. Information on the data used for the study is given (date, vessel, duration, water depth, species, data type, length frequency mode) together with the number of detection at each WBT (70 kHz, 120 kHz, 200 kHz) for each record. The length frequency for the data collected by the Alida (SCH6) FV on 2017/12/04 was not available (only weight measurements) and is calculated using a weight frequency relationship (see footnote) [65].</i> . | 94 |

Justification

Report C076/19

Project Number: 4311400004 EFMZV Real-time broadband.

The scientific quality of this report has been peer reviewed by a colleague scientist and a member of the Management Team of Wageningen Marine Research

Approved: Harriet van Overzee
Researcher

Signature:



Date: 6th of August 2019

Approved: Jakob Asjes
Manager Integration

Signature:



Date: 6th of August 2019

Annex I: calibration additional information

Table I.1: summary table for the calibration settings of all the data sets from *Tridens II* analysed in this study (Section 3).

| vessel | date_year | frequency | sphere_size | n_good_pings | depth_sphere | std_Gf | SNR | mean_error | pulse_length | slope | f_start | f_stop |
|------------|-----------|-----------|-------------|--------------|--------------|----------|---------|------------|--------------|-----------|---------|--------|
| Tridens II | 2015 | 70 | 38mm | 1783 | 15.697 | 0.082967 | 28.5679 | -0.087203 | 0.002048 | 0.021701 | 45 | 90 |
| Tridens II | 2015 | 120 | 38mm | 800 | 15.7185 | 0.13983 | 27.2987 | -1.2864 | 0.002048 | 0.01028 | 95 | 160 |
| Tridens II | 2015 | 200 | 22mm | 1576 | 13.4381 | 0.48293 | 28.7908 | -1.8414 | 0.002048 | 0.0061035 | 160 | 260 |
| Tridens II | 2015 | 200 | 38mm | 494 | 15.7359 | 0.21703 | 29.1637 | -0.86765 | 0.002048 | 0.0061035 | 160 | 260 |
| Tridens II | 2016 | 70 | 38mm | 3531 | 16.5531 | 0.66928 | 18.6186 | -0.11319 | 0.002048 | 0.043403 | 45 | 90 |
| Tridens II | 2016 | 120 | 38mm | 396 | 16.5158 | 0.47241 | 17.5096 | 3.5079 | 0.002048 | 0.020559 | 95 | 160 |
| Tridens II | 2016 | 200 | 38mm | 2085 | 16.5258 | 0.49963 | 12.5968 | -1.6002 | 0.002048 | 0.0061035 | 160 | 260 |
| Tridens II | 2017 | 70 | 38mm | 1908 | 12.9608 | 0.28148 | 23.7472 | -0.16795 | 0.001024 | 0.043403 | 45 | 90 |
| Tridens II | 2017 | 120 | 22mm | 2416 | 15.5559 | 0.66074 | 14.6793 | -0.035264 | 0.001024 | 0.021701 | 90 | 170 |
| Tridens II | 2017 | 120 | 25mm | 3211 | 18.6784 | 0.62526 | 13.7281 | -1.3426 | 0.001024 | 0.021701 | 90 | 170 |
| Tridens II | 2017 | 120 | 38mm | 869 | 13.0003 | 0.6362 | 15.9078 | -1.7749 | 0.001024 | 0.021701 | 90 | 170 |
| Tridens II | 2017 | 200 | 22mm | 1164 | 15.7844 | 0.47383 | 15.3097 | -1.4728 | 0.001024 | 0.012207 | 160 | 260 |
| Tridens II | 2017 | 200 | 25mm | 1458 | 18.9114 | 0.44538 | 13.8456 | -1.5099 | 0.001024 | 0.012207 | 160 | 260 |
| Tridens II | 2018 | 70 | 25mm | 1369 | 15.2147 | 0.29612 | 23.1208 | 0.084679 | 0.002048 | 0.021701 | 45 | 90 |
| Tridens II | 2018 | 70 | 38mm | 3444 | 15.9392 | 0.6388 | 21.806 | -0.046024 | 0.002048 | 0.021701 | 45 | 90 |
| Tridens II | 2018 | 120 | 25mm | 950 | 15.381 | 0.16915 | 26.149 | 0.13993 | 0.002048 | 0.010851 | 90 | 170 |
| Tridens II | 2018 | 120 | 38mm | 1116 | 15.1667 | 0.55593 | 27.9572 | -0.6744 | 0.002048 | 0.010851 | 90 | 170 |
| Tridens II | 2018 | 200 | 25mm | 1329 | 15.078 | 0.20609 | 25.6335 | 0.29276 | 0.002048 | 0.0061035 | 160 | 260 |
| Tridens II | 2018 | 200 | 38mm | 843 | 15.176 | 0.16612 | 28.5493 | 0.077439 | 0.002048 | 0.0061035 | 160 | 260 |
| Tridens II | 2019 | 70 | 25mm | 323 | 14.7651 | 0.63729 | 16.2245 | -0.13963 | 0.001024 | 0.043403 | 45 | 90 |
| Tridens II | 2019 | 70 | 38mm | 403 | 15.908 | 0.17873 | 21.6577 | -0.66108 | 0.001024 | 0.043403 | 45 | 90 |

| | | | | | | | | | | | | |
|------------|------|-----|------|-----|---------|---------|---------|----------|----------|----------|-----|-----|
| Tridens II | 2019 | 120 | 25mm | 150 | 14.9538 | 0.25215 | 20.2613 | 0.25622 | 0.001024 | 0.021701 | 90 | 170 |
| Tridens II | 2019 | 120 | 38mm | 725 | 15.7094 | 0.46649 | 25.6688 | -1.0247 | 0.001024 | 0.021701 | 90 | 165 |
| Tridens II | 2019 | 200 | 22mm | 191 | 17.9876 | 1.0413 | 17.4644 | 5.0783 | 0.001024 | 0.012207 | 160 | 260 |
| Tridens II | 2019 | 200 | 25mm | 398 | 15.453 | 0.25021 | 21.372 | -0.25131 | 0.001024 | 0.012207 | 160 | 260 |
| Tridens II | 2019 | 200 | 38mm | 479 | 17.7723 | 1.0656 | 23.6094 | 3.693 | 0.001024 | 0.011837 | 165 | 260 |

Table 1.2: summary table for the calibration settings of all the data sets from FVs analysed in this study (Section 3).

| vessel | date_year | frequency | sphere_size | n_good_pings | depth_sphere | std_Gf | SNR | mean_error | pulse_length | slope | f_start | f_stop | fc |
|--------|-----------|-----------|-------------|--------------|--------------|---------|---------|------------|--------------|-----------|---------|--------|-------|
| Afrika | 2016 | 70 | 22mm | 553 | 14.4097 | 0.22793 | 19.509 | -0.66165 | 0.002048 | 0.021701 | 45 | 90 | 67.5 |
| Afrika | 2016 | 70 | 25mm | 593 | 16.2248 | 0.29252 | 14.8626 | -1.026 | 0.002048 | 0.021701 | 45 | 90 | 67.5 |
| Afrika | 2016 | 70 | 38mm | 602 | 18.1528 | 0.2924 | 15.3454 | -0.87045 | 0.002048 | 0.021701 | 45 | 90 | 67.5 |
| Afrika | 2016 | 120 | 22mm | 633 | 13.4704 | 0.32108 | 16.4091 | 0.035166 | 0.002048 | 0.010851 | 90 | 170 | 130 |
| Afrika | 2016 | 120 | 25mm | 772 | 15.1962 | 0.286 | 14.6638 | -1.3441 | 0.002048 | 0.010851 | 90 | 170 | 130 |
| Afrika | 2016 | 120 | 38mm | 950 | 17.0404 | 0.30678 | 20.1028 | -2.3597 | 0.002048 | 0.010851 | 90 | 170 | 130 |
| Afrika | 2016 | 200 | 22mm | 784 | 14.0733 | 0.75931 | 13.7236 | 0.62558 | 0.002048 | 0.0061035 | 160 | 260 | 210 |
| Afrika | 2016 | 200 | 25mm | 28 | 15.6176 | 0.61309 | 10.5882 | 1.3576 | 0.002048 | 0.0061035 | 160 | 260 | 210 |
| Afrika | 2016 | 200 | 38mm | 93 | 17.6478 | 0.57284 | 10.3116 | 1.7009 | 0.002048 | 0.0061035 | 160 | 260 | 210 |
| Alida | 2015 | 70 | 15mm | 837 | 15.9415 | 0.30677 | 25.1794 | -0.20521 | 0.001024 | 0.021701 | 45 | 90 | 67.5 |
| Alida | 2015 | 70 | 22mm | 1026 | 17.0125 | 0.34212 | 27.7784 | 0.19384 | 0.001024 | 0.021701 | 45 | 90 | 67.5 |
| Alida | 2015 | 70 | 38mm | 1144 | 19.4975 | 0.34645 | 26.8499 | -0.06725 | 0.001024 | 0.021701 | 45 | 90 | 67.5 |
| Alida | 2015 | 120 | 15mm | 1171 | 15.8896 | 0.11466 | 23.276 | -2.0533 | 0.001024 | 0.01028 | 95 | 160 | 127.5 |
| Alida | 2015 | 120 | 22mm | 1173 | 16.9618 | 0.22481 | 27.1121 | -1.2587 | 0.001024 | 0.01028 | 95 | 160 | 127.5 |
| Alida | 2015 | 120 | 38mm | 1173 | 19.4487 | 0.1451 | 24.8974 | -1.4208 | 0.001024 | 0.01028 | 95 | 160 | 127.5 |
| Alida | 2015 | 200 | 15mm | 993 | 15.9212 | 0.37235 | 20.2707 | -1.0209 | 0.001024 | 0.0061035 | 160 | 260 | 210 |
| Alida | 2015 | 200 | 22mm | 1087 | 16.9928 | 0.43441 | 25.5497 | 2.7443 | 0.001024 | 0.0061035 | 160 | 260 | 210 |
| Alida | 2015 | 200 | 38mm | 1137 | 19.4782 | 0.16882 | 28.4675 | -0.23989 | 0.001024 | 0.0061035 | 160 | 260 | 210 |
| Alida | 2016 | 70 | 22mm | 268 | 14.947 | 0.11034 | 25.743 | -0.85351 | 0.002048 | 0.021701 | 45 | 90 | 67.5 |
| Alida | 2016 | 70 | 25mm | 426 | 18.5293 | 0.13633 | 24.293 | -1.2075 | 0.002048 | 0.021701 | 45 | 90 | 67.5 |

| | | | | | | | | | | | | | |
|-------|------|-----|------|------|---------|---------|---------|-----------|----------|-----------|-----|-----|-------|
| Alida | 2016 | 70 | 38mm | 628 | 21.7642 | 0.11502 | 26.2847 | -1.0192 | 0.002048 | 0.021701 | 45 | 90 | 67.5 |
| Alida | 2016 | 120 | 22mm | 241 | 15.9823 | 0.13971 | 25.4149 | -0.24662 | 0.002048 | 0.01028 | 95 | 160 | 127.5 |
| Alida | 2016 | 120 | 25mm | 374 | 19.6752 | 0.16784 | 25.5068 | -1.2701 | 0.002048 | 0.01028 | 95 | 160 | 127.5 |
| Alida | 2016 | 120 | 38mm | 498 | 23.2951 | 0.15727 | 25.4809 | -0.46317 | 0.002048 | 0.01028 | 95 | 160 | 127.5 |
| Alida | 2016 | 200 | 22mm | 627 | 15.164 | 0.73757 | 24.6775 | 1.8268 | 0.002048 | 0.0061035 | 160 | 260 | 210 |
| Alida | 2016 | 200 | 25mm | 897 | 18.742 | 0.92364 | 24.2131 | -0.72316 | 0.002048 | 0.0061035 | 160 | 260 | 210 |
| Alida | 2016 | 200 | 38mm | 1406 | 22.0742 | 0.91996 | 26.0473 | 0.42103 | 0.002048 | 0.0061035 | 160 | 260 | 210 |
| Alida | 2017 | 70 | 25mm | 610 | 13.2469 | 0.18778 | 23.0748 | -1.183 | 0.001024 | 0.043403 | 45 | 90 | 67.5 |
| Alida | 2017 | 70 | 38mm | 1009 | 17.9985 | 0.15592 | 24.3529 | -0.96246 | 0.001024 | 0.043403 | 45 | 90 | 67.5 |
| Alida | 2017 | 120 | 25mm | 149 | 14.7346 | 0.60243 | 17.5268 | -1.9021 | 0.001024 | 0.021701 | 90 | 170 | 130 |
| Alida | 2017 | 120 | 38mm | 273 | 19.6424 | 0.83106 | 16.8312 | -1.6059 | 0.001024 | 0.021701 | 90 | 170 | 130 |
| Alida | 2017 | 200 | 25mm | 291 | 13.9331 | 0.65766 | 11.3243 | -1.0824 | 0.001024 | 0.012207 | 160 | 260 | 210 |
| Alida | 2017 | 200 | 38mm | 219 | 19.0456 | 0.64583 | 10.4512 | -0.33535 | 0.001024 | 0.012207 | 160 | 260 | 210 |
| Alida | 2018 | 70 | 15mm | 417 | 9.7486 | 1.0323 | 21.436 | -0.089681 | 0.001024 | 0.043403 | 45 | 90 | 67.5 |
| Alida | 2018 | 70 | 22mm | 579 | 13.184 | 0.94519 | 26.0824 | 0.15201 | 0.001024 | 0.043403 | 45 | 90 | 67.5 |
| Alida | 2018 | 70 | 38mm | 683 | 16.8935 | 0.95976 | 28.0973 | -0.083344 | 0.001024 | 0.043403 | 45 | 90 | 67.5 |
| Alida | 2018 | 120 | 15mm | 156 | 10.2664 | 0.64997 | 29.8885 | -0.78241 | 0.001024 | 0.021701 | 90 | 170 | 130 |
| Alida | 2018 | 120 | 22mm | 198 | 13.7603 | 0.74993 | 30.2143 | 0.41552 | 0.001024 | 0.021701 | 90 | 170 | 130 |
| Alida | 2018 | 120 | 38mm | 315 | 17.4372 | 0.67892 | 28.4328 | -0.94398 | 0.001024 | 0.021701 | 90 | 170 | 130 |
| Alida | 2018 | 200 | 15mm | 181 | 10.1606 | 0.68754 | 21.2352 | -0.48193 | 0.001024 | 0.012207 | 160 | 260 | 210 |
| Alida | 2018 | 200 | 22mm | 345 | 13.6689 | 0.56378 | 19.6465 | 2.5304 | 0.001024 | 0.012207 | 160 | 260 | 210 |
| Alida | 2018 | 200 | 38mm | 454 | 17.399 | 0.49668 | 25.006 | 0.51939 | 0.001024 | 0.012207 | 160 | 260 | 210 |

Annex II: automatic report generation

R codes were compiled to automatically generate some representative tables, maps and plots in the format of a short report to summarize the trawl catch and acoustic recordings of each fishing trip. For this, the R-studio functionalities and relevant R packages (e.g. "rmarkdown", "knitr" and "ggplot2") were used. The document gives an overall overview on how the catch characteristics that can be important in interpretation of the acoustic data (e.g. Table 1). In the document, there is a map showing the position of the hauls relative to the schools with an indication of total amount per species for a haul (figure 5). There are bar plots showing total catch per species relative to date and duration of haul per species (e.g. figure 2 and 3). E.g. in the figure 2 the bar corresponding to December 3rd indicate high amount of herring catch in a short duration in the first haul of the day. This catch was followed by horse mackerel catches as can be seen on figure 3 for the second and third haul. This is an indication that horse mackerel and herring co-occur in the area therefore one should be careful in the interpretation of the schools on the echograms when generating the ground truth table. The histograms on the figure 4 gives a summary of the length distribution across the hauls e.g. whether there is a structure in the distribution of length composition across the hauls that can be used for species identification.

Summary of the catch
Table 1 Catch Summary

| Date | No.Haul | Tot.Duration | Tot.Catch | HER | HOM | MAC | SPR | OTHER |
|------------|---------|--------------|-----------|-----|-------|-----|-----|-------|
| 2017-12-02 | 1 | 2.8 | 10 | 0 | 0.0 | 0 | 10 | 0 |
| 2017-12-03 | 3 | 3.2 | 290 | 120 | 170.0 | 0 | 0 | 0 |
| 2017-12-04 | 1 | 0.8 | 120 | 0 | 120.0 | 0 | 0 | 0 |
| 2017-12-05 | 3 | 7.1 | 155 | 40 | 115.0 | 0 | 0 | 0 |
| 2017-12-06 | 3 | 4.4 | 110 | 76 | 30.0 | 0 | 0 | 4 |
| 2017-12-07 | 4 | 5.6 | 160 | 130 | 0.0 | 0 | 0 | 30 |
| 2017-12-08 | 3 | 6.1 | 90 | 70 | 0.0 | 0 | 0 | 20 |
| 2017-12-09 | 3 | 4.4 | 145 | 145 | 0.0 | 0 | 0 | 0 |
| 2017-12-10 | 1 | 1.1 | 40 | 20 | 0.0 | 20 | 0 | 0 |
| 2017-12-11 | 2 | 0.4 | 95 | 95 | 0.0 | 0 | 0 | 0 |
| 2017-12-15 | 4 | 9.4 | 55 | 0 | 4.8 | 15 | 0 | 35 |
| 2017-12-16 | 1 | 1.3 | 5 | 0 | 0.0 | 0 | 0 | 5 |

Catch Composition / Haul Duration

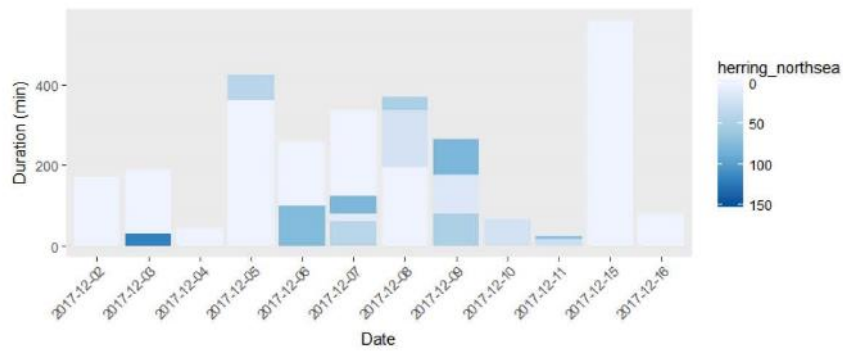


Figure 2 Total haul duration (bar length) and total **herring** catch (colour) per date

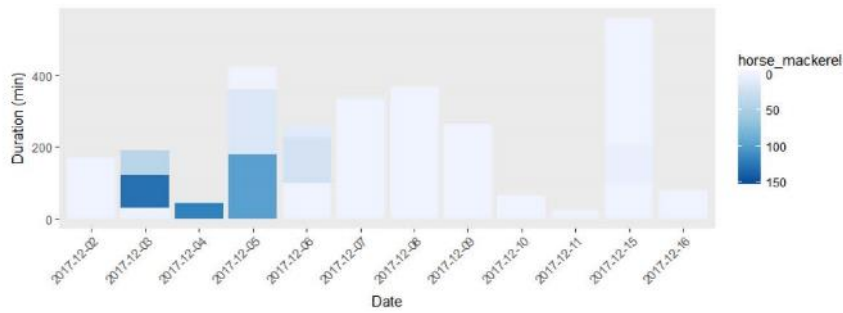


Figure 3 Total haul duration (bar length) and total **horse mackerel** catch (colour) per date

Length distribution

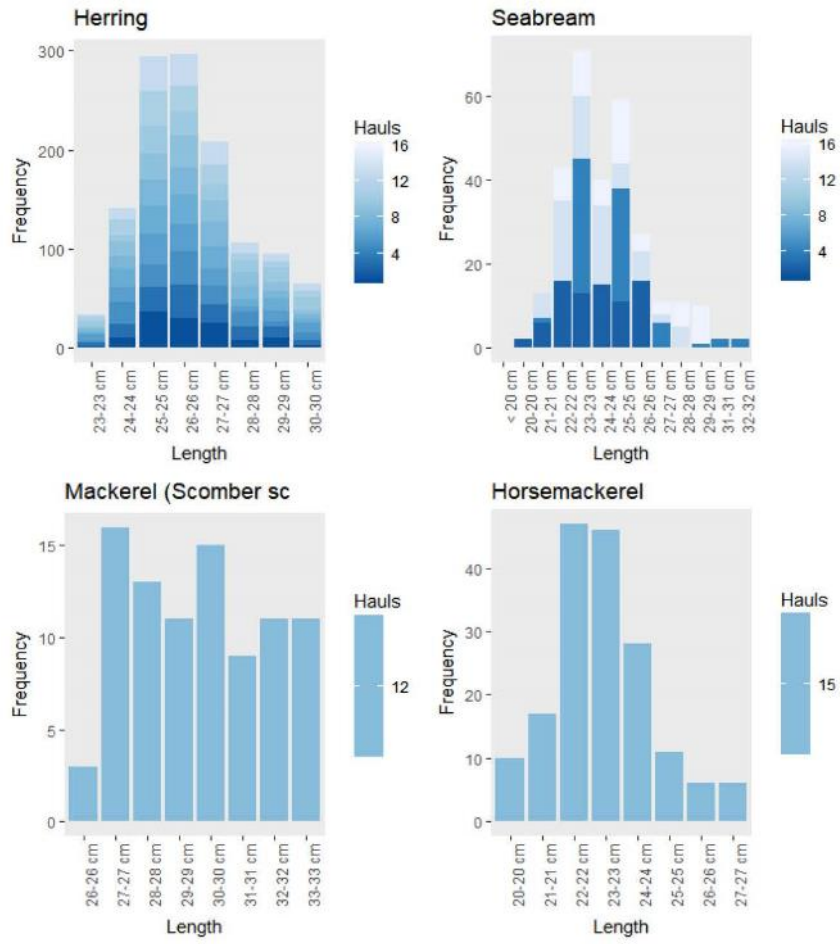


Figure 4 Length distribution species/hauls

Fishing trip map

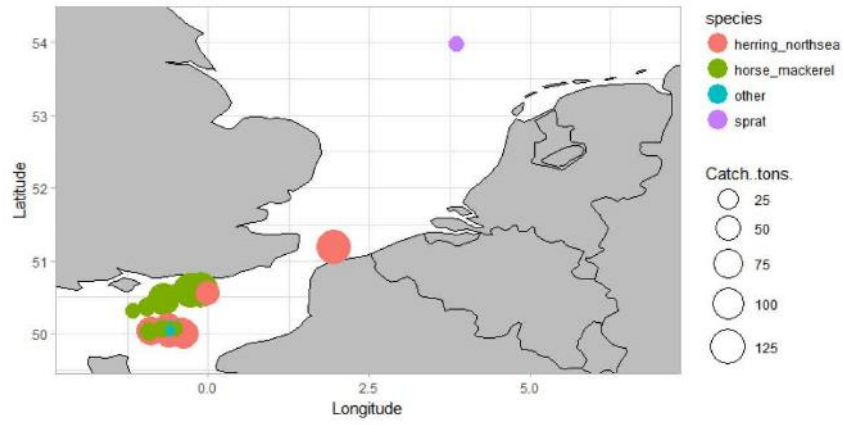
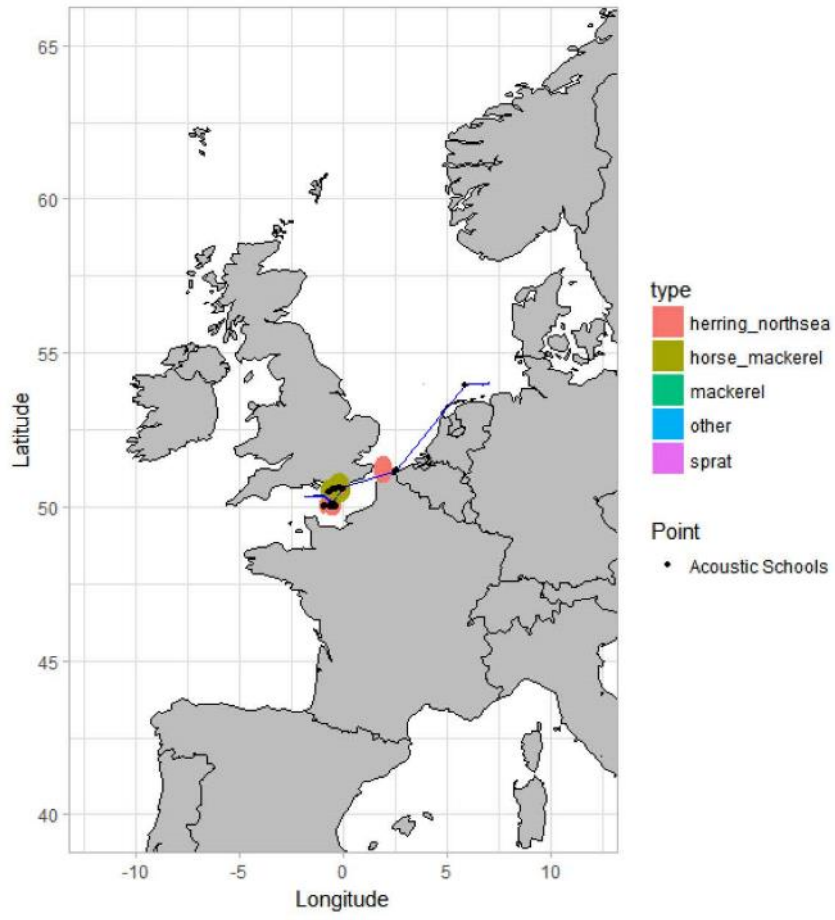


Figure 5 Location of the trawl hauls and catch composition and amount (bubble plot)

Overview Map



Annex III: Calibration manual

EK80 calibration manual

Benoit Berges – Wageningen Marine Research – benoit.berges@wur.nl

Version 1.0

Data: 20/08/2018

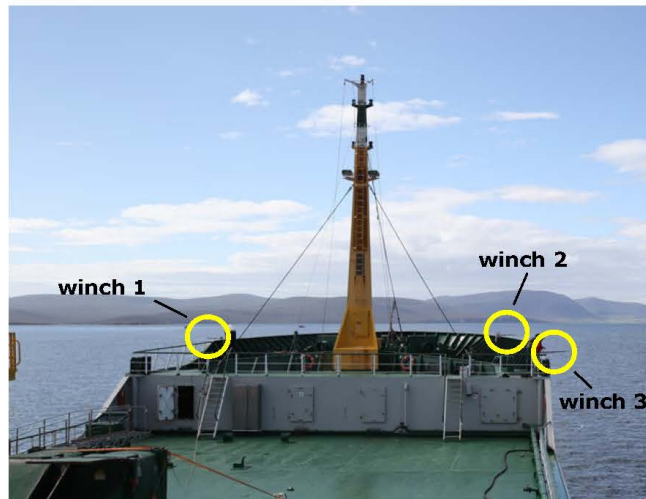
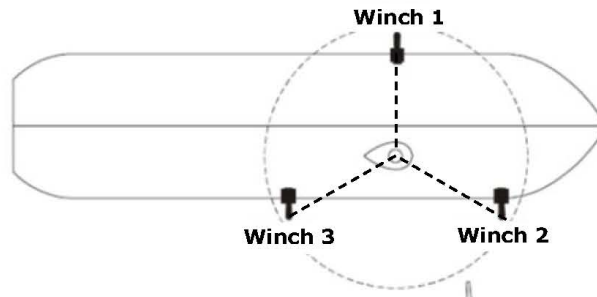
1

Contents

| | | |
|-------|---|----|
| 1 | Calibration kit setup | 3 |
| 2 | Calibration procedure | 4 |
| 2.1 | Getting the sphere into position under the ship | 4 |
| 2.2 | EK80 software setup | 5 |
| 2.2.1 | EK80 CW (narrow band) and EK80 FM (broadband) | 6 |
| 3 | Calibration procedure – graphical guide | 7 |
| 3.1 | Getting the sphere into position under the ship | 7 |
| 3.2 | EK80 software setup | 11 |
| 3.2.1 | EK80 CW (narrow band) | 14 |
| 3.2.2 | EK80 FM (broadband) | 16 |
| | Appendix 1 – calibration log form | 18 |

1 Calibration kit setup

BEFORE DROPPING THE ANCHOR!!!: Attach 3 winches at pre-specified locations (centred around the transducer), adjusting as needed for best control of sphere



2 Calibration procedure

- Calibration should be attempted prior to a survey or as soon as convenient at the beginning of the fishing trip, and/or if possible at the end. Calibration during a fishing trip (instead of at the end) is also acceptable if it will be: (a) in better conditions and/or (b) save significant time.
- Calibrate during relatively calm sea states. Stabilizing the vessel with two point anchor is optimal, e.g., using a trawl door for stern anchor. If anchoring, allow for 30-50 m of water under the boat. When conditions are very calm, calibrating while drifting is acceptable. A single anchor is not usually as workable.
- The main engine should be off during calibration.
- Make sure there are few, if any, fish in the water column. Daytime is best to avoid fish. Calibration data can be collected at night if fish are absent.

Install the calibration equipment and select the calibration sphere for the appropriate frequency(s). Use VHS radios to communicate between the bridge and the calibration winch operator(s). Alternatively, you can use remotely-operated winches if available and control them from the bridge.

The following steps should be performed for a 3 point calibration procedure

- a) Start the echosounder in the EK80 software. Select: OPERATION => Normal
- b) Set transceiver mode to "Active" for visualisation.
- c) Switch echosounder on, start pinging: OPERATION => PING => ON.

2.1 Getting the sphere into position under the ship

- d) Attach 3 winches at pre-specified locations (centred around the transducer), adjusting as needed for best control of sphere
- e) Using one person on port and one on starboard, drop a rope with a weight attached in the middle over bow, allowing enough slack to clear the bow, anchor, and any other protrusions (e.g. sonar head) between bow and transducer.
- f) Walk the rope along each side until the rope is even with the single (e.g. starboard) winch.
- g) Tie the starboard winch line to the rope and while feeding out starboard line with slack, pull the rope up on the portside at the forward port winch.
- h) Remove the rope and attach the lines from all 3 winches together.
- i) Only now: Anchor the vessel
- j) Dip the clean, dry, calibration sphere in water with dish washing liquid (e.g., 'dref').
- k) Attach the sphere to the middle point of the 3 monofilament calibration lines; attach a stabilizing weight ~ 3-5 m below the sphere.
- l) Carefully lower the sphere and the weight over the side - do not touch the side of the vessel with the sphere.
- m) Reel out the same amount of line, on all 3 winches in order to place the sphere in the middle under the transducer.
- n) Look for the sphere on the echogram. Let out line on all the winches until the sphere is visible on the EK80 screen (but do not let out so much line that weight/sphere hits the bottom...). The sphere must be placed 15-20m below the transducer!!
- o) Set Ping rate to Maximum just for the calibration: OPERATION => PING MODE: Maximum. This will collect more single target data on the sphere, and make it easier to correct the calibration files for a known systematic error in the EK80 system.

2.2 EK80 software setup

- p) Measure water salinity and temperature using the CTD device. Enter the parameters in the Environment dialogue box in the EK80 software: SETUP => INSTALLATION => ENVIRONMENT.
- q) Setup bottom detection parameters (ACTIVE => BOTTOM DETECTION) with a minimum depth of 2m and a maximum depth of 50m
- r) Setup output directory (OPERATION => OUTPUT) to the appropriate data recording location
- s) Setup single target detection parameters (ACTIVE => SINGLE TARGET DETECTION):

| | |
|--|-------------|
| Min Threshold | -50 |
| Min Echo Length | 0.6 |
| Max Echo Length | 1.8 |
| Max CW phase deviation or Maximum FM phase deviation | 8 25 |
| Max Gain Comp (one-way) | 6 |
| Min Echo Spacing | 0 |

- t) Setup echosounder channels with the following parameters (OPERATION => NORMAL OPERATION):

> **FM (broadband):**

| Channel | Pulse type | Pulse duration (ms) | Power (W) | Start Frequency (Hz) | End Frequency (Hz) | Ramping |
|---------|------------|---------------------|-----------|----------------------|--------------------|---------|
| 38 kHz | LFM Up | 1.024 | 2000 | 35000 | 45000 | Fast |
| 70 kHz | LFM Up | 1.024 | 750 | 45000 | 90000 | Fast |
| 120 kHz | LFM Up | 1.024 | 250 | 90000 | 170000 | Fast |
| 200 kHz | LFM Up | 1.024 | 120 | 160000 | 260000 | Fast |
| 333 kHz | LFM Up | 1.024 | 50 | 280000 | 450000 | Fast |

> **CW (narrowband):**

| Channel | Pulse type | Pulse duration (ms) | Power (W) | Ramping |
|---------|------------|---------------------|-----------|---------|
| 18 kHz | CW | 1.024 | 2000 | Fast |
| 38 kHz | CW | 1.024 | 2000 | Fast |
| 70 kHz | CW | 1.024 | 750 | Fast |
| 120 kHz | CW | 1.024 | 250 | Fast |
| 200 kHz | CW | 1.024 | 120 | Fast |
| 333 kHz | CW | 1.024 | 50 | Fast |

- u) Start recoding data (OPERATION => Record RAW).
- v) Setup the mode of the channel being calibrated (OPERATION => NORMAL OPERATION) as **Active** and other channels as **passive**. This is to ensure the best data quality, reducing noise generated by other channels.
- w) Record calibration date and time, target sphere and channel on log form (Appendix 1).

2.2.1 *EK80 CW (narrow band) and EK80 FM (broadband)*

- x) Start Calibration wizard (SETUP => CALIBRATION) and select the channel being calibrated together with the target sphere.
- y) Start the collection of calibration data by pressing the Start button in the calibration wizard. The progress of the calibration is monitored by the calibration wizard (target detection, % coverage). Make sure the target sphere is within the minimum and maximum depth parameters. One can increase the TS deviation parameter if the target sphere is within the max/min depth parameters and the system does not give any detections.
- z) When coverage is 90% or higher, stop calibration data recording by pressing the Stop button in the calibration wizard.
 - aa) Press the Next button in the calibration wizard and save results
 - bb) Press the Finish button in the calibration wizard. While exiting the calibration wizard, save the results and update the echosounder with the new calibration
 - cc) Start again from Step w if more channels are to be calibrated

3 Calibration procedure – graphical guide

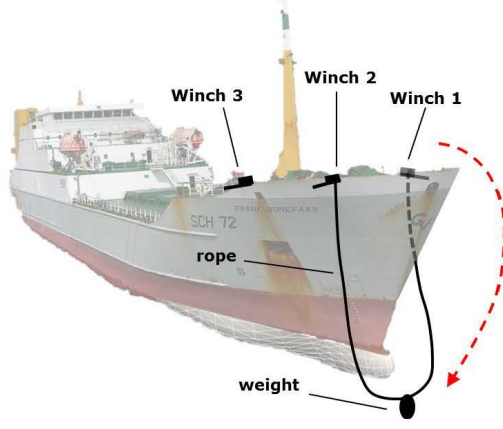
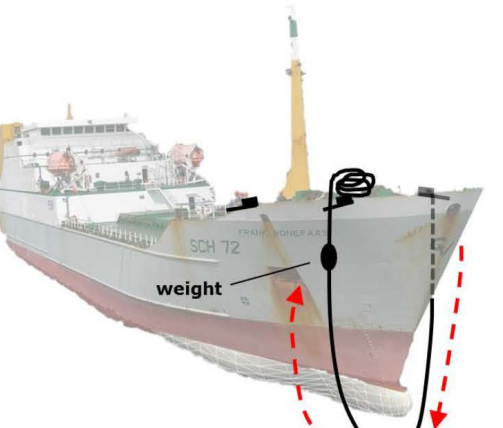
(a) Start the echosounder in the EK80 software. Select: OPERATION => Normal

(b) Set transceiver mode to "Active" for visualisation.

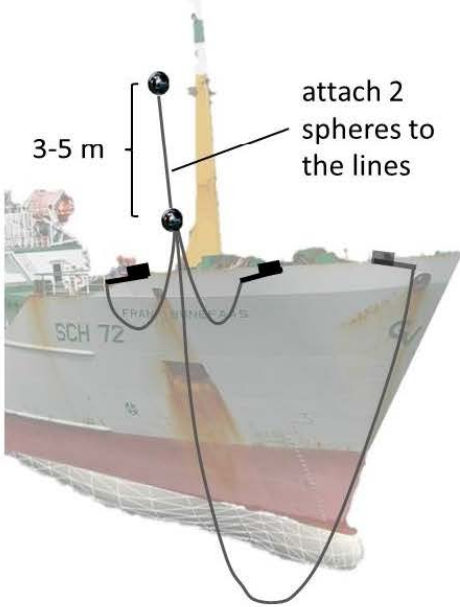

(c) Switch echosounder on, start pinging: OPERATION => PING => ON.

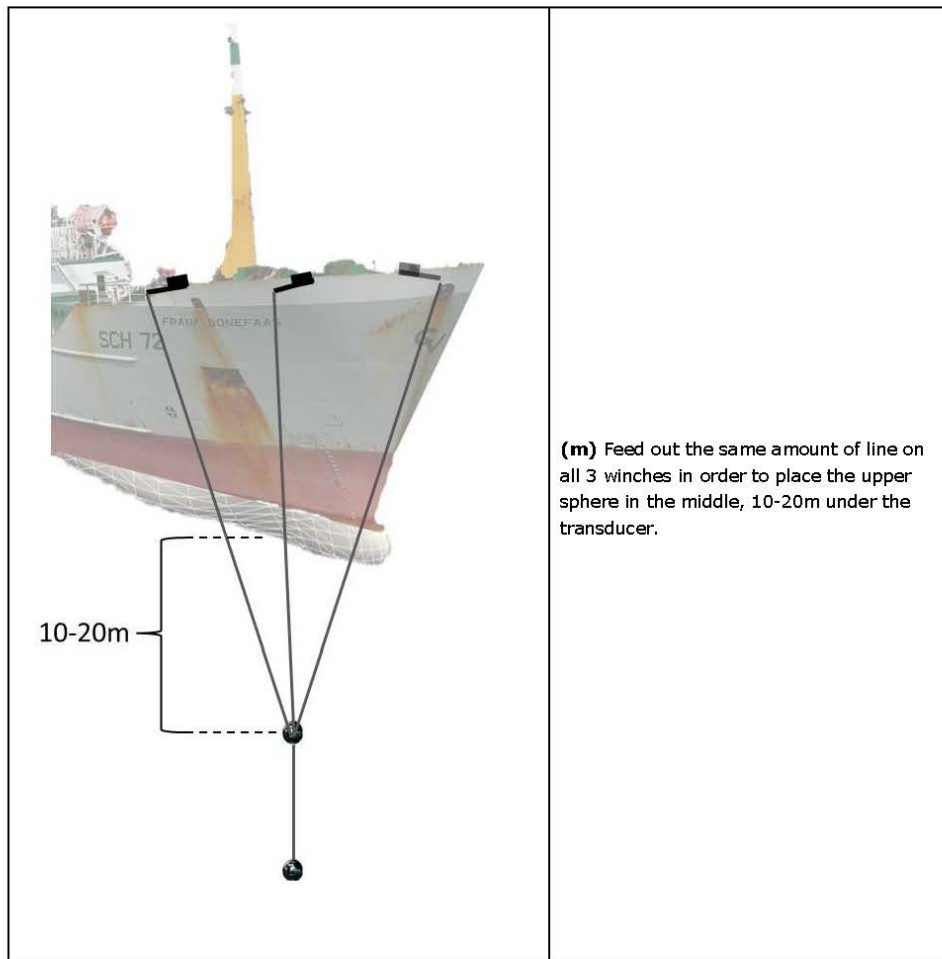
3.1 Getting the sphere into position under the ship

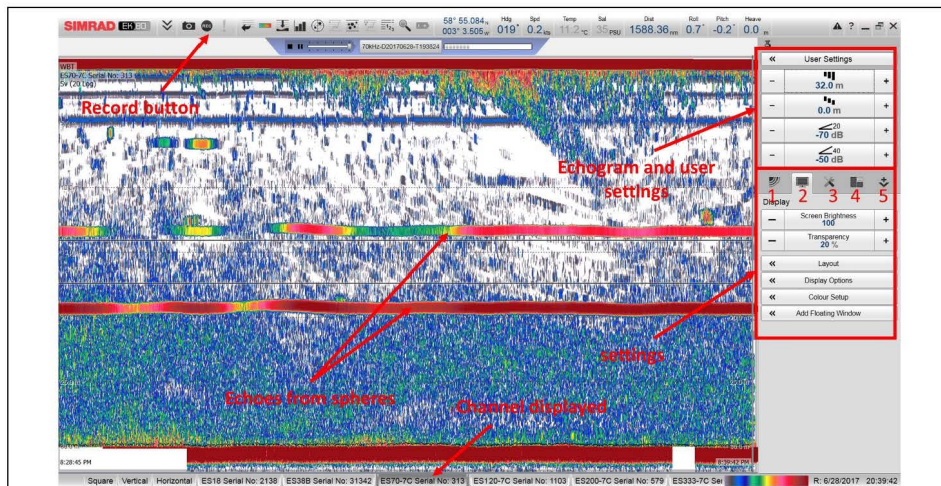
(d) Attach 3 winches at pre-specified locations (centred around the transducer), adjusting as needed for best control of sphere

| | |
|--|--|
|  <p>The diagram shows a 3D model of the bow of a ship. Three winches are labeled: Winch 1 on the starboard side, Winch 2 in the center, and Winch 3 on the port side. A rope is shown being lowered from the bow area, with a weight attached to its end. Red dashed arrows indicate the path of the rope as it is being lowered and then walked along the deck.</p> | <p>(e) Using one person on port and one on starboard, drop a rope with a weight attached in the middle over the bow, allowing enough slack to clear the bow, anchor, and any other protrusions (e.g. sonar head) between bow and transducer.</p> |
|  <p>The diagram shows the same 3D model of the ship's bow. The rope with the weight is now being walked along the deck from the bow towards the transducer. Red dashed arrows indicate the path of the rope as it is being walked along each side of the ship.</p> | <p>(f) Walk the rope along each side until the rope is even with the single (port-side) winch. Feed rope out on the port side and pull it up on starboard side until the weight can be taken on board. Take the weight off the rope.</p> |

| | |
|--|---|
| | <p>(g) Tie the thin line of the port winch to the rope and while feeding out port line <u>with slack</u>. Pull the rope up on the starboard side at the forward starboard winch.</p> |
| | <p>(h) Remove the rope and attach the lines from all 3 winches together. (i) <u>Only now:</u> Anchor the vessel.</p> |
| | <p>(j) Dip the clean, dry, calibration sphere in water with dish washing liquid (e.g., 'drecht').</p> |

| | |
|---|--|
|  <p>3-5 m</p> <p>attach 2 spheres to the lines</p> | <p>(k) Attach the sphere to the middle point of the 3 monofilament calibration lines; attach a second sphere as stabilizing weight ~3-5 m below the first sphere.</p> |
|  | <p>(l) Carefully lower the 2 spheres over the side – do not touch the side of the vessel with the spheres.</p> |

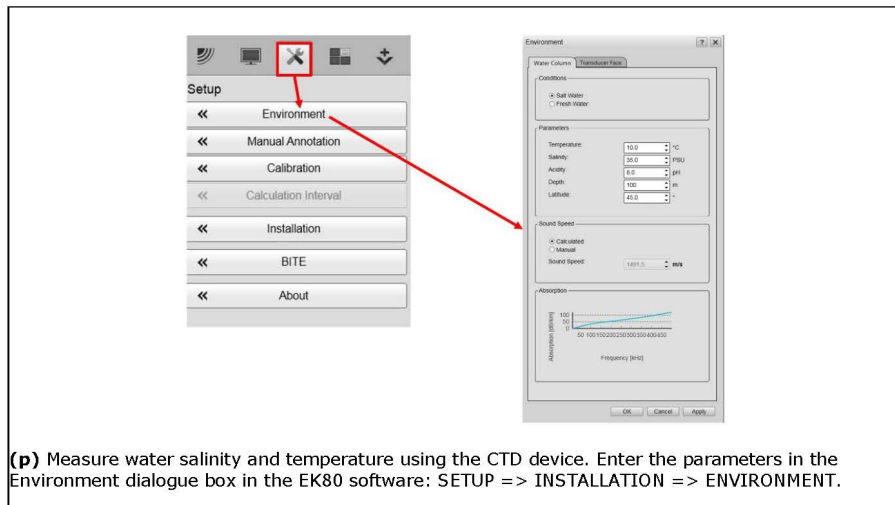




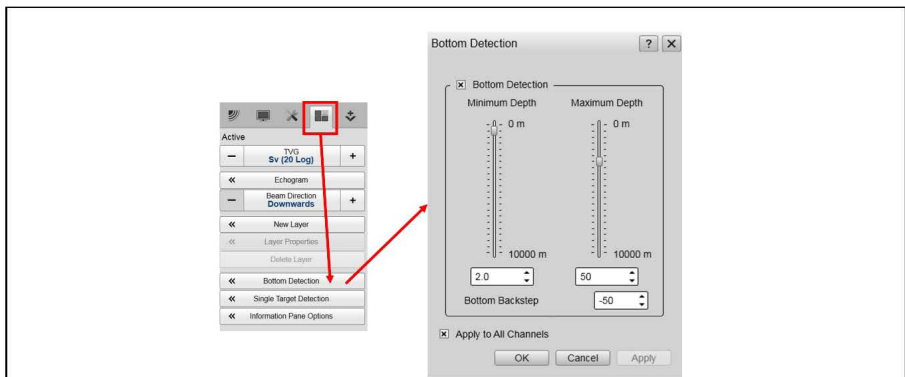
Echogram display with spheres in the water. (n) Look for the 2 sphere echoes on the echogram (visible as 2 dark lines). Lower the sphere until the sphere it is visible on the EK80 screen (but do not let out too much line so that the lower sphere hits the bottom...). **The upper sphere must be placed 10-20 metres below the transducer!!**

(o) Set Ping rate to Maximum just for the calibration: OPERATION => PING MODE: Maximum. This will collect more single target data on the sphere, and make it easier to correct the calibration files for a known systematic error in the EK80 system.

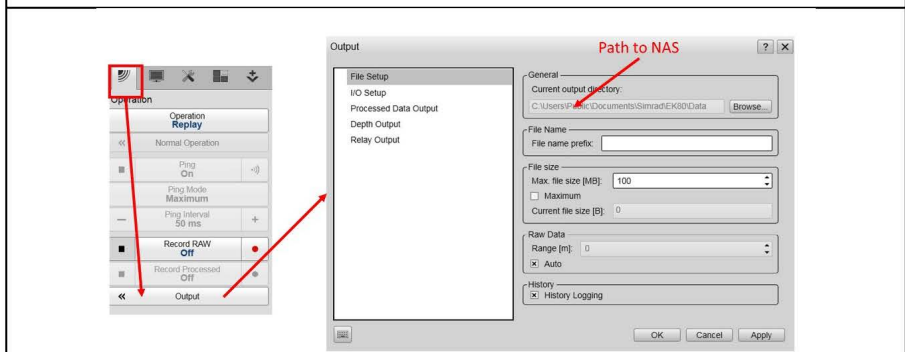
3.2 EK80 software setup



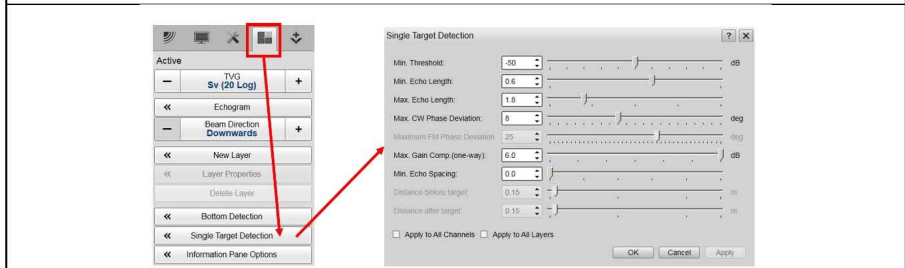
(p) Measure water salinity and temperature using the CTD device. Enter the parameters in the Environment dialogue box in the EK80 software: SETUP => INSTALLATION => ENVIRONMENT.



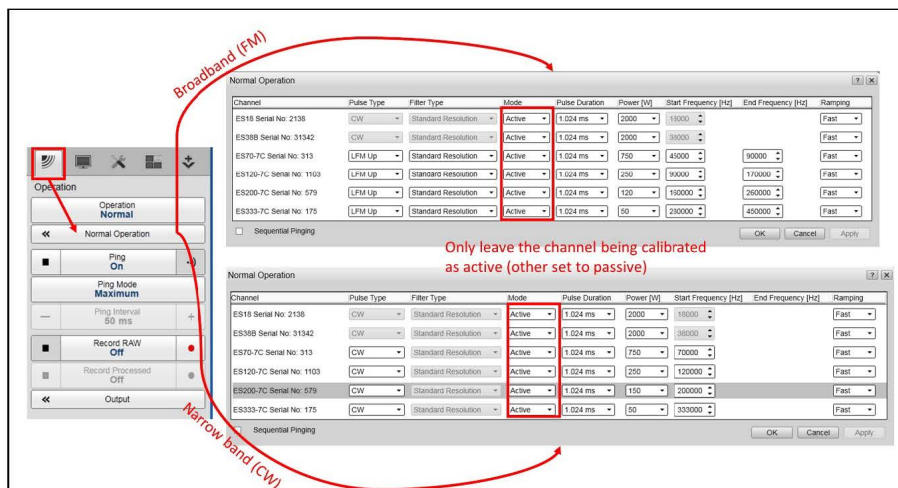
(q) Setup bottom detection parameters (ACTIVE => BOTTOM DETECTION) with a minimum depth of 2m and a maximum depth of 50m.



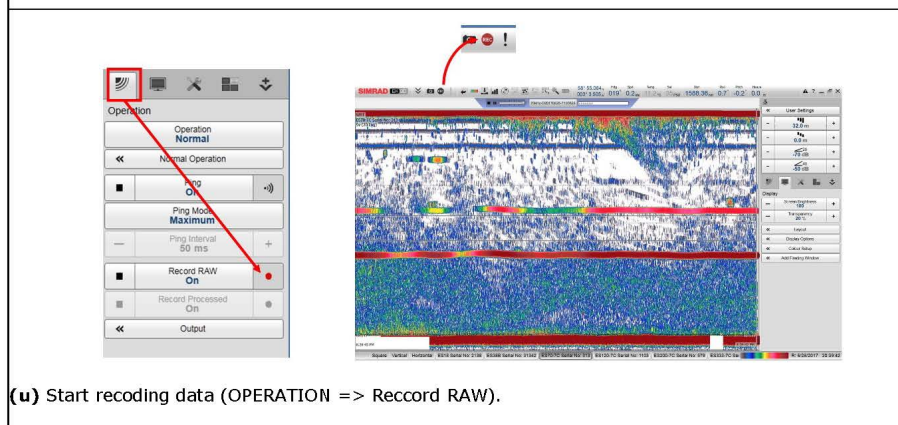
(r) Setup output directory (OPERATION => OUTPUT) to the appropriate data recording location.



(s) Setup single target detection parameters (ACTIVE => SINGLE TARGET DETECTION).



(t) Setup echosounder channels (OPERATION => NORMAL OPERATION).

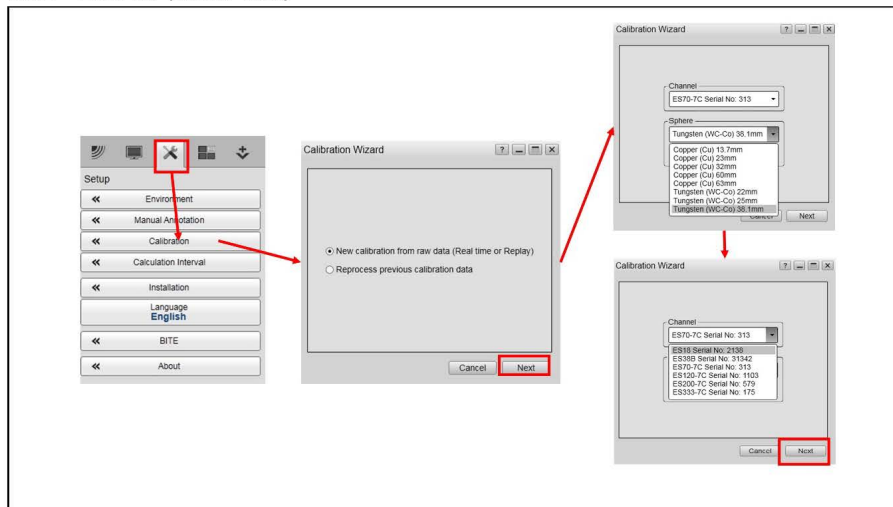


(u) Start recoding data (OPERATION => Record RAW).

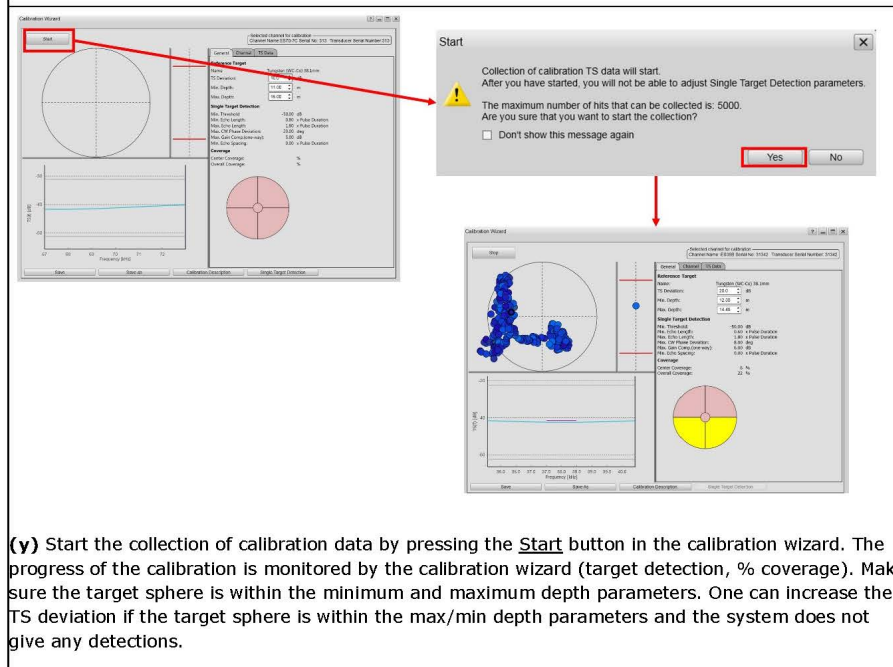
(v) Setup the mode of the channel being calibrated (OPERATION => NORMAL OPERATION) as **Active** and other channels as **passive**. This is to ensure the best data quality, reducing noise generated by other channels.

(w) Record calibration date and time, target sphere and channel on log form (Appendix 1).

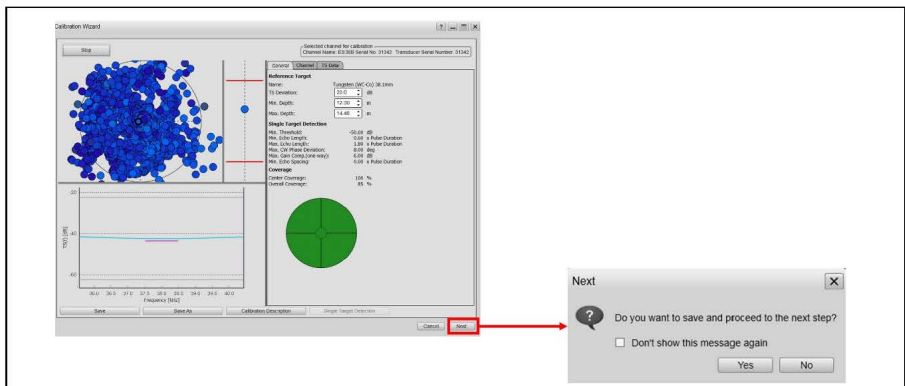
3.2.1 EK80 CW (narrow band)



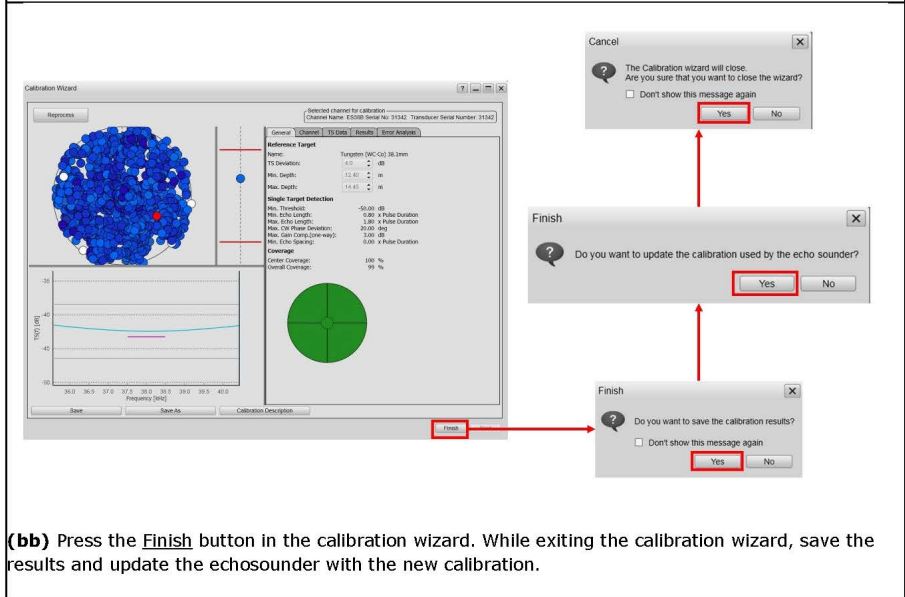
(x) Start Calibration wizard and select the channel being calibrated together with the target sphere.



(y) Start the collection of calibration data by pressing the **Start** button in the calibration wizard. The progress of the calibration is monitored by the calibration wizard (target detection, % coverage). Make sure the target sphere is within the minimum and maximum depth parameters. One can increase the TS deviation if the target sphere is within the max/min depth parameters and the system does not give any detections.



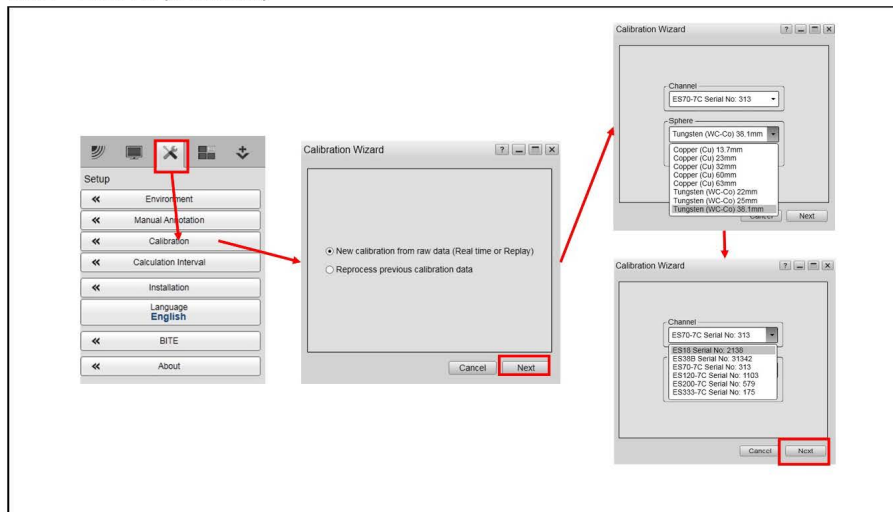
(z) When coverage is 90% or higher, stop calibration data recording by pressing the **Stop** button in the calibration wizard. **(aa)** Press the **Next** button in the calibration wizard and save results



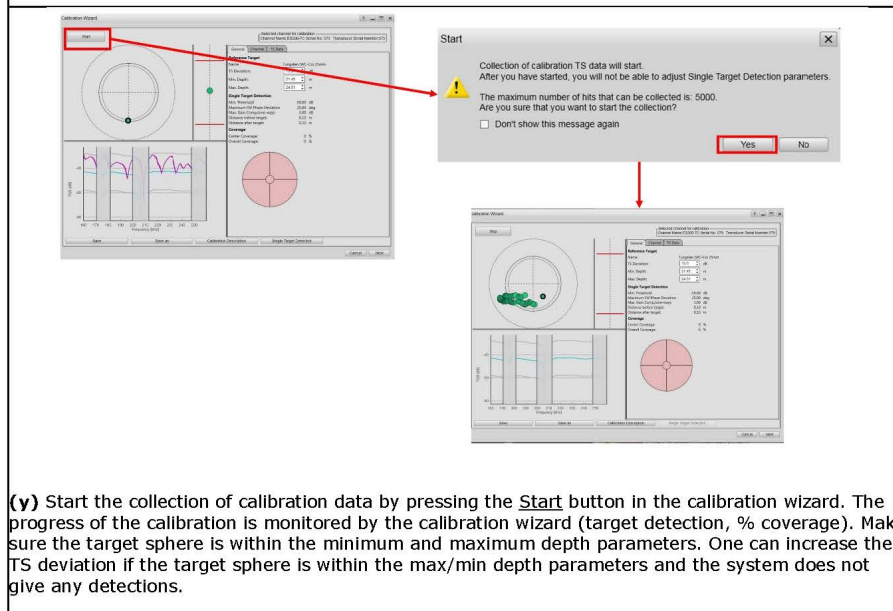
(bb) Press the **Finish** button in the calibration wizard. While exiting the calibration wizard, save the results and update the echosounder with the new calibration.

(cc) Start again from **Step w** if more channels to be calibrated.

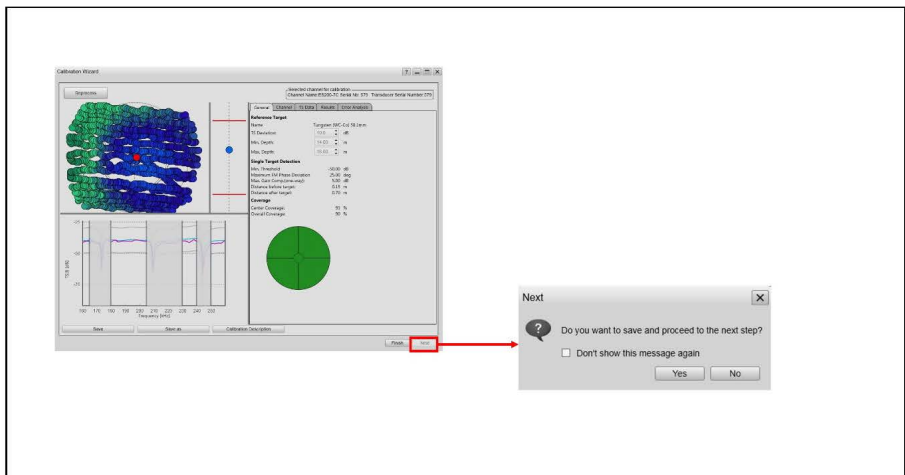
3.2.2 EK80 FM (broadband)



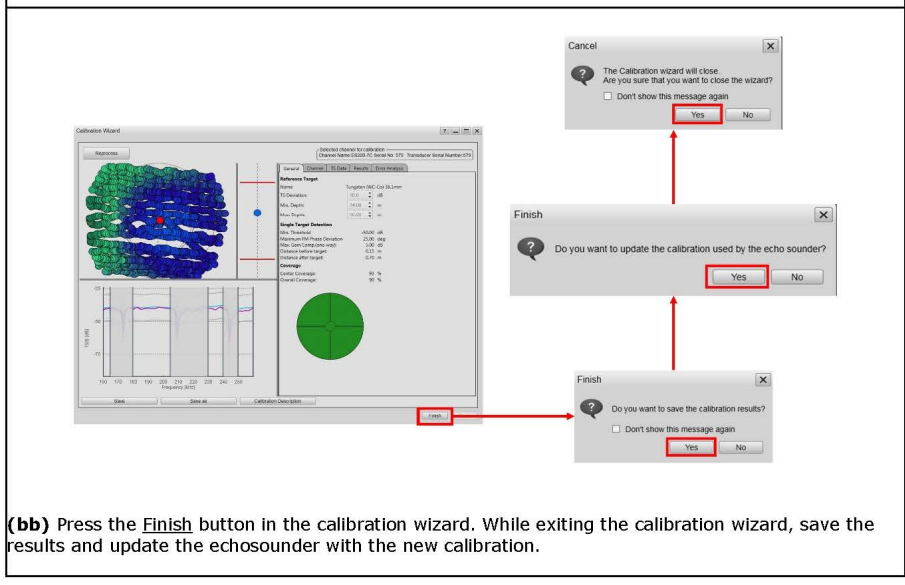
(x) Start Calibration wizard and select the channel being calibrated together with the target sphere.



(y) Start the collection of calibration data by pressing the Start button in the calibration wizard. The progress of the calibration is monitored by the calibration wizard (target detection, % coverage). Make sure the target sphere is within the minimum and maximum depth parameters. One can increase the TS deviation if the target sphere is within the max/min depth parameters and the system does not give any detections.



(z) When coverage is 90% or higher, stop calibration data recording by pressing the Stop button in the calibration wizard. **(aa)** Press the Next button in the calibration wizard and save results



(bb) Press the Finish button in the calibration wizard. While exiting the calibration wizard, save the results and update the echosounder with the new calibration.

(cc) Start again from Step w if more channels to be calibrated.

Annex V: project dissemination and presentations

IV.1 presentation at the 2017 ASA conference (Boston, USA)



28 June 2017 | Jeroen van de Sande
 2 | Classification of Pelagic Fish Using Wideband Echo Sounders

CONTENTS

- › Background
- › Research goal
- › Data collection
- › Processing chain & results
- › Conclusions and way ahead

28 June 2017 | Jeroen van de Sande
 3 | Classification of Pelagic Fish Using Wideband Echo Sounders

BACKGROUND

- › European Commission introduced landing obligation for commercial fisheries under the common fisheries policy (Jan 2015 for pelagic fisheries, to be extended to all fisheries in 2019)
- › Need for better species selectivity
- › Different options are being developed / investigated:
 - › Optical (cameras in the net)
 - › Mechanical (net mesh size, grids)
 - › Acoustical offers the advantage to provide information prior to the catch.

REFERENCES

Ten percent of fish caught in oceans get dumped: study

By Mike Peck | 06/27

Fishing fleets dump about 10 percent of the fish they catch back into the ocean as an "ecosystem service" of low-value fish, despite some progress in landing catches in recent years, scientists said on Monday.

Of discarding fish, the fish global marine catch 2015 and landed around by 100 percent, with the rate of discards was still high across a decade from a peak in the late 1990s. Discarded fish are usually dead or dying.

Almost 10 million tonnes of about 100 million tonnes of fish caught annually in the past decade were thrown back into the sea, according to the "Ocean Waste" survey by the University of British Columbia and the University of Western Australia.

Invasive alien species (fish and shellfish) are also dumped, however, how much is of an unclear species. It includes fish species such as the Atlantic cod, for instance, may throw back into the sea.

Discards are an "ecosystem service," especially at a time when wild capture fisheries are under global stress, under growing demands for food security and human nutritional health," they wrote in the journal *PLoS ONE*.

The report revealed the global discards from a peak of about 10 million tonnes in 1990.

28 June 2017 | Jeroen van de Sande
 4 | Classification of Pelagic Fish Using Wideband Echo Sounders

BACKGROUND

- › European Commission introduced landing obligation for commercial fisheries under the common fisheries policy (Jan 2015 for pelagic fisheries, to be extended to all fisheries in 2019)
- › Need for better species selectivity
- › Different options are being developed / investigated:
 - › Optical (cameras in the net)
 - › Mechanical (net mesh size, grids)
 - › Acoustical offers the advantage to provide information prior to the catch.

28 June 2017 | Jeroen van de Sande
 5 | Classification of Pelagic Fish Using Wideband Echo Sounders

RESEARCH GOAL

- › Assess classification performance using wideband acoustical information of homogeneous schools of commercial, pelagic fish species:
 - › Herring
 - › Mackerel
 - › Horse Mackerel
- › Use of SIMRAD EK80 wideband echo sounders:
 - › 45-90 kHz
 - › 90-160 kHz
 - › 160-260 kHz
- › Data recorded on a commercial freezer-trawler

28 June 2017 | Jeroen van de Sande
 6 | Classification of Pelagic Fish Using Wideband Echo Sounders

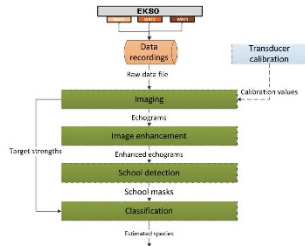
DATA COLLECTION

- › Data collection during three fishing trips

| Species | Amount |
|----------------|------------|
| Herring | 5 schools |
| Horse Mackerel | 7 schools |
| Mackerel | 38 schools |

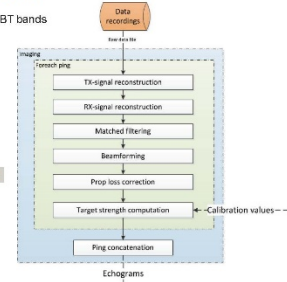
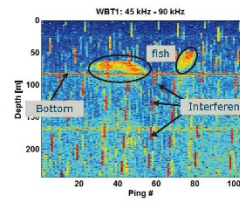
PROCESSING CHAIN

- Recorded, raw EK60 data is converted to a classification output per school
- All data is automatically processed:



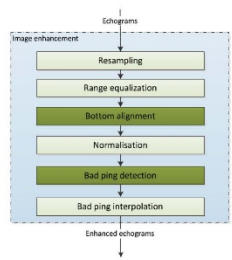
PROCESSING CHAIN

- Convert raw, recorded EK60 data in the three WBT bands to echograms



PROCESSING CHAIN

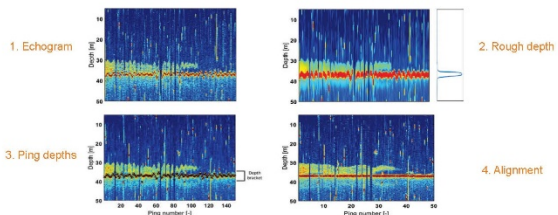
- Recorded data can be of poor quality as a result of:
 - Interferences of other sonars
 - Severe ship motion causing:
 - "empty" pings
 - school deforming



- Echograms need processing to:
 - Align bottom
 - Indicate artefacts
 - Combine transducers

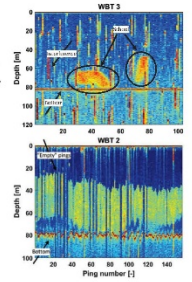
PROCESSING CHAIN

- Through the sensor bottom alignment to facilitate school detection



PROCESSING CHAIN

- Bad pings reduce the image quality as a result of distorted data caused by:
 - Acoustic or electronic interference during reception of the data
 - Problems during transmission (no contact between transceiver and water, air bubbles below transceiver)
- Bad ping detection and/or replacement required, since they:
 - Could split schools in two in case of "empty" pings
 - Do not represent the actual time signal at the concerning location
- All have their effect on school detection and classification



PROCESSING CHAIN

- 1. Image quality estimation to derive template filter length

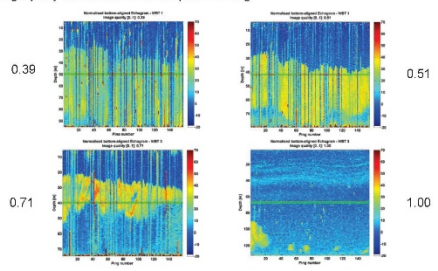


Image enhancement PROCESSING CHAIN BAD PING DETECTION

2. Creating image template

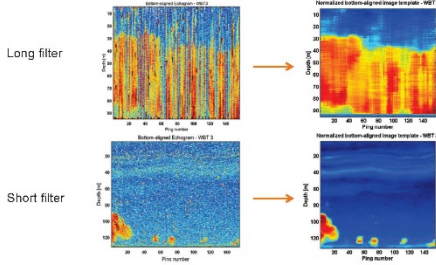


Image enhancement PROCESSING CHAIN BAD PING DETECTION

3. Bad pixel determination

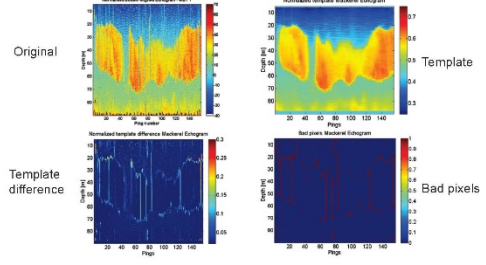
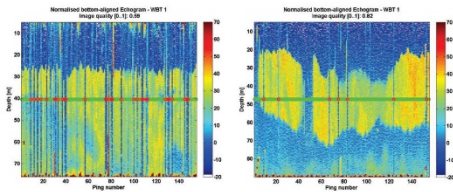


Image enhancement PROCESSING CHAIN BAD PING DETECTION

4. Determining bad pings: a ping is 'bad' if in this subset of pixels the ratio of bad pixels exceeds a certain threshold

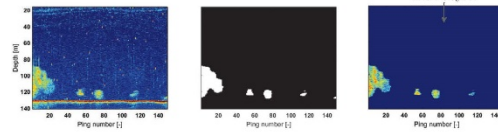
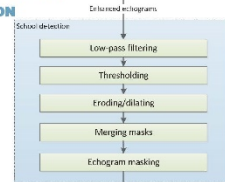


School detection PROCESSING CHAIN SCHOOL DETECTION

Collect pixels that together form fish schools

Transducers are combined to do additional noise reduction

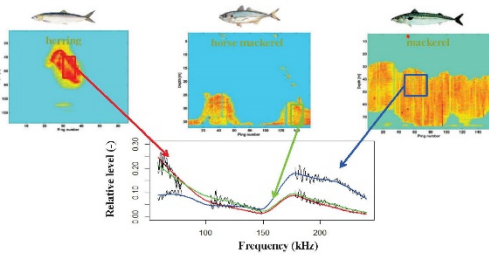
The masked echograms are used to do feature computation and classification on



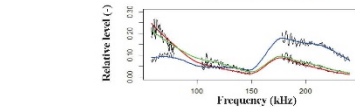
Classification PROCESSING CHAIN CLASSIFICATION

Use of Dynamic Factor Analysis (Zuur et al. 2003) to do trend-based classification

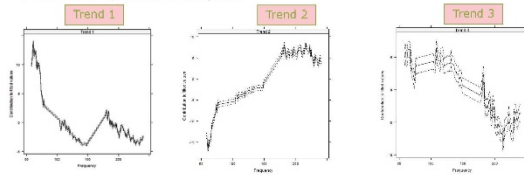
Average frequency response per species:



Classification PROCESSING CHAIN CLASSIFICATION



Common trend patterns identified by DFA:



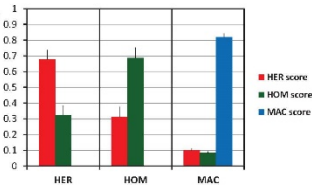
Classification

PROCESSING CHAIN CLASSIFICATION

- › Similarity between school spectrum and trends used as input features for classifier

- › Results: misclassification of only 1 Horse Mackerel school in the (relatively small) list of:
 - › 5 Herring schools
 - › 7 Horse Mackerel schools, and
 - › 38 Mackerel schools

Average confidence levels



CONCLUSIONS AND WAY AHEAD

- › The use of wideband echo sounders shows potential to distinguish Herring, Mackerel and Horse Mackerel based on their relative frequency response trends
- › At this stage there is already dealt with the interfering circumstances related to deployment on a commercial fishing vessel
- › Way ahead:
 - › More data is being collected to further test and develop the classification algorithm (varying seasons, areas, sizes). More species will be added
 - › Estimation of fish length (to support classification)
 - › An online demonstrator system has been installed on FV SCH24 'Afrika' (22nd June)

ACKNOWLEDGEMENTS

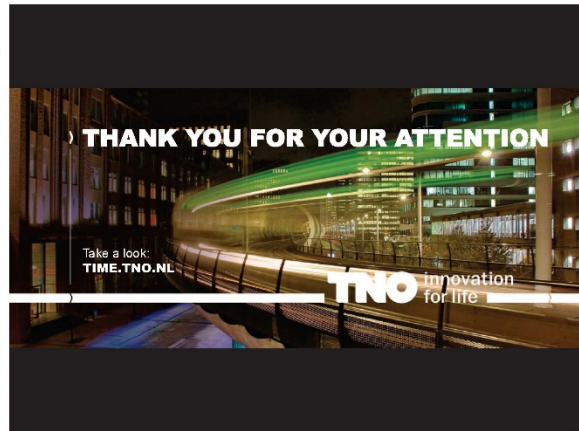
- › Crew and skipper of the SCH6 'Alida' are acknowledged for their efforts in data collection
- › The project was selected for the Dutch Operational Programme "Perspectives for a Sustainable Fishery" and co-financed by the European Fisheries Fund



Netherlands Enterprise Agency



The European Fisheries Fund
 Investing in Sustainable Fisheries
 MarineTraffic.com



IV.2 presentation at 2019 WGFAS (Galway, Ireland)

Fish species recognition using broadband acoustics

B. J. P. Bergès*, J. J. M. van de Sande†, B. Quesson†, S. Sakinani†, D. Burggraaf†, M. Pastoors†
 * Wageningen Marine Research (WUR), Lelystad, The Netherlands
 † TNO, Den Haag, The Netherlands
 ‡ Polaris 101, Zandvoort (P.A.), Zandvoort, The Netherlands
 § beritzberg@wur.nl

Wageningen University
 TNO innovation for life
 RVZ
 Europese Unie, Europees Fonds voor Maritieme Zakelijke Onderneming

Summary

- Project brief
- Data collection
- Data management
- Trend analysis & Species identification
- ECHO software
- Conclusion

Wageningen University
 TNO innovation for life
 RVZ
 Europese Unie, Europees Fonds voor Maritieme Zakelijke Onderneming

Project brief

- Motivation: reduce bycatch by providing tools allowing better selectivity
- Develop software (MATLAB) to aid skippers during fishing
- Data collection from 3 commercial vessels
- Classification using EK80FM (70, 120, 200 kHz)
- Real time classification
- Species of interest: Herring, Horse Mackerel, Mackerel, potentially Sprat and Sardine

Wageningen University
 TNO innovation for life
 RVZ
 Europese Unie, Europees Fonds voor Maritieme Zakelijke Onderneming

Data collection

- Data collected only during fishing operations
- ~20TB of FM data collected so far (80% from one vessel)
- Catch composition and length frequency from catch samples
- Calibration performed on each vessel
- Number of matching schools:
 - HER: 174 schools
 - HOM: 218 schools
 - MAC: 33 schools

Wageningen University
 TNO innovation for life
 RVZ
 Europese Unie, Europees Fonds voor Maritieme Zakelijke Onderneming

Data base

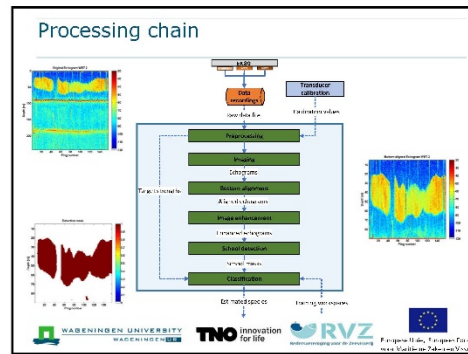
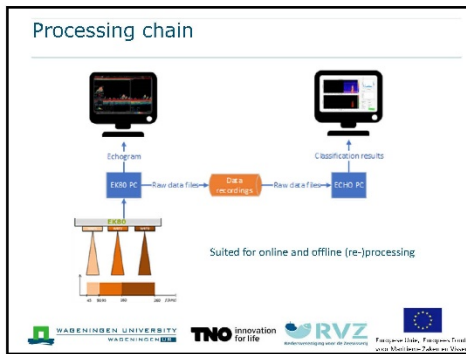
- Automatic routines to detect and extract large schools
- Manual checks of results
- Raw data reduced to individual schools with specific format
- Database used for:
 - Normalizing data sets
 - Automatized training
 - Batch data analysis

Wageningen University
 TNO innovation for life
 RVZ
 Europese Unie, Europees Fonds voor Maritieme Zakelijke Onderneming

Data base

- Automatic routines to detect and extract large schools
- Manual checks of results
- Raw data reduced to individual schools with specific format
- Database used for:
 - Normalizing data sets
 - Automatized training
 - Batch data analysis

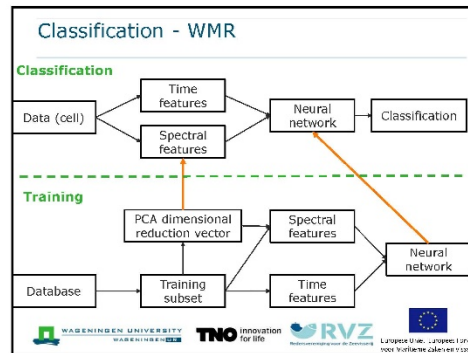
Wageningen University
 TNO innovation for life
 RVZ
 Europese Unie, Europees Fonds voor Maritieme Zakelijke Onderneming



Classification

- Classification done per cell (1.5 m in height)
- Signal features are computed for each cell
 - Time features
 - Spectral features
- Classification using machine learning
 - 2 classification methods
 - TNO (supervised machine learning)
 - WMR (Neural Network)

WAGENINGEN UNIVERSITY | TNO innovation for life | RVZ | European Union



Classification - WMR

- Time features:
 - Time features (per channel)
 - SNR
 - Std of Sv distribution
 - Skewness of Sv distribution
- Spectral features:
 - Spectral features
 - 10 principal components
 - dimensional reduction
- Not as robust as TNO classifier

| Output Class \ Target Class | HER | HOM | MAC |
|-----------------------------|-------------|---------------|---------------|
| HER | 71% 1150 | 17.4% 1416 | 2.1% 310 |
| HOM | 0.1% 100 | 74.7% 620 | 24.5% 270 |
| MAC | 0.3% 40 | 0.2% 20 | 94.2% 1100 |

Accuracy: 71.4%

WAGENINGEN UNIVERSITY | TNO innovation for life | RVZ | European Union

Classification - TNO

- Evaluation approach:
 - Independent training and test set
 - Each fish school bound to deliver max. number of cells

| Actual species \ Estimated species | HER | HOM | MAC |
|------------------------------------|-------|-------|-------|
| HER | 94.7% | 6.0% | 0.9% |
| HOM | 5.2% | 92.1% | 3.7% |
| MAC | 0.0% | 1.8% | 95.2% |

Scores when using all data

WAGENINGEN UNIVERSITY | TNO innovation for life | RVZ | European Union

Classification - TNO

- Robustness tests:
 - All data (reference):
 - Average score > 90%
 - Train with data of a few trips, test on data of another trip
 - Average score > 80%
 - Simulate calibration errors
 - Introduce WBT offset error or linear error
 - Rough estimate of score reduction of 25% per 1 dB (relative) error

Example: 1 dB offset error WBT3

The graph shows two lines: a blue line for 'Original values' and a purple line for 'Altered values'. The x-axis is 'Freq (kHz)' from 0 to 300, and the y-axis is 'Level (dB)' from 22 to 32. The altered values show a consistent downward shift of approximately 1 dB across the frequency range.

Logos: Wageningen University, TNO innovation for life, RVZ, European Union.

ECHO software

The screenshot shows the ECHO software interface. It features a large spectrogram on the left, a smaller spectrogram on the right, and a control panel at the bottom with various settings and buttons. The interface is designed for acoustic data analysis.

Logos: Wageningen University, TNO innovation for life, RVZ, European Union.

Conclusion

Conclusions:

- Broadband echosounder is promising though challenging
- Data management is key when using EK80FM
- Workflow/procedure in place for further data collection and analysis
- Herring and Horse Mackerel marks come as very close
- Classification exemplifies satisfying results to date

Logos: Wageningen University, TNO innovation for life, RVZ, European Union.

Acknowledgements

Crew and skippers of SCH6 'Alida', SCH24 'Afrika' and SCH302 'Willem van der Zwan' (and especially Bas) are acknowledged for their efforts in data collection

Questions?

Logos: Wageningen University, TNO innovation for life, RVZ, European Union.

Extra slides

Logos: Wageningen University, TNO innovation for life, RVZ, European Union.

Data sets

| Year | Month | Day | Time | Lat | Lon | Depth (m) | Species | Count |
|------|-------|-----|-------|-------|------|-----------|---------|-------|
| 2018 | 08 | 01 | 08:00 | 52.15 | 4.10 | 10 | Herring | 15 |
| 2018 | 08 | 01 | 08:05 | 52.15 | 4.10 | 10 | Herring | 12 |
| 2018 | 08 | 01 | 08:10 | 52.15 | 4.10 | 10 | Herring | 18 |
| 2018 | 08 | 01 | 08:15 | 52.15 | 4.10 | 10 | Herring | 14 |
| 2018 | 08 | 01 | 08:20 | 52.15 | 4.10 | 10 | Herring | 16 |
| 2018 | 08 | 01 | 08:25 | 52.15 | 4.10 | 10 | Herring | 13 |
| 2018 | 08 | 01 | 08:30 | 52.15 | 4.10 | 10 | Herring | 17 |
| 2018 | 08 | 01 | 08:35 | 52.15 | 4.10 | 10 | Herring | 14 |
| 2018 | 08 | 01 | 08:40 | 52.15 | 4.10 | 10 | Herring | 16 |
| 2018 | 08 | 01 | 08:45 | 52.15 | 4.10 | 10 | Herring | 13 |
| 2018 | 08 | 01 | 08:50 | 52.15 | 4.10 | 10 | Herring | 17 |
| 2018 | 08 | 01 | 08:55 | 52.15 | 4.10 | 10 | Herring | 14 |
| 2018 | 08 | 01 | 09:00 | 52.15 | 4.10 | 10 | Herring | 16 |
| 2018 | 08 | 01 | 09:05 | 52.15 | 4.10 | 10 | Herring | 13 |
| 2018 | 08 | 01 | 09:10 | 52.15 | 4.10 | 10 | Herring | 17 |
| 2018 | 08 | 01 | 09:15 | 52.15 | 4.10 | 10 | Herring | 14 |
| 2018 | 08 | 01 | 09:20 | 52.15 | 4.10 | 10 | Herring | 16 |
| 2018 | 08 | 01 | 09:25 | 52.15 | 4.10 | 10 | Herring | 13 |
| 2018 | 08 | 01 | 09:30 | 52.15 | 4.10 | 10 | Herring | 17 |
| 2018 | 08 | 01 | 09:35 | 52.15 | 4.10 | 10 | Herring | 14 |
| 2018 | 08 | 01 | 09:40 | 52.15 | 4.10 | 10 | Herring | 16 |
| 2018 | 08 | 01 | 09:45 | 52.15 | 4.10 | 10 | Herring | 13 |
| 2018 | 08 | 01 | 09:50 | 52.15 | 4.10 | 10 | Herring | 17 |
| 2018 | 08 | 01 | 09:55 | 52.15 | 4.10 | 10 | Herring | 14 |
| 2018 | 08 | 01 | 10:00 | 52.15 | 4.10 | 10 | Herring | 16 |
| 2018 | 08 | 01 | 10:05 | 52.15 | 4.10 | 10 | Herring | 13 |
| 2018 | 08 | 01 | 10:10 | 52.15 | 4.10 | 10 | Herring | 17 |
| 2018 | 08 | 01 | 10:15 | 52.15 | 4.10 | 10 | Herring | 14 |
| 2018 | 08 | 01 | 10:20 | 52.15 | 4.10 | 10 | Herring | 16 |
| 2018 | 08 | 01 | 10:25 | 52.15 | 4.10 | 10 | Herring | 13 |
| 2018 | 08 | 01 | 10:30 | 52.15 | 4.10 | 10 | Herring | 17 |
| 2018 | 08 | 01 | 10:35 | 52.15 | 4.10 | 10 | Herring | 14 |
| 2018 | 08 | 01 | 10:40 | 52.15 | 4.10 | 10 | Herring | 16 |
| 2018 | 08 | 01 | 10:45 | 52.15 | 4.10 | 10 | Herring | 13 |
| 2018 | 08 | 01 | 10:50 | 52.15 | 4.10 | 10 | Herring | 17 |
| 2018 | 08 | 01 | 10:55 | 52.15 | 4.10 | 10 | Herring | 14 |
| 2018 | 08 | 01 | 11:00 | 52.15 | 4.10 | 10 | Herring | 16 |
| 2018 | 08 | 01 | 11:05 | 52.15 | 4.10 | 10 | Herring | 13 |
| 2018 | 08 | 01 | 11:10 | 52.15 | 4.10 | 10 | Herring | 17 |
| 2018 | 08 | 01 | 11:15 | 52.15 | 4.10 | 10 | Herring | 14 |
| 2018 | 08 | 01 | 11:20 | 52.15 | 4.10 | 10 | Herring | 16 |
| 2018 | 08 | 01 | 11:25 | 52.15 | 4.10 | 10 | Herring | 13 |
| 2018 | 08 | 01 | 11:30 | 52.15 | 4.10 | 10 | Herring | 17 |
| 2018 | 08 | 01 | 11:35 | 52.15 | 4.10 | 10 | Herring | 14 |
| 2018 | 08 | 01 | 11:40 | 52.15 | 4.10 | 10 | Herring | 16 |
| 2018 | 08 | 01 | 11:45 | 52.15 | 4.10 | 10 | Herring | 13 |
| 2018 | 08 | 01 | 11:50 | 52.15 | 4.10 | 10 | Herring | 17 |
| 2018 | 08 | 01 | 11:55 | 52.15 | 4.10 | 10 | Herring | 14 |
| 2018 | 08 | 01 | 12:00 | 52.15 | 4.10 | 10 | Herring | 16 |

Logos: Wageningen University, TNO innovation for life, RVZ, European Union.

Calibration

- 2-3 Spheres in the water
- Non optimal conditions for calibration
- Custom software used for data processing
- Variations between years in the order of 0.5-1 dB
- Variation problematic with classifier sensitivity

| Year | Distance | Species | Volume | Time | Depth | Lat | Long |
|------|----------|---------|--------|-------|-------|-------|------|
| 2014 | 1000 | HER | 100 | 10:00 | 10 | 52.00 | 5.00 |
| 2014 | 1000 | HOM | 100 | 10:05 | 10 | 52.00 | 5.00 |
| 2014 | 1000 | MAC | 100 | 10:10 | 10 | 52.00 | 5.00 |
| 2015 | 1000 | HER | 100 | 10:00 | 10 | 52.00 | 5.00 |
| 2015 | 1000 | HOM | 100 | 10:05 | 10 | 52.00 | 5.00 |
| 2015 | 1000 | MAC | 100 | 10:10 | 10 | 52.00 | 5.00 |

WAGENINGEN UNIVERSITY
TNO innovation for life
RVZ
European Union, European Fisheries and Aquaculture Innovation Programme

Spectral trend analysis

- Spectra in each cell of each school
- Analysis of relative trends between schools and species
- Use distance between Z-normalized/smooth spectra
- Use multi-dimensional scaling for analysis

WAGENINGEN UNIVERSITY
TNO innovation for life
RVZ
European Union, European Fisheries and Aquaculture Innovation Programme

Spectral trend analysis

- Expectedly, HER and HOM are close but exemplify differences
- Absolute level and time features potentially adds more discrimination power

WAGENINGEN UNIVERSITY
TNO innovation for life
RVZ
European Union, European Fisheries and Aquaculture Innovation Programme



European
Commission



Sea trial of the software on board a Dutch fishing vessel
© photo copyright Wageningen Marine Research



GENERAL INFORMATION

Member State:
Netherlands

EMFF measure:
Innovation linked to conservation of marine biological resources

Total operation budget:
EUR 797 428

EU budget contribution:
EUR 598 071

- Keywords:**
- Landing obligation
 - Sustainable production
 - Marine fisheries

Operation dates:
2016-2019

Contact details:
Wageningen Marine Research
and Redersvereniging voor de
Zeevisserij, NL

STORY OF THE MONTH

SUPPORTED BY THE EMFF (European Maritime and Fisheries Fund)

Identifying fish species with echo sounder data

Operation description

Under EU sustainability rules, fishermen are not allowed to catch fish below a certain minimum size. Nor are they any longer allowed to throw unwanted fish overboard. Instead, they must land everything they catch. As a result, the fishing industry requires new and better ways of identifying fish species and sizes *before* bringing the catch aboard.

The RealFishEcho project in the Netherlands, financed with nearly €600 000 from the EMFF, is developing methods to identify fish species and to estimate their size in close to real time. Using broadband echo sounder data, fishermen are able to avoid unwanted catches. This allows them to only bring aboard the fish they are targeting – mainly herring, mackerel, and horse mackerel –, making their fishing practices more sustainable.

The funding has allowed fishermen and researchers to collect and analyse more data. This has not only made the technology more accurate and reliable; it can also recognise more fish species than before. Data are collected from commercial freezer trawlers and research vessels.

For more information:

<https://www.wur.nl/en/Publication-details.htm?publicationId=publication-way-353333383235>

Maritime Affairs
and Fisheries

IV.4 Presentation at PFA science day

Fish species recognition using broadband acoustics

B. J. P. Bergást¹, J. J. M. van de Sandel², B. Quesson³, S. Sekman⁴, A.W.R. van Heljingen⁵, E. van Helmond¹, D. Burggraaf¹, M. Pastoor⁶

¹ Wageningen Marine Research (WUR), Gronau, The Netherlands
² TNO, Den Haag, The Netherlands
³ Pelagic Fish Association (PFA), Zierikzee, The Netherlands
⁴ van.de.sandel@wur.nl
⁵ bergast@wur.nl

European Union, Erasmus+ (under Marie Skłodowska Curie)

RVZ
 Nederlandse Vereniging voor de Zeevisserij
 Innovation for life
 TNO
 WAGENINGEN UNIVERSITY
 WAGENINGEN

Collected data

Classification success rate

| | HR | CM | RMSE |
|------|-------|-------|-------|
| HR | 2.0 | 37.2% | 56.2% |
| RMSE | 84.7% | 39.2% | 56.2% |

WAGENINGEN UNIVERSITY
 WAGENINGEN

Project brief

- Species identification
- Data collection from 3 commercial vessels
- Classification using EK80FM (70, 120, 200 kHz)
- Real time classification
- Species of interest: Herring, Horse Mackerel, Mackerel, potentially Sprat and Sardine

WAGENINGEN UNIVERSITY
 TNO Innovation for life
 RVZ
 European Union, Erasmus+ (under Marie Skłodowska Curie)

Advantages of broadband echosounders

- High spatial resolution
 - Target tracking
 - Target sizing
- High frequency resolution
 - Species identification

WAGENINGEN UNIVERSITY
 TNO Innovation for life
 RVZ
 European Union, Erasmus+ (under Marie Skłodowska Curie)

Improved resolution

WAGENINGEN UNIVERSITY
 TNO Innovation for life
 RVZ
 European Union, Erasmus+ (under Marie Skłodowska Curie)

Continuous frequency response

WAGENINGEN UNIVERSITY
 TNO Innovation for life
 RVZ
 European Union, Erasmus+ (under Marie Skłodowska Curie)

Challenges: noise

- Noise (stripes) in the echograms
- More prone to interferences and cross talks
- There is ways to filter stripe noise

ALID_HER_2016_08_Rishshool_003_WBTTN02_c-000016

WAGeningen UNIVERSITY | TNO Innovation for life | RVZ | European Union

Challenges: data volume

- For a 6 frequencies echosounder:
 - EK60: ~5 GB / 24h
 - EK80 CW: ~40 GB / 24h
 - EK80 FM: ~1 TB / 24h
- Automatic processing
- Data selectivity/reduction

WAGeningen UNIVERSITY | TNO Innovation for life | RVZ | European Union

Data collection

- ~20TB of FM data collected so far (80% from one vessel)
- Catch composition and length frequency from catch samples
 - HER: 217 schools
 - HOM: 266 schools
 - MAC: 62 schools
 - SPR: 19 schools
 - PIL: 7 schools

WAGeningen UNIVERSITY | TNO Innovation for life | RVZ | European Union

Data collection

WAGeningen UNIVERSITY | TNO Innovation for life | RVZ | European Union

WMR classifier

All data together Accuracy: 75.4%

| Actual \ Target Class | HER | HOM | MAC |
|-----------------------|--------------|--------------|------------|
| HER | 1708 1743 | 873 2039 | 236 183 |
| HOM | 2296 2202 | 1773 1547 | 219 187 |
| MAC | 976 891 | 129 402 | 567 473 |

Performance per data set

WAGeningen UNIVERSITY | TNO Innovation for life | RVZ | European Union

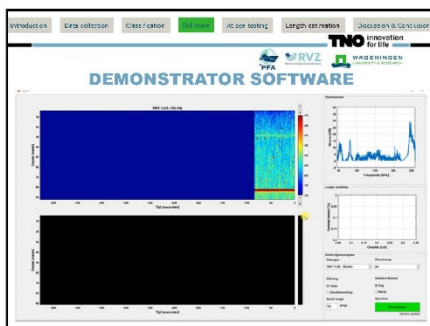
TNO classifier

All data together All data - 64 averaging cell(s)

| Actual species \ Estimated species | HER | HOM | MAC |
|------------------------------------|-------|-------|-------|
| HER | 84.7% | 13.9% | 1.2% |
| HOM | 5.6% | 94.2% | 0.1% |
| MAC | 1.1% | 0.5% | 98.3% |

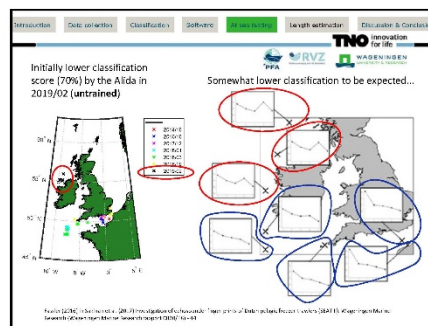
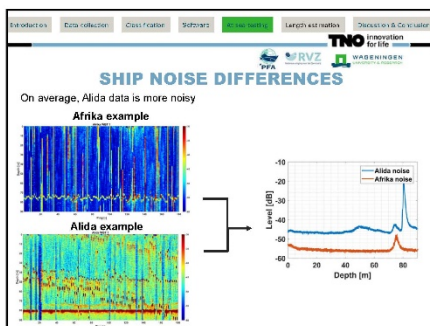
Performance per data set

WAGeningen UNIVERSITY | TNO Innovation for life | RVZ | European Union

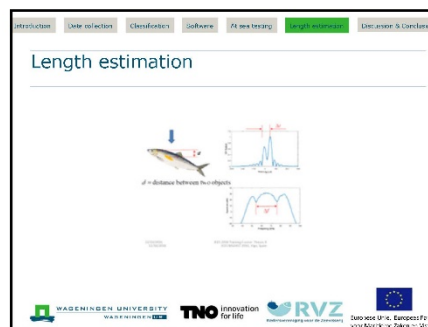


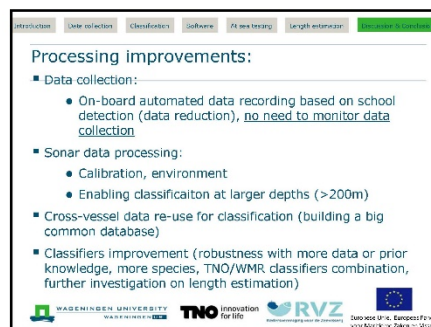
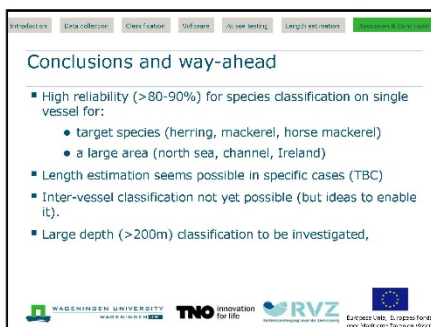
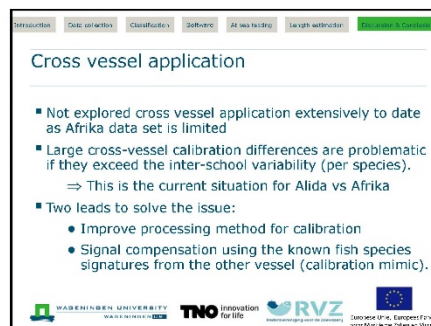
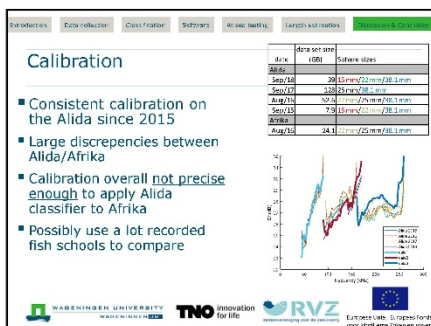
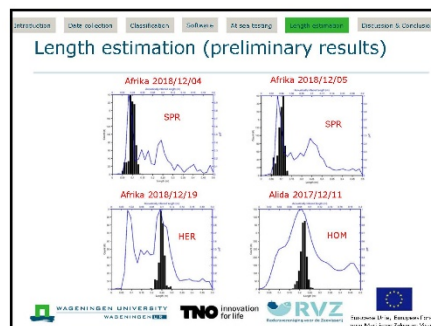
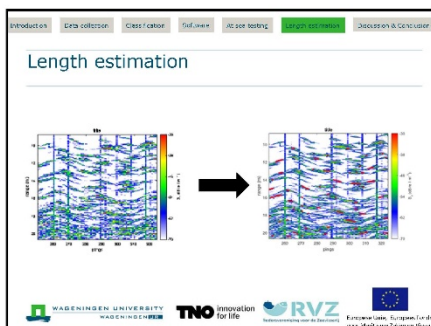
AT SEA TESTING

- › Demonstrator functioning in real time on Afrika and Alida
- › Some issues:
 - › Higher noise on the Alida => more false detections. Workaround implemented.
 - › Evaluation at Alida in 2019/02: North-West Ireland Horse Mackerel not in database yet => lower score (70%)
 - › Cross-platform application (use Alida data for Afrika) still difficult due to calibration



- › Classifier had not 'seen' Ireland-type of Horse Mackerel, so initially scores lower (70%)
- › **After training** the new type, it is able to score **95%**
- › **Conclusion:** also works for Horse Mackerel in that area now
- › Good news: the three schools back in the Channel scored 96% => stability over the years






Acknowledgements

Crew and skippers of SCH6 'Alida', SCH24 'Afrika' and SCH302 'Willem van der Zwan' (and especially Bas) are acknowledged for their efforts in data collection

Questions/feedback?



Wageningen Marine Research
T +31 (0)317 48 09 00
E: marine-research@wur.nl
www.wur.eu/marine-research

With knowledge, independent scientific research and advice, **Wageningen Marine Research** substantially contributes to more sustainable and more careful management, use and protection of natural riches in marine, coastal and freshwater areas.

Visitors' address

- Ankerpark 27 1781 AG Den Helder
- Korringaweg 7, 4401 NT Yerseke
- Haringkade 1, 1976 CP IJmuiden



Wageningen Marine Research is part of Wageningen University & Research. Wageningen University & Research is the collaboration between Wageningen University and the Wageningen Research Foundation and its mission is: 'To explore the potential for improving the quality of life'
